



University
of Glasgow

Masre, Siti Fathiah (2015) *Analysis of ROCK2 activation in transgenic mouse skin carcinogenesis*. PhD thesis.

<http://theses.gla.ac.uk/6628/>

Copyright and moral rights for this thesis are retained by the author

A copy can be downloaded for personal non-commercial research or study

This thesis cannot be reproduced or quoted extensively from without first obtaining permission in writing from the Author

The content must not be changed in any way or sold commercially in any format or medium without the formal permission of the Author

When referring to this work, full bibliographic details including the author, title, awarding institution and date of the thesis must be given

Analysis of ROCK2 Activation in Transgenic Mouse Skin Carcinogenesis

Siti Fathiah Masre

A Thesis submitted to the University of Glasgow
In fulfilment of the requirements for the
Degree of Doctor of Philosophy

School of Medicine
College of Medical, Veterinary and Life Sciences
University of Glasgow

August 2015

Summary

The purpose of this study was to investigate ROCK2 activation in squamous cell carcinogenesis and assess its co-operation with ras^{Ha} and fos oncogene activation together with loss of PTEN mediated AKT regulation. The analysis of ROCK deregulation with these genes in the MAP Kinase and PI3K pathways, two of the most commonly deregulated signalling systems, employed a well-characterised, transgenic mouse skin model of multi-stage carcinogenesis. A major goal was to study co-operation between these genes in the conversion of benign tumours to malignancy and investigate subsequent progression to aggressive carcinomas, given these are the most significant clinical stages of carcinogenesis from a patient's viewpoint; and also investigated effects of ROCK2 deregulation on the processes of normal epidermal differentiation.

ROCK2 is an effector protein of RhoA, which is a member of the ras superfamily and ROCK2 activation has been associated with tumour progression via an increase in tissue stiffness mediated by changes in actomyosin cytoskeleton leading to increased cellular motility. Thus, ROCK2 expression is commonly associated with the later events in cancer. Furthermore, there are many studies investigating ROCK2 in cancer given that it may be a useful therapeutic target in being downstream of oncogenic ras signalling. Yet, relatively few studies have explored the possibilities of a definite link that confirms the co-operation status of ROCK2 activation with ras/MAPK/fos and /or PTEN/PI3K/AKT pathways in SCC aetiology. Thus, questions exist as to exactly when does ROCK2 activation become causal; and what are the collaborating genes involved in the mechanism that drive the early or late stage events in carcinogenesis.

To begin to answer these questions, inducible ROCK2 activation has been introduced into a well-characterised transgenic mouse skin carcinogenesis model that expressed a combination of ras and fos activation, driven by a modified human keratin 1 vector (HK1). Thus, exclusive epidermal expression of activated ras^{Ha} and fos oncogenes, in proliferative basal layers, gave hyperplasia and papillomatogenesis; but with no evidence of spontaneous malignant conversion.

This stability of phenotype is thus ideal to assess roles for multiple transgene co-operations in the development of benign tumours and their conversion to malignancy. Hence, ROCK transgenic mice that expressed a conditionally active, 4-hydroxytamoxifen (4-HT)-regulated of human ROCK2 transgene were crossed with mice expressing activated ras^{Ha} and /or fos exclusively in epidermal transit amplifying keratinocytes (*HK1.ras*, *HK1.fos*). Inducible PTEN tumour suppressor gene mutation via exon 5 ablation (*K14.Cre/Δ5PTEN^{flx}*) and thus loss of AKT regulation was also incorporated into this model. This was achieved via deletion of exon 5 employing the RU486-mediated cre/loxP system, driven by keratin K14 promoter expression in basal layer keratinocytes. Therefore, to facilitate this investigation, a new and unpublished inducible ROCK2 system was employed in order to target the identical keratinocytes as PTEN loss. This new transgenic line of *Isl.ROCK^{er}* transgenic mice employed the same 4-HT inducible ROCK^{er} transgene but now driven by a generic CAG promoter following cre mediated ablation of the stop cassette once treated with RU486.

In bi-genic *K14.ROCK^{er}/HK1.ras¹²⁰⁵* mice, synergism between ROCK2 activation and (wound-promotion) sensitive *HK1.ras¹²⁰⁵* line showed direct co-operation and achieved malignant conversion of benign papillomas to well-differentiated squamous cell carcinoma (wdSCCs) histotypes (12 weeks of 4-HT treatment). This placed ROCK2 activity as the causal event driving malignant conversion, but in the absence of a wound promotion stimulus (loss of ear tag), papillomas did not convert. The correct papilloma context was required for ROCK to become causal proved to be the case on employing the wound insensitive *HK1.ras¹²⁷⁶* line. Here, *K14.ROCK^{er}/HK1.ras¹²⁷⁶* mice failed to exhibit any papillomas and required the constitutive promotion stimulus from additional fos activation. Interestingly, following cessation of 4-HT, two intriguing observations were recorded. Firstly, that once bi-genic ROCK/ ras^{1205} achieved malignancy, exogenous ROCK^{er} expression appeared to show no involvement once squamous cell carcinomas (SCCs) progressed to poorly differentiated squamous cell carcinomas (pdSCCs), given the elevated expression of endogenous ROCK upon malignant progression. Secondly, the rapid growth of papilloma appeared upon cessation of 4-HT with highly intense p21 expression indicated the requirement of exogenous ROCK2 for malignant conversion and the possibility of a papilloma inhibition by 4-HT anti-cancer activity.

Another major novel finding demonstrated ROCK2 activation could act as an initiator in co-operation with fos activation. Direct co-operation between ROCK2 and fos activation produced benign squamous papillomas yet, whereas ROCK2 activation alone induced hyperplasia as did fos activation alone at this time point, given papilloma formation in *HK1.fos* mice occur over 4-5 months. However, unlike deregulation of MAP Kinase signalling in bi-genic ROCK/*ras*¹²⁰⁵ mice, in bi-genic ROCK/fos mice, no malignant conversion was observed due to high levels of compensatory p53/p21 expression. Thus, this bi-genic *K14.cre/Isl.ROCK^{er}/HK1.fos* model suggests the requirement of additional mutation event for malignant conversion. An unexpected result appeared in bi-genic ROCK/ Δ 5PTEN^{flx} co-operation experiments where *K14.cre/Isl.ROCK^{er}/ Δ 5PTEN^{flx}* cohorts exhibited epidermal hyperplasia with folded papillomatous appearance to the epidermis, but without papillomatogenesis even after seven month of period. This either indicates a weak co-operation between ROCK2 and Δ 5PTEN^{flx} which may be due to the unexpected low levels of p-AKT from a compensatory increased p21 expression; and additional events needed to fill in the oncogenic gap in this bi-genic ROCK/ Δ 5PTEN^{flx} model, or may possibly highlight redundancy in the oncogenic hits provided by ROCK and PTEN. This latter suggest similar links exist between their normal roles in the epidermis which may be accountable for the alterations observed in keratinocyte differentiation. In both *in vitro* and *in vivo* experiments, *K14.cre/Isl.ROCK^{er}/ Δ 5PTEN^{flx}* cohorts showed alterations in epidermal differentiation via anomalous K1 and low levels of K6 expression.

Interestingly, activated ROCK2 appeared to induce or accelerate differentiation activity in *K14.cre/Isl.ROCK^{er}* keratinocytes via increased K1 (early differentiation marker) and reduced K6 (proliferation marker) expression profiles. These results were consistent with *in vivo* data where K6 was expressed in low levels in *K14.cre/Isl.ROCK^{er}* hyperplasia histotypes. In contrast, in *K14.cre/Isl.ROCK^{er}/ Δ 5PTEN^{flx}* keratinocytes, inactivation of PTEN-mediated AKT activity may be accountable for restored keratin K6 and anomalous keratin K1 expression; as keratin K1 was expressed in a similar fashion of normal keratinocytes in *K14.cre/Isl.ROCK^{er}/fos* keratinocytes.

Interestingly, all tri-genic cohorts: *K14.cre/Isl.ROCK^{er}/*ras*¹²⁷⁶/fos*, *K14.cre/Isl.ROCK^{er}/fos/ Δ 5PTEN^{flx}* and *K14.cre/Isl.ROCK^{er}/*ras*¹²⁷⁶/ Δ 5PTEN^{flx}* synergisms exhibited malignant conversion and /or malignant progression in all

animals highlighting a novel role of ROCK2 activation. Further, the stage-specific consequences in each model in this study were shown to be influenced by p53/p21 status, where typically p53 expression disappeared in late stage papillomas yet, p21 expression persisted. This demonstrated the importance of compensatory p53/p21 expression in modulating tumour pathogenesis in all these models. Given that this study incorporated PTEN mutation, the influence of AKT activity was investigated in the SCC progression of tri-genic ROCK/ras¹²⁷⁶/PTEN^{fix} and ROCK/fos/PTEN^{fix} cohorts; revealing a crucial antagonism between p21 and AKT. However, this study revealed that the malignancy in tri-genic ROCK/ras¹²⁷⁶/fos cohorts was not influenced by p-AKT expression, and as this tri-genic model achieved wdSCCs only. This suggests that as the roles of ROCK in altering cytoskeletal organisation leading to increase in tissue stiffness are overlaid onto both MAP Kinase and AKT deregulation, the outcome is a very aggressive pdSCC. Thus, suggesting ROCK signalling to be a potential therapeutic target for ras/MAPK/fos pathway in carcinogenesis. Overall, this study showed the involvement of ROCK2 activation in the initiation stage for papillomatogenesis with fos oncogene, and demonstrated ROCK2 as a converter again and also in malignant progression with ras/fos/ Δ 5PTEN^{fix} mutations. This indicates the link of ROCK2 signalling with both MAPK and PI3K pathways, thus targeting ROCK2 would aid in development of cancer therapy.

Table of contents

Summary	2
List of tables.....	10
List of figures.....	11
Appendix.....	17
Acknowledgement.....	18
Author's declaration	19
Abbreviations	20
Chapter 1 – Introduction	23
1.1 General introduction	23
1.2 ROCK.....	25
1.2.1 ROCK: an overview	25
1.2.2 The structure of ROCK	28
1.2.3 ROCK and cancer	32
1.3 Models of multistage skin carcinogenesis	36
1.3.1 Epidermal physiology	36
1.3.2 The classic mouse skin model of chemical carcinogenesis.....	39
1.3.3 The HK1 transgenic mouse model of skin carcinogenesis.....	42
1.4 Targeting genes to the epidermis: A mimic of classic two stage DMBA/TPA mediated chemical carcinogenesis.....	45
1.4.1 Targeting activated ras ^{Ha} to the epidermis: A model of tumour initiation and papilloma formation.....	46
1.4.2 Targeting v-fos to the epidermis: A model of tumour promotion	52
1.4.3 Inactivation of PTEN tumour suppressor gene mediated AKT regulation	55
1.4.4 Analysis of endogenous ROCK expression in the ras/fos/PTEN ^{flx} skin carcinogenesis model	58
1.5 Hypothesis and Aims of the study	63
Chapter 2 – Materials and Methods.....	64
2.1 Materials.....	64
2.1.1 PCR materials	64
2.1.2 Immunohistochemistry and immunofluorescence materials	65
2.1.3 Cell culture materials.....	66
2.1.4 Western blot materials	67
2.2 Methods.....	68
2.2.1 Transgenic mouse genotypes and breeding.....	68
2.2.2 Polymerase chain reaction (PCR).....	69
2.2.3 Immunohistochemistry and immunofluorescence	72

2.2.4 Primary keratinocytes cell culture	73
2.2.5 Western blot analysis	74
2.2.6 BrdU-labelling analysis	75
Chapter 3 – Results	76
3.1 PCR analysis and genotyping of transgenic mice	76
3.1.1 Confirmation of gene switch activation	79
3.2 ROCK2 activation in transgenic mouse skin carcinogenesis.....	82
3.2.1 ROCK ^{er} transgenic mouse skin induces hyperplasia	82
3.2.2 Expression of differentiation markers in ROCK hyperplasia	87
3.2.3 Summary	89
3.3 Co-operation of ROCK2 and <i>HK1.ras</i> activation in transgenic mouse skin carcinogenesis	90
3.3.1 Confirmation of ROCK ^{er} transgene in bi-genic ROCK/ras ¹²⁰⁵ mouse and expression of downstream targets	91
3.3.2 ROCK2 co-operates with ras ^{Ha} to elicit benign tumours (at 8 weeks) ..	94
3.3.3 ROCK2 co-operates with ras ^{Ha} to elicit malignant conversion (at 12 weeks)	99
3.3.4 Expression of p53 and p21 in bi-genic ROCK/ras ¹²⁰⁵ tumours	104
3.3.5 BrdU-labelling of bi-genic ROCK/ras ¹²⁰⁵ tumours	108
3.3.6 Tenascin C expression in bi-genic ROCK/ras ¹²⁰⁵ tumours.....	110
3.3.7 Cessation of 4-HT treatment in bi-genic ROCK/ras ¹²⁰⁵ tumours	112
3.3.7 Wound promotion for development of appropriate late-stage papilloma prior to ROCK ^{er} causality.	121
3.3.8 Summary	124
3.4 Co-operation of ROCK2 and <i>HK1.fos</i> in transgenic mouse skin carcinogenesis	125
3.4.1 ROCK2 co-operates with activated fos to elicit benign tumours	126
3.4.2 Expression of p53 and p21 in bi-genic ROCK/fos mice	136
3.4.3 BrdU-labelling of bi-genic ROCK/fos mice	138
3.4.4 Summary	140
3.5 Co-operation of ROCK2 and <i>K14.cre/Δ5PTEN^{flx}</i> in transgenic mouse skin carcinogenesis	141
3.5.1 Confirmation of <i>Isl.ROCK^{er}</i> expression in bi-genic ROCK/Δ5PTEN ^{flx} mice	142
3.5.2 ROCK2 co-operates with Δ5PTEN ^{flx} to elicit hyperplasia with papillomatous appearance	145
3.5.3 Expression of differentiation markers in bi-genic ROCK/Δ5PTEN ^{flx} ...	149
3.5.4 Expression of p53, p21 and p-AKT1 in bi-genic ROCK/Δ5PTEN ^{flx} mice	151
3.5.5 BrdU-labelling of bi-genic ROCK/Δ5PTEN ^{flx} mice	155
3.5.6 Summary	157

3.6 Analysis of ROCK2 activation <i>in vitro</i> : effects on differentiation not carcinogenesis.	158
3.6.1 Establishment of primary transgenic mouse keratinocyte culture	159
3.6.2 Expression of keratinocyte differentiation markers <i>in vitro</i>	166
3.6.3 Summary	172
3.7 Co-operation of ROCK2, <i>HK1.ras</i> and <i>HK1.fos</i> in transgenic mouse skin carcinogenesis	175
3.7.1 ROCK2 co-operates with <i>HK1.ras/fos</i> to elicit malignant progression.	176
3.7.2 Expression of differentiation markers in tri-genic ROCK/ <i>ras</i> ¹²⁷⁶ / <i>fos</i> ...	180
3.7.3 Expression of p53 and p21 in tri-genic ROCK/ <i>ras</i> ¹²⁷⁶ / <i>fos</i> mice	182
3.7.4 BrdU-labelling of tri-genic ROCK/ <i>ras</i> ¹²⁷⁶ / <i>fos</i> tumours	188
3.7.5 Summary	190
3.8 Co-operation of ROCK2, <i>HK1.fos</i> and <i>K14.cre/Δ5PTEN^{flx}</i> in transgenic mouse skin carcinogenesis	191
3.8.1 ROCK2 co-operates with <i>HK1.fos/Δ5PTEN^{flx}</i> to produce malignant progression to SCC not keratoacanthomas.....	192
3.8.2 Expression of tumour progression marker keratin K1 in tri-genic ROCK/ <i>fos/Δ5PTEN^{flx}</i> carcinogenesis.....	198
3.8.3 Expression of late differentiation markers filaggrin and loricrin in tri-genic ROCK/ <i>fos/Δ5PTEN^{flx}</i> carcinogenesis	201
3.8.4 Expression of p53 and p21 in tri-genic ROCK/ <i>fos/Δ5PTEN^{flx}</i> tumours	206
3.8.5 BrdU-labelling of tri-genic ROCK/ <i>fos/Δ5PTEN^{flx}</i> mice	210
3.8.6 Expression of p-AKT1 in tri-genic ROCK/ <i>fos/Δ5PTEN^{flx}</i> tumours	212
3.8.7 Summary	214
3.9 Analysis of the co-operation between ROCK2 and <i>ras^{Ha}</i> activation, and loss of PTEN regulation in transgenic mouse skin carcinogenesis.....	216
3.9.1 ROCK2 co-operates with <i>HK1.ras¹²⁷⁶/Δ5PTEN^{flx}</i> to elicit malignant progression	217
3.9.2 Expression of tumour progression marker keratin K1 in ROCK/ <i>ras¹²⁷⁶/Δ5PTEN^{flx}</i> carcinogenesis	222
3.9.3 Expression of p53 and p21 in tri-genic ROCK/ <i>ras¹²⁷⁶/Δ5PTEN^{flx}</i> mice	224
3.9.4 BrdU-labelling of tri-genic ROCK/ <i>ras¹²⁷⁶/Δ5PTEN^{flx}</i> tumours.....	228
3.9.5 Expression of p-AKT1 in tri-genic ROCK/ <i>ras¹²⁷⁶/Δ5PTEN^{flx}</i> tumours..	230
3.9.6 ROCK2 rapidly elicits malignant conversion and progression to aggressive, poorly differentiated SCCs in co-operation with <i>HK1.ras¹²⁰⁵/Δ5PTEN^{het}</i> mice.....	233
3.9.7 Summary	244
Chapter 4 – Discussion	246
4.1 ROCK2 activation in transgenic mouse skin carcinogenesis.....	246
4.2 Co-operation of ROCK2 and <i>HK1.ras</i> in transgenic mouse skin carcinogenesis	250

4.3 Co-operation of ROCK2 and <i>HK1.fos</i> in transgenic mouse skin carcinogenesis	253
4.4 Co-operation of ROCK2 and <i>K14.cre/Δ5PTEN^{fix}</i> in transgenic mouse skin carcinogenesis	257
4.5 Analysis of ROCK2 activation <i>in vitro</i> : effects on differentiation not carcinogenesis.	260
4.6 Co-operation of ROCK2, <i>HK1.ras</i> and <i>HK1.fos</i> in transgenic mouse skin carcinogenesis	262
4.7 Co-operation of ROCK2, <i>HK1.fos</i> and <i>K14.cre/Δ5PTEN^{fix}</i> in transgenic mouse skin carcinogenesis	265
4.8 Co-operation of ROCK2, <i>HK1.ras</i> and <i>K14.cre/Δ5PTEN^{fix}</i> in transgenic mouse skin carcinogenesis	270
Chapter 5 – Conclusions and future studies	275
Appendix A	281
Appendix B	282
Appendix C	283
List of references	285

List of tables

Table No.		Page
2.1	Antibodies used in IHC and IFC procedures	65
2.2	Antibodies used in western analysis.	67
2.3	Master mix solution	70
2.4	Oligos and programmes used in PCR analysis.	71

List of figures

Figure No.		Page
1.1	Rho/ROCK signalling pathway.	26
1.2	Structure of ROCK (1 and 2).	29
1.3	Activation of ROCK.	31
1.4	Schematic diagrams of (a) K14.ROCK ^{er} and (b) Isl.ROCK ^{er} transgenic mice.	35
1.5	Schematic diagram of a typical stratified normal epidermis and typical markers associated with terminal differentiation through each layer.	38
1.6	Classic mouse skin model of chemical carcinogenesis	40
1.7	Operational stages of skin carcinogenesis.	40
1.8	The histotype of typical tumour pathology and expression of tumour markers in multistage mouse skin carcinogenesis as typified by <i>HK1.ras/fos/Δ5PTEN^{flx}</i> transgenic mice.	44
1.9	Schematic diagram of the structure of Ras/MAPK pathway.	48
1.10	Tumourigenesis in <i>HK1.ras</i> transgenic mice	51
1.11	Schematic diagram of the heterodimerisation of fos family genes with members of the jun family	54
1.12	Tumourigenesis in <i>HK1.fos</i> transgenic mice	54
1.13	Schematic diagram of PTEN/PI3K/AKT pathway.	57
1.14	Histology analysis of <i>K14.cre/Δ5PTEN^{flx}</i> transgenic mice	57
1.15	Immunohistochemical analysis of ROCK1 and ROCK2 expressions in <i>HK1.ras/fos/Δ5PTEN^{flx}</i> tumours.	61

3.1	PCR analysis of ROCK ^{er} genotypes.	78
3.2	PCR analysis of <i>HK1.ras</i> and <i>HK1.fos</i> genotypes.	78
3.3	PCR analysis of K14.creP and Δ 5PTEN ^{fix} genotypes	81
3.4	PCR analysis of Δ 5PTEN and ROCK ^{er} expression in RU486-treated K14.cre/ Δ 5PTEN ^{fix} and K14.cre/Isl.ROCK ^{er} ear-tagged biopsies.	81
3.5	<i>K14.ROCK^{er}</i> and <i>K14.cre/Isl.ROCK^{er}</i> transgenic mice at 20 weeks	84
3.6	IHC analysis of GFP-tagged ROCK ^{er} transgene and p-Mypt1 of ROCK substrate	86
3.7	Immunofluorescence analysis of keratin K1 and K6 markers in RU486-/4-HT-treated <i>K14.cre/Isl.ROCK^{er}</i> hyperplasia.	88
3.8	IHC analysis of GFP and p-MYPT1 expression in <i>K14.ROCK^{er}/HK1.ras¹²⁰⁵</i> tumours.	93
3.9	Phenotypes of <i>K14.ROCK^{er}/HK1.ras¹²⁰⁵</i> mice at 8 weeks	95
3.10	Histotypes of <i>K14.ROCK^{er}/HK1.ras¹²⁰⁵</i> papillomas at 8 weeks.	96
3.11	Immunofluorescence analysis of K1/K14 and K6/K14 expression at 8 weeks in 4-HT-treated <i>K14.ROCK^{er}/HK1.ras¹²⁰⁵</i> and <i>HK1.ras¹²⁰⁵</i> tumours	98
3.12	Phenotypes of <i>K14.ROCK^{er}/HK1.ras¹²⁰⁵</i> and <i>HK1.ras¹²⁰⁵</i> mice at 12 weeks	100
3.13	Histotypes of 4-HT-treated <i>K14.ROCK^{er}/HK1.ras¹²⁰⁵</i> and <i>HK1.ras¹²⁰⁵</i> tumours at 12 weeks.	101
3.14	Immunofluorescence analysis of K1/K14 and K6/K14 expression at 12 weeks in 4-HT-treated <i>K14.ROCK^{er}/HK1.ras¹²⁰⁵</i> and <i>HK1.ras¹²⁰⁵</i> tumours	103
3.15	IHC analysis of p53 expression in 4-HT-treated <i>K14.ROCK^{er}/HK1.ras¹²⁰⁵</i> and <i>HK1.ras¹²⁰⁵</i> tumours.	105

3.16	IHC analysis of p21 expression in 4-HT-treated <i>K14.ROCK^{er}/HK1.ras¹²⁰⁵</i> and <i>HK1.ras¹²⁰⁵</i> tumours	107
3.17	BrdU-labelling of bi-genic ROCK/ras ¹²⁰⁵ carcinogenesis	109
3.18	IHC analysis of tenascin C in 4-HT-treated <i>K14.ROCK^{er}/HK1.ras¹²⁰⁵</i> tumours.	111
3.19	Phenotypes of <i>K14.ROCK^{er}/HK1.ras¹²⁰⁵</i> mice after termination of 4-HT for 2 weeks.	113
3.20	Histotype of <i>K14.ROCK^{er}/HK1.ras¹²⁰⁵</i> biopsies at 16 weeks, after 2 weeks termination of 4-HT.	116-117
3.21	Histotype of <i>K14.ROCK^{er}/HK1.ras¹²⁰⁵</i> tumour from the additional papilloma growth at 16 weeks, after 2 weeks termination of 4-HT.	120
3.22	Phenotype and histopathology of 4-HT-treated <i>K14.ROCK^{er}/HK1.ras</i> line 1205 and 1276.	123
3.23	Phenotypes of <i>K14.cre/Isl.ROCK^{er}/HK1.fos</i> and <i>HK1.fos</i> mice at 12 weeks.	128
3.24	Histotype of <i>K14.cre/Isl.ROCK^{er}/HK1.fos</i> and <i>HK1.fos</i> mice at 12 weeks.	129
3.25	Immunofluorescence analysis of K1/K14 and K6/K14 expression in 4-HT-treated <i>K14.cre/Isl.ROCK^{er}/HK1.fos</i> mice at 12 weeks.	131
3.26	Phenotypes of <i>K14.cre/Isl.ROCK^{er}/HK1.fos</i> and <i>HK1.fos</i> mice at 20 weeks.	133
3.27	Histotype of <i>K14.cre/Isl.ROCK^{er}/HK1.fos</i> and <i>HK1.fos</i> epidermis at 20 weeks of 4-HT treatment.	133
3.28	Immunofluorescence analysis of K1/K14 and K6/K14 expression in <i>K14.cre/Isl.ROCK^{er}/HK1.fos</i> and <i>HK1.fos</i> mice at 20 weeks of 4-HT treatment.	135
3.29	IHC analysis of p53 and p21 in RU486-/4-HT-treated <i>K14.cre/Isl.ROCK^{er}/HK1.fos</i> and <i>HK1.fos</i> cohorts.	137
3.30	BrdU-labelling of bi-genic ROCK/fos carcinogenesis.	139

3.31	IHC analysis for the GFP-tagged ROCK ^{er} transgene and p-Mypt1 of ROCK substrate.	144
3.32	Phenotypes of <i>K14.cre/Isl.ROCK^{er}/Δ5PTEN^{flx}</i> and <i>K14.cre/Δ5PTEN^{flx}</i> mice at 27 weeks treatment.	146
3.33	Histotype of <i>K14.cre/Isl.ROCK^{er}/Δ5PTEN^{flx}</i> and <i>K14.cre/Δ5PTEN^{flx}</i> mice at 27 weeks.	148
3.34	Immunofluorescence analysis of K1/K14 and K6/K14 expression at 27 weeks of 4-HT treatment.	150
3.35	IHC analyses of p53 and p21 in RU486-/4-HT-treated <i>K14.cre/Isl.ROCK^{er}/Δ5PTEN^{flx}</i> papillomatous hyperplasia.	153
3.36	Immunofluorescence analysis of p-AKT1 in RU486-/4-HT-treated <i>K14.cre/Isl.ROCK^{er}/Δ5PTEN^{flx}</i> folded hyperplasia.	154
3.37	BrdU-labelling of bi-genic ROCK/Δ5PTEN ^{flx} carcinogenesis.	156
3.38	Morphology of primary <i>K14.cre/Isl.ROCK^{er}</i> keratinocytes in media containing different calcium concentrations.	160
3.39	Morphology of <i>K14.cre/Isl.ROCK^{er}/HK1.fos</i> mouse keratinocytes in media containing different calcium concentrations.	162
3.40	Morphology of <i>K14.cre/Isl.ROCK^{er}/Δ5PTEN^{flx}</i> mouse keratinocytes in media containing different calcium concentrations.	163
3.41	Morphology of primary <i>K14.cre/Isl.ROCK^{er}/HK1.ras¹²⁷⁶</i> mouse keratinocytes.	165
3.42	<i>K14.cre/Isl.ROCK^{er}</i> is activated after RU486-/4-HT treatment.	167
3.43	Western analysis of K1 and K6 differentiation marker expression in primary keratinocytes.	171
3.44	Phenotypes of <i>K14.cre/Isl.ROCK^{er}/ras¹²⁷⁶/fos</i> transgenic mice at 13 weeks.	177
3.45	Histopathology of <i>K14.cre/Isl.ROCK^{er}/ras¹²⁷⁶/fos</i> and	179

	<i>HK1.ras¹²⁷⁶/fos</i> tumours at 13 weeks.	
3.46	IFC analysis of K1/K14 and K6/K14 expression in RU486-/4-HT-treated <i>K14.cre/Isl.ROCK^{er}/ras¹²⁷⁶/fos</i> tumours at 13 weeks.	181
3.47	IHC analysis of p53 expression in malignant RU486-/4-HT-treated <i>K14.cre/Isl.ROCK^{er}/ras¹²⁷⁶/fos</i> histotypes.	183
3.48	IHC Analysis of p21 expression in RU486-/4-HT-treated <i>K14.cre/Isl.ROCK^{er}/ras¹²⁷⁶/fos</i> malignant histotypes.	185
3.49	Immunofluorescence analysis of p-AKT1 expression in RU486-/4-HT-treated <i>K14.cre/Isl.ROCK^{er}/ras¹²⁷⁶/fos</i> malignant histotypes.	187
3.50	BrdU-labelling of tri-genic <i>ROCK/ras¹²⁷⁶/fos</i> carcinogenesis.	189
3.51	Phenotypes of <i>K14.cre/Isl.ROCK^{er}/fos/Δ5PTEN^{flx}</i> transgenic mice at approximately 9 weeks.	194
3.52	Histotypes of <i>K14.cre/Isl.ROCK^{er}/fos/Δ5PTEN^{flx}</i> biopsies at 9 weeks.	197
3.53	Immunofluorescence analysis of K1/K14 and K6/K14 expression in <i>K14.cre/Isl.ROCK^{er}/fos/Δ5PTEN^{flx}</i> carcinogenesis.	200
3.54	Immunofluorescence analysis of filaggrin/K14 expression in RU486-/4-HT-treated <i>K14.cre/Isl.ROCK^{er}/fos/Δ5PTEN^{flx}</i> tumours.	203
3.55	Immunofluorescence analysis of loricrin/K14 expression in RU486-/4-HT-treated <i>K14.cre/Isl.ROCK^{er}/fos/Δ5PTEN^{flx}</i> tumours.	205
3.56	IHC analysis of p53 expression in RU486-/4-HT-treated <i>K14.cre/Isl.ROCK^{er}/fos/Δ5PTEN^{flx}</i> tumours.	207
3.57	IHC analysis of p21 expression in RU486-/4-HT-treated <i>K14.cre/Isl.ROCK^{er}/fos/Δ5PTEN^{flx}</i> tumours.	209
3.58	BrdU-labelling of RU486-/4-HT-treated	211

	<i>K14.cre/Isl.ROCK^{er}/fos/Δ5PTEN^{flx}</i> carcinogenesis.	
3.59	Immunofluorescence analysis of p-AKT1 expression.	213
3.60	Phenotypes of <i>K14.cre/Isl.ROCK^{er}/ras¹²⁷⁶/Δ5PTEN^{flx}</i> transgenic mice at 22 weeks.	219
3.61	Histotypes of RU486-/4-HT-treated <i>K14.cre/Isl.ROCK^{er}/ras¹²⁷⁶/Δ5PTEN^{flx}</i> biopsies at 22 weeks.	221
3.62	Immunofluorescence analysis of K1/K14 expression at 22 weeks.	223
3.63	IHC analysis of p53 expression.	225
3.64	IHC analysis of p21 expression.	227
3.65	BrdU-labelling of <i>K14.cre/Isl.ROCK^{er}/ras¹²⁷⁶/Δ5PTEN^{flx}</i> carcinogenesis.	229
3.66	Immunofluorescence analysis of p-AKT1 expression in RU486-/4-HT-treated <i>K14.cre/Isl.ROCK^{er}/ras¹²⁷⁶/Δ5PTEN^{flx}</i> tumours.	232
3.67	Rapid tumourigenesis developed in <i>K14.ROCK^{er}/HK1.ras¹²⁰⁵/Δ5PTEN^{het}</i> transgenic mice.	235
3.68	Histotypes of RU486-/4-HT-treated <i>K14.ROCK^{er}/HK1.ras¹²⁰⁵/Δ5PTEN^{het}</i> biopsies at 6 weeks.	237
3.69	Histotypes of RU486-/4-HT-treated <i>K14.ROCK^{er}/HK1.ras¹²⁰⁵/Δ5PTEN^{het}</i> biopsies at 6 weeks.	238
3.70	IHC analysis of p53 expression in <i>K14.ROCK^{er}/HK1.ras¹²⁰⁵/Δ5PTEN^{het}</i> carcinogenesis.	240
3.71	IHC analysis of p21 expression in <i>K14.ROCK^{er}/HK1.ras¹²⁰⁵/Δ5PTEN^{het}</i> carcinogenesis.	241
3.72	Immunofluorescence analysis of p-AKT1 and keratin K1 expression in <i>K14.ROCK^{er}/HK1.ras¹²⁰⁵/Δ5PTEN^{het}</i> carcinogenesis.	243

Appendix

A	Cell lines of primary keratinocytes	282
B	Abstract/Publication	283
C	Personal licence holder training record.	284

Acknowledgement

I would like to offer my appreciations and gratitude to Dr. David A. Greenhalgh, my main supervisor and Prof. Dr. Michael F. Olson, my co-supervisor who have guided and taught me uncountable precious knowledge and life lessons along the journey of my PhD. My utmost gratitude goes to the Ministry of Higher Education Malaysia and Universiti Kebangsaan Malaysia for the financial support throughout my PhD and also Scott Endowment for Dermatology Research.

I would like to acknowledge Dr. Jean Quinn for her thoughtful advice, Dennis Duggan (Animal Centre) for his continuous help in animal husbandry and Nicola Rath (Beatson Cancer Research Institute) for her assistance with western analysis.

Finally, I would like to express my gratitude to my parents, Zainon Suratman and Masre Jaafar. Thank you for their unceasing encouragement and patience over the past few years and make my PhD journey endurable.

Author's declaration

I declare that this thesis is the result of my own work.

Siti Fathiah Masre
1107578M

Abbreviations

4-HT	4-hdroxytamoxifen
BSA	Bovine serum albumin
BrdU	5-Bromo-2-deoxyuridine
Cre	Cyclisation recombination gene of bacteriophage P1
DAB	3,3'-Diaminobenzidine
DMBA	Dimethylbenzanthracene
DMEM	Dulbecco's modified eagle medium
DNA	Deoxyribonucleic acid
dNTPs	Deoxynucleotide Triphosphates
g	Gram
EDTA	Ethylenediaminetetra-acetate
FCS	Fetal calf serum
GAP	GTPase Activating
GDP	Guanine diphosphate
GEF	Guanine-nucleotide exchange factor
GFP	Green Fluorescent Protein
GSK3 β	Glycogen synthase kinase beta

GTP	Guanine triphosphate
H&E	Hematoxylin and eosin
HCL	Hydrochloric acid
HK1.ras	Transgenic mice expressing v-rasHa from a modified human keratin K1 vector
IFC	Immunofluorescent
IHC	Immunohistochemistry
LIMK	Lim kinase
MAPK	Mitogen activated protein kinase
µg	microgram
mg	milligram
µl	microlitre
ml	millilitre
MLC	Myosin light chain
NFκβ	Nuclear factor kappa-light-chain-enhancer of activated B cells
PBS	Phosphate buffered saline
PCR	Polymerase chain reaction
pdSCC	Poorly differentiated squamous cell carcinoma
p53	Protein 53

PI3K	Phosphatidylinositol 3-kinase
PIP3	Phosphatidylinositol 3,4,5-triphosphate
pMYPT	phospho-myophos
PTEN	Protein phosphatase and tensin homologue
ROCK	Rho kinase
SCC	Squamous cell carcinoma
SDS	Sodium dodecyl sulphate
SDS-PAGE	SDS polyacrylamide gel electrophoresis
TBST	Tris-buffered saline and Tween20
TPA	12-O-tetradecanoylphorbol-13-acetate
TSG	Tumour suppressor gene
wdSCC	Well differentiated squamous cell carcinoma

Chapter 1 – Introduction

1.1 General introduction

Cancer is a disease that involves changes in the genetic alterations that transform normal cells into malignant derivatives (Hanahan and Weinberg, 2000, 2011). Carcinogenesis is not just the result of exposure to environmental carcinogens; it requires multiple stages involving many pathways before a tumour develops. Various irreversible genetic mutations that co-operate to disrupt normal homeostasis at several levels drive the mechanism of carcinogenesis. Initiating mutations can lead to pre-neoplastic lesions that can regress, persist or convert to malignancy and metastasis. However, the factors that determine whether a pre-neoplastic lesion converts to malignancy, remains benign or regresses are still unclear and will depend on tumour contexts created by each combination of specific mutations.

To investigate this complex process, the development of various *in vitro* and *in vivo* models has been greatly beneficial in cancer studies in allowing investigators to explore the underlying mechanisms of molecular carcinogenesis. To examine these complex mechanisms *in vivo*, transgenic mice expressing inducible transgenes have proved extremely valuable (Leder et al., 1986, Hanahan, 1988). Furthermore, a transgenic mouse skin model that combines the classic mouse skin cancer model with genetic engineering offers a useful approach to study molecular carcinogenesis. The mouse skin model has been widely utilised to explore many cancer theories and its use is beneficial in almost all areas of cancer biology and genetics (Brown et al., 1990, Greenhalgh et al., 1993a, Balmain and Yuspa, 2014).

It is through the use of such transgenic mouse skin models that the causally related mutations that drive stage-specific tumour progression can be tested either via gene over-expression or knockdown. Moreover, the mechanism of multistage tumourigenesis following the acquisition of subsequent mutations can be explored in these models. The development of transgenic mouse models for multistage carcinogenesis has been greatly enhanced by using the appropriate regulatory

element to target particular genes or genetic pathways in specific tissues in the context of the whole organism (Abate-Shen et al., 2008). Typically, transgenic mouse skin models employ keratin promoters to target proliferative and stem cell keratinocytes and the outcome of tumour phenotypes from transgenic mouse skin models enable assessment of particular molecular pathways for each stage of skin carcinogenesis: from hyperplasia through benign tumour formation and conversion to malignancy (Greenhalgh and Roop, 1994).

Genes that are involved in the formation of cancer fall into many different groups, but in brief they act as oncogenes or tumour suppressor genes. Oncogenes are cancer-causing and drive progression through each stage. For example: *ras*^{Ha} and *c-fos* are well known oncogenes where direct mutation or overexpression of the normal (proto-oncogene) protein has been linked to many cancers and as outlined below, their mutations have been shown to mimic the classic two stage mouse chemical carcinogenesis model (Greenhalgh et al., 1993a-c, Fernández-Medarde and Santos, 2011). On the other hand, tumour suppressor genes are cancer-preventing. Normally, they may inhibit tumour formation by one or more of mechanisms such as inhibiting cell proliferation and growth or accelerating differentiation or apoptosis. PTEN, p21 and p53 are classic examples of tumour suppressor genes that are most commonly mutated in cancer (Cooper, 2000).

Transgenic mouse skin models that express specific oncogenes or loss of tumour suppressor genes in the epidermis have been developed to study multistage carcinogenesis, or to investigate epidermal physiology in terms of growth regulation and terminal differentiation, failure of which are often associated with the signalling pathways and transcriptional events that drive cancer (Greenhalgh et al., 1993a-c, Dyke and Jacks, 2002, Yao et al., 2006, 2008, Macdonald et al., 2014). Therefore, by examining the key genes thought to be responsible for the driver mutations that cause tumours at each stage and investigating their co-operation; the results may be beneficial in identifying the specific stage at which mutations become active. These findings may help to design new drugs for therapies and provide the most appropriate animal models to stringently test them prior to clinical trials. The genes chosen for analysis in this study represent some of the most frequently mutated genes in human cancers that are normally responsible for regulating cell growth, apoptosis and homeostasis.

1.2 ROCK

This study investigates the role of ROCK2 in the multistage carcinogenesis model as it transpires that ROCK, an effector of the Rho family proteins RhoA and RhoC, plays an essential role in actomyosin contraction driving the elevation of cellular tension which affects tissue homeostasis and promotes tumour progression (Shimizu et al., 2003, Samuel et al., 2011). ROCK also has important roles in proliferation, differentiation, and cellular transformation (Olson, 2008). Moreover, in humans it has been shown that ROCK activation is involved in several types of cancer including lung, bladder and testicular (Kamai et al., 2003, Rath and Olson, 2012) and elevated expression of ROCK has most often been implicated in the late stages of carcinogenesis including invasion and metastasis. Therefore, studies targeting ROCK gene signalling may help to identify those genes involved in causing or preventing malignant conversion, as conversion to malignancy is one of the most significance clinical events from a clinician's view point.

1.2.1 ROCK: an overview

Rho-associated kinases (ROCK) are downstream effectors of RhoA and RhoC proteins, which are members of the Rho-GTPase family within the Ras superfamily, that help propagate signalling from external signals such as ligand-receptor interactions (Leung et al., 1995, Ishizaki et al., 1996). The three most well studied members of the Rho-GTPase family are: RhoA, Rac1, and CDC42; all of which play pivotal roles in regulation of the actin cytoskeleton network, cell morphology, cell proliferation, apoptosis and many other cellular functions (Rath and Olson, 2012, Pan et al., 2013) (figure 1.1). The signalling function of each of these Rho GTPases is activated by guanine nucleotide exchange factors (GEFs) and deactivated by GTPase-activating proteins (GAPs), thus switching between an inactive GDP-bound and an active GTP-bound protein complex (Rossman et al., 2005).

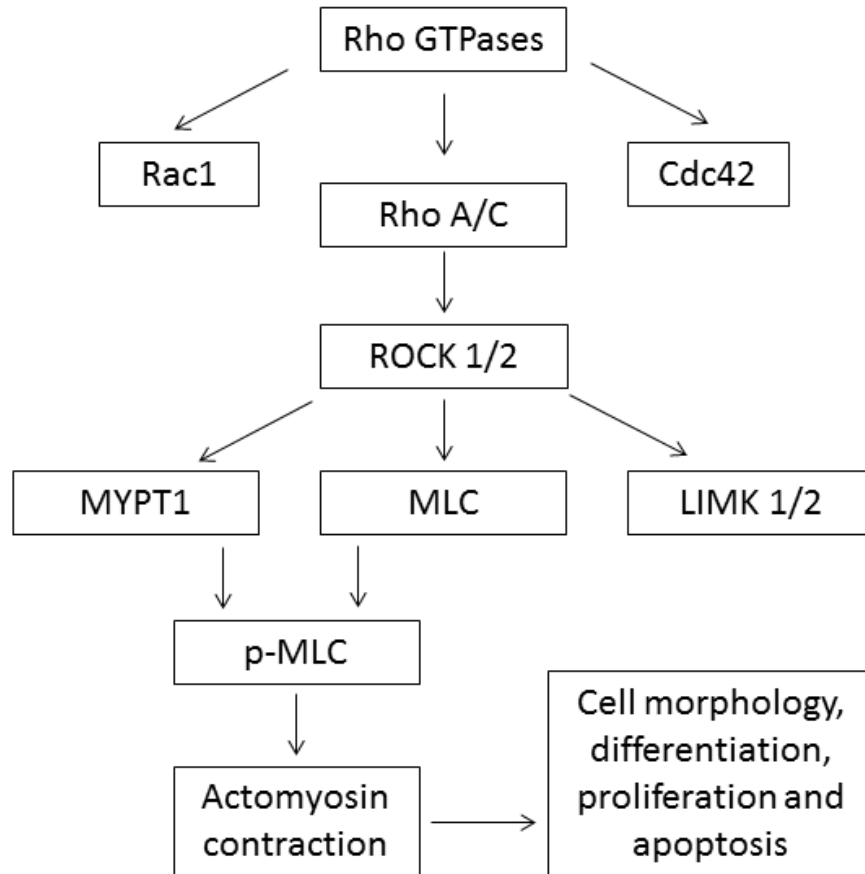


Figure 1.1 Rho/ROCK signalling pathway regulates cellular functions including actomyosin contraction, differentiation, proliferation and apoptosis. (Figure was modified from Rath and Olson, 2012).

ROCK2 was the first ROCK homologue identified as an effector of RhoA, encoding a 150-kDa protein (Leung et al., 1995). Following the finding of ROCK2 (also known as ROK α) (Leung et al., 1995), ROCK1 was later discovered (also known as ROK β) as a RhoA GTP-binding protein encoding a 160-kDa protein (Ishizaki et al., 1996). ROCK1 and ROCK2 are two homologues of Rho effector proteins that are well known to have roles in promotion of actin cytoskeleton contractility (Amano et al., 1996, Leung et al., 1996, Olson and Sahai, 2009). ROCK (1 and 2) generates its actomyosin contraction activity by mediating phosphorylation of several downstream targets including LIM kinases (LIMK 1 and 2), myosin light chain (MLC) and myosin binding subunit of myosin phosphatase (myosin phosphatase targeting protein) (Mypt1). Phosphorylation of LIMK results in inactivation of cofilin and this contributes to stabilisation of the actin filament (Wickman et al., 2010, Rath and Olson, 2012); whilst phosphorylation of MLC promotes actomyosin contraction and through phosphorylation of MYPT1, ROCK inhibits the dephosphorylation of MLC. Thus, the net effect of MLC phosphorylation is actomyosin contraction (Wickman et al., 2010), which develops stress fibers and focal adhesion formation. This in turn leads to increased cellular tension that influences cell morphology and cell movement which consequently contributes to a wide variety of events in cancer (Samuel et al., 2011) (figure 1.1).

ROCK is also involved in numerous other cellular activities including cell proliferation and differentiation (Rath and Olson, 2012); these seemingly contrasting observations may depend upon the experimental conditions and /or cell type under study. Pirone et al., (2006) have shown that ROCK-mediated actomyosin contraction could promote cell proliferation activity in bovine pulmonary artery endothelial cells. In epidermal keratinocytes, specific knockdown of ROCK2 expression in cultured human keratinocytes led to inhibition of terminal differentiation whereas depletion of ROCK1 expression induced terminal differentiation (Lock and Hotchin, 2009). Conditional ROCK2 activation in keratinocytes induced terminal differentiation and induced expression of differentiation markers (McMullan et al., 2003). Taken together, these studies have reported important roles for ROCK in regulating keratinocyte differentiation and proliferation. Thus, as a consequence, deregulation of ROCK activity which contributes to changes in normal keratinocyte physiology may lead to cancer formation. The questions these observations raise include: at what stage do these

ROCK2 changes become important, and what genes are collaborators or inhibitors?

Previous studies indicated the involvement of ROCK activity in cancer formation in several ways (Wickman et al., 2010). ROCK activity was reported to be elevated during tumour invasion and metastasis, suggesting a role in the later stages of the disease consistent with its role in cell migration (Croft et al., 2004, Pan et al., 2013). Furthermore, studies of ROCK inhibition demonstrated that potent ROCK inhibitors were able to suppress K-Ras driven lung tumour growth, suggesting that it may be a therapeutic target for Ras-induced cancers (Rath and Olson, 2012) which so far have not been successfully treated (Castellano and Downward, 2011).

1.2.2 The structure of ROCK

ROCK kinases are serine/threonine protein kinases first discovered to act as downstream effectors of Rho proteins (Leung et al., 1995, Nakagawa et al., 1996). There are two ROCK homologues called ROCK1 (ROCK β) and ROCK2 (ROCK α) (Rath and Olson, 2012). Both share about 90% identities in the kinase domains (Amano et al., 2000, Mueller et al., 2005). ROCK is most closely homologous to members of the AGC kinase group, such as myotonic dystrophy protein kinase (DMPK) (Riento and Ridley, 2003), myotonic dystrophy kinase-related Cdc42-binding kinase (MRCK) (Wilkinson et al., 2005) and citron kinase (Yamashiro et al., 2003). Generally, these kinases share homologous catalytic domains located at the amino terminus that phosphorylate several of the same substrates (Mueller et al., 2005, Wickman et al., 2010). In both ROCK1 and ROCK2, the amino terminus is followed by a coiled-coil region containing the Rho binding domain (RBD), and a pleckstrin homology region with an internal cysteine-rich domain (CRD) in the carboxyl terminus (Riento and Ridley, 2003, Mueller et al., 2005) (figure 1.2).

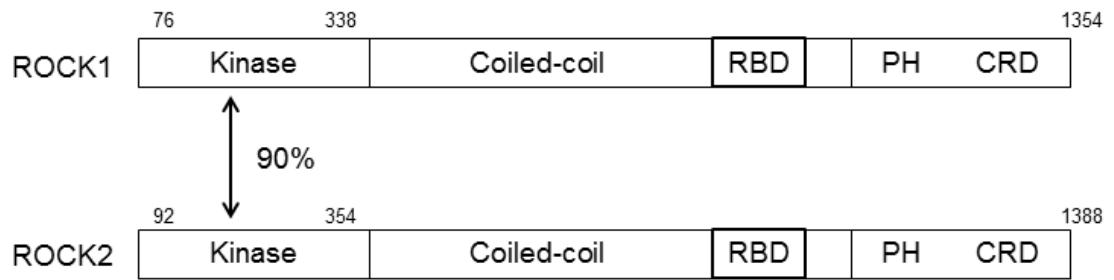


Figure 1.2 Structure of ROCK (1 and 2). ROCK 1 and 2 have approximately 90% identity in kinase domain. Both ROCK 1 and 2 have a coiled-coil region containing rho binding domain (RBD) and followed by a pleckstrin homology (PH) region with an internal cysteine-rich domain (CRD) in the carboxyl terminus (Figure modified from Mueller et al., 2005).

Despite the high homology between ROCK1 and ROCK2 protein sequences, there is a striking difference in the tissue distribution of each isoform (Nakagawa et al., 1996, Mueller et al., 2005). ROCK1 is enriched in liver, spleen, kidney and testis; while ROCK2 is preferentially expressed in brain and muscle (Nakagawa et al., 1996). Moreover, previous studies have shown that ROCK2 is localised in the cytoplasm and cell membrane, with the majority expressed in the cytoplasmic area (Leung et al., 1995, Riento and Ridley, 2003). In terms of the skin, it has been demonstrated that ROCK2 rather than ROCK1 plays a significant role in keratinocyte differentiation (Lock and Hotchin, 2009); and as shown below, ROCK may be integral to the strength of the spinous layer as this is where a broad cytoskeletal network of intermediate keratin filaments is constructed (Fuchs, 1990) alongside that of the actomyosin cytoskeleton. This would be a logical facet to a molecule associated with tensile strength in a tissue associated with a major barrier function.

It has been postulated that ROCK is maintained in an inactive state by its carboxyl terminus region which forms an auto-inhibitory loop by binding directly to the catalytic kinase domain (Mueller et al., 2005). Thus, binding of active GTP-bound Rho to the RBD in the coiled-coiled region of ROCK disrupts this auto-inhibitory structure and results in increased kinase activity (Pan et al., 2013) (figure 1.3a). In addition, some lipids, particularly arachidonic acid, can activate chicken gizzard smooth muscle ROCK2 approximately 5-6-fold *in vitro*, independent of RhoA. This finding demonstrates that lipid activation may be an alternative ROCK activator in smooth muscle cells (Feng et al., 1999, Miyazaki et al., 2006).

During apoptosis, ROCK can be activated by granzym B (for ROCK2) or by caspase 3 (for ROCK1) through cleavage of the carboxyl-terminal region (Riento and Ridley, 2003) adding greater complexity to ROCK signalling (figure 1.3b). While some GTP-binding proteins act as positive regulators of ROCK as shown for RhoA, RhoB and RhoC, other GTP-binding proteins, like RhoE, Gem (in the case of ROCK1) and Rad (in the case of ROCK2), inactivate ROCKs by binding to sites distinct from the RBD (Olson, 2008, Rath and Olson, 2012).

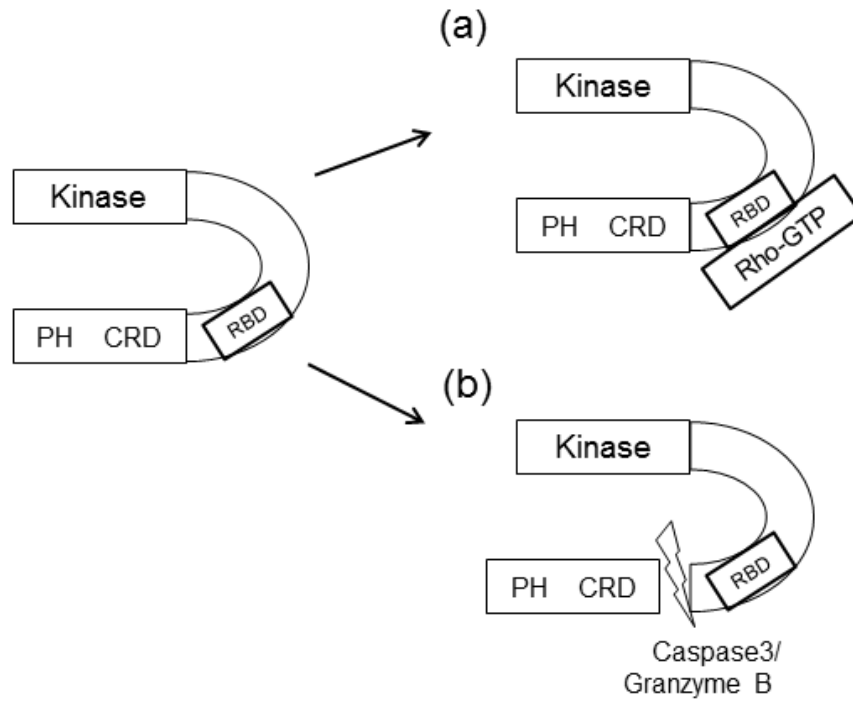


Figure 1.3 Activation of ROCK. The carboxyl terminus of ROCK forms an auto-inhibitory loop to maintain ROCK in an inactive state. (a) Upon binding of Rho-GTP to RBD, it disrupts the auto-inhibitory loop structure and results in the activation of kinase. (b) ROCK can also be activated by granzyme B (for ROCK2) or caspase 3 (for ROCK1) through cleavage of the carboxyl-terminal region. (Figure modified from Julian and Olson, 2014).

1.2.3 ROCK and cancer

Extensive research has been conducted into the association between ROCK expression and cancer (Horiuchi et al., 2008, Routhier et al., 2010) in relation to changes in cell shape and motility. As outlined above, many studies have demonstrated the role of ROCK as an essential regulator for actomyosin contraction (Riento and Ridley, 2003, Kumper and Marshall, 2011). This ROCK-mediated increase in actomyosin contraction leading to increased cellular tension has been shown to promote tumour progression (Samuel et al., 2011) with ROCK expression associated with the later stages of tumour progression to an invasive and metastatic phenotype (Croft et al., 2004, Wickman et al., 2010). In addition to elevated ROCK expression, it was shown that increased levels of Rho proteins, may also be associated with late cancer events (Croft et al., 2004). For example, RhoA over-expression could promote cell invasion contributing to cancer progression (Yoshioka et al., 1999). Collectively, this suggests that ROCK activation acts in later events during tumourigenesis which is consistent with its roles associated with the cytoskeleton and cell movement.

Increased cellular tension influences subsequent changes in cellular structure including cell-cell adhesion and extracellular matrix (ECM) remodelling leading to elevated tissue stiffness (DuFort et al., 2011, Samuel et al., 2011). Stiffness contributes to tumour formation via deposition and changes in ECM components such as collagen, which can also upregulate signal transduction pathways that eventually drive tumour formation and cell proliferation (Kumper and Marshall, 2011, Samuel et al., 2011). Moreover, increased tissue stiffness has been implicated in changes to cell shape (DuFort et al., 2011) which may also trigger the activation of pathways including Rho-ROCK signalling that fuel the remodelling of the actin cytoskeleton (Samuel et al., 2011, Rath and Olson, 2012).

Inhibition of ROCK proteins has the potential to become an Achilles heel for MAPK signalling as it acts as an effector downstream of ras (Castellano and Downward, 2011). As ras inhibitors have not yet proved successful, inhibition of ROCK is a potential alternative therapeutic approach to reduce tumour development (Olson, 2008, Rath and Olson, 2012, Morgan-Fisher et al., 2013). Previous studies have reported successful application of ROCK inhibitors to suppress tumour growth

using *in vivo* and *in vitro* models (Patel et al., 2012, Zhang et al., 2012), yet there is no ROCK inhibitor that has been clinically established for cancer therapy (Morgan-Fisher et al., 2013). Furthermore, most studies have indicated important roles for ROCK in promoting invasion and metastasis which are involved in the later stages of cancer (Croft et al., 2004, Samuel et al., 2011), suggesting that inhibiting ROCK at these stages would be the most likely scenario to be of benefit. However, whether ROCK can also promote early stages of cancer is still unclear (Morgan-Fisher et al., 2013) hence, model studies of ROCK pathway activation may highlight new targets in the mechanisms driving carcinogenesis.

In one such study involving ROCK2 transgenic mice (*K14.ROCK^{er}*), ROCK activation significantly influenced tumour formation and progression to invasive carcinomas in a two stage chemical carcinogenesis skin cancer model. Conversely, application of ROCK inhibitor Y27632 led to reductions in tumour growth and conversion (Samuel et al., 2011). However, the two-stage chemical carcinogenesis protocol induces many unknown mutations and there is little clear indication of which genes directly co-operate with one another. Nevertheless, this study implicates an important consequence of ROCK activation in skin tumour formation and provides an opportunity to assess ROCK activation in co-operation with other genes in classic mouse skin carcinogenesis.

Experiments in this study have included two models that targeting ROCK2 activation: *K14.ROCK^{er}* (Samuel et al., 2009a) and *Isl.ROCK^{er}* transgenic mice. In order to assess the stage-specific roles of ROCK2 activation in multistage skin carcinogenesis, both transgenic models (*K14.ROCK^{er}* (Samuel et al., 2009a) and *Isl.ROCK^{er}*) consist of a conditionally-active human ROCK2 kinase domain with part of the coiled-coil region fused to the estrogen receptor (ER) hormone binding domain at the carboxyl terminus and enhanced green fluorescent protein (GFP) at the amino terminus (Croft and Olson, 2006) (figure 1.4). Although this ROCK2^{er} fusion protein doesn't have all the domains at the carboxyl terminus including the pleckstrin homology domain which modulates membrane localisation of ROCK, it does reflect the consequences of increased actomyosin contraction (per communication with Olson). Both ROCK1 and ROCK2 are expressed in keratinocytes with ROCK2 being more predominant (McMullan et al., 2003). By exchanging RBD in ROCK2 with the ER, the model is conditionally activated by 4-HT via the K14 promoter, conditionally-active ROCK2 can be selectively

expressed in the proliferative basal layers. As shown in a previous study by Samuel et al., (2009a), ROCK2^{er} transgene was expressed on the superficial cell layer of embryoid bodies through GFP staining, consistent with the K14-driven specific expression. Activated ROCK2^{er} was also expressed throughout the epidermal layers, including hair follicles of *K14.ROCK^{er}* mouse skin as demonstrated by phosphorylated Mypt1 expression, again, consistent to the area targeted by K14 promoter (Samuel et al., 2011). The new unpublished *Isl.ROCK^{er}* transgenic model employs the same ROCK transgene but it is now placed downstream of a loxP flanked stop codon and is driven by a general CAG-promoter. This *Isl.ROCK^{er}* model requires cre recombinase to evict the stop cassette located between loxP sites. Thus, mating with K14.creP mice (K14 promoter) (Berton et al., 2000b) is required to achieve tissue specificity on the proliferative basal layers and follicles.

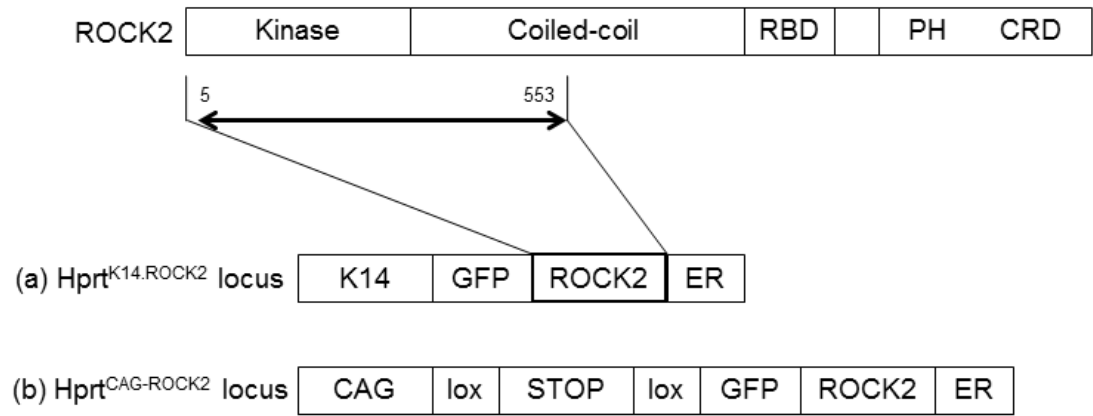


Figure 1.4 Schematic diagrams of (a) $K14.ROCK2^{ef}$ and (b) $Isl.ROCK2^{ef}$ transgenic mice. (Figure modified from Croft and Olson, 2006).

1.3 Models of multistage skin carcinogenesis

1.3.1 Epidermal physiology

Prior to exploring the use of transgenic mouse models for skin carcinogenesis, it is essential to understand the overall physiology of the epidermis including its organisation, structure and cell types as each has the potential to influence cancer formation. It is worth remembering that the primary function of the epidermis is to act as a barrier, hence it is logical to consider the contribution of ROCK-mediated signalling to the tensile strength and integrity of the epidermis which may be a latent problem that later contributes to cancer progression via increased tissue stiffness. Since the transgenic mouse models employed in this study are primarily geared to test the roles of genes in cancer; they are equally valid to investigate an interrelationship between keratinocyte proliferation and differentiation during normal epidermal functions. By understanding these key aspects of epidermal physiology, the changes induced by alteration of the normal proliferation and differentiation pathways will facilitate the diagnostic analysis of pre-malignant and malignant tumours.

The epidermis forms the outer layer of the skin and mainly consists of keratinocytes which are organised into four main layers or compartments: basal layer, spinous layer, granular layer and cornified layer (Alonso and Fuchs, 2003, Fuchs, 2008) (figure 1.5). It should be noted that in mice, and most animals covered in fur, the epidermis is seldom more than one layer thick. The exceptions to this are the ear and neonatal epidermis, which is naturally hyperplastic until hair follicles form at day 3 to 4, then the epidermis thins out and remains constant (Sundberg, 2004) hence, 24 to 48 hour neonates are used to derive keratinocytes for culture). The basal layer contains cells which are attached to an epidermal basement membrane. This layer consist of occasional interfollicular epidermal stem cells but mainly proliferating transit amplifying cells (Alonso and Fuchs, 2003). Typically these proliferative basal layer keratinocytes express keratins K5 and K14 (Yuspa et al., 1989, Yuspa, 1994), whilst the majority of pluripotent stem cells reside in the hair follicle bulge region and express markers such as K15 and K17. The hair follicles also typically express keratin K6, a keratin marker which is expressed in wounded or hyperproliferative epidermis (Rothnagel et al., 1999) or

at time of stress, such as overexpression of TGF β in transgenic mouse epidermis (Sellheyer et al., 1993, Akhurst and Hata, 2012). As basal cells commit to differentiate and move from the basement membrane toward the spinous layer, they lose proliferative capability and express early differentiation markers such as K1 and K10 (Yuspa et al., 1989, Yuspa, 1994). It is these cells of the spinous layer that gain adaptability to mechanical stress that provides the epidermis with its tensile strength by strengthening their cytoskeletal filaments and cell-cell connections via e.g. adherent junctions, a process influenced by ROCK isoforms (Amano et al., 1997, Amano et al., 2000). As differentiation progresses, spinous cells migrate into the granular layer and express late stage terminal differentiation markers including loricrin, filaggrin and keratinocyte transglutaminase (Yuspa, 1994) and these differentiation associated genes are regulated by AP1 (DiSepio et al., 1995), hence the interest in developing the original fos transgenic mice.

Cells of the granular layer subsequently form the cornified envelope by cross linking proteins including filaggrin and loricin mediated by transglutaminase. Granular cells also produce lamellar granules containing lipids which attach to proteins of the cornified envelope to offer a water-resistant seal for epidermal water barrier function (Kalinin et al., 2002, Alonso and Fuchs, 2003, Candi et al., 2005). Upon progression to the last stages of terminal differentiation, granular cells undergo the final processes of cornification producing the outermost layer of epidermis called the cornified layer (Alonso and Fuchs, 2003, Candi et al., 2005), again a feature regulated by c-fos (Fisher et al., 1991). Of significant importance to *in vitro* studies, this epidermal differentiation programme is regulated in part by an epidermal gradient of calcium (Ca²⁺). This Ca²⁺ ion concentration gradually increases from low concentrations in the basal layer, increases in the spinous layer to high concentrations of Ca²⁺ in the granular layer (Hennings et al., 1980) and this can be mimicked *in vitro* to both grow and induce the terminal differentiation of primary keratinocytes and some keratinocyte cell lines (Hennings et al., 1980, Greenhalgh et al., 1989). Further resistance to this differentiation switch can be employed to test keratinocyte transformation (Greenhalgh et al., 1989, Morgan et al., 1992).

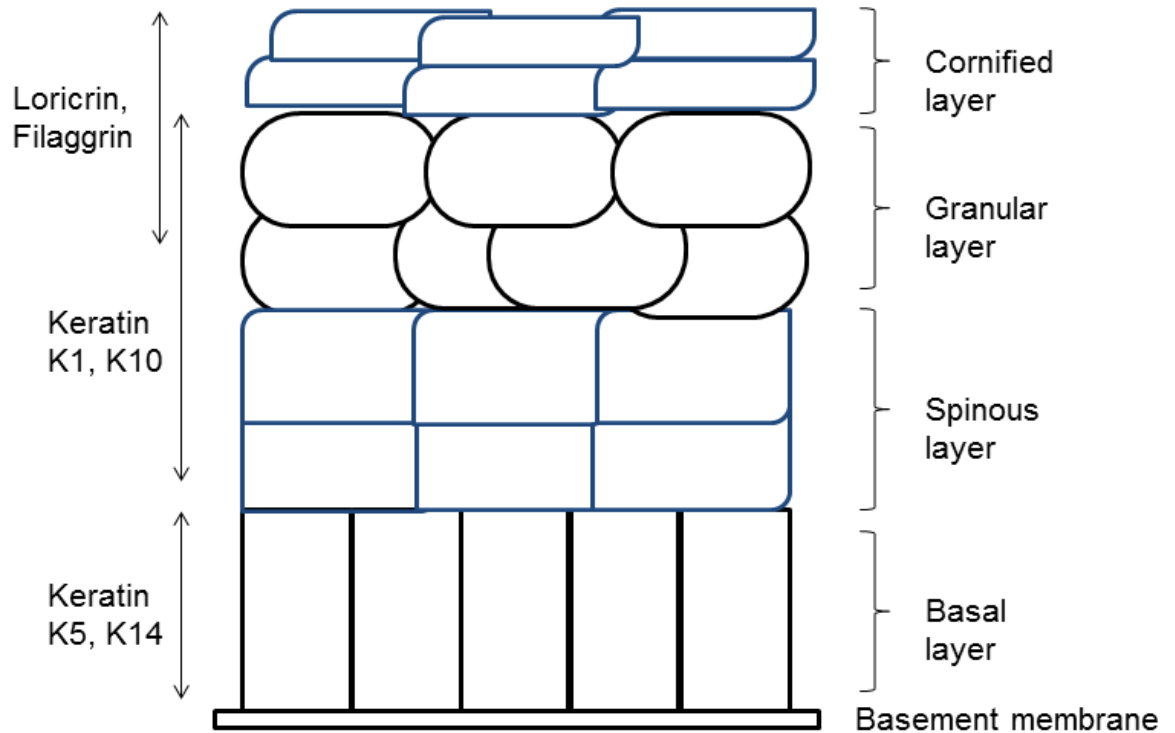


Figure 1.5 Schematic diagram of a typical stratified normal epidermis and typical markers associated with terminal differentiation through each layer. Keratin K5 and K14 indicate the proliferative compartment; K1 and K10 are early differentiation markers expressed as keratinocytes commit to differentiation and leave the basal layer and, loricrin and filaggrin are late stage markers. Omitted from this diagram is keratin K6 which is normally expressed in hair follicles and is expressed in all layers indicating anomalous pre-neoplastic hyperplasia or epidermal stress.

1.3.2 The classic mouse skin model of chemical carcinogenesis

One of the most successful *in vivo* models used to study molecular carcinogenesis over the last 100 years has been the mouse skin model of two-stage chemical carcinogenesis (Yuspa et al., 1991). This two-stage chemical carcinogenesis protocol was amongst the first to define the stages of initiation, through promotion to a benign tumour, and later malignant conversion or progression (figure 1.6). The model employs many regimes involving chemicals which possess initiating activity, activity associated with promotion or with both initiation and promotion activities (Yuspa, 1994). The most common treatment regime typically involves the application of a mutagen such as 7, 12-dimethyl-benzanthracene (DMBA), which at low level doses provides an initiation step that leads to irreversible DNA damage, such as mutation at codon 61 of the ras^{Ha} gene (Balmain, 1985, Roop et al., 1986) but at this low level dose, tumour formation requires promotion. Promotion can happen immediately or up to one year later, thus demonstrating that these cells are most likely the cancer stem cell targets (Yuspa, 1998).

The initiated cell populations are expanded by tumour promoters, such as weekly application of 12-O-Tetradecanoylphorbol-13-acetate (TPA) and this treatment regime can continue for up to 60 weeks. TPA is the classic promoting agent typically employed and activates numerous pathways including c-fos signalling in the AP-1 complex (Greenhalgh and Yuspa, 1988, Greenhalgh et al., 1990). The combined effect of (DMBA) initiation and (TPA) promotion results initially in squamous cell papillomas that appear by 8 to 10 weeks and which can persist (TPA independent), regress (on cessation of TPA) and approximately 10 to 20% of these papillomas progress to carcinomas. Typically the papillomas that appear in the first 3 months are most likely to persist and convert (Hennings et al., 1993). However, such malignant conversion and papilloma number is also dependent on the doses of both initiator and promoter (Hennings et al., 1993, Yuspa, 1994, Abel et al., 2011) and their specific strengths to act as initiators or promoters. For example sunlight is a strong initiator but is a weak promoter (Brash et al., 1991).

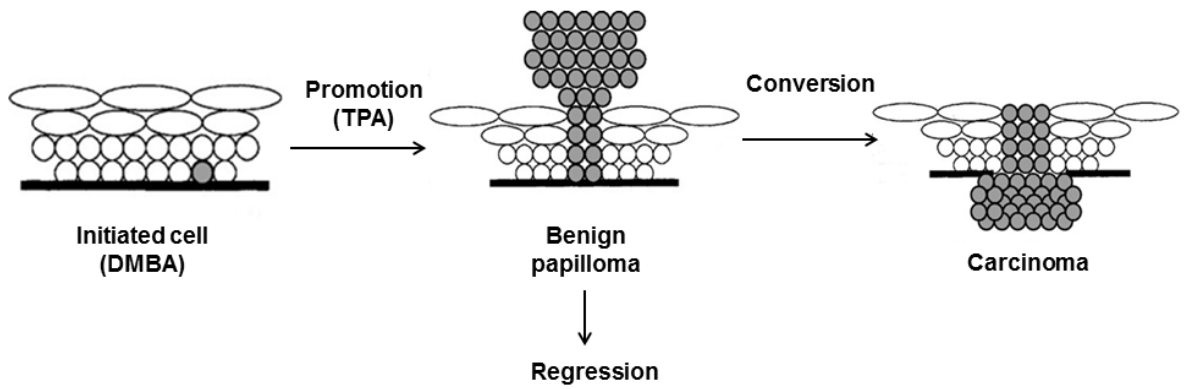


Figure 1.6 Classic mouse skin model of chemical carcinogenesis from DMBA initiation to TPA promotion leading to formation of benign papilloma that can persist, regress or convert to carcinoma.

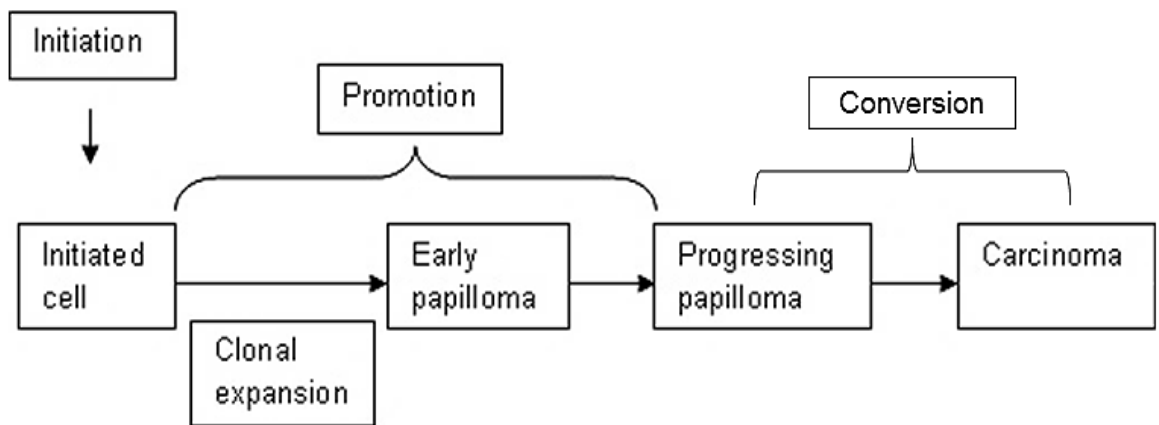


Figure 1.7 Operational stages of skin carcinogenesis. The initiated cell remains for the lifespan of the animal and thus could be considered a cancer stem cell; the early appearing papillomas are more prone to convert (like *ras/fos/PTEN*) while papillomas appearing later are more likely to be TPA dependent and regress on cessation of treatment. This model demonstrates the necessity for multiple genetic insults for malignant tumours to occur.

Figure 1.7 shows the operational stages of skin carcinogenesis which illustrates that multiple events are required for development of most cancers (Yuspa and Poirier, 1988, Yuspa, 1994). First, exposure to carcinogen (example: DMBA) induces the initiation stage which is irreversible and amongst the many genes that are mutated, the ras^{Ha} gene is most frequently activated with over 85% of papillomas expressing ras^{Ha} mutation at codon 61 (Balmain, 1985, Quintanilla et al., 1986). The stem cell unit in the bulge region of the hair follicle and in the proliferative basal layers are the key targets in this initiation stage (Morris, 2004).

The next stage involves promotion induced by promoters (example: TPA or wounding) where initiated cells expand, increase in proliferative activity in the basal layers leading to epidermal hyperplasia, observed skin thickening and benign tumour formation (Yuspa et al., 1982). These benign squamous papillomas may progress to squamous cell carcinoma (SCC) by additional mutation (Greenhalgh et al., 1990, Greenhalgh et al., 1993a-c, Yuspa et al., 1994). During keratinocytes begin to lose the ability to differentiate in an orderly fashion, alter their size and shape and begin to express keratins such as K6. Of note, and exploited throughout this study, is the reduction and eventual loss of expression of the early differentiation marker keratin K1 which is an indicator of malignant conversion and the degree of malignant progression achieved (Greenhalgh et al., 1993a-c, Slaga et al., 1995). This and other pathological markers such as loss of p53 and p21 tumour suppressor genes (TSGs) have been valuable in evaluating the tumour development, and appear to be good indicators of tumour progression into malignancy (Yao et al., 2006, Yao et al., 2008, Macdonald et al., 2014).

This classic DMBA/TPA two-stage chemical carcinogenesis protocol was previously used on ROCK transgenic mice and results showed increased malignant progression compared to controls (Samuel et al., 2011). However, while it was assumed to co-operate with ras^{Ha} activation in this model, many other mutations are induced by application of DMBA and single treatment without TPA to assess ROCK as a promoter in early stage carcinogenesis were not reported. Thus, whether ROCK activation could exert an earlier initiating role or later promoting role remained unclear and this has been investigated in this project; as the HK1 model was specifically designed to mimic this classic two-stage chemical carcinogenesis protocol. Furthermore, these studies directly assess ROCK activation together with the co-operating mutations implicated in the chemical

carcinogenesis mechanism such as ras and /or fos oncogene activation and then progress to assess inactivation of PTEN tumour suppressor gene regulation of AKT, and the roles played by p53/p21 in the unfolding mechanism.

1.3.3 The HK1 transgenic mouse model of skin carcinogenesis

The mechanism of carcinogenesis is driven by irreversible genetic mutations that cooperate to disrupt normal homeostasis. In skin carcinogenesis, initial mutations can lead to pre-neoplastic epidermal hyperplasia and pre-malignant benign squamous papillomas which can regress, persist or convert to malignancy and (rarely) eventually become metastatic (Balmain et al., 1984, Hennings et al., 1985). When coupled to the well-characterised mouse skin carcinogenesis models, transgenic mice that are designed to investigate particular gene expression or knockout, this presents a manageable approach to verify roles in each stage of carcinogenesis: initiation, promotion and malignant conversion. At the same time, pathways that help inhibit or induce carcinogenesis in responses to these specific driving mutations may be discovered through this model.

Here the epidermis is an attractive target tissue where genes are expressed through a variety of promoters given the understanding of epidermal differentiation. In addition, the use of an inducible system not only gives expression in specific tissues, but also at times designated by the investigator; such as in adulthood thus avoiding complications during embryogenesis or post-natal development. These inducible systems also facilitate gene expression at a particular stage of the cancer process and cessation of treatment with the inducing agent can also provide insight as to causality and oncogene dependence. The multistage nature of carcinogenesis in mouse skin presents as a pathology with easy accessibility to assist both observations on tumour progression and treatment with biological agents. Hence, the transgenic mouse skin model can be used to investigate various cancer hypotheses, identify the stage-specific causal factors and possibly provide a model system to aid in testing new drugs for the prevention and treatment of cancer.

Given that ras^{Ha} is the oncogene extensively activated following DMBA treatment (Balmain and Pragnell, 1983, Balmain et al., 1984, Roop et al., 1986), previous

transgenic mouse studies have mimicked the initiation steps of chemical carcinogenesis via the expression of activated proto-oncogene ras^{Ha} (*HK1.ras*). Numerous groups have expressed activated ras in the epidermis, by employing keratin promoters, to initiate carcinogenesis in transgenic mice and this often results in benign squamous papillomas which can lead to a rapid carcinogenesis or not depending upon the cell population targeted (Bremner and Balmain, 1990, Greenhalgh et al., 1993a-c). As detailed below, to mimic the second, promotion stage addition of e.g. $v-fos$ (*HK1.fos*) oncogene activation Greenhalgh et al., 1993c), can be employed given it is a major facet of TPA promotion (Schlingemann et al., 2003). It has already been shown to co-operate with ras^{Ha} oncogene activation in the transformation of primary keratinocytes and papilloma cell lines (Greenhalgh and Yuspa, 1988, Greenhalgh et al., 1990). In transgenic models ras/fos resulted in papillomas that persisted, but without spontaneous progression to malignancy (Greenhalgh et al., 1993c). This ras/fos co-operation makes it an ideal model to study the mechanism driving conversion of benign tumours; such as inactivation of AKT regulation via mutation of PTEN exon5 in transgenic *HK1.ras/fos/ Δ 5PTEN^{flx}* transgenic mice (Macdonald et al., 2014).

This HK1 transgenic mouse model of multistage skin carcinogenesis is summarised in figure 1.8 and depicts the classic stages of chemical skin carcinogenesis. The data from individual oncogene experiments are reviewed in detail below in each section, but in brief, the HK1 mouse skin model employs a truncated keratin K1 targeting vector (HK1) modified to specifically target the proliferative epidermal keratinocytes with activated ras^{Ha} and $v-fos$ expression to create *HK1.ras* and /or *HK1.fos* transgenic mice (Greenhalgh et al., 1993a-c). This model recapitulates each stage of skin carcinogenesis and has a unique feature in that progression through each stage requires another genetic event; e.g. co-expression of ras^{Ha} and fos elicited persistent papillomas without spontaneous conversion (Greenhalgh et al., 1993a-c), making these models ideal to assess conversion. Experiments in this study have included PTEN mutation (Yao et al., 2006, 2008) and the assessment of stage-specific roles for ROCK2 activation.

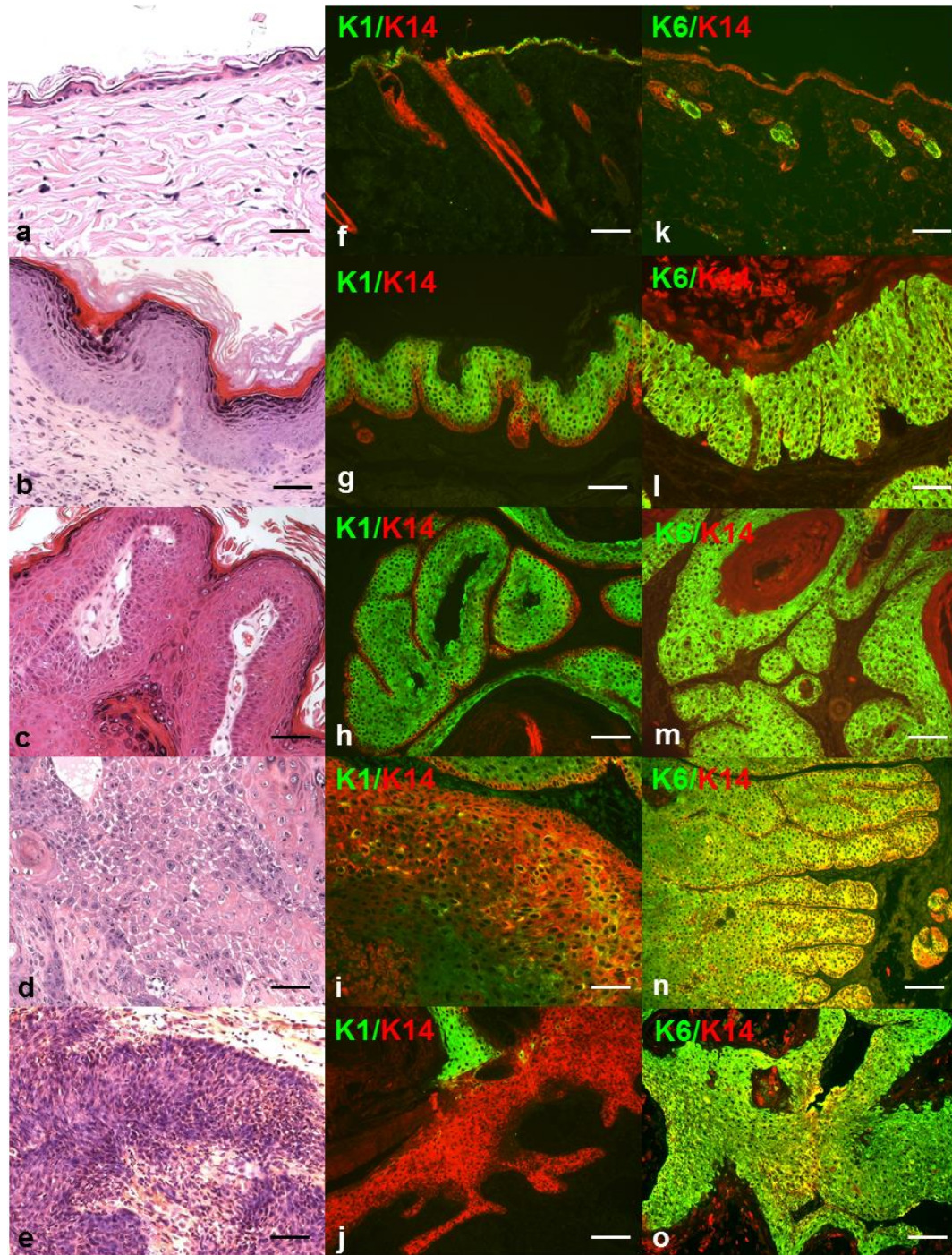


Figure 1.8 The histotype of typical tumour pathology and expression of tumour markers in multistage mouse skin carcinogenesis as typified by *HK1.ras/fos/Δ5PTEN^{flx}* transgenic mice.

This progress from (a) normal epidermis, to (b) epidermal hyperplasia, followed by (c) benign squamous cell papilloma and subsequent malignant conversion to (d) well-differentiated squamous cell carcinoma (wdSCC) then continued with further progression to (e) poorly-differentiated SCC (pdSCC).

IFC analysis of keratin K1 showed strong supra-basal expression from (f,g,h) normal to benign papilloma before K1 expression became reduced upon malignancy in (i) wdSCC and disappeared in (j) pdSCC. IFC analysis of keratin K6 showed (k) typical expression in hair follicles of normal epidermis, and (l-o) persistent expression throughout *HK1.ras/fos/Δ5PTEN^{flx}* carcinogenesis consistent with its association with excessive proliferation.

In addition, as detailed below throughout these experiments, keratin K1 an early marker of terminal differentiation, served as an excellent marker of tumour progression status (figure 1.8f-j); as during carcinogenesis, supra-basal K1 expression fades as benign papillomas convert to wdSCC and disappears in pdSCC by TPA promotion (figure 1.8f-j). Whilst keratin K6, a keratin that normally is expressed in hair follicles and also associated with excessive proliferation or epidermal stress, appeared persistently throughout carcinogenesis in these *HK1.ras/fos/Δ5PTEN^{fix}* transgenic mice (figure 1.8k-o). Collectively, this model supplies the ability to assess ROCK2 activation in both MAPK and PTEN/AKT signalling deregulation and to assess co-operation at each stage following the mechanism via p53/p21, AKT status and differentiation markers expression.

1.4 Targeting genes to the epidermis: A mimic of classic two stage DMBA/TPA mediated chemical carcinogenesis

One clear lesson from HK1 transgenic mice was that progression requires more than one oncogene; for example: ras^{Ha} requires promotion, fos required initiation and malignancy required additional events despite co-operation of two powerful oncogenes (v-ras^{Ha} and v-fos). Given the many studies on ROCK activation in carcinogenesis (Sahai and Marshall, 2003, Samuel et al., 2011), the stable phenotypes produced in the HK1 model presented an ideal opportunity to examine the causal relationship between ROCK signalling deregulation and *ras/fos/PTEN* tumorigenesis giving a valuable approach to understand the events that both drive or inhibit tumour formation.

One crucial step is the design of the transgenic mouse model that allows induction of a specific gene or expression in specific cell types. To study the mechanism of how ROCK2 activation is involved in multistage carcinogenesis, transgenic mice expressing tamoxifen-regulated, conditionally active ROCK2-estrogen receptor fusion transgene, under control of the keratin K14 promoter have been developed. These showed that deregulated ROCK2 expression in the basal layers induced keratinocyte hyperplasia, epidermal thickening and elevated collagen deposition (Samuel et al., 2009a, 2011, Rath and Olson, 2012). Studies using the classic two-

stage DMBA/TPA promotion suggested that ROCK2 deregulation was involved in the later stages increasing the number of carcinomas. Thus, investigation of ROCK activation in this HK1 transgenic mouse model will be used to identify partner genes in co-operative studies and examine ROCK2 deregulation in the earlier stages of tumour development and progression.

1.4.1 Targeting activated ras^{Ha} to the epidermis: A model of tumour initiation and papilloma formation

The ras gene family has three members: H-ras, K-ras and N-ras, that form a superfamily of membrane bound signalling systems; a molecule turnstile that takes external signalling from tyrosine kinase receptors such as epidermal growth factor (EGF) and transmits to downstream signalling pathways (Der et al., 1986, Bos, 1989, Kimmelman, 2015). The biological molecular turnstile activity of ras functions by swapping between active GTP-bound and inactive GDP-bound forms to switch binding on downstream effectors. Multiple downstream effectors are thus being stimulated by Ras-GTP (figure 1.8) and when mutated, it is permanently on and this deregulation of signalling contributes to tumourigenesis.

The activation of the ras/MAPK pathway that contributes to cell proliferation and sustains cell survival in combination with the activation of PTEN/AKT that increases proliferation and gives resistance to apoptosis, show the significant potential of both interacting pathways to drive malignant transformation (Chang et al., 2003, McCubrey et al., 2007, Macdonald et al., 2014); hence, the interest in adding the consequences of ROCK signalling and to assess the effects of cell rigidity and tissue stiffness on malignant conversion and invasion (Samuel et al., 2011, Rath and Olson, 2012).

It has been frequently reported that ras genes play a pivotal role in different types of tumours and are a causal factor in tumour development through specific point mutations at codons 12, 31 and 61 that activate ras oncogenes (Der et al., 1986, Karnoub and Weinberg, 2008). Moreover, ras genes also actively participate in carcinogenesis with almost 30% mutated ras being found in all types of human tumours (Baines et al., 2011). Ras genes were identified as critical intermediates located between receptor tyrosine kinases and downstream kinases (MAPK)

which channel their mitogenic signals to the nucleus leading to malignant transformation (Roberts and Der, 2007) (figure 1.9). In human skin cancer studies, it has been estimated that up to 50% of SCCs have been demonstrated to have a high occurrence of ras^{Ha} gene mutation at codon 12 in skin cancer derived from UV exposure (Pierceall et al., 1991). This ras^{Ha} mutation frequency depends mainly on latitude (Bos, 1989, Baines et al., 2011) and the skin type exposed to UV-B which acts as both initiator; e.g activating ras^{Ha}, inactivating p53 (Brash et al., 1991) and over subsequent years acts as a promoter which includes the role of UV-induced c-fos expression (Basset-Seguin et al., 1990).

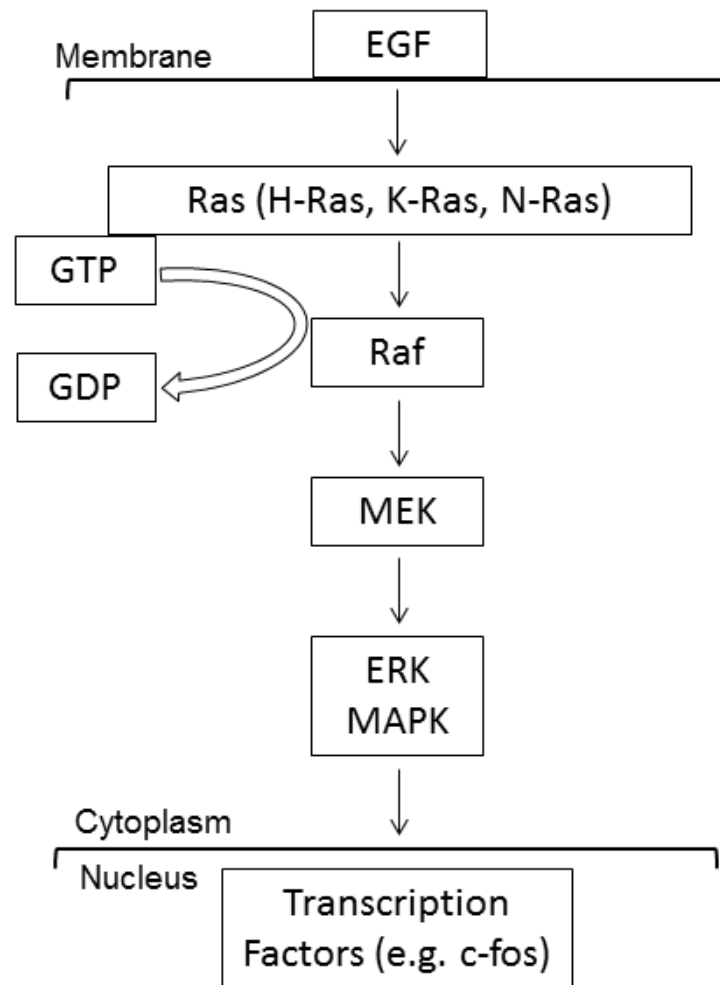


Figure 1.9 Schematic diagram of the structure of Ras/MAPK pathway. Tyrosine kinase receptors such as epidermal growth factor (EGF) channel external signalling to downstream pathway. Thus, GTP binds to Ras and becomes active followed by activation of Raf. Activated Raf leads to phosphorylation of MEK which activates MAPK (ERK). Activated MAPK enters the nucleus and activates transcription factors. (Figure modified from Roberts and Der, 2007).

In the classic DMBA-TPA mouse carcinogenesis models, ras^{Ha} gene mutation at codon 61 appears as a main target in more than 90% cases (Balmain and Pragnell, 1983, Balmain et al., 1984, Roop et al., 1986). This proved to be the initiation event as demonstrated by the transfection of primary keratinocytes with v-ras^{Ha} followed by grafting onto nude mouse skin which resulted in the formation of papillomas (Roop et al., 1986). Whilst ras activation was able to mimic the initiating event of chemical carcinogenesis, v-ras^{Ha} initiation required a promoting agent such as TPA or wounding at the graft site to give rise to benign papillomas (Brown et al., 1986). This grafted skin system also offered a co-operation approach to identify other genes in multistage skin carcinogenesis, typified by co-operation with *fos* when transfected into papilloma cell lines (Greenhalgh and Yuspa, 1988).

In order to study the role of ras^{Ha} activation, a transgenic mouse model was developed where activated v-ras^{Ha} was incorporated into a truncated human keratin K1 vector (HK1) to generate the *HK1.ras* transgene (Greenhalgh et al., 1993a). This truncated form of the keratin K1 gene was based on a 12kb EcoR1 clone that had lost several 3' control elements, later shown to be required for correct expression in terminal differentiation (Roop et al., 1987, DiSepio et al., 1995). This allows the HK1 vector to target gene expression exclusively in the epidermis from a late stage of embryo development (approximately day 19) and fortunately is expressed in 20 to 30% of the proliferative transit amplifying keratinocytes of the basal layers and importantly is still expressed following malignant conversion. In contrast, the endogenous mouse keratin K1 is lost during tumour progression and serves as a very useful marker for the degree of transformation achieved (Greenhalgh et al., 1993a-c).

HK1.ras transgenic mice initially presented with a phenotype of neonatal hyperplasia which resolved by day 10 and after that the adult mice were the same as their normal siblings. Two lines of *HK1.ras* mice have been maintained over the years: *HK1.ras*¹²⁰⁵ and *HK1.ras*¹²⁷⁶ (Greenhalgh et al., 1993a). While both lines exhibited identical neonatal phenotypes proving that their epidermis was initiated in adults, they presented very different and very useful alternate phenotypes in terms of tumour formation. This has been instrumental in the ability to make a multistage skin carcinogenesis model. The *HK1.ras*¹²⁰⁵ line formed benign squamous papillomas in 100% of animals that received a wound promotion

stimulus from ear tagging. This wound promotion stimulus was required and if the ear tag fell out, the papilloma regressed in a similar fashion to that observed in the two-stage chemical carcinogenesis model that required either continuous TPA promotion (Balmain et al., 1984) or the wounding associated with xenografts (Strickland et al., 1988) for tumour formation. Hence, these *HK1.ras*¹²⁰⁵ papillomas are considered to be regression prone. In contrast, and for reasons unknown, *HK1.ras*¹²⁷⁶ mice are not prone to developing papillomas in the absence of an additional hit (example: fos activation or PTEN mutation) but again uniquely and luckily, once papillomas developed; just as with *HK1.ras*¹²⁰⁵ papillomas, persistent tumours arising on a bi-genic 1276 background do not undergo spontaneous progression (Greenhalgh et al., 1993a,c, Yao et al., 2006).

As shown in figure 1.10(a), *HK1.ras*¹²⁰⁵ transgenic mice produced benign squamous papillomas at approximately 10 to 12 weeks of age and typically after ear tag wounding. In the absence of the ear tag, these mice only exhibited papillomas at sites of excessive scratching or bites. Also despite an initial wrinkly phenotype in neonates, adults appeared grossly normal, yet their epidermal histopathology was typically hyperplastic (figure 1.10b) without wound promotion. Upon promotion by application of TPA, *HK1.ras*¹²⁰⁵ developed rapid onset large papillomas, whilst *HK1.ras*¹²⁷⁶ formed smaller sporadic tumours over a longer time (Greenhalgh et al., 1996). However, all *HK1.ras*¹²⁰⁵ tumours regressed on the removal of TPA promotion (Greenhalgh et al., 1996). Therefore, development of ras^{Ha} autonomous papillomas required additional events in order to proceed to papilloma progression or malignant conversion.

Here, double-labelled immunofluorescence analysis of keratin K1 expression showed strong expression in the supra-basal epidermal layers. As demonstrated by the red keratin K14 counterstain that highlights the proliferative basal layers and follicles, this result was routinely exploited to confirm the benign nature of tumours (figure 1.10c). Furthermore, keratin K6 which is typically expressed in hair follicles only or in pathological conditions from wounding or stress (Sellheyer et al., 1993) showed uniform expression in proliferative epidermal hyperplasia (figure 1.9d) and was also consistent with this *HK1.ras* histotype.

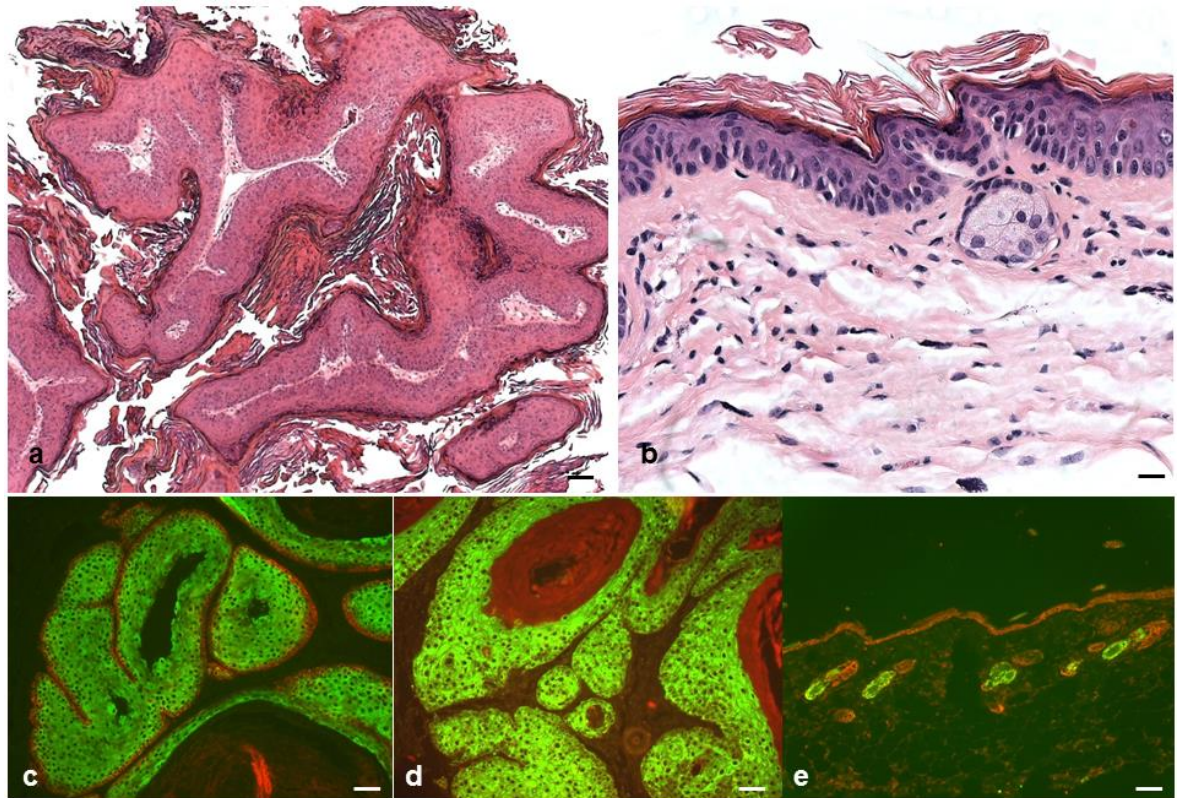


Figure 1.10 Tumourigenesis in *HK1.ras* transgenic mice showed (a) histotype of benign squamous papilloma by 3 months after wounding in the *HK1.ras*¹²⁰⁵ and (b) mild epidermal hyperplasia without wounding in the *HK1.ras*¹²⁷⁶. (c) IFC analysis of keratin K1 expressed in the supra-basal layers of *HK1.ras* papilloma. (d) Typical keratin K6 marker expression in *HK1.ras* papilloma, whilst (e) in normal epidermal, keratin K6 was only expressed in hair follicles. (Scale: 50-100µm).

1.4.2 Targeting v-fos to the epidermis: A model of tumour promotion

Fos was first recognised as the transforming gene of Finkel-Biskis-Jenkins murine osteosarcoma virus (*FBJ-MSV*) which was isolated from a spontaneous osteosarcoma in CF1 mouse (Finkel et al., 1966). The viral v-fos produced more than 90% of the bone tumour in mice and induced transformation of fibroblasts *in vitro* (Ransone and Verma, 1990). Fos in itself cannot form dimers or bind to DNA, but heterodimerisation of fos family genes with members of the jun family form the activator protein 1 (AP1) complex and these achieve flexibility as transcription factors and thus control many physiological processes including cellular proliferation, transformation, differentiation and apoptosis which all contribute to tumourigenesis (Shaulian and Karin, 2002, Malnou et al., 2007) (figure 1.11).

Previous analysis of the skin of transgenic mice containing a lacZ/fos fusion construct showed constitutive expression of fos with β -galactosidase staining in all epidermal layers including hair follicle (Smeyne et al., 1992). In normal human adult skin, fos is expressed in the proliferative basal layers (Basset-Seguin et al., 1990) and in the upper keratinocyte layers (Fisher et al., 1991) which suggest its role is not restricted to proliferation but that it is also involved in the differentiation process and its alteration generates a potential target for tumourigenesis.

The AP1 complex has been shown to be one of the major transcription factor targets of RAS/MAPK signalling pathway (Deng and Karin, 1994, Chang et al., 2003). As outlined above, if activation of ras oncogene is equivalent to the initiation event, then, activation of fos oncogene may acts as a promoter to mimic the TPA promotion stages of DMBA/TPA chemical carcinogenesis (Schlingemann et al., 2003). In support of this idea, analysis of c-fos knockout mice transfected with v-ras^{Ha} together with TPA application revealed no evidence of tumour formation (Saez et al., 1995); whilst tumours formed in c-fos wild type mice with v-ras^{Ha} were successfully converted to malignancy, thus demonstrating that c-fos was crucial for late stage of carcinogenesis (Greenhalgh et al., 1990).

In order to study the role of fos activation in the transgenic mouse model, a *HK1.fos* transgene was generated that resulted in constitutive expression of v-fos

in the epidermis. This v-fos construct served to amplify the functions of endogenous c-fos proto-oncogene in all of its epidermal roles. Initially the *HK1.fos* transgenic mice were indistinguishable from normal mice as effects on proliferation were counterbalanced by effects on differentiation; such that the only observation was an increased mitotic index. Ultimately, with wound promotion from the ear tag, *HK1.fos* transgenic mice formed hyperplastic and hyperkeratotic phenotypes which had a long latency period (> 5 months) before eventually proceeding to form highly keratotic papillomas (> 12 months) and although consistent with a promotion role, they remained benign (Greenhalgh et al., 1993b). As shown in figure 1.12, *HK1.fos* transgenic mice took a longer time to produce a hyperplastic histotype with hyperkeratosis also a prominent feature at approximately 6 to 8 months of age with wounding. Thus, *HK1.fos* mice require an additional of secondary event for further tumour progression. Yet, upon TPA treatment of *HK1.fos* mice, no changes were recorded until small papillomas appeared after 22 weeks that all contained an activated ras^{Ha} which was the initiating event (Greenhalgh et al., 1995).

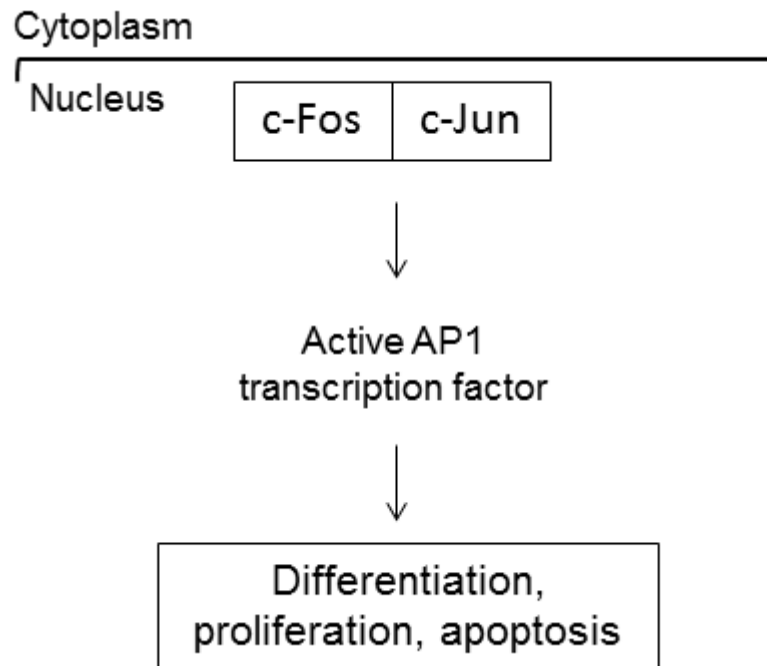


Figure 1.11 Schematic diagram of the heterodimerisation of fos family genes with members of the jun family to form the activated AP1 transcription factor resulting in various cellular activities including differentiation, proliferation and apoptosis.

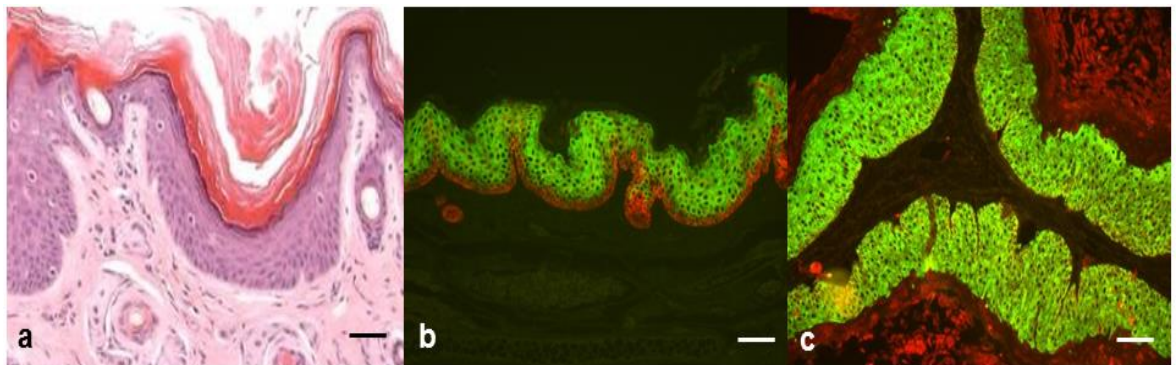


Figure 1.12 Tumourigenesis in *HK1.fos* transgenic mice showed (a) mixed histotype of hyperplasia and hyperkeratosis that took approximately 6 to 8 months to develop with wounding. (b) IFC analysis of keratin K1 expressed in the supra-basal layers of *HK1.fos* hyperplasia. (c) Typical keratin K6 marker expression in *HK1.fos* epidermal layers indicative of hyperplasia. (Scale: 100 μ m).

1.4.3 Inactivation of PTEN tumour suppressor gene mediated AKT regulation

The phosphatase and tensin homologue deleted at chromosome ten (PTEN) was identified in 1997 by mapping of homozygous deletions on chromosome 10q23 which majorly occurred in breast, brain and prostate cancers (Li et al., 1997, Hopkins et al., 2014). PTEN is commonly interrupted in sporadic tumours and is also present as a germline mutation associated with the hereditary cancer syndrome Cowden disease which is typified by early onset of cutaneous hyperkeratosis suggesting an important role for PTEN in epidermal differentiation (Yao et al., 2008, Song et al., 2012).

The ability of PTEN to dephosphorylate protein and lipid substrates means that it is known as a dual-specificity phosphatase (Myers et al., 1997, Maehama and Dixon, 1998). The phosphatase domain of PTEN is highly important in its tumour suppressor role (Myers et al., 1997). PTEN acts as a negative regulator of the PI3K/AKT pathway to inhibit cell growth, cell migration and survival by dephosphorylating its main substrate, phosphatidylinositol-3,4,5-trisphosphate (PIP₃) to PIP₂ (Stambolic et al., 1998, Hollander et al., 2011) (figure 1.13). As it is well documented that PIP₃ recruits AKT to the membrane by binding to its pleckstrin homology (PH) domain, resulting in AKT being phosphorylated at threonine 308 by 3-phosphoinositide-dependent kinase (PDK1) and at serine 473 by mammalian target of rapamycin complex 2 (mTORC2) (Song et al., 2012, Hopkins et al., 2014). Furthermore, in addition to its function as a negative regulator of the PI3K/AKT pathway, a study has shown that PTEN helps restrict MDM2 activity, which is a substrate of AKT; via indirectly inhibiting p-MDM2 from entering the nucleus to degrade p53 which is essential in the regulation of apoptosis (Mayo and Donner, 2002). Therefore, loss of PTEN functions are implicated in AKT activation that drives many cellular events such as cell proliferation and cell survival; and also contributes to p53 degradation leading to tumourigenesis (Chalhoub and Baker, 2009, Song et al., 2012, Hopkins et al., 2014).

There have been many studies investigating the important roles of tumour suppressor PTEN in carcinogenesis. In PTEN knockout mice, its loss proved to be lethal, (Cristofano et al., 1998, Hollander et al., 2011), therefore chemical

carcinogenesis studies employed a heterozygous mouse model (Mao et al., 2004). These studies have shown that deletion of one allele of PTEN resulted in tumour development (Marsh et al., 1998). However, PTEN-induced tumourigenesis is dependent on the type of tissue targeted. Studies demonstrated that homozygous PTEN loss in mammary gland (Li et al., 2002) and prostate (Wang et al., 2003) resulted in the rapid onset of tumour development. In contrast, there was no evidence of tumour formation when PTEN was lost in pancreatic β cells (Stiles et al., 2006) or in intestine (Marsh et al., 2008).

Homozygous PTEN loss in transgenic mice resulted in death during embryogenesis, whereas heterozygous PTEN loss in mice produced several tumours in different tissues, therefore, a conditional knockout of PTEN has been developed to study its role in tumourigenesis (Lesche et al., 2002, Freeman et al., 2006). Exon 5 of PTEN which encodes the phosphatase domain is highly associated with mutations in many tumours. Thus, PTEN floxed at exon 5 transgenic mice have been generated by flanking exon 5 with LoxP sequences (Lesche et al., 2002). As shown in figure 1.14a, cre recombinase fused with a progesterone ligand binding domain (PLBD) and driven by keratin K14, is responsive to RU486 which is an agonist of progesterone and activates the recombinase activity (Kellendonk et al., 1996). This Cre-Progesterone fusion protein then enters the nucleus to ablate the stop codon in the context of loxP-stop-loxP (which is applicable to *Isl.ROCK^{er}* line) or the exon5 flanked by loxP ($\Delta 5PTEN^{flx}$). The result of using this regulator transgene is illustrated in figure 1.14b, where expression of β -gal appeared in the interfollicular and follicular cells of *K14.creP/ROSA26* mice at 5 weeks post RU486 treatment, thus proving expression in stem cells (Berton et al., 2000b). Also, the histology of RU486-treated *K14.cre/ $\Delta 5PTEN^{flx}$* transgenic mice is shown which developed a mild hyperplasia histotype identical to that of Cowden disease (figure 1.14c).

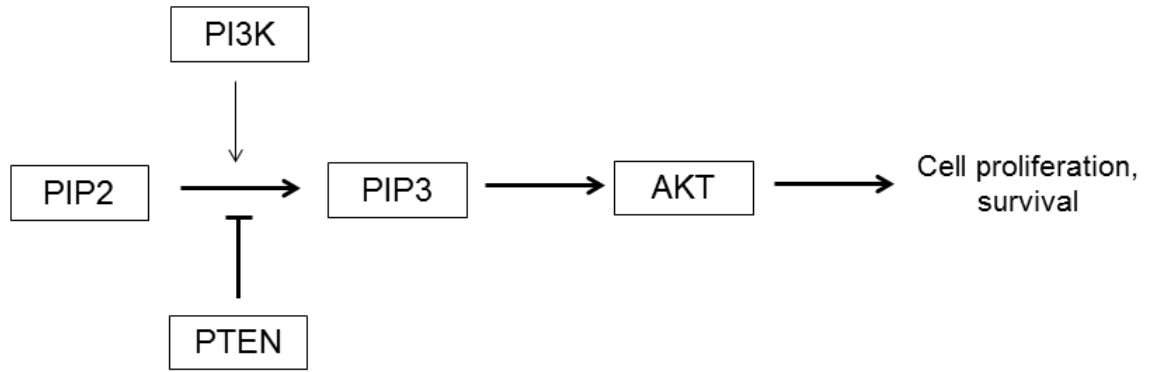


Figure 1.13 Schematic diagram of PTEN/PI3K/AKT pathway. PTEN acts as a negative regulator to PI3K by inhibiting the phosphorylation of PIP₂ to PIP₃ that can activate AKT to induce cell proliferation and cell survival leading to tumourigenesis.

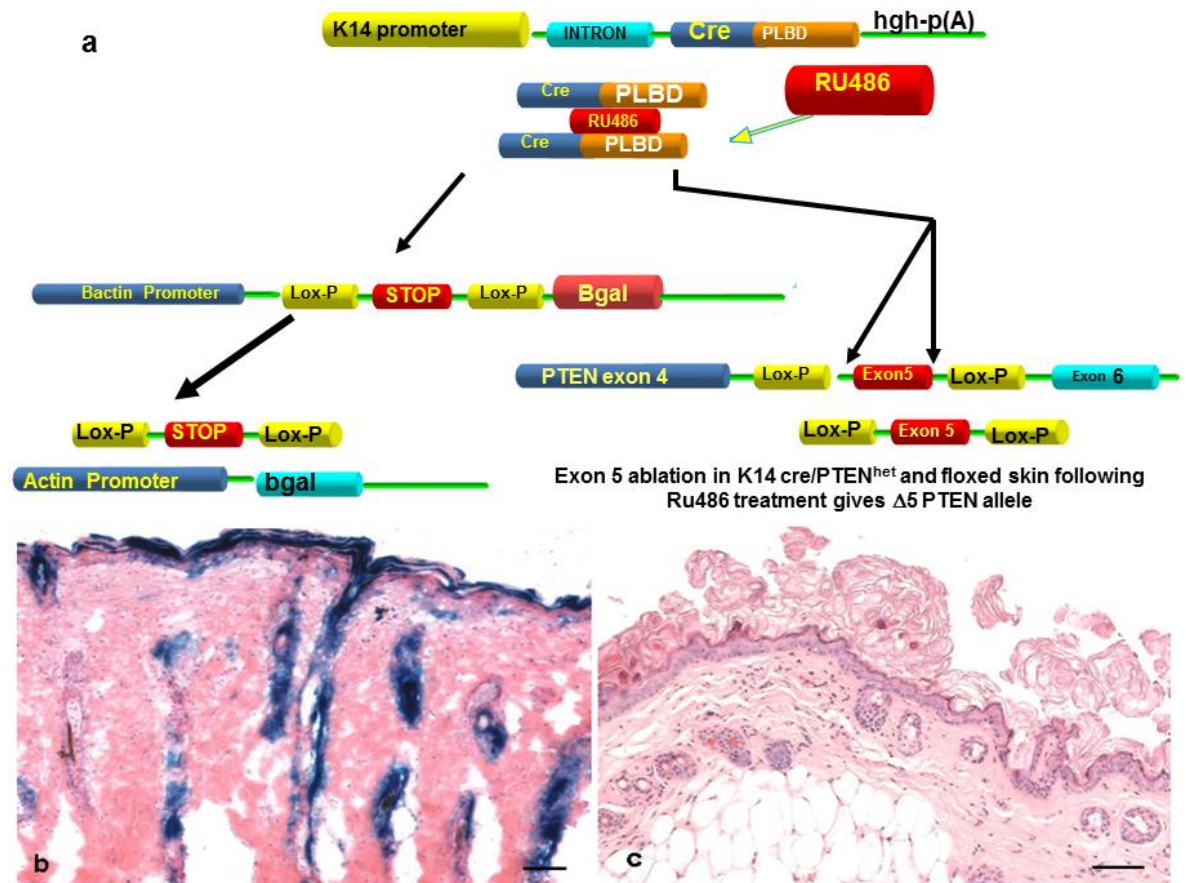


Figure 1.14 Histology analysis of *K14.cre/Δ5PTEN^{fix}* transgenic mice demonstrated (a) the cre/loxP system. Upon introduction of RU486, cre recombinase became activated and excised the stop codon or exon5 flanked by loxP ($\Delta 5PTEN^{fix}$). (b) Expression of β -gal staining in interfollicular and follicular cells of *K14.creP/ROSA26* mice after RU486 treatment. (c) Histotype of *K14.cre/Δ5PTEN^{fix}* mice revealed epidermal hyperplasia at 6 to 8 months of age with wounding, but no evidence of tumour formation. (Scale: 150 μ m).

Through co-operation of PTEN with other oncogenes or with loss of other tumour suppressor genes there is a high probability of cancer formation. As mentioned earlier, PI3K is downstream of ras oncogene and ras can activate PI3K signalling thus promoting cell proliferation and cell survival (Vivanco and Sawyers, 2002, Castellano and Downward, 2010). Previous studies by Yao et al., (2006) showed that ras^{Ha} activation in co-operation with PTEN loss lead to benign papilloma with no sign of conversion, whilst fos activation in co-operation with PTEN loss produced keratoacanthomas (KAs) but not carcinomas (Yao et al., 2008). This provides an exciting opportunity to include ROCK signalling and to assess the interaction of ROCK with ras/fos/PTEN in these epidermal specific mutation models; and ask whether it would be redundant or induce conversion.

1.4.4 Analysis of endogenous ROCK expression in the ras/fos/PTEN^{flx} skin carcinogenesis model

It is well known that certain oncogenes can cooperate with each other to accelerate the progression of tumourigenesis (Hunter, 1991, Macdonald et al., 2014). It is also likely that there is co-operation between particular oncogenes and /or loss of tumour suppressor genes in tumour development depending on their function, and when they become causal to drive progression to the next stage. It is the context created by each mutation that facilitates their co-operation or their redundancy. Thus, this subchapter assesses whether changes in ROCK signalling in mouse skin carcinogenesis could be observed at each stage involving activation of the ras/MAPK pathway to fos/AP1 signalling, together with deregulation of PTEN/AKT signalling pathways.

The HK1 model demonstrates ras activation as an initiator whilst fos activation acts as a promoter (Greenhalgh et al., 1993a-c, Yao et al., 2008). Alternatively, in a separate context, whilst co-operation studies between ras and PTEN loss gave papillomas (Yao et al., 2006), conversely, fos activation and PTEN loss drives tumour development into highly differentiated keratoacanthomas (KAs) rather than to papillomas or carcinomas (Yao et al., 2008). Moreover, co-operation of ras oncogene and loss of PTEN resulted in tumours that still remained benign and failed to convert into carcinoma (Yao et al., 2006). Given that ROCK is a member of the ras superfamily of small GTPases, it is reasonable to predict that there will

be a link between ROCK and ras signalling deregulation. In addition from these previous studies, it is highly probable that there will be co-operation between ROCK activation and the epidermal specific *fos*/ Δ 5PTEN^{flx} mutations as all these transgenes interact with many of the same target molecules and signalling pathways. The question remains as to whether this linkage is redundant, as both are on similar pathways or that the extra changes mediated by ROCK signalling with respect to tissue stiffness (Samuel et al., 2011, Rath and Olson, 2012) will be additive and at what stage of carcinogenesis do they become causal?

It has already been reported that some Rho GTPases, mainly RhoA and RhoC contribute to oncogenic ras transformation (Zohn et al., 1998). Sahai et al., (2011) demonstrated a high level of Rho activity in ras-transformed cells and elevated Rho suppressed p21 expression leading to cell proliferation, and p21 alongside p53 is a critical indicator of tumour progression in the HK1 model (Macdonald et al., 2014). However, again demonstrating the importance of mutation timing and tumour context, reverse involvement of Rho activity in ras-transformed cells has also been reported (Izawa et al., 1998).

Previous studies have demonstrated the interaction between rho kinase and ras activation *in vitro* (Qiu et al., 1995, Olson et al., 1998, Sahai et al., 2001), however there remains a relative lack of direct co-operation studies between ROCK2 and ras^{Ha} activation. Moreover, though the application of DMBA/TPA on ROCK2 resulted in carcinogenesis (Samuel et al., 2011), yet, there is not enough evidence from either DMBA or TPA alone on ROCK2 and at which stage ROCK2 co-operation with ras^{Ha} becomes causal. Thus, this study proves this expectation between ROCK2 and ras^{Ha} through transgenic mouse models that mimic the DMBA/TPA chemical carcinogenesis model. It is well documented that activated ras^{Ha} can act as a tumour initiator, however, deregulated ROCK expression was showed to be elevated in the later stages of events during chemical carcinogenesis (Samuel et al., 2011, Ibbetson et al., 2013). Therefore, as a baseline, the levels of endogenous ROCK1 and ROCK2 were assessed at each stage in the HK1 model of tumourigenesis, which would be augmented by the additional expression of exogenous ROCK.

An indication that ROCK signalling is clearly involved in this carcinogenesis model is demonstrated in figure 1.15 which analysed multistage tumourigenesis in tri-

genic *ras/fos/ΔPTEN^{fix}* mice. These results showed expression of both ROCK1 and 2 in both early epidermal hyperplasia and in benign papillomas and also demonstrated that ROCK2 appeared to be more prominent than ROCK1, which correlated well in this study. As keratinocyte differentiation follows a relatively normal pathway sequence in these early histotypes of epidermal hyperplasia and benign papillomas (Greenhalgh et al., 1993a-c, Yao et al., 2006, 2008), there was a suggestion that both ROCK 1 and 2 expression appeared predominantly in the supra-basal layers of the epidermis (figure 1.15 – arrows). This important finding would be consistent with a role for ROCK signalling in maintaining epidermal integrity and its role in increasing the tensile strength of tumour tissues (Samuel et al., 2011) would be a logical facet in the spinous layer of the epidermis that would contribute to the barrier functions of the skin (Byrne et al., 1994, Fuchs, 2007).

This relative lack of basal layer expression would thus provide an ideal opportunity to deregulate ROCK in these proliferative layers given expression of the ROCK2^{er} transgene from a keratin K14 promoter (Samuel et al., 2009a) where the cancer target keratinocytes reside and thus directly assess effects of ROCK2 activation in these early phenotypes. Analysis of ROCK protein expression also demonstrated that ROCK2 was elevated further in *HK1.ras/fos/Δ5PTEN^{fix}* malignant tumours (figure 1.15c,f), and of note, this expression was now found in the basal cell compartment. Again, these data were consistent with a later role of ROCK at the malignant and invasive stage.

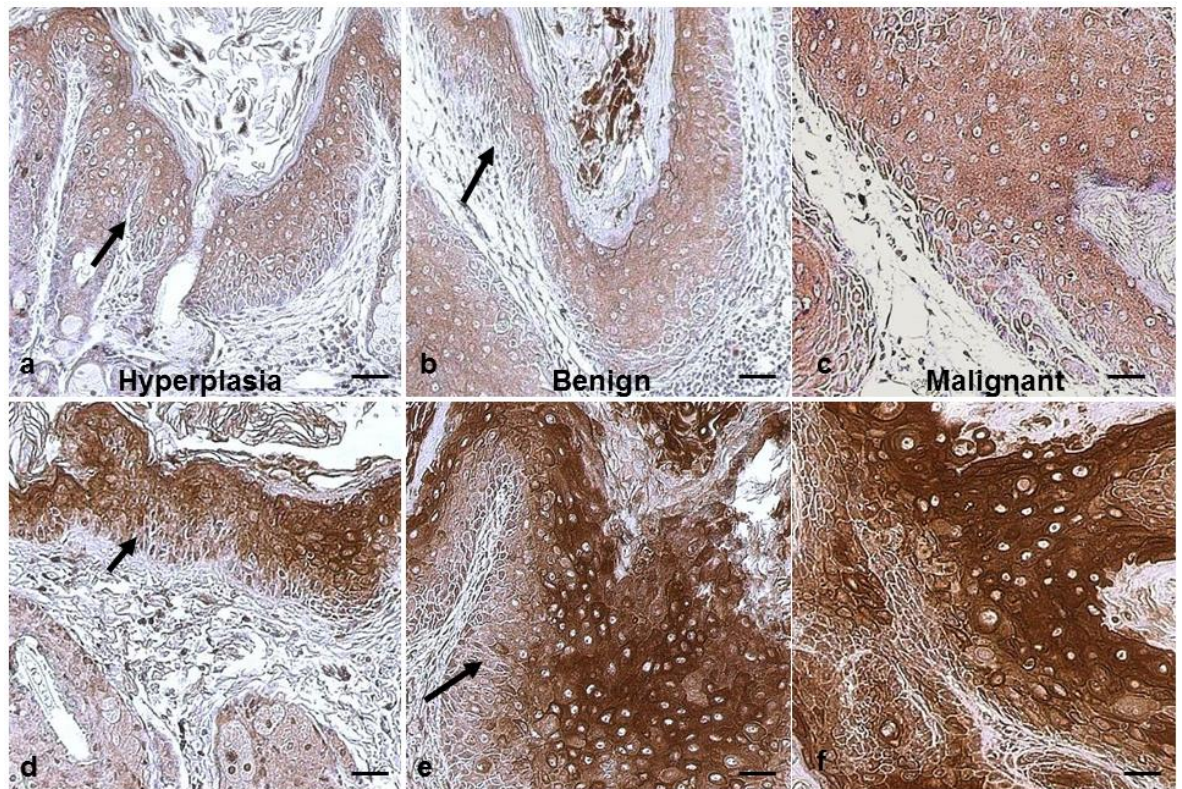


Figure 1.15 Immunohistochemical analysis of ROCK1 (a, b, c) and ROCK2 (d, e, f) expression in *HK1.ras/fos/Δ5PTEN^{fix}* tumours. Endogenous ROCK1 (a, b) and ROCK2 (d, e) are expressed in the supra-basal layer (arrows) of *HK1.ras/fos* hyperplasia and benign papillomas whilst both ROCK1 (c) and ROCK2 (f) are strongly expressed in all compartments including the basal layer following malignant conversion in *K14.cre/HK1.ras/fos/PTEN^{fix}* SCCs. (Scale: 50-100 μ m).

In addition to potential ROCK and ras co-operation, other studies have reported that RhoA/ROCK signalling is associated with PTEN activity in the regulation of cell proliferation by downregulating AKT activity (Yang and Kim, 2012), and the finding that ROCK is a downstream effector of Rho family signalling to the c-fos serum response element also provides a direct link to fos and regulation of transcription by AP1 (Chihara et al., 1997, Perona et al., 1997).

Taken collectively, these findings suggest that the HK1 model would be an ideal platform to study and analyse the novel co-operation and molecular mechanism which triggers causal roles for ROCK2 and ras/fos activation together with PTEN loss and AKT deregulation. Furthermore, the analysis of PTEN loss includes a new cre/lox responsive ROCK2 transgenic mouse (*Isl.ROCK^{er}*) geared to express ROCK2 in all tissues from a CAG promoter and is ideal to target ROCK and PTEN mutations to the identical *Isl.ROCK^{er}/Δ5PTEN^{flx}* keratinocytes populations and observe any malignant conversion events in both carcinogenesis and epidermal differentiation.

1.5 Hypothesis and Aims of the study

The general aim of this study is to analyse ROCK2 activation in the multistage cancer process by employing a transgenic mouse model that has been established to express commonly mutated genes in cancer: ras, fos and PTEN exclusively in the epidermis. It is hypothesised that ROCK2 can become active in the early stage of cancer in co-operation with ras/fos/PTEN. Thus, the selected co-operative genes permit identification of the cancer stage at which mutations become active.

The specific aims of the study were to:

1. Investigate and compare the outcome of two ROCK2 transgenic mouse models: K14.ROCKer and K14cre/Isl.ROCKer in carcinogenesis.
2. Examine the synergism of ROCK2 with ras, fos and PTEN in multistage carcinogenesis and analyse other oncogenes and /or tumour suppressor genes such as p53, p21 and /or p-AKT in this transgenic mouse skin carcinogenesis model. At the same time, this study will investigate this synergistic process in vitro through low and high calcium changes in transgenic mouse keratinocytes to assess effects on proliferation and differentiation activities.

The relevant background and further elaboration of specific aims are discussed in further detail within each part of the study.

Chapter 2 – Materials and Methods

2.1 Materials

2.1.1 PCR materials

2.1.1.1 Reagents and buffers

Taq DNA polymerase, 10X PCR buffer and 50mM Magnesium Chloride (from Life Technologies);

DNTPs (from Roche diagnostics);

50x PCR running buffer;

6x DNA loading buffer (0.25% bromophenol blue, 0.25% xylene and 30% glycerol);

Proteinase K (from Sigma);

DNA extraction buffer (50mM Tris/HCL pH 8.0, 100mM EDTA Ph 8.0, 100mM NaCl, 1% SDS and 200µg/ml fresh proteinase K).

2.1.2 Immunohistochemistry and immunofluorescence materials

2.1.2.1 Antibodies

Antibody	Dilution	Company
Rabbit anti-keratin1 (#PRB-149P) (Greenhalgh et al., 1993c)	1:50	Covance
Rabbit anti-keratin6 (#PRB-169P) (Greenhalgh et al., 1993c)	1:50	
Guinea pig anti-keratin14 (#20R-CP002) (Yao et al., 2006)	1:500	Fitzgerald
Rabbit anti-ROCK2 (H-85) (#SC-5561) (Lane et al., 2008)	1:100	Santa Cruz Biotechnology
Rabbit anti-ROCK1 (H-85) (#SC-5560) (Lock and Hotchin, 2009)	1:100	
Rabbit anti-p53 (#SC-6243) (Yao et al., 2008)	1:50	
Rabbit anti-p21 (#SC-397) (Yao et al., 2008)	1:50	
Rabbit anti-phospho-Mypt1 (Thr696) (#ABS45) (Samuel et al., 2011)	1:50	Millipore
Biotinylated goat anti-guinea pig IgG (#BA-7000) (Yao et al., 2008)	1:200	Vector Laboratories
Biotinylated goat anti-rabbit IgG (#BA-1000) (Steiniger and Barth, 2000)	1:200	
Streptavidin Texas red (#SA-5006) (Yao et al., 2006)	1:400	
Horseradish peroxidase-conjugated anti rabbit (#PI-1000) (Yao et al., 2008)	1:100	
FITC-labelled anti-rabbit (#711-005-152) (Yao et al., 2006)	1:100	Jackson Laboratories
Rabbit anti-Tenascin C (#T2551) (Schauer et al., 2009)	1:50	Sigma
Rat anti-BRDU (#ab6326) (Illa-Bochaca and Montuenga, 2006)	1:50	Abcam
Rabbit anti-pAKT1 (473) (#ab81283) (Sobinoff et al., 2011)	1:50	
Rabbit anti-GFP living colors A.v. Peptide (#632377) (Samuel et al., 2011)	1:50	Clontech

Table 2.1 Antibodies used in immunohistochemistry and immunofluorescence procedures.

2.1.2.2 Other reagents

Normal goat serum, normal horse serum, and DAB (from Dako);
1x PBS (from Life Technologies);
Ethanol (from VWR chemicals);
Xylene (from Fisher Scientific);
Citrate buffer and PermaFluor mounting medium (from Thermo Scientific);
Pertex mounting medium (from Cell Path);
Paraffin embedding medium (from Ted Pella Inc.);
Hematoxylin and Eosin (H&E), 3% hydrogen peroxide solution, and
Bromodeoxyuridine (BrdU) (from Sigma).

2.1.3 Cell culture materials

2.1.3.1 Reagents and buffers

L-Glutamine, sodium pyruvate, penicillin/streptomycin, Dulbecco's phosphate buffered saline (PBS) without Ca^{2+} and Mg^{2+} , and 2.5% trypsin (all from Life Technologies);
Chelex 100 sodium, ethanol, dimethyl sulfoxide (DMSO), RU486 (mifepristone), 4-Hydroxytamoxifen (4-HT) (all from Sigma-Aldrich).

2.1.3.2 Media

1. DMEM (Dulbecco's Modified Eagle Medium) was purchased from Invitrogen.
2. KGM (Keratinocyte Growth Media 2) and supplement components including: Bovine Pituitary Extract, Epidermal Growth Factor, Insulin, Hydrocortisone, Epinephrine, Transferrin and CaCl_2 were purchased from Promo Cell.
3. The medium used for primary mouse keratinocyte culture was: 10% KGM, 10% chelexed fetal calf serum (FCS), 10% fibroblast conditioned media, 10mM of L-glutamine, 1mM of pyruvate and penicillin/streptomycin in DMEM supplemented with 0.05mM Ca^{2+} .

2.1.4 Western blot materials

2.1.4.1 Reagents and Buffers

4-12% Bis-Tris gel and NuPage transfer buffer (from Life Technologies);

1x MES SDS running buffer, 1x NuPAGE transfer buffer and 1x MOPS buffer (from Invitrogen);

Pageruler Prestained protein ladder (from Thermo Scientific);

6X loading buffer (1M Tris pH6.8, SDS, glycerol, distilled water and bromophenol blue);

1x TBST buffer pH 7.5 (1M Tris pH8, 5M NaCl, Tween 20 and Milli Q water);

1x TBST-TM pH 7.5 (1M Tris pH8, 5M NaCl, Tween 20, Marvel and Milli Q water) and methanol (from Fisher Scientific).

2.1.4.2 Antibodies

Antibody	Dilution	Company
Mouse anti-MRCL3/MRLC2/MYL9 (E-4) (Samuel et al., 2011)	1:1000	Santa Cruz Biotechnology
Alexa fluor 680 donkey anti-rabbit (Samuel et al., 2011)	1:5000	Invitrogen
Goat anti mouse 800 IgG conjugated dylight	1:15000	Jackson
Rabbit anti-keratin1 (Greenhalgh et al., 1993c)	1:1000	Covance
Rabbit anti-keratin6 (Greenhalgh et al., 1993c)	1:1000	

Table 2.2 Antibodies used in western analysis.

2.2 Methods

2.2.1 Transgenic mouse genotypes and breeding

Two transgenic lines were employed to activate ROCK expression in the epidermis. The first transgenic line, *K14.ROCK^{er}* (Samuel et al., 2009a) consists of the human ROCK2 kinase domain fused to mutant 17 β -estradiol-insensitive estrogen receptor (ER) hormone binding domain (HBD) (Littlewood et al., 1995) and enhanced green fluorescent protein (EGFP). This construct is under the control of a keratin *K14* gene promoter and knocked into the HPRT locus which results in gene expression in all epithelial cells but gene activity is exclusive to epidermal cells including interfollicular and follicles due to topical application of 4-HT. The second transgenic line is the new unpublished model, *K14.cre/Isl.ROCK^{er}* which employs the same ROCK^{er} transgene but it is now inserted downstream of a loxP flanked stop cassette and driven by a general CAG-promoter (figure 1.4). Thus, to ensure that the transgene is targeting the same proliferative basal layer and hair follicles, *Isl.ROCK^{er}* mice were mated with K14.creP mice (*K14.cre/Isl.ROCK^{er}*). This model achieves tissue specificity in the epidermis as the keratin K14 vector is targeting the epidermal basal layer and follicles (Berton et al., 2000a). The K14.creP is fused to a progesterone ligand binding domain which is responsive to RU486, a progesterone agonist, thus, activating the recombinase. This cre-fusion protein is translocated to the nucleus to ablate the stop codon flanked by loxP sites. RU486 evicts the stop codon and then, topical application of 4-HT activates the ROCK^{er} transgene as described previously (Samuel et al., 2009b). This new transgenic line is required to turn on ROCK^{er} protein in the same cells and in an identical way to the mechanism of PTEN ablation employed previously where loxP-flanked sequences of PTEN exon 5 were removed to assess its loss in carcinogenesis (*HK1.ras/fos/ Δ PTEN^{fix}*) (Yao et al., 2006, 2008).

In this study, *HK1.ras* (Greenhalgh et al., 1993a), *HK1.fos* (Greenhalgh et al., 1993b) and RU486-inducible K14.creP regulator (Berton et al., 2000a) transgenic mice were maintained as heterozygotes on an outbred ICR line, whilst Δ 5PTEN^{fix} mice were maintained as homozygotes as described previously (Yao et al., 2006, 2008, Macdonald et al., 2014). For *HK1.ras* transgenic mice, two different lines were used in this study: *HK1.ras* 1205 (sensitive to wound promotion) and *HK1.ras*

1276 (insensitive to wound promotion). All transgenic lines were bred under project licence 60/4318 according to the rules and regulations of the UK Home Office. To ablate epidermal PTEN and also the stop cassette, cre recombinase was activated by topical treatment with 2µg RU486 in 20µl ethanol per ear for 1 week. To activate ROCK^{er} transgenes, 15µl of a 10mg/ml solution of 4-hydroxytamoxifen (4-HT) dissolved in ethanol was topically applied on each ear of transgenic mice for 20 weeks with controls received RU486 and ethanol.

2.2.1.1 Tail cutting and DNA isolation

The mice were weaned 21-24 days after birth. To isolate the DNA for genotyping by PCR (at 5 weeks), a 4mm of tail tip biopsy was taken under anaesthetic, and put into a labelled eppendorf tube. 460µl of DNA extraction buffer was added to each tube and the tissue digested overnight at 55°C with occasional vortexing to degrade the tails. Next day, tissue lysate were centrifuged at 13,000 rpm for 15 minutes to ensure that tail genomic DNA was dissolved in supernatant; whilst tissue debris and remnants were pooled as a pellet under the supernatant. 500µl of ethanol was added gently to the supernatant to precipitate tail genomic DNA. The precipitated DNA was collected by gently rolling onto a clean pipette tip and any remaining ethanol allow to evaporate off. The DNA was transferred into a new labelled eppendorf tube which contained 280µl dH₂O and left to dissolve at 55°C for 1 hour.

2.2.2 Polymerase chain reaction (PCR)

2.5µl of tail DNA was used as a template in a 25µl reaction volume comprising 2.5mM MgCl₂, 0.5µM reverse and forward primers for each transgene, 0.25mM dNTPs and 1 unit Taq DNA polymerase (1U/ µl) set in a 200µl PCR tube (Table 2.3). PCR was performed for each transgene in a thermal cycler according to the programmes listed in Table 2.4. PCR products were maintained at 4°C after the final step. Electrophoresis was performed on the PCR products by using a 1% (K14CreP, Ras, Fos and ROCK^{er}) and 1.5% (PTEN) agarose gels that were stained with ethidium bromide to visualise the bands under UV lights and to ensure that PCR amplified the DNA from each transgene.

Component	Volume	Final Concentration
DNA	2.5 μ l	
10x PCR buffer	2.5 μ l	1x
50mM MgCl ₂	2.0 μ l	2.5mM
Forward primer	0.5 μ l	0.5 μ M
Reverse primer	0.5 μ l	0.5 μ M
dNTP	0.25 μ l	0.25 μ M
Taq polymerase	0.25 μ l	1 unit
dH ₂ O	To 25 μ l	

Table 2.3 Master mix solution

Name	Sequences	Programmes
ROCK ^{er}	2F CGACCACTACCAGCAGAACA 2R GACGAACCAACTGCACTTCA	Denaturation at 95 ^o C (5mins), Annealing at 60 ^o C (1min), Extension at 72 ^o C (45secs), Final extension at 72 ^o C (5mins).
K14CreP	1F CGGTCGATGCAACGAGTGAT 2R CCACCGTCAGTACGTGAGAT	Denaturation at 94 ^o C (5mins), Annealing at 58 ^o C (45secs), Extension at 72 ^o C (45secs), Final extension at 72 ^o C (5mins).
Ras	1F GGATCCGATGACAGAATACAAGC 2R ATCGATCAGGACAGCACACTTGCA	Denaturation at 95 ^o C (5mins), Annealing at 56 ^o C (1min), Extension at 72 ^o C (45secs), Final extension at 72 ^o C (10mins).
Fos	1F GGATCCATGATGTTCTCGGGTTTC 2R CGATTATTGCCACCCTGCCATG	Denaturation at 95 ^o C (2mins), Annealing at 62 ^o C (30seconds), Extension at 72 ^o C (45secs), Final extension at 72 ^o C (10mins).
PTEN	1F ACTCAAGGCAGGGATGAGC 2R GTCATCTTCACTTAGCCATTGG 3R GCTTGATATCGAATTCCTGCAGC	Denaturation at 95 ^o C (2mins), Annealing at 62 ^o C (30seconds), Extension at 72 ^o C (45secs), Final extension at 72 ^o C (10mins).

Table 2.4 Primers and programmes used in PCR analysis.

2.2.3 Immunohistochemistry and immunofluorescence

2.2.3.1 Preparation of skin biopsy sample

Mice were injected with 125 mg/kg 5-bromo-4-deoxyuridine (BrdU, Sigma) (15.625mg of Brdu was dissolved in 1ml of 0.9% sterile NaCl solution, pH 7) intraperitoneally and biopsied after 2 hours. Mice were sacrificed and biopsies of dorsal skin, tail and ears were taken. Each biopsy was cut in half and one half was fixed in 10% buffered formalin for 24 to 48 hours at 4°C before being processed for histology and H&E staining in the Beatson Research Institute, while the other half was snap frozen in liquid nitrogen and stored at -70°C.

2.2.3.2 Immunohistochemistry analysis

Paraffin sections (5-7µm) were incubated at 65°C for 30 minutes to soften the wax and then immediately placed in xylene for 20 minutes to remove the wax. Sections were immersed in absolute ethanol for 1 minute, and then washed in 1x PBS for 10 minutes to rehydrate the section; followed by antigen retrieval with 1x commercial citrate buffer (Thermo Scientific) for 2 minutes in microwave at high power. Sections were left to cool at room temperature for 20 minutes before being immersed in 3% hydrogen peroxide to block endogenous peroxidase enzyme. Sections were washed with 1x PBS then blocked in 10% normal goat serum (diluted in 1x PBS) for 10 minutes and then incubated with primary antibodies diluted in blocking solution (10% normal goat serum) overnight at 4°C.

After incubation with primary antibody, sections were washed in 1x PBS for 10 minutes and incubated with secondary horseradish peroxidase-conjugated anti rabbit antibody diluted in 20% bovine serum albumin (diluted in 1x PBS), for 1 hour at room temperature. Sections were washed in 1x PBS and DAB (3,3'-diaminobenzidine) substrate solution (Dako) was freshly prepared then added to sections for 5 minutes at room temperature. Sections were immediately washed in water for 3 minutes and counterstained with Haematoxylin for 20 to 30 seconds. Next, sections were washed for 3 times in running tap water and dipped in acid alcohol 3 times to remove excess stain; then, washed again in running tap water before immersion in Scott's water for 1 minute to blue the Haematoxylin stain

followed by washing in running tap water 3 times. Sections were immersed in absolute ethanol for 3 minutes followed by xylene for 3 minutes, left dried before being mounted with Permount solution and covered with a coverslip. Finally, sections were visualised by using Carl-Zeiss microscope Axiovision software.

2.2.3.3 Immunofluorescence analysis

For double-labelled immunofluorescence staining, paraffin sections (5-7 μ m) were incubated at 65°C for 30 minutes and placed in xylene for 20 minutes to remove the wax. Next, sections were placed in absolute ethanol for 1 minute to remove xylene and then washed in 1x PBS for 10 minutes. Antigen retrieval was performed using 1x commercial citrate buffer (boiled for 2 minutes in microwave at high power). Sections were allowed to cool at room temperature for 20 minutes and washed with 1x PBS for 10 minutes. To prevent non-specific binding, sections were blocked in 10% normal horse serum or 10% normal goat serum diluted in 1x PBS for 10 minutes. Slides were incubated with primary antibodies diluted in the blocking solution overnight at 4°C.

The next day, sections were washed in 1x PBS for 10 minutes before being incubated with biotinylated goat anti-species of the primary antibody (usually rabbit) diluted in 20% bovine serum albumin (diluted in 1x PBS) for 60 minutes at room temperature. Sections were washed with 1x PBS for 10 minutes; and incubated with FITC to highlight the selected target protein from primary antibody and Texas red avidin to highlight the epidermis and follicles as a background (diluted in 20% bovine serum albumin) for 60 minutes at room temperature. Sections were washed in 1x PBS for 10 minutes before being mounted with Permafluor and then stored at 4°C.

2.2.4 Primary keratinocytes cell culture

Keratinocytes were isolated from normal and transgenic neonatal mice, as described by Yuspa et al., (1980) and modified by Greenhalgh et al., (1989). Briefly, 24hour old newborn mice were sacrificed through an overdose of pentobarbital by intra-peritoneal injection and transported to the lab in 70 % ethanol which served as a sterilization step. Individual mice were placed in 60mm

dishes and tail biopsies taken for DNA isolation and overnight PCR analysis for genotype confirmation. The skin was carefully removed and stretched on the cover of each 60mm dish with the dermis face down for approximately 30minutes. Each skin was carefully floated onto 5 ml of 0.25% trypsin (diluted in 1x sterile PBS with Ca^{2+} and Mg^{2+}) and incubated overnight at 4°C. Care was taken to avoid the edges of the skins curling up.

The next day, with the epidermis side down on petri dish, the epidermis was separated from the dermis with sterile forceps. Once genotype was confirmed, skins of the same genotype were combined together into a 50ml centrifuge tube which contained 40ml of high calcium DMEM media to inhibit the trypsin action. To separate keratinocyte cells from the epidermal sheet, the tubes were gently inverted for 20minutes and the cornified layer was removed by filtering through sterile gauze. The resultant filtrate was centrifuged at 900rpm for 3minutes and the pellet resuspended in DMEM medium supplemented with 10% chelexed fetal calf serum (FCS), L-glutamine, penicillin/streptomycin and 0.05mM calcium as previously described (Hennings et al., 1980). Cells were counted using a haemocytometer and typically 1 mouse skin yielded $(5-8) \times 10^6$ cells. Thus, cells were plated out in the same number of mouse equivalents (0.5 mouse equivalents per each 60mm petri dish) to standardise plating density. After overnight incubation to allow the keratinocyte to attach, cells were washed twice with 1x sterile PBS (without Ca^{2+} and Mg^{2+}) to remove unattached and differentiated cells and fed with the same low calcium media. To activate ROCK^{er} *in vitro*, *K14.cre/Isl.ROCK^{\text{er}}* keratinocytes were treated with RU486 (10^{-9}M) on day 1; and 4-HT (10^{-9}M) on day 2 in the low calcium medium for 4 days. The calcium concentration was increased to 0.10mM on day 4 for 24 hours to induce keratinocyte terminal differentiation, then to 1.5mM calcium on day 5 for 24hours. Cells were harvested every 4 to 6 days when cells were 90% confluent or 24 hours after the second calcium switch.

2.2.5 Western blot analysis

For analysis of non-soluble keratin proteins (keratin 1 and 6), cells were washed with PBS and lysed in buffer with 50mM Tris (pH 6.8), 1% SDS and 2% β -mercaptoethanol. The cells were gently homogenised using a syringe and then

heated at 80°C for 10 minutes. All cells were then transferred to eppendorf tubes, centrifuged at 13,000 rpm for 5 minutes and the supernatant was transferred to fresh eppendorf tubes. The protein concentration was determined using the BCA total protein assay kit as per manufacturer's instruction (Thermo Scientific). 20µg of each lysate was mixed with 6x loading buffer and run out on a NuPAGE Bis-Tris mini gel with one lane was loaded in 5µl pageruler prestained protein ladder. Gels were run at 200V for 60minutes and transferred to nitrocellulose membrane by electro-transfer at 100V for 60minutes. After transfer, the membrane was washed in 5% skimmed milk with 1x Tris-buffered saline and Tween20 (TBST) for 15 minutes to block non-specific binding. Primary antibodies (keratin K1 anti rabbit, keratin K6 anti rabbit, and tMLC anti mouse) were diluted in 5% skimmed milk in 1x TBST buffer, applied to the membrane and incubated overnight at 4°C. The next day, the membrane was washed in 1x TBST buffer (3 x 5 minutes) then incubated in the dark for 1 hour, with Licor fluorescent-labelled conjugated secondary antibody (680 anti-rabbit and 800 anti-mouse) in 5% skimmed milk diluted in 1x TBST. The membrane was washed with 1x TBST (3 x 5minutes), then washed in distilled water (5minutes) before being stored in water, in the dark until scanned by LICOR Odyssey system to capture the image.

2.2.6 BrdU-labelling analysis

All mice received 5-Bromo-4-deoxyuridine (BrdU, 125mg/kg) through intraperitoneal injection 2 hours prior biopsy. For BrdU staining, following antigen retrieval with 1x commercial citrate buffer, paraffin sections were incubated overnight with anti-rat BrdU antibody and anti-guinea pig keratin K14 at 4°C. Expression was visualised via Alexa Fluor anti-rat IgG and counterstained with biotinylated anti-guinea pig/ Streptavidin-Texas red. Data for BrdU-labelling was calculated manually using three sections per tumour (three independent tumours), and three independent readings per image, at a 20x magnification. Data were presented as the percentage (%) of all nuclei that was immuno-labelled for BrdU from total of 100 cells in each area. Statistical analysis of variance test (ANOVA) was performed to determine any significant difference between cohorts, with p value of <0.05 was considered as significant.

Chapter 3 – Results

3.1 PCR analysis and genotyping of transgenic mice

The genotype of each transgenic mouse was confirmed by routine PCR analysis of tail or biopsy DNA. DNA was also isolated from tumour biopsies to confirm their identity and RU486-mediated cre activity. As outlined above in the methods, two transgenic mouse strains of 4-HT-inducible ROCK2 activation (*K14.ROCK^{er}* and *Isl.ROCK^{er}*) were employed in this study with both ROCK^{er} transgenes being expressed directly or indirectly from a keratinocyte specific K14 promoter (Berton et al., 2000b, Samuel et al., 2011). Initial studies involved breeding of *HK1.ras*, *HK1.fos*, *K14.ROCK^{er}* and *Isl.ROCK^{er}* mice. The *K14.ROCK^{er}* transgene which was integrated at the HPRT gene locus, and topical application of 4-HT was previously shown induce epidermal hyperplasia in these mice (Samuel et al., 2009a, 2011). For experiments involving PTEN mutations, and to ensure ROCK activation and inducible PTEN exon 5 loss occurred in the identical epidermal cells, later studies employed transgenic mice expressing a K14.creP regulator transgene: where a single RU486 treatment activates cre activity in the epidermis; and after cre-mediated removal of loxP-flanked stop cassette, the same 4-HT inducible ROCK2 transgene was expressed from a generic CAG promoter downstream of loxP-flanked stop codons (*K14.cre/Isl.ROCK^{er}*). Hence, following a single RU486 treatment K14 mediated cre activity removes the stop cassette thus expressing ROCK^{er} ready to be activated by topical 4-HT treatment.

Using specific primers (Table 2.4) for ROCK^{er}, a 589-bp fragment was observed which indicated positive ROCK^{er} transgenic mice (figure 3.1). Similarly, analysis of tail DNA for *HK1.ras* or *HK1.fos* transgenes employing specific primers gave a 743-bp and 800-bp bands respectively (figure 3.2). The RU486-inducible *K14.creP* regulator transgene produced a 600-bp band and $\Delta 5$ PTEN^{flx} transgenic mice a 1.3-kbp band, indicative of the floxed allele, and 1.2-kbp band indicative of the wild type allele (figure 3.3). ROCK^{er} mice were created by integrating the transgene in the HPRT locus on the X-chromosome. Thus in this study, most ROCK^{er} transgenic mice maintained on treatment procedures were males due to potential X-linked chromosome inactivation in ROCK^{er} female mice. Similarly, all *HK1.ras*,

HK1.fos and *K14.creP* transgenic mice were maintained as heterozygous lines on a background of outbred ICR mice.

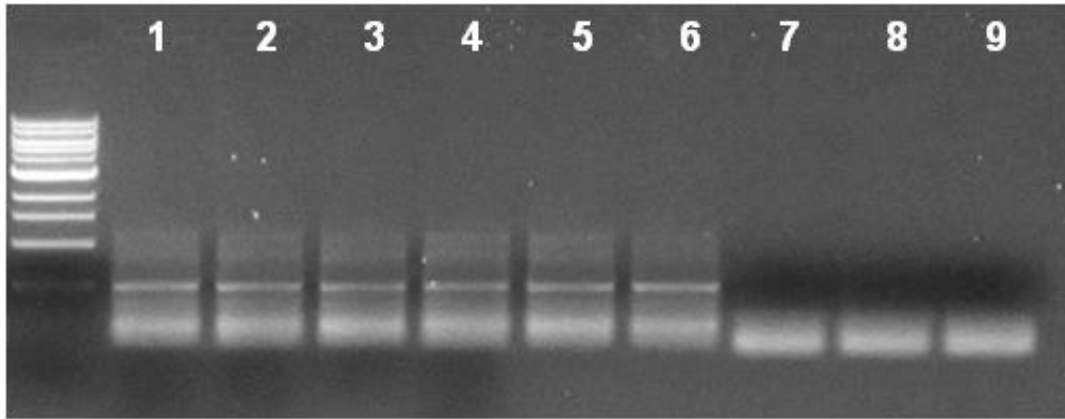


Figure 3.1 PCR analysis of $ROCK^{er}$ genotypes. PCR product represents $ROCK^{er}$ transgenic line. $ROCK^{er}$ positive progenies were identified from genomic tail DNA derived from *K14.ROCK^{er}* mice (lane 1 to 3) and *Isl.ROCK^{er}* mice (lane 4 to 6). 589-bp fragment represents $ROCK^{er}$ positive transgenic mice (lane 1 to 6) and is absent in the three negative controls from non transgenic ICR mice (lane 7 to 9). (DNA ladder is Biolabs 1kb).

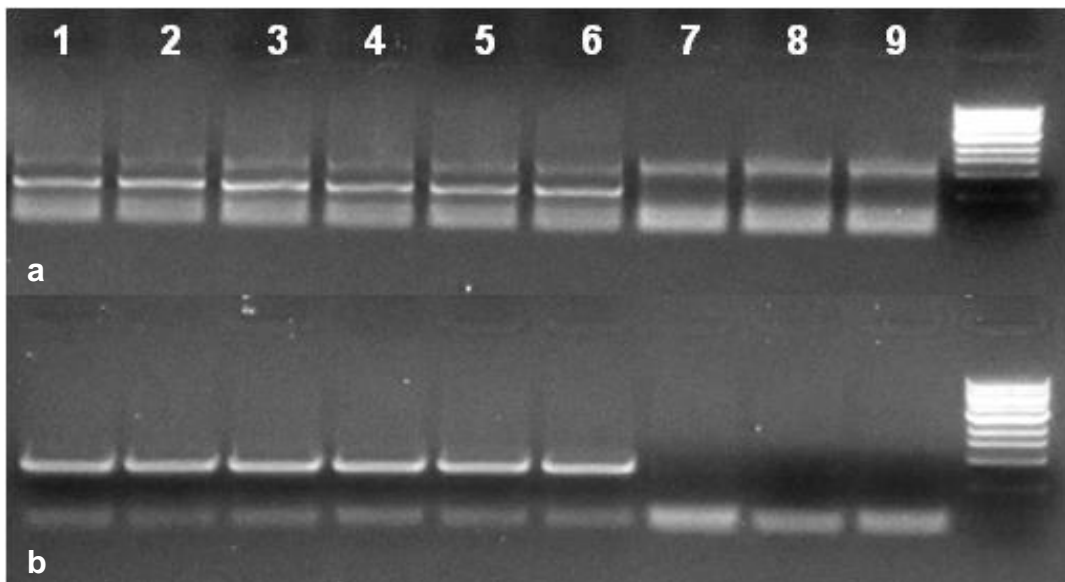


Figure 3.2 PCR analysis of *HK1.ras* and *HK1.fos* genotypes. (a) 743-bp band represents *HK1.ras* positive transgenic lines (lane 1 to 6) and is absent in the three negative controls from non transgenic ICR mice (lane 7 to 9). (b) 800-bp band represents *HK1.fos* positive transgenic lines (lane 1 to 6) and is absent in the three negative controls from non transgenic ICR mice (lane 7 to 9). (DNA ladder is Biolabs 1kb).

3.1.1 Confirmation of gene switch activation

This study incorporates an inducible cre/loxP gene switch system so that PTEN loss or ROCK^{er} activation can be limited to specific sites on the mouse skin and once the mouse has fully developed. The cre recombinase is fused to the progesterone ligand binding domain which is induced to dimerise and translocate to the nucleus by topical application of RU486. This acts to evict a stop cassette in the ROCK^{er} transgene or exon 5 of PTEN. This regulator transgene is driven by a keratin K14 promoter (Berton et al., 2000b). Thus the transgene is exclusively expressed in epidermal basal layers, including hair follicles and stem cells. These mice have been successfully used to ablate lox-P flanked PTEN exon 5 ($\Delta 5$ PTEN) and eliminate the inhibition of AKT (Wu et al., 2003) along with ras and fos activation (Yao et al., 2006, Macdonald et al., 2014).

To produce bi-genic *K14.cre/ $\Delta 5$ PTEN^{flx}* mice, two matings of heterozygous *K14.cre* were set with floxed PTEN homozygous ($\Delta 5$ PTEN^{flx}) to firstly generate bi-genic mice heterozygous for the $\Delta 5$ PTEN allele (*K14.cre/ $\Delta 5$ PTEN^{wt/flx}*) and in the second round the desired floxed PTEN homozygous *K14.cre/ $\Delta 5$ PTEN^{flx}* genotype was produced by mating between $\Delta 5$ PTEN^{flx} and *K14.cre/ $\Delta 5$ PTEN^{wt/flx}* mice. This allowed the assessment of the effects of PTEN heterozygosity and was occasionally essential when a floxed homozygous $\Delta 5$ PTEN^{flx} background gave a phenotype too severe for the Home Office UK regulations, for example in the HK1.ras 1205 transgenic line when crossed with homozygous *K14.cre/ $\Delta 5$ PTEN^{flx}* genotypes.

For PTEN analysis, as shown in figure 3.3, using primer sequences positioned in exon 4 (PTEN1F) and in exon 5 (PTEN2R) specific PTEN products, 1.3-kbp (floxed), 1.2-kbp (wild type) and 1.3/1.2-kbp (heterozygous), were produced. To verify the functional RU486 cre activity and elimination of exon 5 after topical RU486 treatment, bi-genic *K14.cre/ $\Delta 5$ PTEN^{flx}* or *K14.cre/ $\Delta 5$ PTEN^{wt/flx}* mice produced a 500-bp band when primer sequences positioned in exon 4 (PTEN1F) and in exon 6 (PTEN3R) were used (figure 3.4). This band was absent in wild type mice, *K14.cre*P-negative $\Delta 5$ PTEN^{flx} siblings or RU486-untreated bi-genic *K14.cre/ $\Delta 5$ PTEN^{flx}* mice.

A similar analysis was performed to identify *K14.cre/Isl.ROCK^{er}* mice in which cre acted to ablate the stop cassette in the *Isl.ROCK^{er}* transgene construct. The CAG expressed form of *Isl.ROCK^{er}* was detected using ROCK3F (forward) and ROCK4R (reverse). Results (figure 3.4) confirmed that RU486-mediated stop codon ablation occurred in RU486-treated *K14.cre/Isl.ROCK^{er}* mice by the presence of a 500-bp band, but not in either RU486-untreated mice or mice without K14.creP transgene. Collectively, these data consistently indicated a thriving cre/lox system in RU486-treated homozygous PTEN, heterozygous PTEN, and *Isl.ROCK^{er}*. These conditions were applied to confirm the identity of routine tumour biopsy DNA.

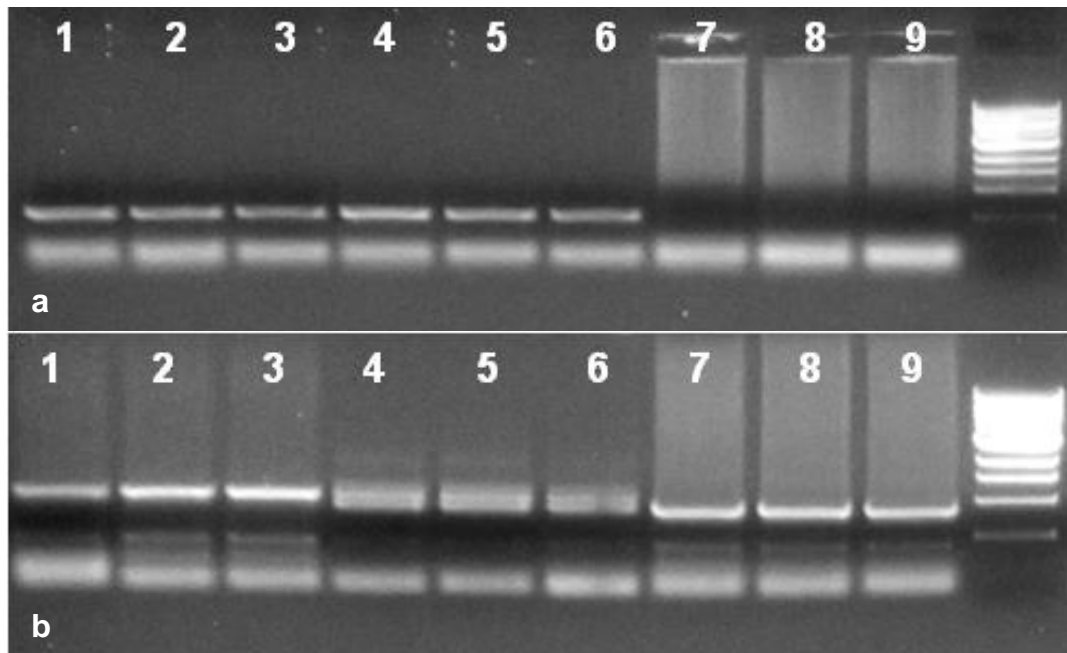


Figure 3.3 PCR analysis of *K14.creP* and $\Delta 5PTEN^{flx}$ genotypes. (a) 600-bp band represents *K14.creP* positive transgenic mice (lane 1 to 6) and is absent in the three negative controls (lane 7 to 9). (b) 1.3-kbp band represents floxed *PTEN* (lane 1 to 6), 1.3/1.2-kbp band represents heterozygous *PTEN* (lane 4 to 6) and 1.2-kbp band wild-type *PTEN* (lane 7 to 9) transgenic mice. (DNA ladder is Biolabs 1kb).

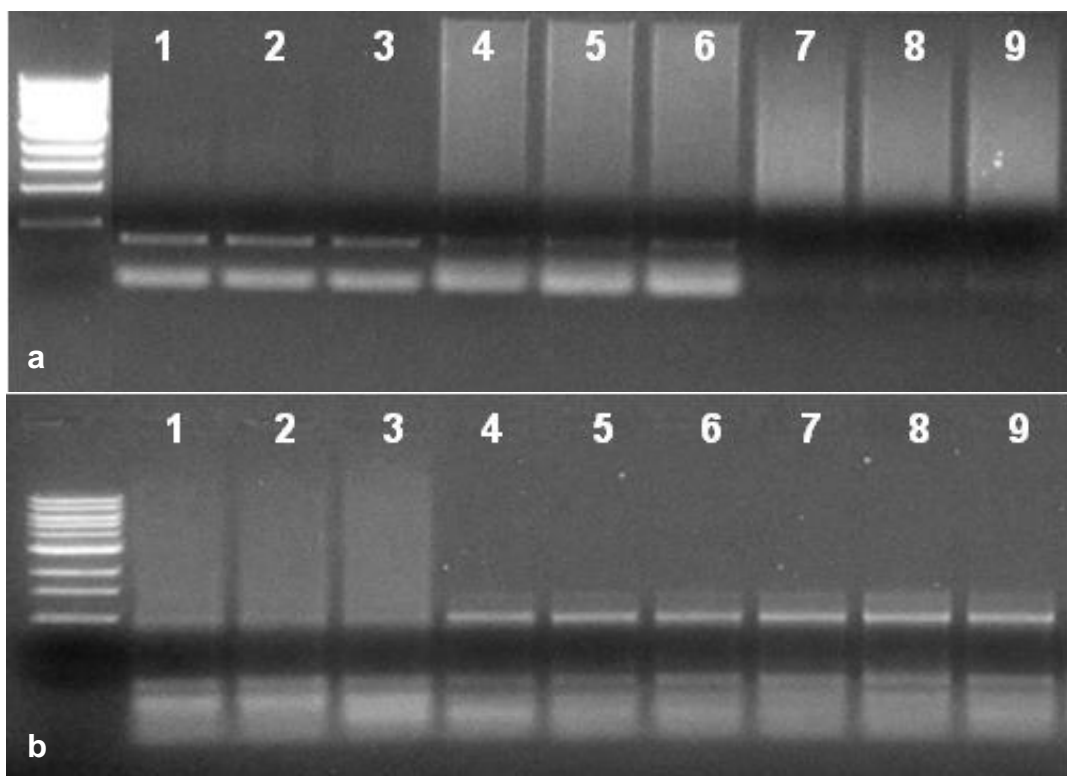


Figure 3.4 PCR analysis of $\Delta 5PTEN^{flx}$ and *ROCK^{er}* expression in RU486-treated *K14.cre/\Delta 5PTEN^{flx}* and *K14.cre/Isl.ROCK^{er}* ear-tagged biopsies. (a) RU486-treated heterozygous *PTEN* (lane 1 to 3), homozygous *PTEN* (lane 4 to 6), wild type *PTEN* (lane 7) and RU486-untreated *K14.cre/\Delta 5PTEN^{flx}* mice (lane 8 to 9). (b) RU486-untreated *K14.cre/Isl.ROCK^{er}* (lane 1 to 3) and RU486-treated *K14.cre/Isl.ROCK^{er}* mice (lane 4 to 9). (DNA ladder is Biolabs 1kb).

3.2 ROCK2 activation in transgenic mouse skin carcinogenesis

As mentioned in the introduction, ROCK plays a major role in actomyosin contraction leading to increased cellular tension which contributes to tumour progression (Rath and Olson, 2012). Therefore, the first phase of this study focused on ROCK^{er} activation alone in carcinogenesis. Previously, Samuel et al. (2011) reported that 4-HT inducible ROCK^{er} activation resulted in epidermal hyperplasia using a *K14.ROCK^{er}* transgenic mouse model. In this section, experiments focused on assessment of ROCK activation alone not only to repeat the earlier studies again this time in the background of outbred ICR mice, but also by employing a new cre/lox responsive ROCK system: *K14.cre/Isl.ROCK^{er}*. These transgenic mice were put on procedure to confirm similar results in the epidermis. This new ROCK model was necessary to activate the ROCK^{er} transgene in the same keratinocytes in the *K14.cre/PTEN^{flx}* strains and in *ras/fos/Δ5PTEN^{flx}* in the next co-operative study.

3.2.1 ROCK^{er} transgenic mouse skin induces hyperplasia

All ROCK^{er} transgenic mice were first analysed for ROCK^{er} transgene expression exploiting the green fluorescent protein (gfp) tag. This would confirm the presence and location within the epidermis of ROCK^{er} (EGFP- ROCK^{er}). Unfortunately, the GFP fluorescence was not detectable, thus, analysis of GFP expression was confirmed by immunohistochemical (IHC) techniques. As shown in figure 3.5, RU486/4-HT-treated *K14.cre/Isl.ROCK^{er}* (figure 3.5a) and 4-HT-treated *K14.ROCK^{er}* epidermis (figure 3.5b), together with RU486-treated/4-HT-untreated *K14.cre/Isl.ROCK^{er}* mouse skin (figure 3.5c) exhibited the expected EGFP-ROCK^{er} expression profile in all epidermal layers compared to control 4-HT-treated non-transgenic ICR mouse skin (figure 3.5d).

ROCK^{er} is activated upon application of 4-HT due to the estrogen receptor (er) fusion protein and activated ROCK phosphorylates its substrates, Mypt1. Thus, to determine that ROCK^{er} was activated by 4-HT treatment, *K14.cre/Isl.ROCK^{er}* and *K14.ROCK^{er}* skin biopsies were analysed for phosphorylation of the myosin

phosphatase targeting subunit (p-Mypt1) (Samuel et al., 2009a). Consistent with prior findings (Samuel et al., 2009a, 2011), RU486-/4-HT-treated *K14.cre/lsl.ROCK^{er}* and 4-HT-treated *K14.ROCK^{er}* mice (figure 3.5 e,f) showed strong Mypt1 phosphorylation throughout the follicular and interfollicular layers, thus confirming their expression from a K14 promoter. In contrast, little trace of p-Mypt1 was observed in RU486-treated/4-HT-untreated *K14.cre/lsl.ROCK^{er}* mice (figure 3.5g) whilst p-Mypt1 was undetectable in non-transgenic normal skin (figure 3.5h). Therefore, these experiments confirmed expression of the ROCK^{er} protein and its activation upon 4-HT application, in all epidermal layers including hair follicles in *K14.ROCK^{er}* and *K14.cre/lsl.ROCK^{er}* mice.

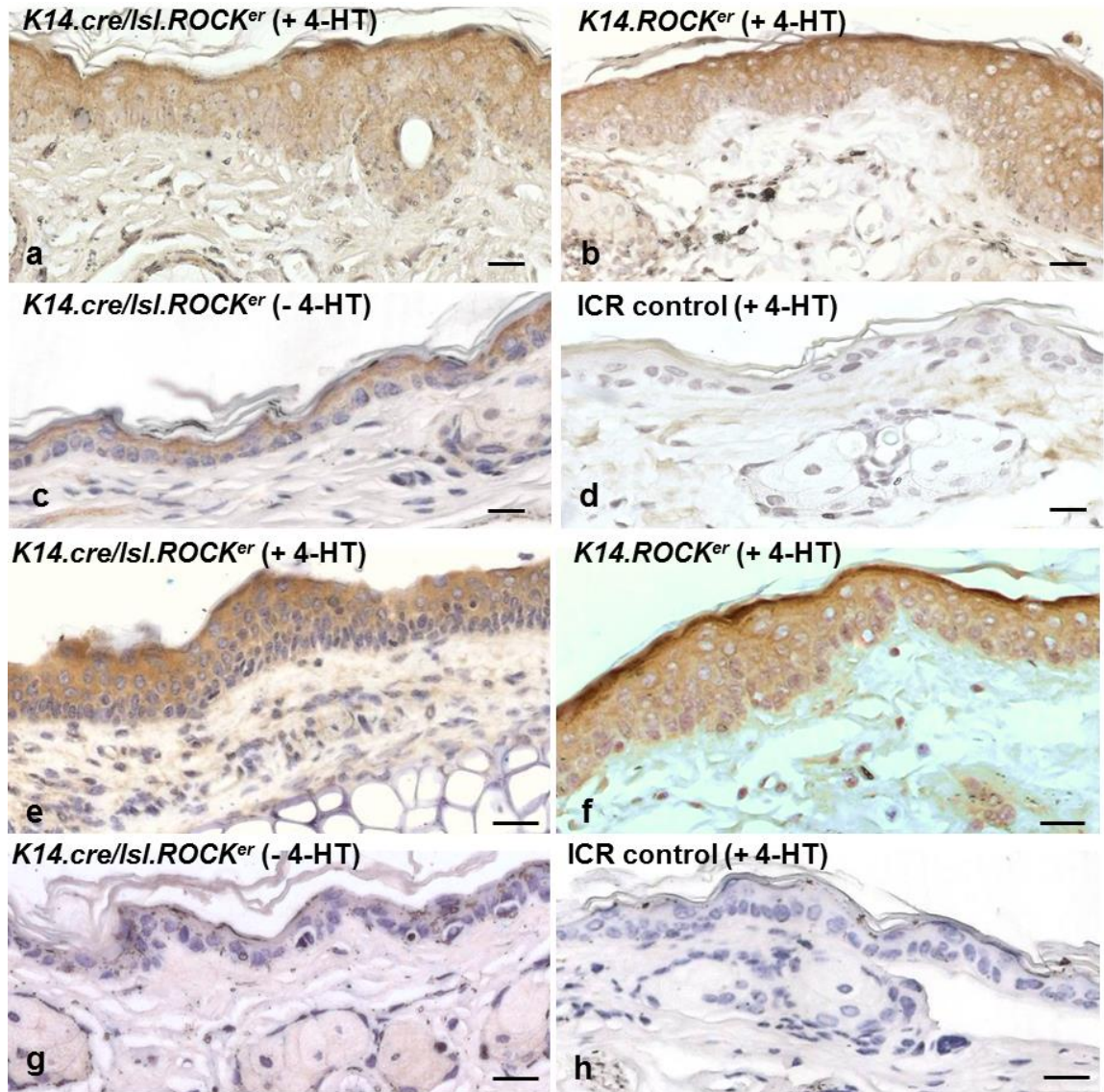


Figure 3.5 IHC analysis of GFP-tagged ROCK^{er} transgene [a-d] and p-Mypt1 of ROCK substrate [e-h]. (a) Strong expression (brown) of exogenous ROCK (EGFP- ROCK^{er}) throughout epidermal layers of RU486-/4-HT-treated *K14.cre/lsl.ROCK^{er}* and (b) 4-HT-treated *K14.ROCK^{er}* hyperplasia histotypes. (c) GFP expression was manifested in normal epidermis of RU486-treated/4-HT-untreated *K14.cre/lsl.ROCK^{er}*. (d) GFP was not expressed in normal epidermal layer of 4-HT-treated control ICR.

Elevated p-Mypt1 expression appears in all epidermal layers and follicles of (e) RU486/4-HT-treated *K14.cre/lsl.ROCK^{er}* skin and (f) 4-HT induced *K14.ROCK^{er}* hyperplasia. (g) Little trace of p-mypt1 was detected in normal histotype of RU486-treated/4-HT-untreated *K14.cre/lsl.ROCK^{er}* and (h) p-Mypt1 was undetectable in 4-HT-treated control epidermis. (Scale bar: 100µm).

In order to compare the *K14.ROCK^{er}* and *K14.cre/lsl.ROCK^{er}* models to see if they gave the same outcomes as in previous experiments, 4-5 weeks old *K14.ROCK^{er}* adult mice were first bred onto the HK1 ICR background (4 rounds of breeding) and a cohort of 10 male heterozygous mice were put on procedure. Topical treatment with a volume of 15µl of a 10mg/ml solution of 4-hydroxytamoxifen (4-HT) dissolved in ethanol on both tagged and untagged ears was performed three times per week to activate ROCK^{er} in the epidermis. Transgenic mice controls (n= 6 per cohort) received ethanol alone and ICR controls (n= 6 per cohort) received 4-HT. *K14.cre/lsl.ROCK^{er}* mice received identical treatment but the adult mice were also pre-treated with RU486 (2µg RU486 in 20 µl ethanol per ear) for one week.

After 20 weeks of treatment, mice were assessed for phenotypes and biopsied to investigate the histotypes of ROCK activation. All 4HT-treated ROCK^{er} mice showed a very mild, extremely subtle phenotype of a slightly thickened ear, while no phenotypes were obtained in 4-HT-untreated ROCK^{er} mice or control normal ICR mice treated with 4-HT (figure 3.6a-f). Histological analysis revealed that both 4HT-treated *K14.ROCK^{er}* (figure 3.6g) and *K14.cre/lsl.ROCK^{er}* mice (figure 3.6h) had induced epidermal hyperplasia. Control RU486-treated/4-HT-untreated *K14.cre/lsl.ROCK^{er}* mice and 4-HT-treated non-transgenic ICR mice remained normal (figure 3.6i,j).

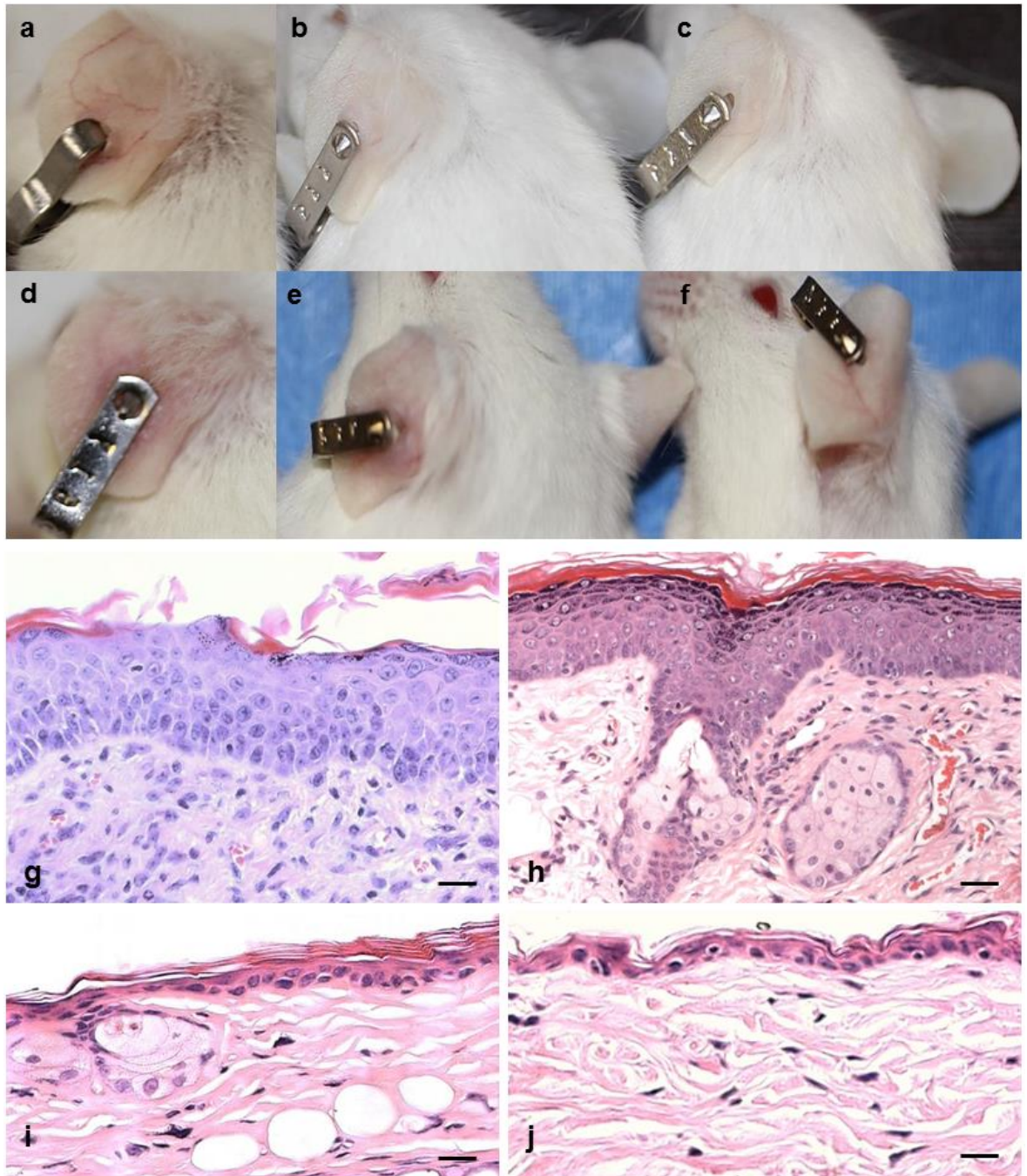


Figure 3.6 (a) 4-HT-untreated *K14.ROCK^{ef}*, (b) RU486-treated/4-HT-untreated *K14.cre/Isl.ROCK^{ef}* transgenic mice and (c) 4-HT-untreated non-transgenic ICR control mice; together with (d) 4-HT-treated *K14.ROCK^{ef}*, (e) RU486/4-HT-treated *K14.cre/Isl.ROCK^{ef}* transgenic mice and (f) 4-HT-treated non-transgenic ICR control mice at 20 weeks showed no differences in phenotypes.

However, from histology analysis; (g) 4-HT-treated *K14.ROCK^{ef}* and (h) RU486-/4-HT-treated *K14.cre/Isl.ROCK^{ef}* epidermis showed thickened layers and hyperplasia histotypes. (i) RU486-treated/4-HT-untreated *K14.cre/Isl.ROCK^{ef}* and (j) 4-HT-treated non-transgenic ICR epidermis showed a similar typical normal histotype. (Scale bar: 100 μ m).

3.2.2 Expression of differentiation markers in ROCK hyperplasia

Keratin K1 was analysed by double-labelled immunofluorescence and its expression examined to assess any changes in early keratinocyte differentiation. Keratin K1 is expressed in all supra-basal layers of the epidermis as they commit to differentiate. Keratin K1 expression is not only an important marker for early epidermal differentiation, but it is also an important indicator of the differentiation state and has been successfully employed as a marker of tumour progression as decreased expression of K1 marker appears as tumours convert to carcinomas (Greenhalgh et al., 1993a-c, Yao et al., 2006, 2008, Macdonald et al., 2014). Analysis of keratin K1 expression in hyperplastic *K14.cre/Isl.ROCK^{er}* epidermis showed a normal, relatively ordered expression in the supra-basal epidermal layers. Keratin K1 expression appears scattered unevenly in non-transgenic ICR normal epidermis due to the supra-basal layer being only one cell thick (figure 3.7a,b).

Skin biopsies were also analysed for the expression of keratin K6 by double-labelled immunofluorescence. Typically, keratin K6 shows no expression in normal interfollicular epidermis, but expression appears in the upper part of the hair follicles. In addition, in wounded or stressed, interfollicular epidermis keratin K6 expression is always very strong and often associated with wounding or keratinocyte hyperproliferation (Rothnagel et al., 1999). As shown in figure 3.7c, keratin K6 expression was correctly limited to the hair follicles of normal non-transgenic ICR epidermis. Interestingly, K6 expression is patchy in hyperplastic *K14.cre/Isl.ROCK^{er}* epidermis (figure 3.7d). Consistent with a study by Rothnagel et al. (1999), K6 which is a marker of proliferation was expressed in all epidermal layers of *HK1.ras* and *HK1.fos* hyperplasia (figure 3.7e,f). Both keratin K1 and K6 were counterstained with keratin K14 (red) which represents the keratinocytes. In ROCK hyperplasia K14 was expressed throughout the epidermis and hair follicles (figure 3.7a-f).

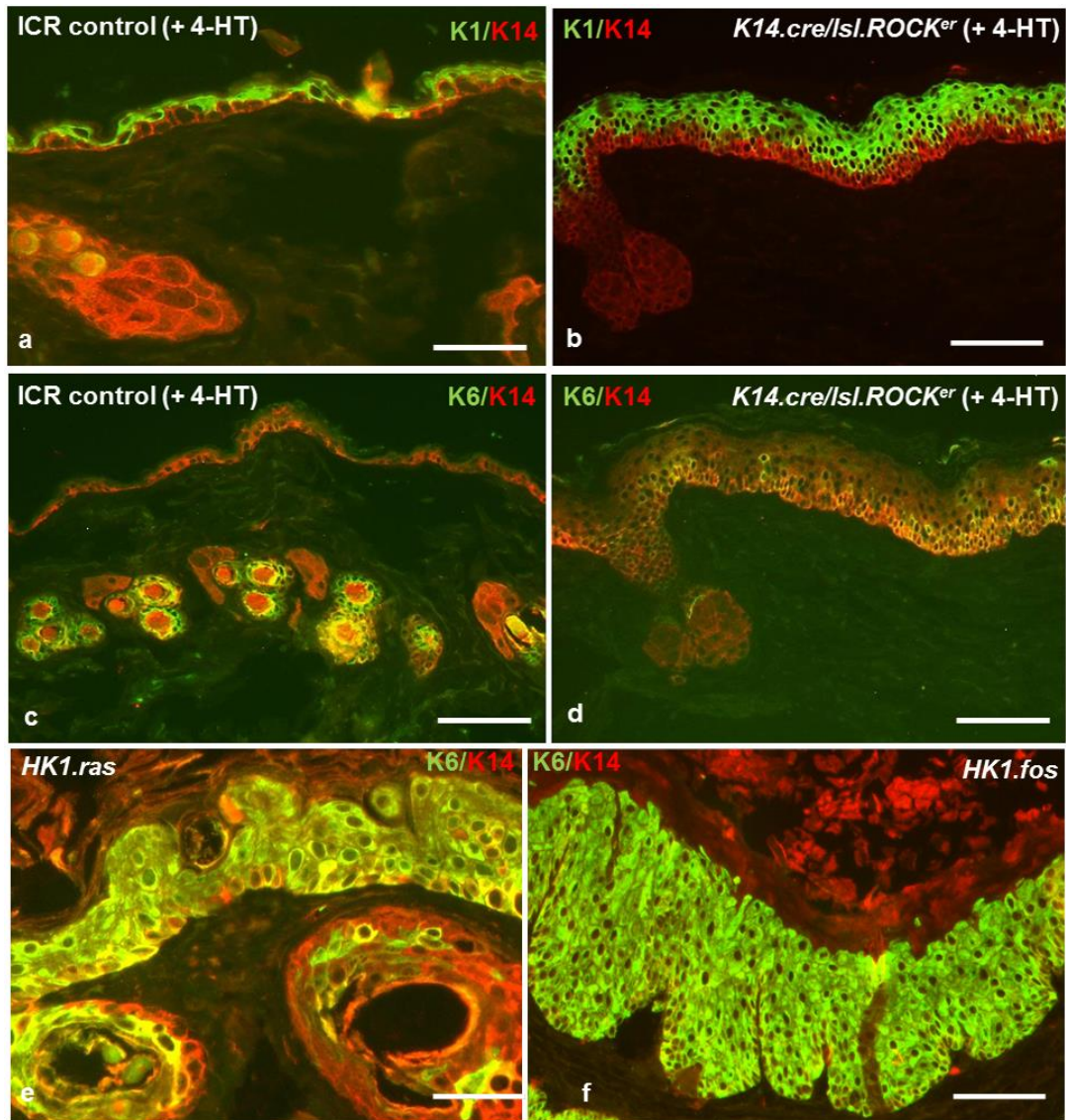


Figure 3.7 Immunofluorescence analysis of keratin K1 and K6 markers in RU486-/4-HT-treated *K14.cre/lsl.ROCK^{er}* hyperplasia. (a) Normal non-transgenic ICR epidermis shows K1 expression in one cell thick layer. (b) Hyperplastic *K14.cre/lsl.ROCK^{er}* epidermis exhibits strong K1 expression in the supra-basal layers. (c) Normal non-transgenic ICR epidermis displays limited K6 expression only in the hair follicles. (d) Patchy K6 expression in hyperplastic *K14.cre/lsl.ROCK^{er}* epidermis. (e) Typical K6 expression in all epidermal layers of *HK1.ras* and (f) *HK1.fos* hyperplasia (Scale bar: 100 μ m).

3.2.3 Summary

Collectively, this study indicated that ROCK2 activation in this latest *cre/lox* ROCK2 model (*K14.cre/lsl.ROCK^{er}*) gave identical results to the previous outcome of ROCK2 activation in *K14.ROCK^{er}* transgenic mice (Samuel et al., 2009a). These data show that even though there were very mild phenotypes in both *K14.ROCK^{er}* and *K14.cre/lsl.ROCK^{er}* mice that were almost undistinguishable from control ICR mice, from histology analysis, ROCK2 activation resulted in an epidermal hyperplastic histotype which was distinguishable from the normal control ICR mice. Thus, as anticipated, there appears to be little or no difference between *K14.ROCK^{er}* and *K14.cre/lsl.ROCK^{er}* mice in terms of both gross phenotype and histotype. Furthermore, although it is well known for keratin K6 to become highly expressed during keratinocyte proliferation *in vivo* and *in vitro* (Rothnagel et al., 1999), or under hyperproliferative conditions mediated by oncogene expression (Greenhalgh et al., 1993a-c); expression of K6 also indicates a stressed epidermal state an example of which is when TGF β 1 overexpression was targeted to the epidermis using the HK1 vector (Sellheyer et al., 1993), this led to inhibition of epidermal proliferation although IFC analysis revealed high levels of K6 expression. In this study, K6 expression suggested that ROCK activation induced differentiation activity which associated with hyperplasia. Lock and Hotchin, (2009) have shown that knockdown of ROCK2 in HaCat cells resulted in reduced differentiation. Therefore, in this study, differentiation is expected to increase with ROCK2 activation but the end result is epidermal hyperplasia. However, the lack of keratin K6 proliferation marker displayed by odd and patchy expression suggests that the differentiation part is still listening to the role of ROCK2 in differentiation. This unique expression of K6 is also seen in Δ 5PTEN^{fix} cohorts that give similar odd differentiation responses (chapter 3.5). There was no sign of tumour formation with ROCK2 activation for up to 5 months of continuous treatment in this study. Therefore, this result suggests that additional mutations are required in co-operation with ROCK2 activation for tumour formation. Accordingly, the next approach in this study investigated the co-operation between ROCK and an activated ras oncogene to examine their potential co-operation in skin carcinogenesis and determine at which stage their co-operation drives progression.

3.3 Co-operation of ROCK2 and *HK1.ras* activation in transgenic mouse skin carcinogenesis

Previous studies have shown that activation of the ras^{Ha} oncogene either by DMBA initiation (Brown et al., 1990, Balmain and Yuspa, 2014), viral infection (Roop et al., 1986) or grafting models of multistage carcinogenesis (Greenhalgh and Yuspa, 1988, Strickland et al., 1988) confirmed an early role leading to formation of papillomas. Of the numerous transgenic mouse studies, Greenhalgh et al., (1993a) demonstrated that exclusive epidermal expression of activated ras^{Ha} driven by truncated human keratin K1 promoter (*HK1.ras*) produced an initiated epidermis (*HK1.ras*¹²⁷⁶) and wound dependent regressing squamous papillomas (*HK1.ras*¹²⁰⁵); but no conversion to carcinoma. These mice were therefore ideal to study the mechanism of papillomatogenesis (Greenhalgh et al., 1993c, 1995, 1996) or malignant conversion (Macdonald et al., 2014).

Earlier data showed that ROCK activation in transgenic mouse skin resulted in epidermal hyperplasia without tumour formation, and two-stage chemical carcinogenesis (DMBA/TPA) on these ROCK mice revealed an increased carcinoma conversion rate (Samuel et al., 2011) that suggested the need for additional, possibly earlier events. Even though this chemical carcinogenesis study suggested the indirect link between ROCK and ras^{Ha} activation, yet there is still no definite evidence of ROCK2 and ras synergism in the skin carcinogenesis models. However, links already exist and can be contradictory.

Studies have demonstrated that the interrelationship between RhoA (which act as an upstream regulator of ROCK) and ras in increasing cell proliferation in Swiss-3T3 cells occurs by inhibiting p21 expression (Olson et al., 1998, Sahai et al., 2001); and these data have implications for the p21 findings in this current model (below). Conversely, studies have also shown that inhibition of ROCK activities have little effect on ras-dependent-proliferation and showed no changes in p21 levels after treatment of fibroblast cell lines with the ROCK inhibitor, Y-27632 (Sahai et al., 2001). Given the complexity and feedback loops in these inter-related signalling pathways it appeared that ERK/MAPK signalling from ras-transformed cells bypassed this inhibition via the downregulation of ROCK (1 and 2) expression (Sahai et al., 2001).

In the chemical carcinogenesis experiments, there is no clear indication as to whether ROCK2 co-operated with ras^{Ha} as in the absence of TPA promotion, a single dose of DMBA on ROCK alone, which supposedly activated endogenous c-ras^{Ha} (Strickland et al., 1988, Greenhalgh et al., 1995) failed to elicit tumours; in a similar fashion to ROCK activation alone (Olson, unpublished data). Thus the questions remains as to what stage of carcinogenesis did this potential ROCK2/ ras^{Ha} synergism become active and what was the underlying mechanism?. Therefore, to investigate any co-operation in multistage tumour formation between ras oncogene and ROCK, ROCK^{er} mice were crossed with both lines of HK1.ras mice and the phenotypes produced by these bi-genic ROCK/ ras progeny were analysed.

3.3.1 Confirmation of ROCK^{er} transgene in bi-genic ROCK/ras^{1205} mouse and expression of downstream targets

$\text{K14.ROCK}^{\text{er}}/\text{HK1.ras}^{1205}$ mice were first analysed for expression of the ROCK^{er} fusion protein-tagged with the green fluorescent protein (EGFP) by IHC analysis. Unfortunately the GFP was not detectable by fluorescence microscopy thus the ROCK^{er} transgene was confirmed in 4-HT-treated $\text{K14.ROCK}^{\text{er}}/\text{HK1.ras}^{1205}$ epidermal layers (figure 3.8a). IHC analysis of p-Mypt1, a downstream substrate of ROCK was performed on the $\text{K14.ROCK}^{\text{er}}/\text{HK1.ras}^{1205}$ mouse skin to further confirm that exogenous ROCK^{er} was activated by induction with 4-HT (figure 3.8b). These results showed that p-Mypt1 was expressed throughout the epidermal layers of $\text{K14.ROCK}^{\text{er}}/\text{HK1.ras}^{1205}$ mice.

Analysis of GFP and p-Mypt1 expression was performed on 4-HT-treated HK1.ras^{1205} (figure 3.8c,d) and 4-HT-untreated $\text{K14.ROCK}^{\text{er}}/\text{HK1.ras}^{1205}$ (figure 3.8e,f) mice. Conversely, GFP was not expressed in 4-HT-treated HK1.ras^{1205} epidermis (figure 3.8c) as compared to 4-HT-untreated $\text{K14.ROCK}^{\text{er}}/\text{HK1.ras}^{1205}$ epidermis (figure 3.8e) where GFP was expressed. However, both mice showed low p-Mypt1 expression (figure 3.8d,f) as exogenous ROCK was not activated compared to 4-HT-treated $\text{K14.ROCK}^{\text{er}}/\text{HK1.ras}^{1205}$ mouse skin (figure 3.8b). These findings confirmed ROCK^{er} transgene expression and activation by 4-HT, again repeating the earlier result in the ROCK activation alone cohorts; and this

finding also indicated that effects of ROCK2 synergism in the bi-genic ROCK/ras¹²⁰⁵ cohorts is mediated in part via phosphorylation of Mypt1.

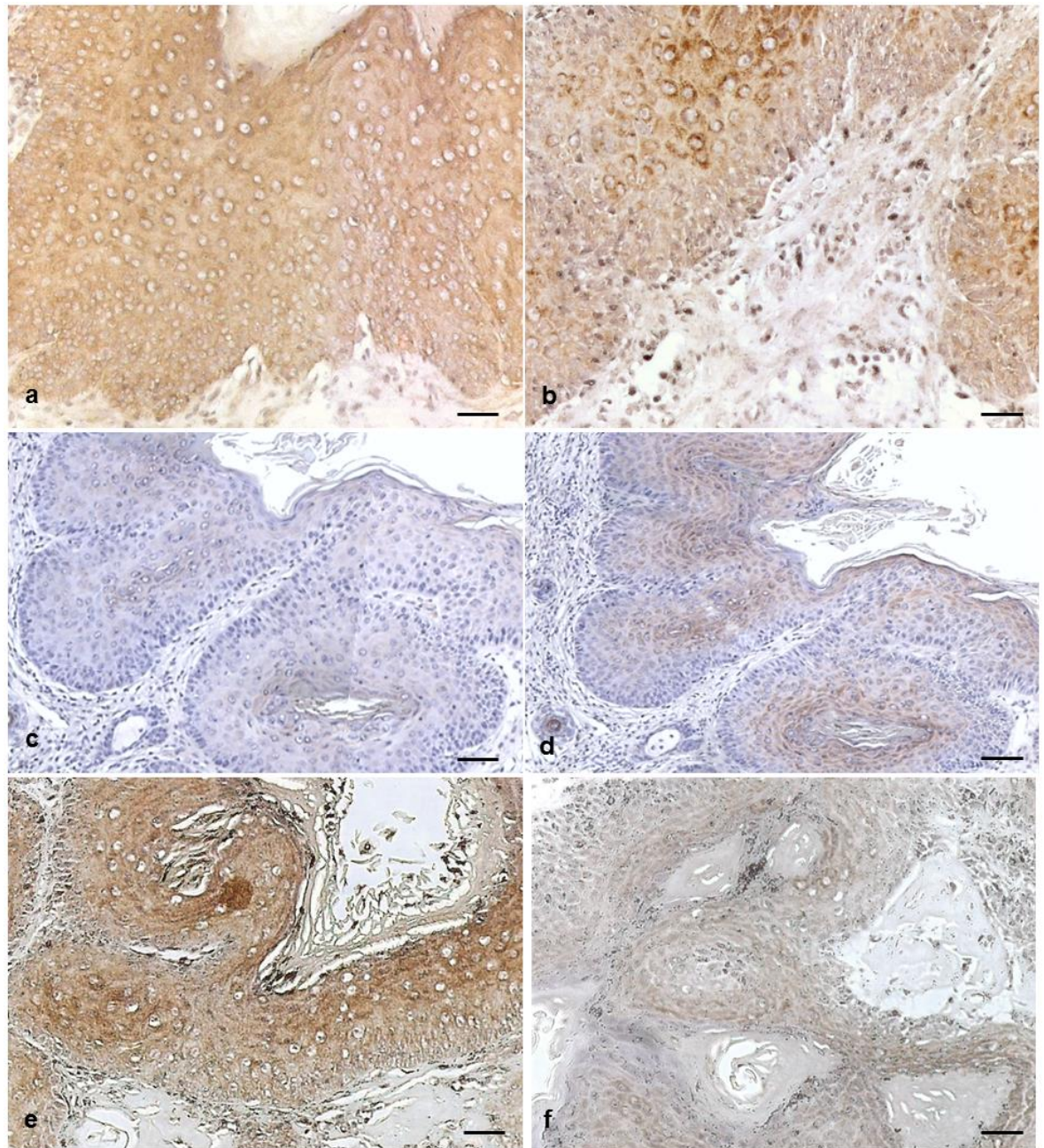


Figure 3.8 IHC analysis of GFP and p-MYPT1 expression in *K14.ROCK^{er}/HK1.ras¹²⁰⁵* tumours. (a) 4-HT-treated *K14.ROCK^{er}/HK1.ras¹²⁰⁵* wdSCC histotype exhibited high expression of GFP and (b) pMypt1 in all epidermal layers. (c) 4-HT-treated *HK1.ras¹²⁰⁵* papilloma showed no expression of GFP and (d) faint expression of p-Mypt1. (e) GFP expression was detected in 4-HT-untreated *K14.ROCK^{er}/HK1.ras¹²⁰⁵* papilloma but (f) only low levels of p-Mypt1 were displayed due to a lack of exogenous ROCK activity. (Scale bar: 100 μ m).

3.3.2 ROCK2 co-operates with ras^{Ha} to elicit benign tumours (at 8 weeks)

As cited in the introduction, two lines of *HK1.ras* mice were employed in these studies. The first series of experiments used the 1205 line resulting in wound sensitive papillomas in 100% of animals. Later cohorts employed the *HK1.ras* line 1276, a less potent oncogenic insult, but its initiation was vital to the success of establishing viable, bi-genic and tri-genic genotypes for later experiments.

In repeated experiments, cohorts of *K14.ROCK^{er}/HK1.ras¹²⁰⁵* (n= 12) and *HK1.ras¹²⁰⁵* (n= 6) age-matched siblings (6-7 week old) were treated with 15µl of 10mg/ml 4-hydroxytamoxifen (4-HT) per dorsal surface of both tagged and untagged ears, initially for up to 12 weeks with *K14.ROCK^{er}/HK1.ras¹²⁰⁵* and *HK1.ras¹²⁰⁵* (n= 5 each) controls receiving ethanol alone. At 8 weeks, both *K14.ROCK^{er}/HK1.ras¹²⁰⁵* and *HK1.ras¹²⁰⁵* mice had developed tumours with little difference when compared to controls either with or without 4-HT treatment (figure 3.9); although there was a suggestion that control *HK1.ras¹²⁰⁵* mice receiving 4-HT resulted in slightly smaller tumours compared to previous studies.

Histological analysis of 4-HT-treated *K14.ROCK^{er}/HK1.ras¹²⁰⁵* tumours (figure 3.10a) showed a typical benign papilloma histotype, with a relatively well-ordered keratinocyte differentiation pattern despite an expansion of each epidermal layer due to the proliferation and subsequent differentiation. This histotype was similar to 4-HT-treated *HK1.ras¹²⁰⁵* papillomas (figure 3.10b). For the *HK1.ras¹²⁰⁵* cohorts, these results are consistent with all previous studies as *HK1.ras¹²⁰⁵* mice produce benign papillomas on the tagged ear due to the wounding which exerts a promotion stimulus (Greenhalgh et al., 1993a, Yao et al., 2006).

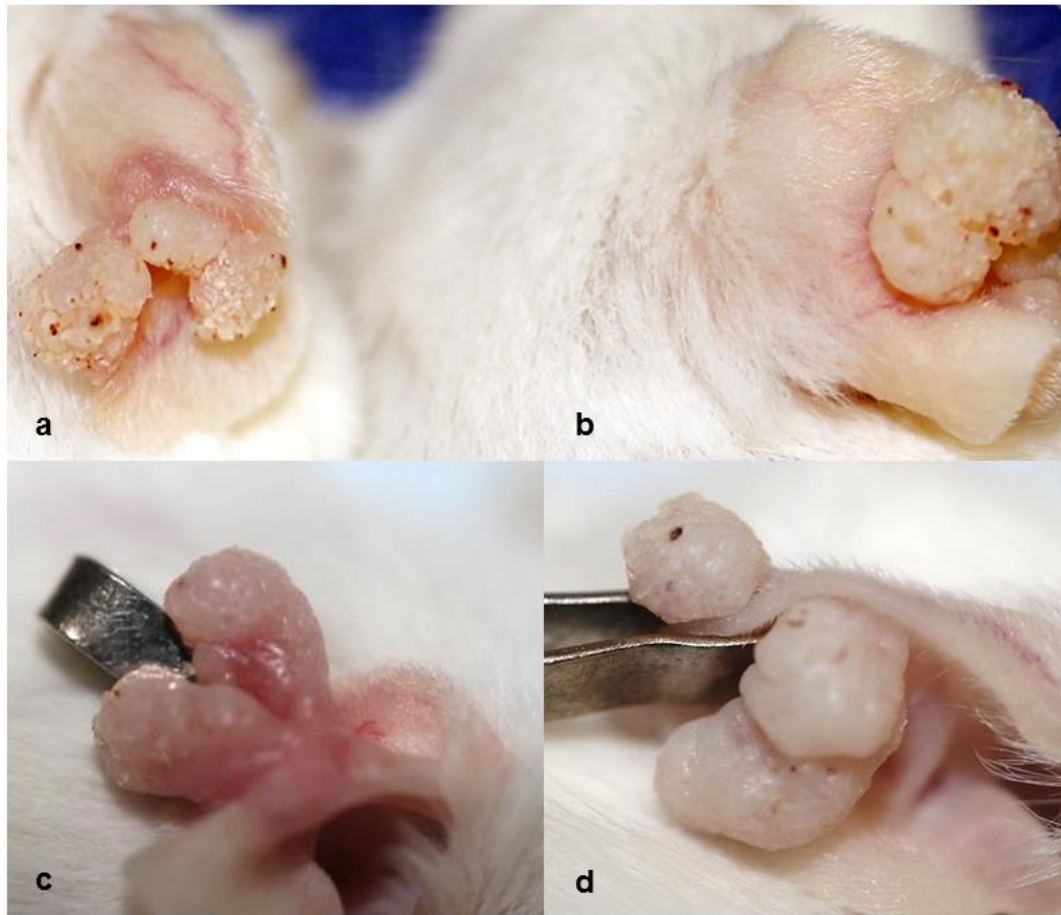


Figure 3.9 Phenotypes of *K14.ROCK^{er}/HK1.ras¹²⁰⁵* mice at 8 weeks. (a) 4-HT-treated *K14.ROCK^{er}/HK1.ras¹²⁰⁵* and (b) *HK1.ras¹²⁰⁵* mice; together with (c) 4-HT-untreated *K14.ROCK^{er}/HK1.ras¹²⁰⁵* and (d) *HK1.ras¹²⁰⁵* mice display papillomas in similar size.

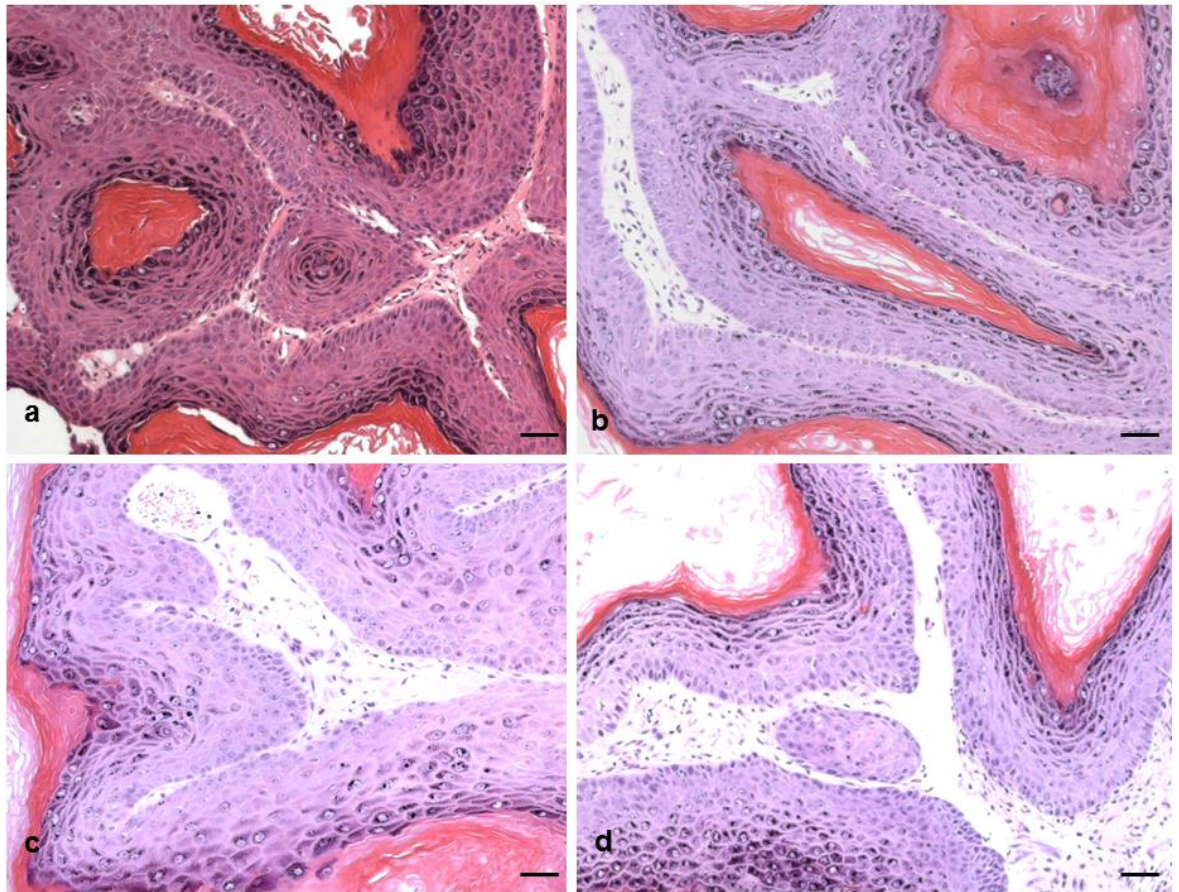


Figure 3.10 H&E staining of *K14.ROCK^{er}/HK1.ras¹²⁰⁵* papillomas at 8 weeks. (a) 4-HT-treated *K14.ROCK^{er}/HK1.ras¹²⁰⁵* and (b) *HK1.ras¹²⁰⁵* epidermis; together with (c) 4-HT-untreated *K14.ROCK^{er}/HK1.ras¹²⁰⁵* and (d) *HK1.ras¹²⁰⁵* epidermis remain benign papillomas with no evidence of conversion at this stage. (Scale: 100 μ m).

Given this lack of overt co-operation, skin biopsies were analysed for the expression of keratins K1 and K6 by a double-labelled immunofluorescence. As shown in figure 3.11(a,b), both 4-HT-treated *K14.ROCK^{er}/HK1.ras¹²⁰⁵* and *HK1.ras¹²⁰⁵* epidermis displayed strong K1 expression (green) in the benign papillomas in a typical, supra-basal expression profile. All biopsies were counterstained with keratin K14 (red) to highlight the epidermis and hair follicles. However, in some *K14.ROCK^{er}/HK1.ras¹²⁰⁵* papillomas (H&E benign), areas of K1 expression showed a more yellow colour as shown by the arrow in figure 3.11(a). This suggested a decreased expression of K1 (green) in that area, which has been suggestive of malignant conversion in all previous *HK1.ras* model studies (Yao et al., 2006, Macdonald et al., 2014) and this prompted a repeat experiment and analysis at later time periods. Both 4-HT-treated *K14.ROCK^{er}/HK1.ras¹²⁰⁵* and *HK1.ras¹²⁰⁵* papillomas demonstrated uniform and intense K6 expression throughout the epidermal layers (figure 3.11c,d), a finding previously associated with both keratinocyte proliferation and situations of epidermal stress.

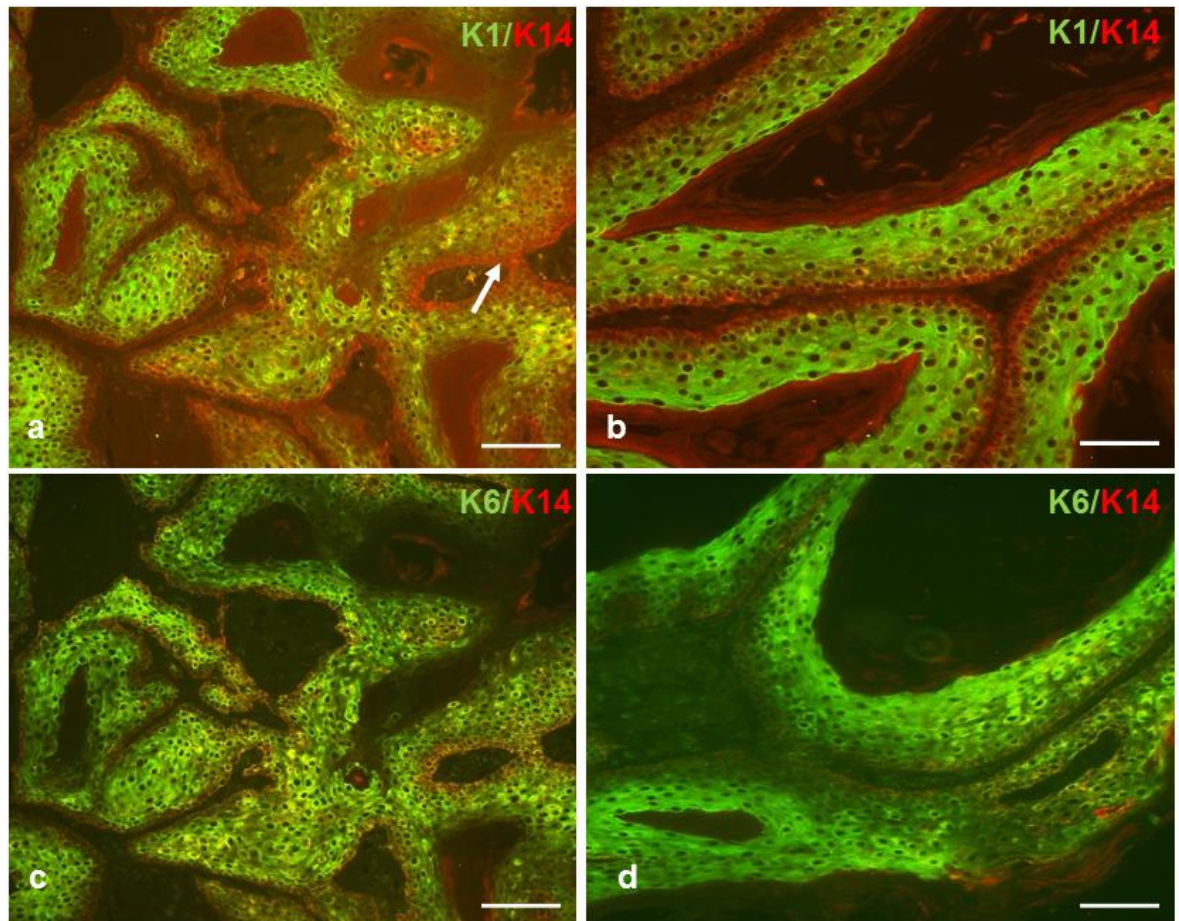


Figure 3.11 Immunofluorescence analysis of K1/K14 and K6/K14 expression at 8 weeks in 4-HT-treated *K14.ROCK^{er}/HK1.ras¹²⁰⁵* and *HK1.ras¹²⁰⁵* tumours. (a) *K14.ROCK^{er}/HK1.ras¹²⁰⁵* and (b) *HK1.ras¹²⁰⁵* epidermis exhibit strong K1 expression in the supra-basal layers confirming that the papillomas remain benign. (c) *K14.ROCK^{er}/HK1.ras¹²⁰⁵* and (d) *HK1.ras¹²⁰⁵* papillomas show K6 expression throughout epidermal layers. (Scale bar: 100 μ m).

3.3.3 ROCK2 co-operates with ras^{Ha} to elicit malignant conversion (at 12 weeks)

Experiments were repeated with cohorts of *K14.ROCK^{er}/HK1.ras¹²⁰⁵* (n= 12) and *HK1.ras¹²⁰⁵* (n= 6) mice due to unique finding of K1 expression in the bi-genic ROCK/ras¹²⁰⁵ benign tumours at 8 weeks. Therefore, all mice were kept on procedure for 12 weeks to test whether the co-operation between ROCK and ras¹²⁰⁵ would produce any malignant tumours. At 12 weeks, again there was little difference in tumour size or appearance between 4-HT-treated *K14.ROCK^{er}/HK1.ras¹²⁰⁵* and *HK1.ras¹²⁰⁵* transgenic mice (figure 3.12). However, at this time point, their histotypes were quite different.

At this time point, the previous suggestion of papilloma progression to a later stage as determined by K1 expression proved to be correct. Histological analysis of 4-HT-treated *K14.ROCK^{er}/HK1.ras¹²⁰⁵* demonstrated a mixed histotype with areas of malignant transformation, predominantly to wdSCC (figure 3.13a); whilst 4-HT-treated *HK1.ras¹²⁰⁵* papillomas remained benign at 12 weeks (figure 3.13b). The composite *K14.ROCK^{er}/HK1.ras¹²⁰⁵* tumour histology highlights a junction between papilloma and carcinoma (figure 3.13a - arrows), while the *HK1.ras¹²⁰⁵* tumour showed a thickened folded papillomatous epidermis (figure 3.13b) which is a typical characteristic of benign tumours. At higher magnification, the area of malignant conversion showed a mainly well-differentiated squamous cell carcinoma (wdSCC) histotype with disorganisation in the epidermal basal layers and exhibited invasive keratinocytes which penetrated through the basal layer into the dermis together with an appearance of mitotic body (figure 3.13c - arrow). It should be noted that at this 12 week time point, *K14.ROCK^{er}/HK1.ras¹²⁰⁵* tumours displayed mainly wdSCC histotype as determined by K1 expression below.

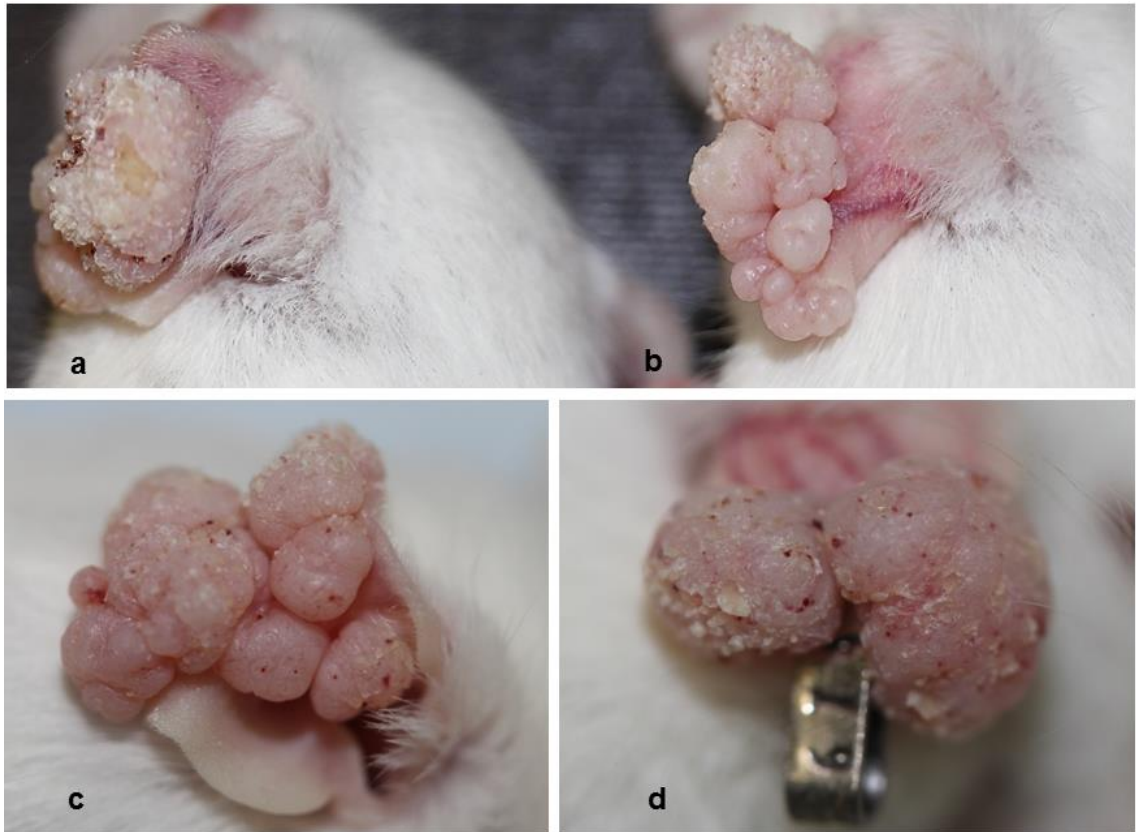


Figure 3.12 Phenotypes of *K14.ROCK^{ef}/HK1.ras¹²⁰⁵* and *HK1.ras¹²⁰⁵* mice at 12 weeks. (a) 4-HT-treated *K14.ROCK^{ef}/HK1.ras¹²⁰⁵* and (b) *HK1.ras¹²⁰⁵* mice; together with (c) 4-HT-untreated *K14.ROCK^{ef}/HK1.ras¹²⁰⁵* and (d) *HK1.ras¹²⁰⁵* mice showed similar-sized papillomas and tumour clusters.

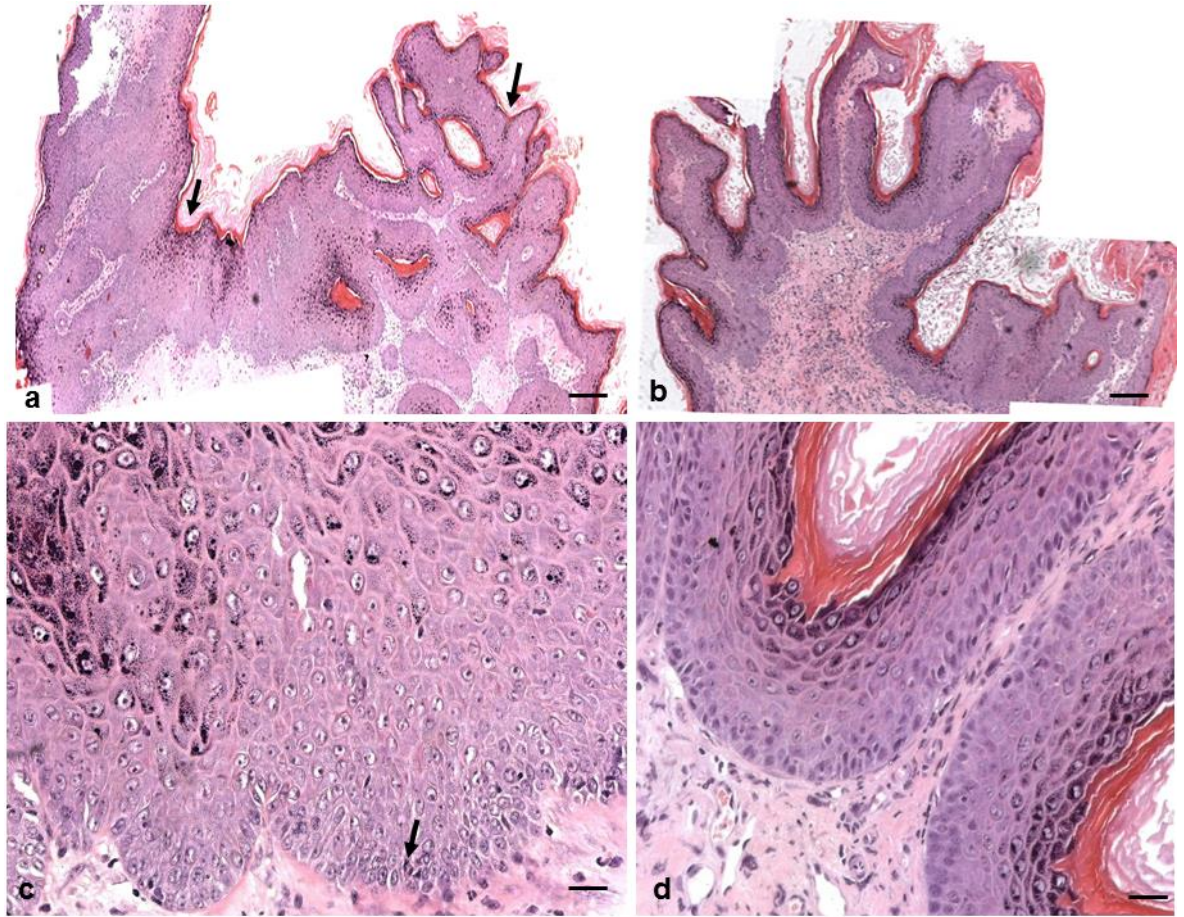


Figure 3.13 H&E staining of 4-HT-treated *K14.ROCK^{er}/HK1.ras¹²⁰⁵* and *HK1.ras¹²⁰⁵* tumours at 12 weeks. (a) Composite micrograph of *K14.ROCK^{er}/HK1.ras¹²⁰⁵* epidermis demonstrating a mixed histotype from benign papilloma (right arrow) to malignant conversion (left arrow) to wdSCC and progression to some SCCs. (b) Conversely, composite micrograph of *HK1.ras¹²⁰⁵* epidermis shows a typical benign papilloma histotype. (c) Higher magnification of *K14.ROCK^{er}/HK1.ras¹²⁰⁵* SCC area shows disorganisation of epidermal architecture especially in basal layers together with the appearance of mitotic figures (arrow). (d) In contrast, higher magnification of *HK1.ras¹²⁰⁵* papilloma exhibit well-organised basal layers. (Scale bar: 100µm in a,b; 50µm in c,d).

Given that decreased K1 expression is a useful marker of tumour progression from benign to carcinoma stages, *K14.ROCK^{ef}/HK1.ras¹²⁰⁵* tumours (at 12 weeks) were analysed for the expression of K1 to confirm malignant conversion. As shown in figure 3.14a, K1 expression became reduced and the micrograph appeared yellow due to the background of uniform K14 expression (red); thus this indicated a wdSCC histotype (Yao et al., 2006, Macdonald et al., 2014). Interestingly, in light of the findings in alternate models, K6 expression in *K14.ROCK^{ef}/HK1.ras¹²⁰⁵* wdSCC appeared in the typical fashion observed previously, with strong uniform expression in all epidermal layers (figure 3.14c). This contrasted with K6 expression in activated ROCK^{ef} hyperplasia (above) and also bi-genic ROCK/ Δ 5PTEN^{flx} (below). In all control genotypes, both K1 and K6 expression after 12 weeks (e.g. 4-HT-treated *HK1.ras¹²⁰⁵* benign histotypes - figure 3.14b,d) remained identical to K1 and K6 expression in *HK1.ras¹²⁰⁵* histotypes at 8 weeks (figure 3.11b,d).

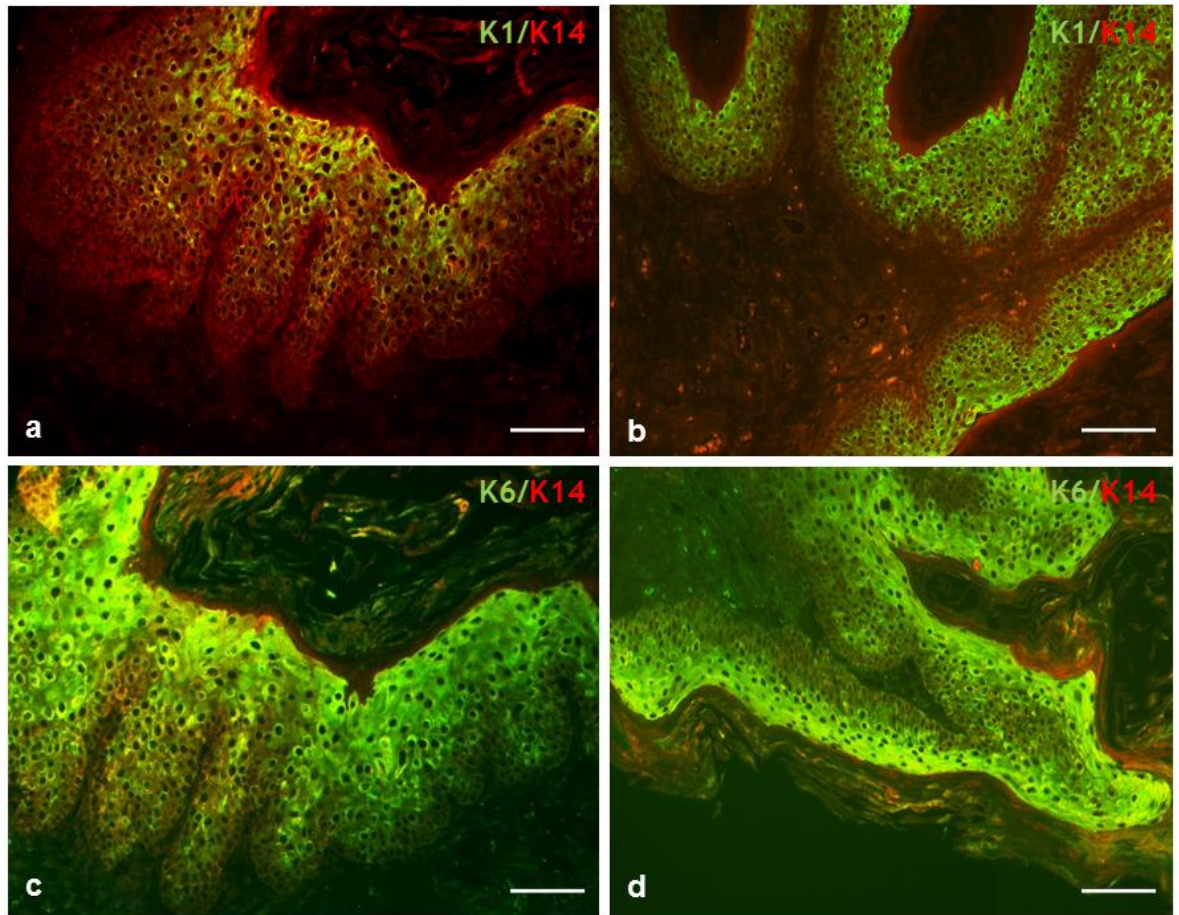


Figure 3.14 Immunofluorescence analysis of K1/K14 and K6/K14 expression at 12 weeks in 4-HT-treated *K14.ROCK^{er}/HK1.ras¹²⁰⁵* and *HK1.ras¹²⁰⁵* tumours. (a) *K14.ROCK^{er}/HK1.ras¹²⁰⁵* epidermis displays reduced K1 expression and indicative of a carcinoma histotype. (b) *HK1.ras¹²⁰⁵* papilloma exhibits strong K1 expression in the supra-basal layers and remained benign. (c) Keratin K6 expression in *K14.ROCK^{er}/HK1.ras¹²⁰⁵* wdSCC and (d) in *HK1.ras¹²⁰⁵* benign papilloma appeared uniform in all epidermal layers which is similar to a typical K6 expression in response to hyperproliferation. (Scale bar: 100µm).

3.3.4 Expression of p53 and p21 in bi-genic ROCK/ras¹²⁰⁵ tumours

Tumour suppressor genes p53 and p21 have an essential role in suppression of tumour development in all cancers and are particularly important in skin carcinogenesis (Topley et al., 1999, Wang et al., 2000, Macdonald et al., 2014). Therefore their status was analysed in *K14.ROCK^{er}/HK1.ras¹²⁰⁵* papillomas and carcinomas. Given these previous studies, and the fact that bi-genic ROCK/ras¹²⁰⁵ papillomas had converted to carcinoma after 12 weeks, it was anticipated that at least p53 expression would be altered at this conversion stage. As shown in figure 3.15a, this proved to be correct as an early 8 weeks *K14.ROCK^{er}/HK1.ras¹²⁰⁵* papilloma expressed relatively high p53 levels in both the nuclei and cytoplasm of basal layer keratinocytes. Following a malignant conversion after 12 weeks treatment, p53 expression in *K14.ROCK^{er}/HK1.ras¹²⁰⁵* wdSCC area became supra-basal and was gradually lost from the basal layer (figure 3.15b), and showed complete loss in SCC area (figure 3.15c). This p53 loss is paralleled with the reduction in K1 expression. In contrast, p53 expression in control *HK1.ras¹²⁰⁵* papillomas remained high and persisted throughout the epidermal layers (figure 3.15d).

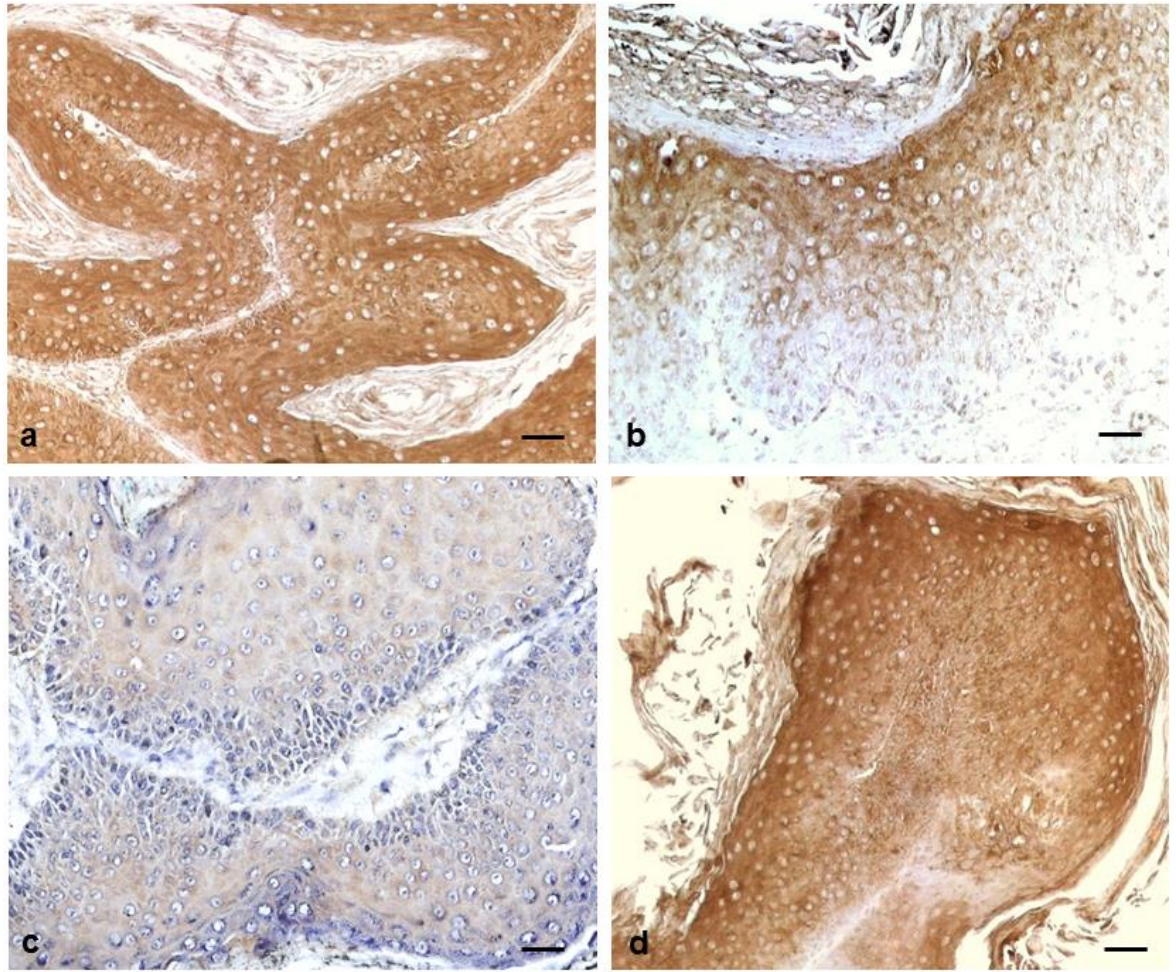


Figure 3.15 IHC analysis of p53 expression in 4-HT-treated *K14.ROCK^{er}/HK1.ras¹²⁰⁵* and *HK1.ras¹²⁰⁵* tumours. (a) Early *K14.ROCK^{er}/HK1.ras¹²⁰⁵* benign papilloma histotype (at 8 weeks) shows high p53 expression in all epidermal layers. (b) Following malignant conversion (at 12 weeks), p53 shows a reduction in expression that became supra-basal in *K14.ROCK^{er}/HK1.ras¹²⁰⁵* wdSCC area. (c) Whilst p53 expression shows complete loss upon progression in *K14.ROCK^{er}/HK1.ras¹²⁰⁵* SCC area. (d) *HK1.ras¹²⁰⁵* benign papillomas exhibit strong and uniform p53 expression throughout the epidermal compartment. (Scale bar: 100µm in a,d; 50µm in b,c).

Whilst p53 expression became reduced as *K14.ROCK^{er}/HK1.ras¹²⁰⁵* papillomas converted to carcinomas, surprisingly p21 a primary effector of p53 and often lost in tandem (el-Deiry et al., 1993), was still retained in bi-genic ROCK/ras¹²⁰⁵ carcinomas. In *K14.ROCK^{er}/HK1.ras¹²⁰⁵* benign papillomas (figure 3.16a), p21 was high and was shown to be somewhat supra-basal, a result perhaps consistent with its role in the induction of keratinocyte differentiation (Topley et al., 1999) and this subtle feature was also similar to its expression in *HK1.ras¹²⁰⁵* benign papilloma (figure 3.16b). Thus, surprisingly, instead of an anticipated p21 loss in conjunction with p53, this study found that reduced p53 expression resulted in elevated p21 expression. As shown in figure 3.16(c,d), p21 expression still remained persist in the *K14.ROCK^{er}/HK1.ras¹²⁰⁵* wdSCC (figure 3.15c) but gradually faded and became supra-basal in the SCC area (figure 3.15d) which was the reverse of the p53 expression profile. Moreover, in wdSCC, p21 expression was confined to basal layer before disappearing in SCC, similar to *K14.ROCK^{er}/HK1.ras¹²⁰⁵* tumours at 16 weeks (a control for cessation of 4-HT) where p21 expression faded upon progression to pdSCC (below). These novel findings suggest that p53 loss was sensed and a feedback system induced p21 expression to act as a backup support for the loss of the anti-tumour effects of p53.

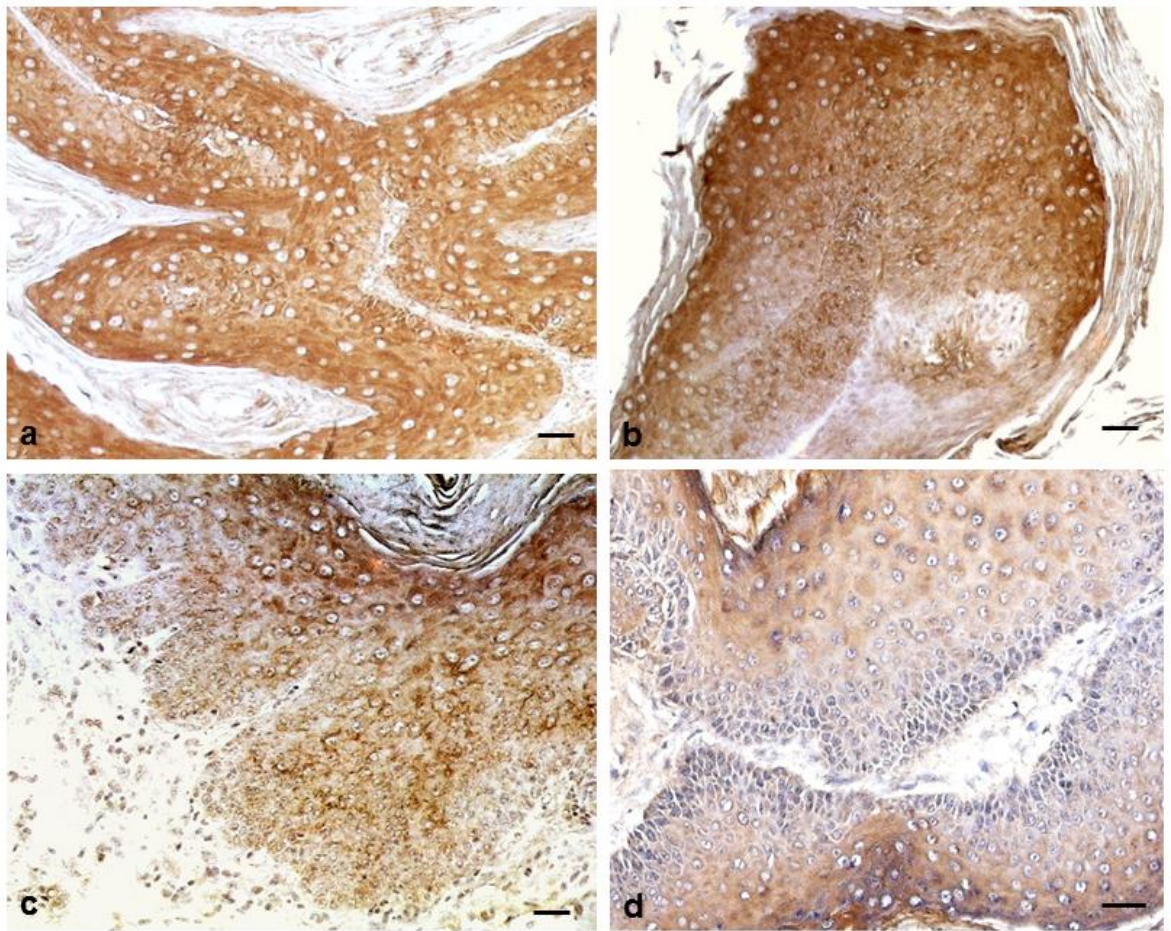


Figure 3.16 IHC analysis of p21 expression in 4-HT-treated *K14.ROCK^{er}/HK1.ras¹²⁰⁵* and *HK1.ras¹²⁰⁵* tumours. (a) Early *K14.ROCK^{er}/HK1.ras¹²⁰⁵* benign papilloma histotype (at 8 weeks) shows strong and uniform p21 expression in all epidermal layers. (b) *HK1.ras¹²⁰⁵* benign papilloma histotype also displays p21 expression throughout the epidermal layers. (c) Following malignant conversion at 12 weeks, p21 expression remained confined to *K14.ROCK^{er}/HK1.ras¹²⁰⁵* wdSCC area. (d) However, p21 expression was lost in the basal layer of *K14.ROCK^{er}/HK1.ras¹²⁰⁵* SCC area and appeared supra-basal upon tumour progression, while p53 expression had completely gone at this stage. (Scale bar: 100µm in a,b; 50µm in c,d).

3.3.5 BrdU-labelling of bi-genic ROCK/ras¹²⁰⁵ tumours

5-bromo-2-deoxyuridine (BrdU) labelling is a typical test to measure cell proliferation (Crane and Bhattacharya, 2013). The purpose of this study was to examine cell proliferation rates in *K14.ROCK^{er}/HK1.ras¹²⁰⁵* papillomas and carcinomas, and *HK1.ras¹²⁰⁵* benign papillomas as an increase in the epidermal proliferation activity is indicative of tumour progression. As shown in figure 3.17, BrdU-labelling revealed that 4-HT-treated *K14.ROCK^{er}/HK1.ras¹²⁰⁵* carcinomas have the highest high proliferation activity (65.1%) followed closely by 4-HT-treated *K14.ROCK^{er}/HK1.ras¹²⁰⁵* benign tumours (45.4%). In contrast, cell proliferation rates were lower and almost similar in almost all control groups that produced papillomas (4-HT-untreated *K14.ROCK^{er}/HK1.ras¹²⁰⁵* 17.7%; 4-HT-treated and 4-HT-untreated *HK1.ras¹²⁰⁵* papillomas: 18% and 16.1%).

These results indicate that cell proliferation rates increased as bi-genic ROCK/ras¹²⁰⁵ tumours converted from benign to the malignant stage. However, the proliferation rates in bi-genic ROCK/ras¹²⁰⁵ papilloma (+ 4-HT) were much higher than control *HK1.ras¹²⁰⁵* papillomas. This result may be due to the bi-genic ROCK/ras¹²⁰⁵ papillomas (+ 4-HT) that have already begun to show signs of malignant conversion (unique K1 expression) at 8 weeks compared to ras¹²⁰⁵ papillomas that were persistently benign. Moreover, the higher proliferation rate in *K14.ROCK^{er}/HK1.ras¹²⁰⁵* carcinomas coincided with the loss of p53 expression (figure 3.15). However, this mitotic index was lower than that observed in previous *HK1.ras¹²⁷⁶/Δ5PTEN^{flx}* cohorts promoted with TPA (Yao et al., 2006). This may indicate the persistence of p21 expression in these tumours, as observed in previous tri-genic ras/fos/Δ5PTEN^{flx} mice (Macdonald et al., 2014); a result also consistent with the further increased cellular proliferation observed in tri-genic ROCK/ras¹²⁷⁶/Δ5PTEN^{flx} cohorts that had lost p21 expression and exhibited high levels of activated AKT (below).

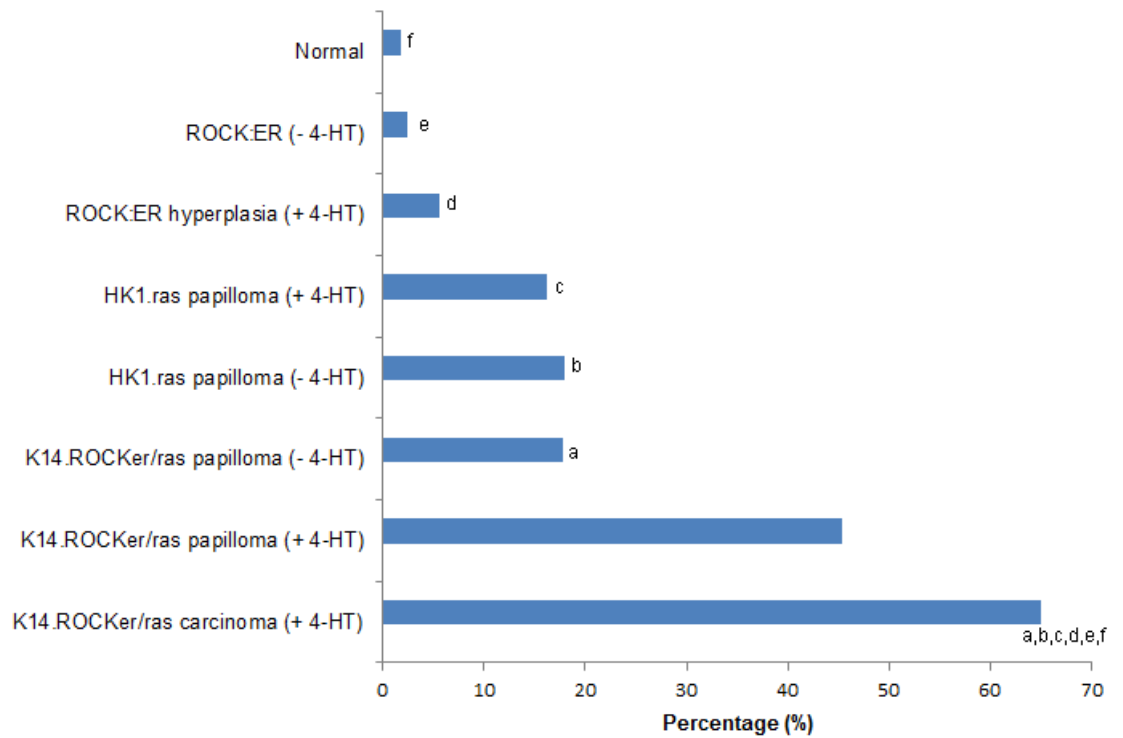


Figure 3.17 BrdU-labelling of bi-genic ROCK/ras¹²⁰⁵ carcinogenesis. Graph displays serial increases in cell proliferation rate upon conversion to carcinomas in 4-HT-treated *K14.ROCK^{er}/HK1.ras¹²⁰⁵* mice. (a,b,c,d,e,f : significantly difference between *K14.ROCK^{er}/HK1.ras¹²⁰⁵* carcinoma (+ 4-HT) and each cohort ($p < 0.05$), but not with *K14.ROCK^{er}/HK1.ras¹²⁰⁵* papilloma (+ 4-HT) ($p > 0.05$)).

3.3.6 Tenascin C expression in bi-genic ROCK/ras¹²⁰⁵ tumours

Given that ROCK molecules are closely involved in tissue integrity and stiffness, experiments progressed to a preliminary analysis of tenascin C. This is another molecule commonly associated with malignant progression and was an attractive target for investigation in this model given its role in the organisation of the ECM and thus may be influenced by ROCK-mediated change in tissue stiffness or cell migration. Tenascin C, a large ECM molecule is expressed at low levels in normal tissues (Midwood and Orend, 2009), yet shows high expression in many cancers and its expression increases with tumour progression (Dang et al., 2006). In this study expression of tenascin C was examined in the multistage cancer event of *K14.ROCK^{er}/HK1.ras¹²⁰⁵* by IHC analysis.

As shown in figure 3.18(a,b), tenascin C was sparsely expressed in both *HK1.ras¹²⁰⁵* and *K14.ROCK^{er}/HK1.ras¹²⁰⁵* papillomas. However, upon conversion of bi-genic ROCK/ras¹²⁰⁵ papilloma to wdSCC (at 12 weeks), tenascin C expression was elevated in both epidermal and dermal areas (figure 3.18c,d). Conversely, tenascin C expression was undetectable in ROCK2 hyperplasia histotype (figure 3.18e) and absent in normal epidermis (figure 3.18f). Therefore, data shows that the elevated presence of tenascin C is associated with tumour progression in the multistage carcinogenesis of *K14.ROCK^{er}/HK1.ras¹²⁰⁵* histotypes.

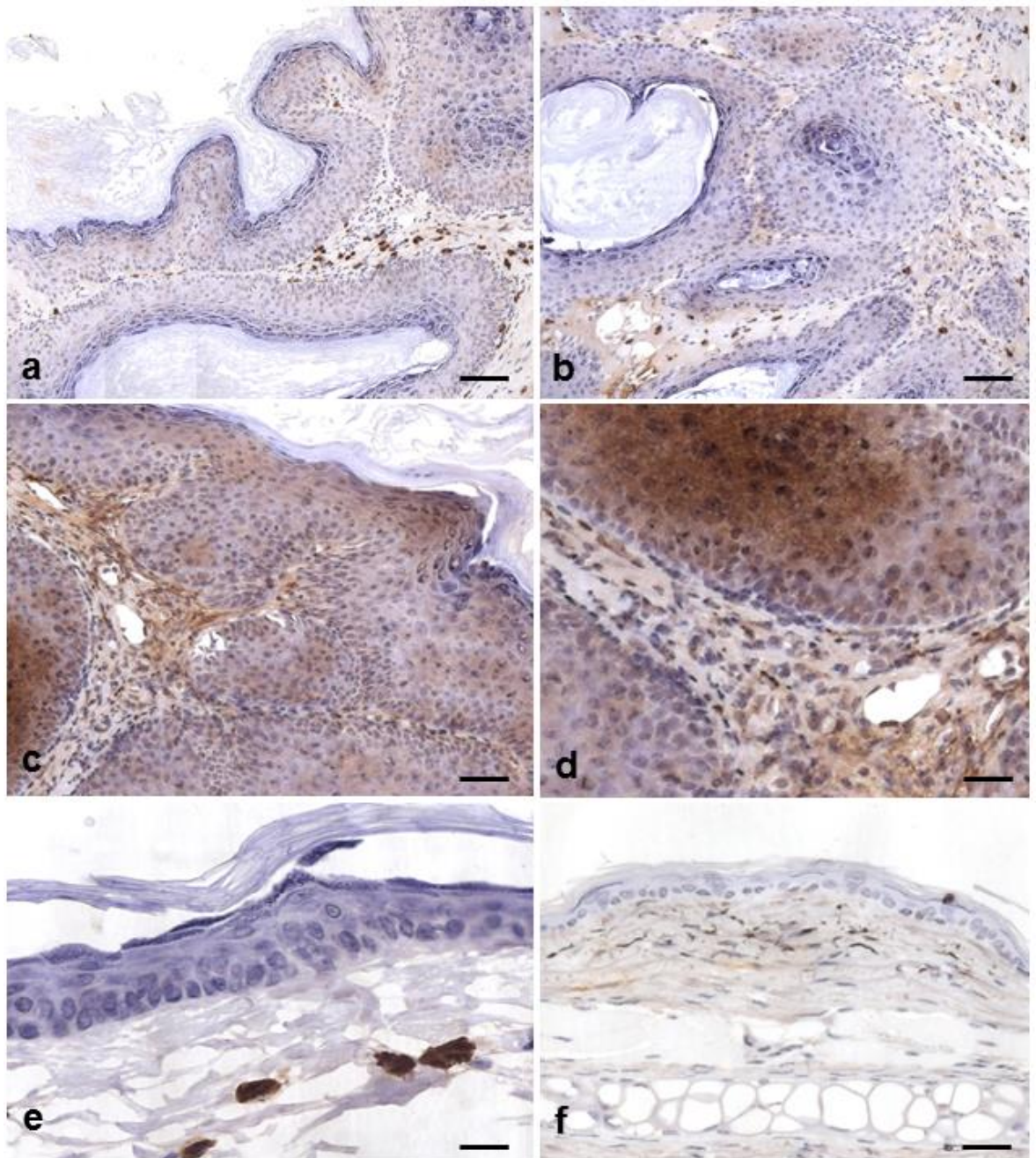


Figure 3.18 IHC analysis of tenascin C in 4-HT-treated *K14.ROCK^{er}/HK1.ras¹²⁰⁵* tumours. (a) Tenascin C was expressed at low levels in both 4-HT-treated *HK1.ras¹²⁰⁵* and (b) *K14.ROCK^{er}/HK1.ras¹²⁰⁵* papillomas. (c) The highest level of tenascin C was displayed upon *K14.ROCK^{er}/HK1.ras¹²⁰⁵* papilloma conversion to wdSCC and (d) showed expression in both epidermal and dermal areas. (e) Tenascin C was undetectable in *K14.cre/Isl.ROCK^{er}* hyperplasia and (f) absent in normal epidermis. (Scale bar: 100µm in a-d,f; 50µm in e).

3.3.7 Cessation of 4-HT treatment in bi-genic ROCK/ras¹²⁰⁵ tumours

One advantage of using this 4-HT inducible form of the transgenic model is the ability to assess oncogene dependence via cessation of treatment. 4-HT treatment was stopped in a cohort of six *K14.ROCK^{er}/HK1.ras¹²⁰⁵* mice that had been topically treated with 4-HT for approximately 14 weeks; and animals were biopsied two to three weeks later. This determined whether bi-genic ROCK/ras¹²⁰⁵ malignant tumours remained dependent on activated ROCK^{er} to either reduce SCC size and show that ROCK2 no longer drives the tumour progression, or whether activated ROCK^{er} had become redundant and progression continued. In these experiments, this smaller cohort of mice were closely examined on a daily basis; as beyond 16 weeks the size of these *K14.ROCK^{er}/HK1.ras¹²⁰⁵* tumours began to give concern to the Home Office Inspector. Hence, a separate procedure was included on the Licence prior to these experiments commencing.

K14.ROCK^{er}/HK1.ras¹²⁰⁵ mice demonstrated larger size of tumours by 14 weeks of 4-HT treatment, which were more obviously SCCs when compared to papillomas of control cohorts (figure 3.19a,b). However, most interestingly, at 16 weeks, two weeks post cessation of 4-HT compared to their size at 14 weeks, all *K14.ROCK^{er}/HK1.ras¹²⁰⁵* tumours became larger (figure 3.19d,e). This result suggested that ROCK2 was no longer involved, but this assumption also proved to be incorrect on detailed analysis (below). The cessation of 4-HT-tumours showed an increased size, but overall they remained pale and had a weakly vascularised appearance at biopsy as compared to aggressive carcinomas produced in e.g. *ras¹²⁷⁶/Δ5PTEN^{flx}* cohorts treated with TPA which appears less keratotic and a highly vascularised red colour (Yao et al., 2006). In contrast, control *HK1.ras¹²⁰⁵* mice post two weeks without 4-HT showed little to no difference in tumour size and remained classical ras papillomas (figure 3.19c,f).

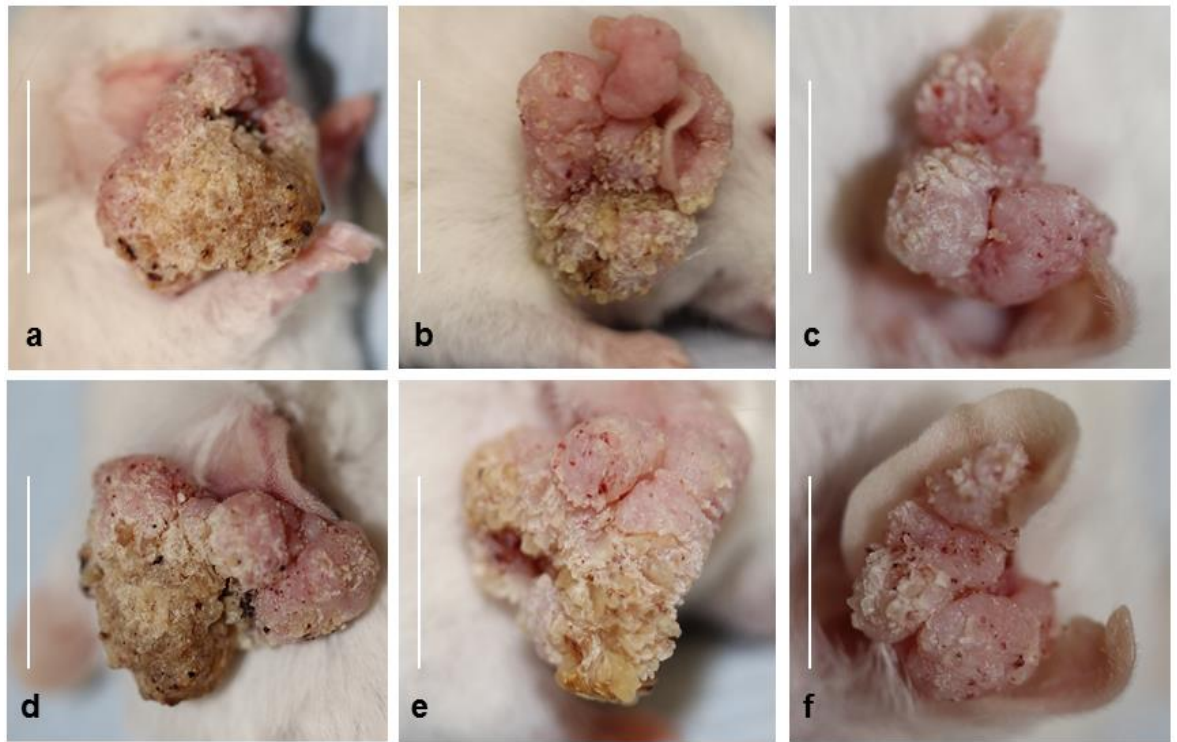


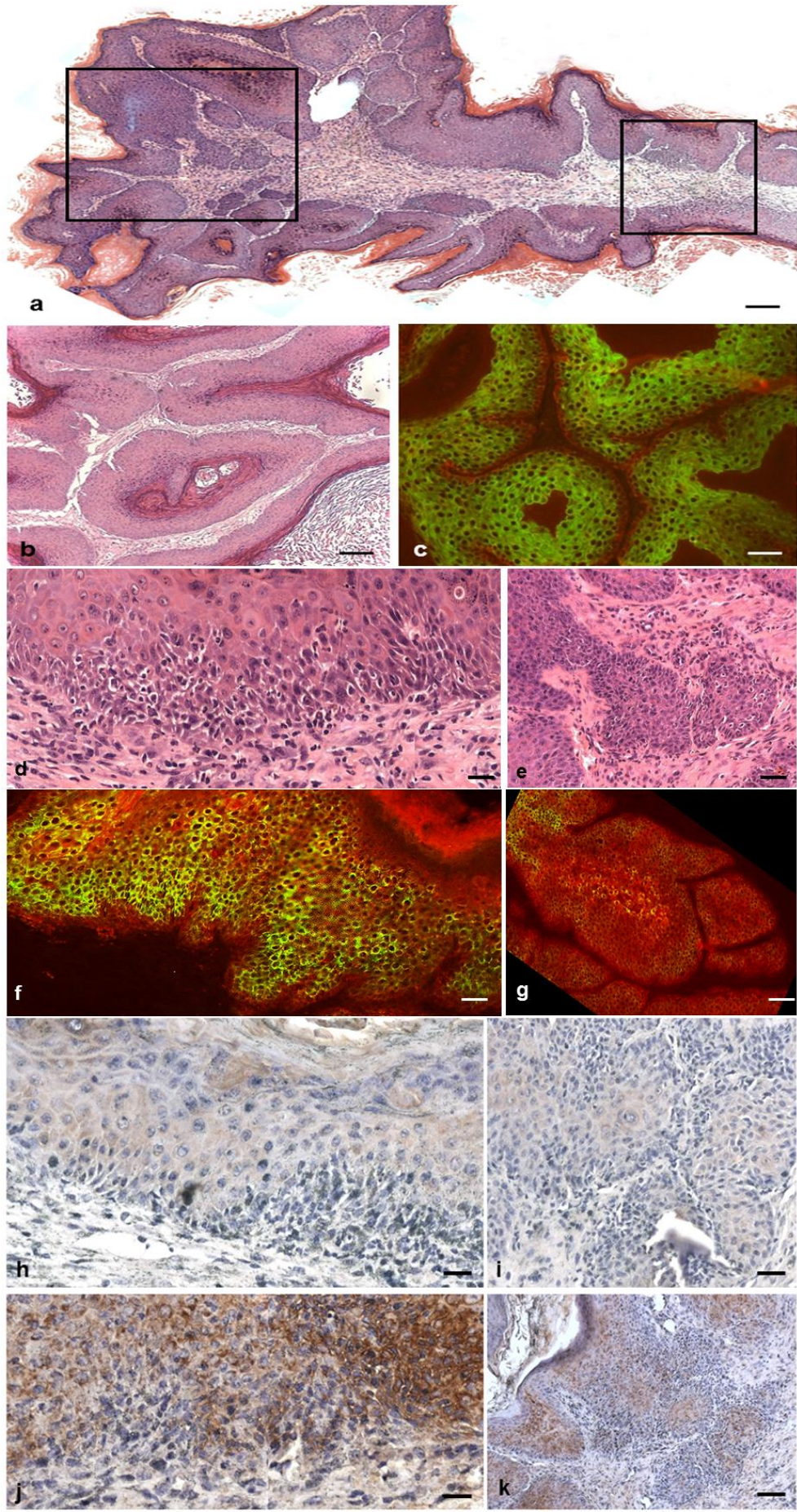
Figure 3.19 Phenotypes of *K14.ROCK^{er}/HK1.ras¹²⁰⁵* mice after termination of 4-HT for 2 weeks. (a, b) *K14.ROCK^{er}/HK1.ras¹²⁰⁵* and (c) *HK1.ras¹²⁰⁵* mice exhibit large tumours at 14 weeks of 4-HT treatment. (d, e) *K14.ROCK^{er}/HK1.ras¹²⁰⁵* mice display larger tumours with a pale and less vascularised appearance after 2 weeks cessation of 4-HT; whilst (f) *HK1.ras¹²⁰⁵* tumour shows no changes in size or phenotypes at 16 weeks.

Typically, older *K14.ROCK^{er}/HK1.ras¹²⁰⁵* tumours possessed a mixed histotype of wdSCC, plus areas of K1/p53 negative-p21 positive SCC (figure 3.20a - small box, figure 3.20d,f,h,j) alongside occasional areas of highly invasive pdSCC (K1/p53/p21 negative) (figure 3.20a - larger box, figure 3.20e,g,i,k). Whereas control littermate *HK1.ras¹²⁰⁵* tumours remained as papillomas (figure 3.20b), with strong K1 expression (figure 3.20c). However, following cessation of 4HT, *K14.ROCK^{er}/HK1.ras¹²⁰⁵* wdSCCs exhibited a disturbed architecture (figure 3.20d). Here, [p53-negative] basal layer keratinocytes became disarranged and appeared to terminally differentiate (as apoptosis is not a preferred option for a tissue involved in barrier maintenance) consistent with the appearance of elevated K1 expression [increased green overtones in wdSCC areas: figure 3.20f]; and elevated p21 (figure 3.20j) also consistent with roles in epidermal differentiation (Devgan et al. 2006).

These data suggest that at this wdSCC stage exogenous ROCK^{er} activation was still required to maintain malignancy. Indeed following cessation of 4-HT treatment, remarkably (and repeatedly) it appeared that at the sites of wdSCC, p21 levels actually increased and this would be consistent with the retention of K1 at such wdSCC sites given the role of p21 in keratinocyte differentiation (Topley et al., 1999, Yao et al., 2008, Macdonald et al., 2014). This persistence appeared in many wdSCCs (below, such as tri-genic ROCK/ras¹²⁷⁶/fos) and a recurrent theme was antagonism with AKT; but here these data suggest that the loss of activated ROCK2 facilitated an anti-progression response involving terminal differentiation (figure 3.20d,f,j). In contrast, in pdSCC histotypes (figure 3.20a – larger box, figure 3.20e), this was not the case. In these more invasive pdSCCs (figure 3.20a – larger box, figure 3.20e), the opposite profile appeared, as K1/p53/p21 expression disappeared completely (figure 3.20g,i,k) and this K1 result, together with analysis of p53/p21 suggest that once *K14.ROCK^{er}/HK1.ras¹²⁰⁵* carcinomas had progressed from wdSCC to pdSCC the presence of exogenous ROCK^{er} expression was redundant.

Analysis of GFP in *K14.ROCK^{er}/HK1.ras¹²⁰⁵* wdSCC and pdSCC showed expression in all epidermal layers (figure 3.20l,m). However, following cessation of 4-HT, p-Mypt1 analysis in both wdSCCs and pdSCC histotypes showed reduced expression that appeared more supra-basal (figure 3.20n,o) compared to previous analysis of uniform and strong p-Mypt1 expression in all epidermal layers

of *K14.ROCK^{er}/HK1.ras¹²⁰⁵* wdSCC at 12 weeks (figure 3.17b). Thus, this may indicate that the cessation of 4-HT has turned off the ROCK2^{er} system. Moreover, these findings suggested that whilst *K14.ROCK^{er}/HK1.ras¹²⁰⁵* tumours remained wdSCC, they relied on exogenous ROCK^{er} to maintain malignancy. However, this 4-HT cessation study suggests that exogenous ROCK^{er} activation is no longer a rate limiting factor once wdSCC has progressed to pdSCCs.



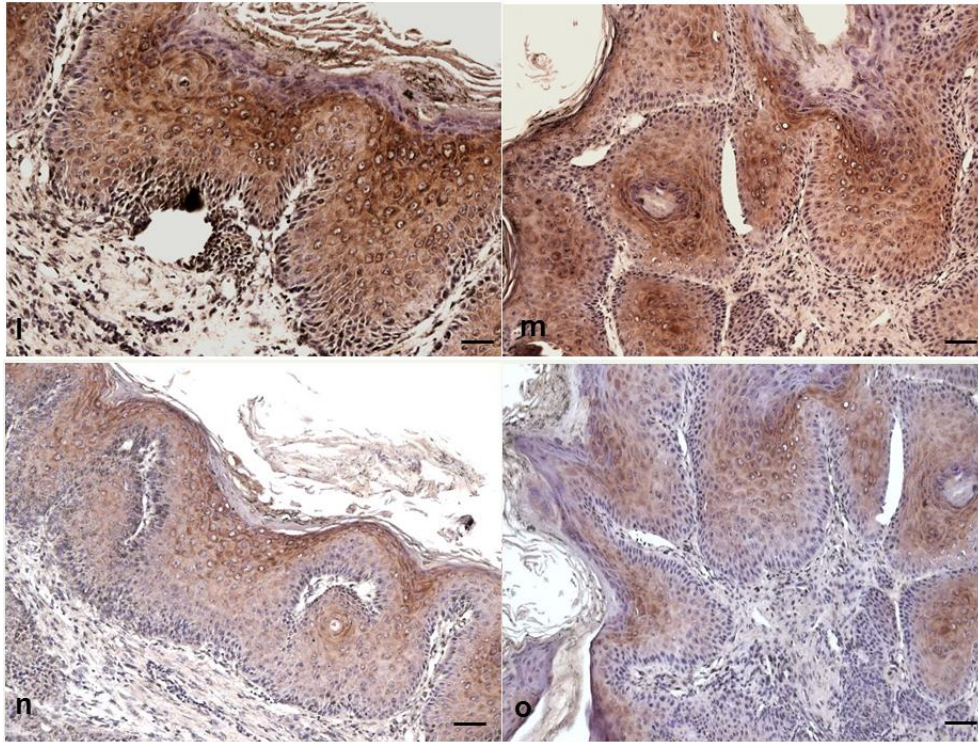


Figure 3.20 Histotype of *K14.ROCK^{er}/HK1.ras¹²⁰⁵* biopsies at 16 weeks, after 2 weeks termination of 4-HT. (a) A low magnification composite *K14.ROCK^{er}/HK1.ras¹²⁰⁵* tumour exhibits a mixed histotype of papilloma, wdscc (small box) and invasive pdscC (large box). (b) In contrast, at this time point control *HK1.ras¹²⁰⁵* tumours still remain as benign papilloma histotype and (c) display a supra-basal keratin K1 expression typical of their benign nature.

(d) At higher magnification, *K14.ROCK^{er}/HK1.ras¹²⁰⁵* wdscc areas display a disorganised basal layer, whilst (e) *K14.ROCK^{er}/HK1.ras¹²⁰⁵* pdscC areas display finger like projections of highly invasive cells into the dermis.

(f) *K14.ROCK^{er}/HK1.ras¹²⁰⁵* wdscc areas demonstrate expression of retained K1, whilst (g) in *K14.ROCK^{er}/HK1.ras¹²⁰⁵* pdscC areas, K1 expression is completely lost.

(h) p53 expression is already totally lost in *K14.ROCK^{er}/HK1.ras¹²⁰⁵* wdscc and (i) again in pdscC histotypes.

(j) p21 expression persists in *K14.ROCK^{er}/HK1.ras¹²⁰⁵* wdscc areas and is elevated, but in (k) *K14.ROCK^{er}/HK1.ras¹²⁰⁵* pdscC areas, p21 expression is disappearing.

(l) *K14.ROCK^{er}/HK1.ras¹²⁰⁵* wdscc and (m) pdscC histotypes exhibit gfp expression in all epidermal layers.

(n) Following cessation of 4-HT, both *K14.ROCK^{er}/HK1.ras¹²⁰⁵* wdscc and (o) pdscC histotypes display p-Mypt1 expression that seems to appear more in the supra-basal layer.

On further investigation, the increase in tumour size was not all it seemed. All *K14.ROCK^{er}/HK1.ras¹²⁰⁵* tumours became larger after cessation of 4-HT, yet it appeared that in the areas of wdSCC, the tissue architecture appeared disrupted; several portions of these tumours were examined more stringently. In all mice, the tumour forming the majority of the additional growth was biopsied to determine the histotype and expression profiles (figure 3.21a). As displayed in figure 3.21b, the histological analysis showed an aggressive late papilloma histotype, not wdSCC or pdSCC; and this was supported by strong expression of K1 and an ordered differentiation pattern as exhibited by K14 (red) expression typical of standard papillomas (figure 3.21c).

The reduced levels of p53 expression in emerging *K14.ROCK^{er}/HK1.ras¹²⁰⁵* tumours were consistent with a late-stage, aggressive papilloma (Macdonald et al., 2014) and this expression faded in several areas (figure 3.21d); this was counteracted by the huge intensity of p21 expression in basal and differentiated layers which was both nuclear and cytoplasmic (figure 3.21e,f). This level of p21 has not been seen in any other tumour analysis in the HK1 model, and this result was repeated in all emerging *K14.ROCK^{er}/HK1.ras¹²⁰⁵* papillomas analysed to date; regardless of technical issues e.g. new p21 antibodies or DAB reagents.

These results suggest several conclusions. It may be that malignant conversion and progression are totally dependent on ROCK2 activation and thus, loss of exogenous ROCK2 activity suddenly induced papillomatogenesis; where perhaps p53 and certainly p21 expression prevented conversion. No tumour aetiology suggests that these were once wdSCC/SCCs that regressed to papilloma. These appeared to be novel tumours. A second hypothesis may be that these are additional papilloma subtypes which arise simply due to cessation of 4-HT. This further suggests that certain papilloma subtypes (Glick et al., 1991, Hennings et al., 1993, Yao et al., 2006) may be sensitive to the nature of 4-HT anti-cancer activities; and consequently another earlier facet of *K14.ROCK^{er}/HK1.ras¹²⁰⁵* co-operation is that it may give rise to a set of papillomas that are destined to become malignant; unlike e.g. *HK1.ras¹²⁷⁶/fos* papillomas. Although why ear-tag tumours arose in 4-HT-treated *HK1.ras¹²⁰⁵* mice is unclear (yet, these do not become malignant (Greenhalgh et al., 1993a)) and this may centre on the wound promotion stimulus, as in all these *K14.ROCK^{er}/HK1.ras¹²⁰⁵* cohorts, if the ear tag had been lost tumours rarely appeared and this was investigated further (below).

The analysis to investigate wound (or fos-mediated) promotion demonstrated that it was vital to attain the papilloma context where ROCK2 activation induced malignant conversion.

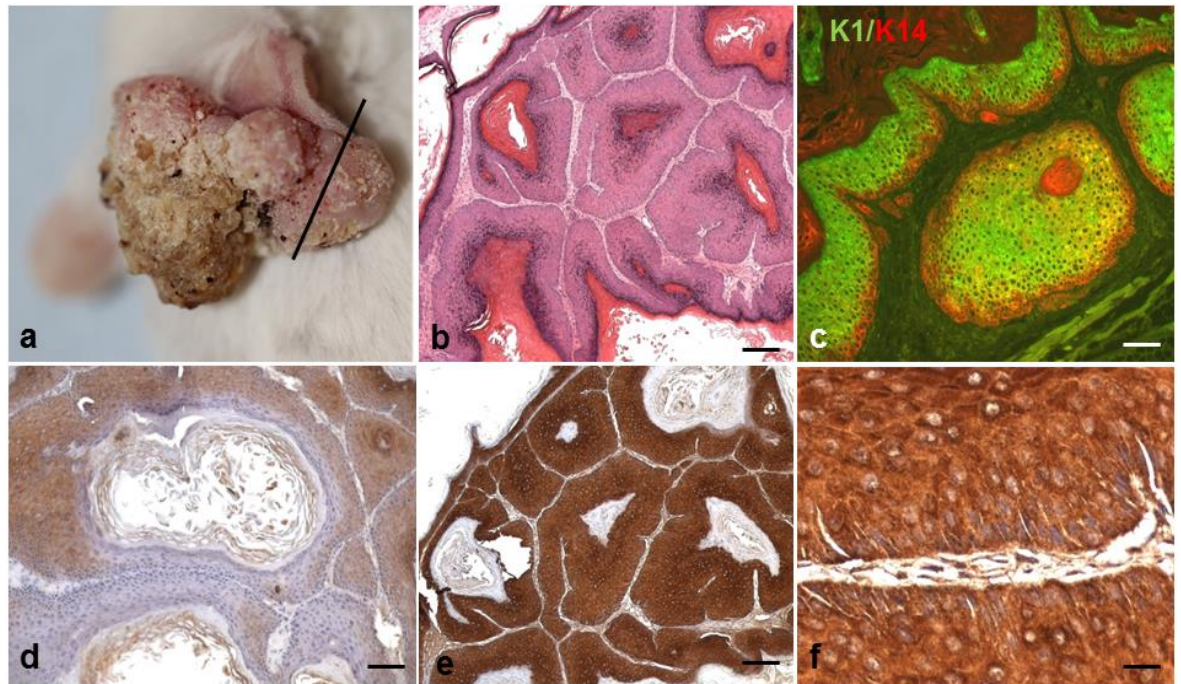


Figure 3.21 Histotype of *K14.ROCK^{er}/HK1.ras¹²⁰⁵* tumour from the additional papilloma growth at 16 weeks, after 2 weeks termination of 4-HT. (a) *K14.ROCK^{er}/HK1.ras¹²⁰⁵* mouse shows the area of additional tumour growth (line). (b) Histology analysis shows a late stage papilloma histotype and confirmed by (c) strong K1 expression which is weak in some areas. (d) Pre-malignant tumour shows faded p53 expression and (e,f) intense p21 expression in all epidermal layers in both the nuclei and cytoplasm.

3.3.7 Wound promotion for development of appropriate late-stage papilloma prior to ROCK^{er} causality.

As shown in results above, bi-genic ROCK/ras¹²⁰⁵ tumours converted from benign papillomas to malignant tumours at approximately 12 weeks continuous 4-HT activation compared to *HK1.ras*¹²⁰⁵ cohorts that still remained benign papillomas. However, if the ear tag falls out prior to overt papillomas forming at approximately 6 weeks of 4-HT treatment; it was noted that despite continued 4-HT treatment, these mice did not develop tumours. Neither did the control ras¹²⁰⁵ cohorts which also lost an ear tag.

Next, the study proceeded to address the possibilities that bi-genic ROCK/ras¹²⁰⁵ tumours required a wound promotion stimulus to establish the appropriate late-stage papilloma context prior to and essential for malignant conversion by ROCK^{er} papillomatogenesis in bi-genic ROCK/ras¹²⁰⁵ mice with and without ear tagging or accidental loss. ROCK associated papillomatogenesis in *HK1.ras* line 1205 papillomas which are normally prone to regression once the ear tag (wound promoter) was lost, were compared to papillomatogenesis in the *HK1.ras*¹²⁷⁶; a background insensitive to wound promotion and later employed in most tri-genic experiments as *HK1.ras*¹²⁰⁵ mice compromise compound transgenic mouse viability.

As shown in figure 3.22a, *K14.ROCK^{er}/HK1.ras*¹²⁰⁵ mice (n= 6) developed tumours at 8 weeks, but there was no sign of tumourigenesis following loss of ear tag (*K14.ROCK^{er}/HK1.ras*¹²⁰⁵ mouse – right (n= 6)) prior to tumours forming around 5 to 6 weeks. At 12 weeks, bi-genic ROCK/ras¹²⁰⁵ mice with intact ear tags possessed typical papillomas on their way to conversion. These appeared bigger and, if papillomas developed but the tags were lost at 7-8 weeks there was no conversion, instead the tumours were smaller which indicated a lack of growth following 4-HT treatment (figure 3.22b).

On loss of ear tag promotion, the histopathology analysis revealed that this *K14.ROCK^{er}/HK1.ras*¹²⁰⁵ papilloma (figure 3.22c) had also failed to achieve malignant conversion confirmed by strong K1 (green) expression (figure 3.22d).

This supports the requirement (some form of) for promotion in this model consistent with the fos models (below). This was further supported by results from line 1276 where in the absence of additional genetic events such as v-fos co-operation (below), *K14.ROCK^{er}/HK1.ras¹²⁷⁶* mice (n= 6) showed a complete lack of tumourigenesis with or without ear tag; even after 16 weeks of 4-HT treatment (figure 3.22e). Here, histology analysis revealed only mild hyperplasia in *K14.ROCK^{er}/HK1.ras¹²⁷⁶* ear epidermis (figure 3.22f) similar to the mild hyperplasia histotype from ROCK^{er} activation alone.

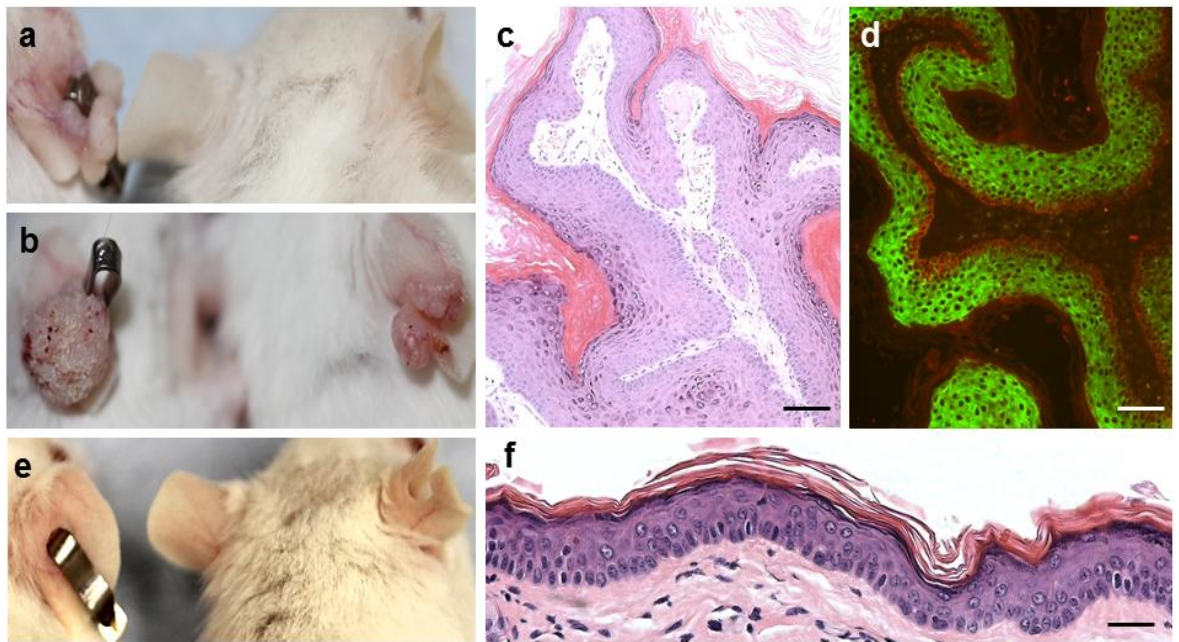


Figure 3.22 Phenotype and histopathology of 4-HT-treated *K14.ROCK^{er}/HK1.ras* lines 1205 and 1276. (a) *K14.ROCK^{er}/HK1.ras¹²⁰⁵* mice at 8 weeks display tumourigenesis on ear tag (left) and exhibit lack of tumour formation on loss of ear tag (right). (b) *K14.ROCK^{er}/HK1.ras¹²⁰⁵* tumours at 12 weeks appear bigger on ear tag (left) and show regression on loss of ear tag (right). (c) Bi-genic *ROCK/ras¹²⁰⁵* tumours on loss of tag ear show benign papilloma histotype and (d) express strong K1 in supra-basal layer. (e) *K14.ROCK^{er}/HK1.ras¹²⁷⁶* mice display no sign of tumourigenesis on ear tag (left) and on loss of ear tag (right). (f) Histology of *K14.ROCK^{er}/HK1.ras¹²⁷⁶* skin on loss of ear tag show hyperplasia histotype.

3.3.8 Summary

Taken together, results in this study indicated that ROCK co-operates with ras^{Ha} to induce conversion of benign papillomas to wdSCC (at 12 weeks) supported by loss of keratin K1, p53 and elevated expression of tenascin C. p21 expression persisted in the bi-genic ROCK/ ras^{1205} wdSCC which suggests it limits further malignant progression. This is consistent with a previous study by Macdonald et al., (2014) that reported on persistent p21 expression in wdSCC histotype of tri-genic $\text{ras}^{1276}/\text{fos}/\Delta 5\text{PTEN}^{\text{fix}}$ mice and suggested that loss of p21 (upon loss of p53) is implicated in advanced carcinoma progression. Data also demonstrated that wound promotion is crucial for the appropriate development of a late-stage papilloma phenotype prior to ROCK causality in ROCK/ ras^{1205} malignant conversion as loss of the ear tag before the papilloma became mature resulted in tumour regression which remained benign. Results from the cessation of 4-HT experiments suggest that upon conversion to malignancy and progression to aggressive carcinomas, exogenous ROCK^{er} is dispensable. Whereas findings indicate that in earlier stages of malignancy, $K14.\text{ROCK}^{\text{er}}/\text{HK1}.\text{ras}^{1205}$ wdSCCs are still dependent on ROCK^{er} expression for continuing progression to aggressive SCCs. Excitingly, after cessation of 4-HT, the appearance of late stage benign papillomas suggested either dependence on ROCK2 activation for conversion or that a subtype of $K14.\text{ROCK}^{\text{er}}/\text{HK1}.\text{ras}^{1205}$ papilloma histotype is sensitive to 4-HT induction. Either way these emerging papillomas had intense p21 expression possibly deriving from the cessation of ROCK^{er} activities. Overall, these data propose that ROCK has an important role in early malignant conversion events in co-operation with ras^{Ha} but only once the appropriate papilloma context had been achieved.

3.4 Co-operation of ROCK2 and *HK1.fos* in transgenic mouse skin carcinogenesis

The transcription factor *fos* has been shown to be a major regulator of keratinocyte proliferation and differentiation, and its deregulation can potentially contribute to tumourigenesis (Basset-Seguín et al., 1990). Since *fos* acts as a nuclear transcription factor and is an eventual downstream target of ras/MAPK pathway (Greenhalgh et al., 1993c, Macdonald et al., 2014), there is a possibility of interaction with Rho/ROCK signalling since data have shown the direct co-operation between ROCK and ras^{Ha} in malignant conversion with ROCK2 being a downstream effector of ras family. Intriguingly, there is still lack of *in vivo* research on co-operation between ROCK and *fos*. In addition, the bi-genic ROCK/ras experiments clearly demonstrated a need for promotion (wounding) and in several experiments, *fos* oncogene was associated with the multistage chemical carcinogenesis model as a major effector of chemical promotion by TPA (Schlingemann et al., 2003). But of greater relevance to these studies, in the HK1 model, activated v-*fos* was involved in promoting papillomatogenesis leading to autonomous papilloma formation through co-operation with v-ras^{Ha} (Greenhalgh et al., 1993c). Interestingly, *fos* activation alone elicits a hyperplasia histotype (Greenhalgh et al., 1993b) after a long latency and is dependent on a wound promotion stimulus. Indeed a *HK1.fos* mouse appears identical to normal mouse except that it has a doubled mitotic index as determined by BrdU labelling. Thus an accelerated differentiation must compensate for this increased proliferation giving a normal histotype (Greenhalgh et al., 1993b). This would be consistent with roles assigned to the *fos* transcription factor via AP1 which acts as a switch to turn pathways on or off such as in the change from proliferation to differentiation (Curran et al., 1984) or granular cells commitment to become cornified (Fisher et al., 1991); hence, often keratins possess several AP1 sites (DiSepio et al., 1995). In stress conditions such as ear tag wounding, v-*fos* interferes with the c-*fos* roles in both proliferation and differentiation in the healing processes, resulting in keratotic hyperplasia by 4 to 6 months and keratotic papillomas around 9 to 12 months (Greenhalgh et al., 1993b). A previous study demonstrated the role of *fos* in the later events of cancer formation. In the HK1 model, v-*fos* provided a constitutive promotion role for *HK1.ras* giving papillomas (Greenhalgh et al., 1993c) and by using a knockout c-*fos* mouse infected with v-ras^{Ha} no tumours

were produced; again demonstrating the importance of *fos* to papilloma formation (Saez et al., 1995). No evidence of tumour formation was recorded in *K14.ROCK^{er}* mice following TPA application (Olson, - unpublished data). Hence, co-operation studies of ROCK and *fos* in a transgenic mouse model would be useful to examine the potential effects of such a combination in tumour formation and keratinocytes differentiation. To investigate co-operation in tumourigenesis between *fos* and ROCK, *K14.cre/Isl.ROCK^{er}* mice were crossed with *HK1.fos* mice to produce bi-genic ROCK/*fos* cohorts.

3.4.1 ROCK2 co-operates with activated *fos* to elicit benign tumours

In these experiments, given that future tri-genic co-operation studies would exploit the new *Isl.ROCK^{er}* genotype, these mice were also used in this bi-genic study and thus phenotypes from bi-genic *K14.cre/Isl.ROCK^{er}/HK1.fos* mice also became useful comparison controls. These mice also employed the K14.creP regulator (Berton et al., 2000b) to express *Isl.ROCK^{er}* following topical treatment with RU486. Initially, 10 individual adult *K14.cre/Isl.ROCK^{er}/HK1.fos* mice and *HK1.fos* age-matched littermates were treated with RU486 at 5/6 weeks of age. This activated cre recombinase to remove the transcriptional stop cassette in the *Isl.ROCK^{er}* transgene and CAG-expressed ROCK^{er} activity was activated by 4-HT (3 times per week) for 12 weeks and biopsies taken. This time point was chosen as bi-genic ROCK/*ras* mice had begun to co-operate and sporadic malignant conversion was observed. Control groups (n= 6 each) included RU486 treatment of *K14.cre/Isl.ROCK^{er}/HK1.fos* mice without 4-HT, and *HK1.fos* mice received treatment of both RU486 and 4-HT. A second experiment involved treated mice (3 times per week) for 20 weeks.

Following 12 weeks treatment with 4HT, both *K14.cre/Isl.ROCK^{er}/HK1.fos* and *HK1.fos* mice showed little difference in phenotypes, but there was a suggestion that *K14.cre/Isl.ROCK^{er}/HK1.fos* mice had a more developed ear thickening and possibly the beginning of tumour formation. At this time point, all control mice had developed scaly and thickened ears particularly on the tagged ear, but with no sign of tumour formation (figure 3.23). This control cohort finding was identical to that reported for *HK1.fos* mice (Greenhalgh et al., 1993b). However, histological

analysis of *K14.cre/Isl.ROCK^{er}/HK1.fos* mice revealed an increased hyperplasia (figure 3.24a) with elevated areas of acanthosis (expansion of the spinous layer) in particular (figure 3.24b). This observation indicates the potential of ROCK activities in supra-basal keratinocytes that may contribute to epidermal strength and the roles assigned to *fos* in the commitment to differentiation (Fisher et al., 1991, Greenhalgh et al., 1993b). This acanthosis again suggests a possible co-operation between ROCK and *fos* and provides a first direct link to a potential co-operation in proliferation and terminal differentiation (figure 3.24b). In comparison, 4-HT-treated *HK1.fos* and 4-HT-untreated *K14.cre/Isl.ROCK^{er}/HK1.fos* control cohorts showed epidermal hyperplasia (figure 3.24c,d) consistent with all previous *HK1.fos* reports (Greenhalgh et al., 1993b,c). At the same time, all bi-genic ROCK/*fos* mice were analysed for expression of ROCK^{er} fusion protein-tagged with GFP (EGFP-ROCK^{er}). IHC analysis of GFP showed that ROCK^{er} transgene was confirmed in RU486-/4-HT-treated *K14.cre/Isl.ROCK^{er}/HK1.fos* epidermis, but GFP was not expressed in 4-HT-treated *HK1.fos* hyperplasia (figure 3.24e,f). IHC analysis of p-Mypt1 was performed to confirm that exogenous ROCK^{er} transgene was activated upon application of 4-HT. As shown in figure 3.24(g), p-Mypt1 was expressed throughout epidermal layers of RU486-/4-HT-treated *K14.cre/Isl.ROCK^{er}/HK1.fos* cohort. Whilst lack of p-Mypt1 expression was demonstrated in 4-HT-treated *HK1.fos* cohort (figure 3.24h). Histologically, *K14.cre/Isl.ROCK^{er}/HK1.fos* appeared to be progressing to papilloma hence, the repeat experiment was extended to 20 weeks.



Figure 3.23 Phenotypes of *K14.cre/Isl.ROCK^{er}/HK1.fos* and *HK1.fos* mice at 12 weeks. (a) RU486-/4-HT-treated *K14.cre/Isl.ROCK^{er}/HK1.fos* mouse exhibits a thickened ear compare to (b) 4-HT-treated *HK1.fos* and (c) RU486-treated/4-HT-untreated *K14.cre/Isl.ROCK^{er}/HK1.fos* mice.

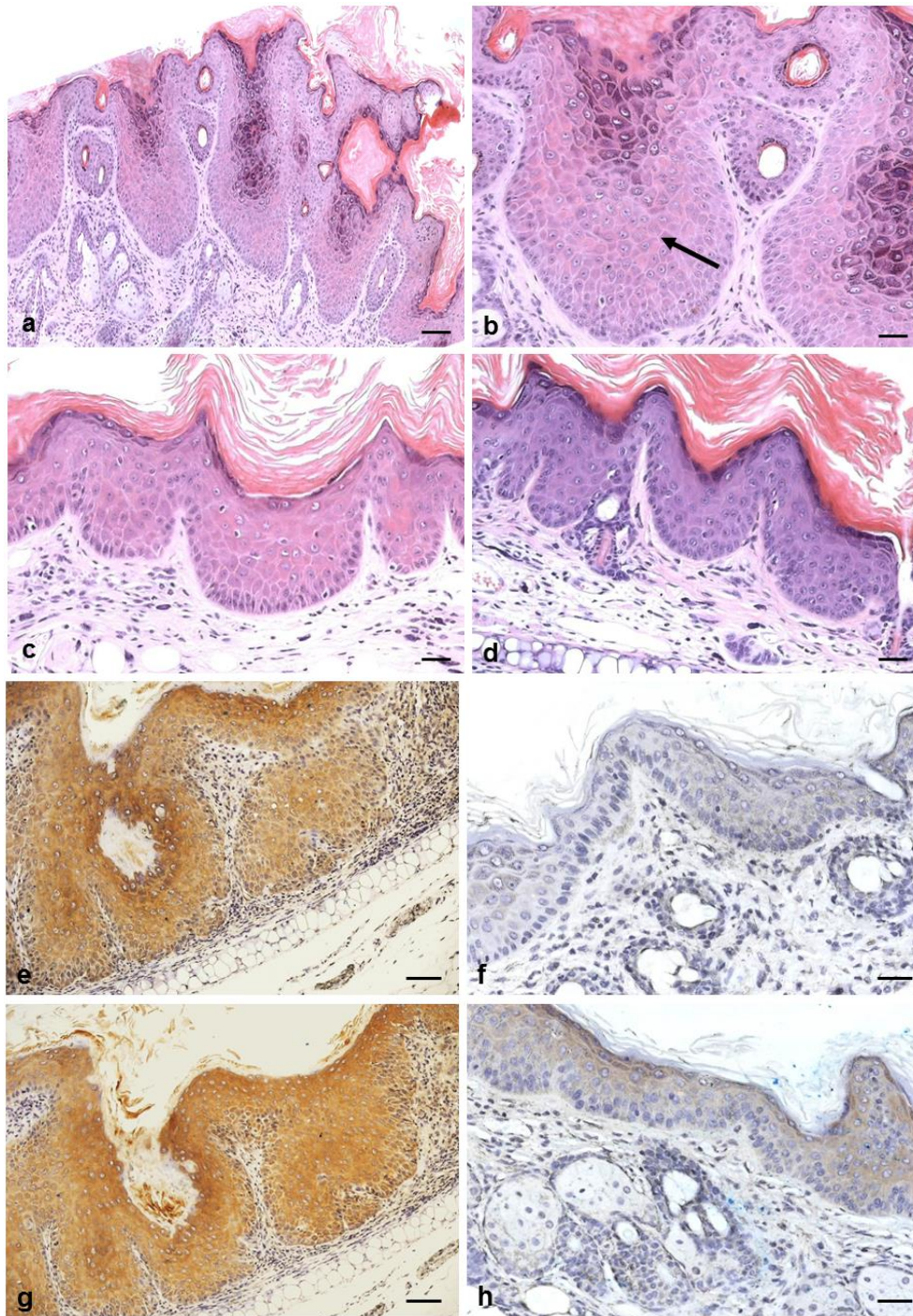


Figure 3.24 Histotype of *K14.cre/Isl.ROCK^{er}/HK1.fos* and *HK1.fos* mice at 12 weeks. (a) RU486-/4-HT-treated *K14.cre/Isl.ROCK^{er}/HK1.fos* epidermis shows hyperplasia with expanded epidermal compartments. (b) At higher magnification, RU486-/4-HT-treated *K14.cre/Isl.ROCK^{er}/HK1.fos* epidermis shows area of acanthosis (arrow) and much thicker hyperplasia compared to (c) 4-HT-treated *HK1.fos* or (d) RU486-treated/4-HT-untreated *K14.cre/Isl.ROCK^{er}/HK1.fos* hyperplastic histotypes. (e) IHC analysis of GFP marker exhibits expression throughout epidermal layers in RU486-/4-HT-treated *K14.cre/Isl.ROCK^{er}/HK1.fos* cohort, but (f) 4-HT-treated *HK1.fos* cohort GFP is undetected. (g) RU486-/4-HT-treated *K14.cre/Isl.ROCK^{er}/HK1.fos* epidermis exhibits strong p-Mypt1 expression but (h) 4-HT-treated *HK1.fos* cohort displays a little trace of p-Mypt1 expression. (Scale bar: b,c,d,f,h: 50 μ m, a,e,g: 100 μ m).

The genotypes allowed exploration of the possible co-operation between ROCK and fos deregulation in keratinocyte differentiation given the observation of acanthosis. Skin biopsies were further analysed for the expression of keratin K1 and K6 by double-labelled immunofluorescence (figure 3.25). These results showed strong K1 expression in both *K14.cre/Isl.ROCK^{er}/HK1.fos* and *HK1.fos* hyperplasia in a normal supra-basal fashion (figure 3.25a,b); however, occasionally in areas of multiple basal layers, at the basal/supra-basal junction, a faint possibility of premature K1 expression could be seen in the upper expanded basal layer of *K14.cre/Isl.ROCK^{er}/HK1.fos* hyperplasia (figure 3.25a – arrows). Analysis of K6 however found a typical uniform high level of K6 expression in both bi-genic ROCK/fos and fos mice in all epidermal layers (figure 3.25c,d) that was classically matched with K6 expression in previous hyperproliferative HK1-transgenic epidermis (Greenhalgh et al., 1993a-c). This was quite different to K6 expression in ROCK^{er} alone but typical of fos (or ras^{Ha}) expression (Greenhalgh et al., 1993a-c) and suggests that fos signalling restores this K6 expression and overrides that of ROCK2; a result that is also observed *in vitro* (below).

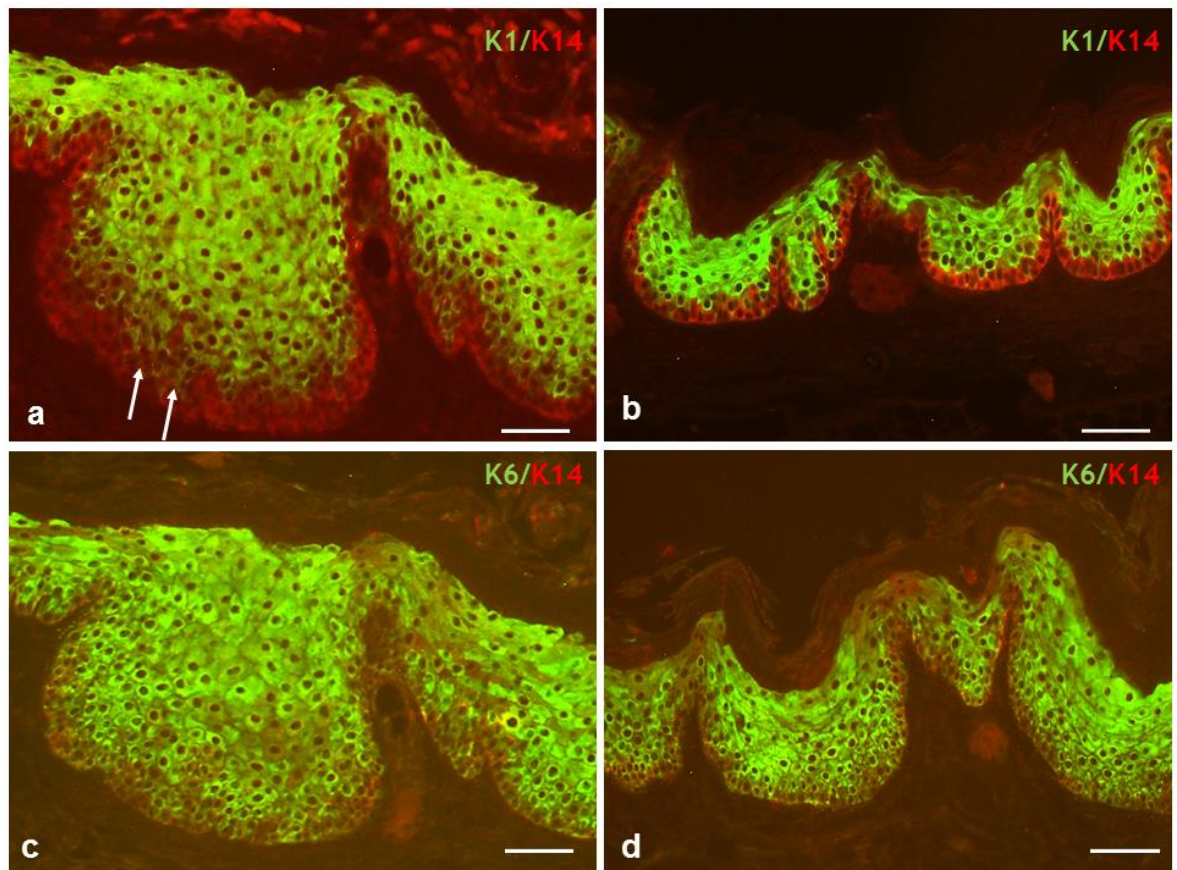


Figure 3.25 Immunofluorescence analysis of K1/K14 and K6/K14 expression in RU486-/4-HT-treated *K14.cre/Isl.ROCK^{ef}/HK1.fos* mice at 12 weeks. (a) *K14.cre/Isl.ROCK^{ef}/HK1.fos* and (b) *HK1.fos* hyperplasia exhibit K1 expression in supra-basal layers. (c) *K14.cre/Isl.ROCK^{ef}/HK1.fos* and (d) *HK1.fos* hyperplasia express K6 throughout epidermal layers. (Scale bar: 100 μ m).

Due to lack of differences in phenotype between bi-genic ROCK/fos and fos mice, in the repeat experiment, a second cohort of mice were kept on procedure for 20 weeks to test whether bi-genic ROCK/fos would produce any tumours. Typically this line of *HK1.fos* mice (Greenhalgh et al., 1993b) failed to develop overt tumours until around 6 to 8 months and these appeared on the tagged ear. In this experiment, at 20 weeks treatment, significant differences in phenotypes were displayed between *K14.cre/Isl.ROCK^{er}/HK1.fos* and *HK1.fos* mice as shown in figure 3.26. Here, during this extra time, *K14.cre/Isl.ROCK^{er}/HK1.fos* mice developed protruding, highly keratotic tumours whilst control untreated mice or *HK1.fos* alone mice presented only increased ear thickening (figure 3.26). On histological analysis, *K14.cre/Isl.ROCK^{er}/HK1.fos* mice displayed highly keratotic papillomas together with a significant number of keratin pearls encircled by classic papilloma histotypes (figure 3.27), again suggestive of roles in keratinocyte terminal differentiation as well as hyperproliferation and papillomatogenesis. In contrast, *HK1.fos* mice exhibited classic hyperplasia, similar to previous results with ROCK^{er} activation alone. However, at this time point, there was no indication of further progression to aggressive papillomas or conversion to malignancy in any *K14.cre/Isl.ROCK^{er}/HK1.fos* mice in these bi-genic experiments.

The lack of malignant conversion is also in stark contrast to that found in *K14.ROCK^{er}/HK1.ras¹²⁰⁵* mice; thus perhaps the context of tumours in *K14.cre/Isl.ROCK^{er}/HK1.fos* mice appears to be distinctly different to the results from the earlier *K14.ROCK^{er}/HK1.ras¹²⁰⁵* study where papillomas had converted to well-differentiated SCC histotypes at approximately 12 weeks. Nonetheless, these exciting data prove for the first time that ROCK2 deregulation co-operates with oncogenic fos in carcinogenesis and moreover, this may be the first example of ROCK being involved in the early stages prior to malignancy; by driving the formation of benign papillomas. This co-operation with fos appears to be a novel finding for ROCK activities and may be consistent with the roles for ROCK2 downstream of ras activation, and possible co-operation in terminal differentiation.



Figure 3.26 Phenotypes of *K14.cre/lsl.ROCK^{er}/HK1.fos* and *HK1.fos* mice at 20 weeks. (a) RU486-/4-HT-treated *K14.cre/lsl.ROCK^{er}/HK1.fos* mouse exhibits a protruding keratotic tumour. (b) 4-HT-treated *HK1.fos* and (c) RU486-treated/4-HT-untreated *K14.cre/lsl.ROCK^{er}/HK1.fos* mice display scaly and thickened ears.

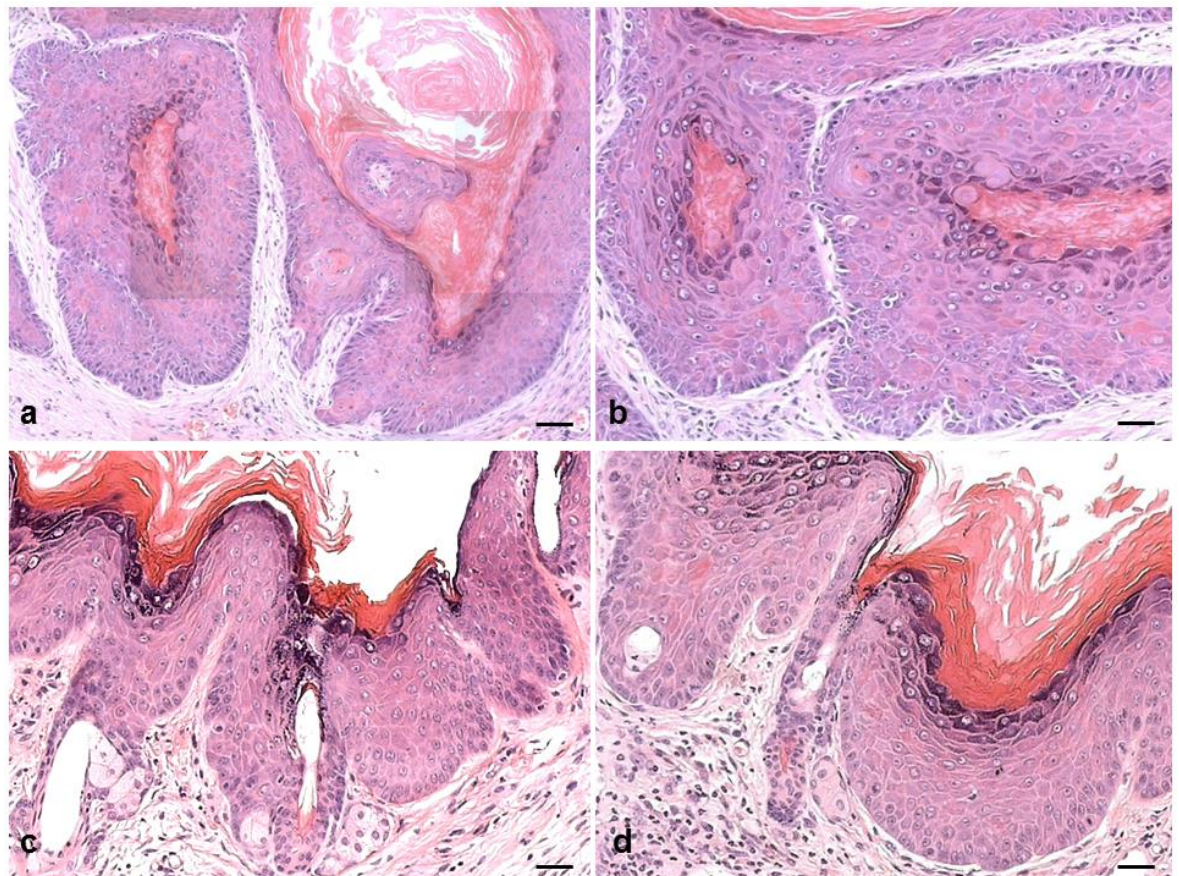


Figure 3.27 Histotype of *K14.cre/lsl.ROCK^{er}/HK1.fos* and *HK1.fos* epidermis at 20 weeks of 4-HT treatment. (a) Composite micrograph of *K14.cre/lsl.ROCK^{er}/HK1.fos* epidermis displays a papilloma histotype with keratin encircled cyst appearing between epidermal layers. (b) Higher magnification of *K14.cre/lsl.ROCK^{er}/HK1.fos* tumour shows a papilloma histotype with the appearance of acanthosis and some odd differentiation in each compartment, but no signs of malignancy as confirmed by K1, p53 and p21 expression (below). (c) RU486-treated/4-HT-untreated *K14.cre/lsl.ROCK^{er}/HK1.fos* epidermis and (d) 4-HT-treated *HK1.fos* shows hyperplasia with papillomatous epidermal layers and a very prominent granular layer associated with *HK1.fos* expression. (Scale bar: a: 100µm, b-d: 50µm)

Expression of keratin K1 confirmed that the tumours produced in *K14.cre/Isl.ROCK^{er}/HK1.fos* mice were benign, whereas bi-genic *ROCK/ras¹²⁰⁵* tumours lost K1 expression by this time following conversion to wdSCC and progression to SCC. Further, as shown in figure 3.28, intense K1 expression appeared in the supra-basal layers of bi-genic *ROCK/fos* mice. This finding again supports the idea that *ROCK^{er}* may accelerate an early differentiation response along with, or amplified by, *HK1.fos* activation particularly with the appearance of keratin pearls and the massive overt keratosis exhibited by these bi-genic *ROCK/fos* papillomas. K6 expression in *K14.cre/Isl.ROCK^{er}/HK1.fos* and *HK1.fos* cohorts showed a distribution more typical of *HK1.fos* phenotypes with expression occurring in a uniform fashion throughout epidermal layers, a result that was typically linked to the active proliferation events that drive tumour promotion.

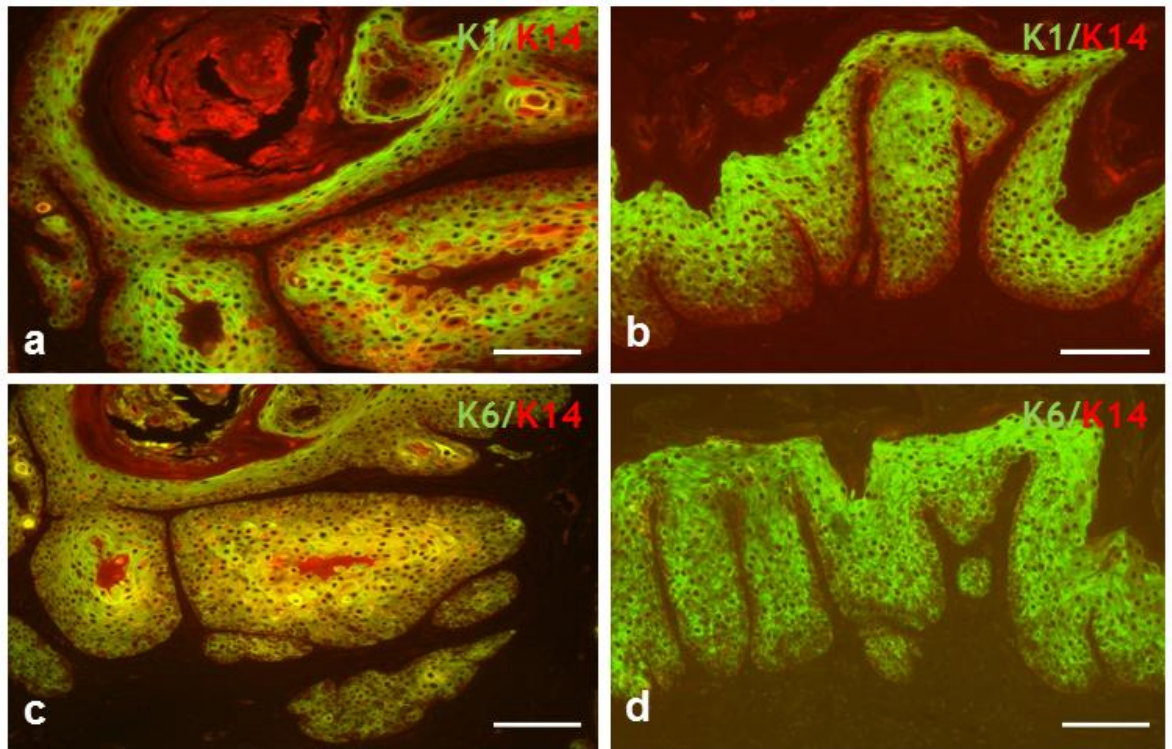


Figure 3.28 Immunofluorescence analysis of K1/K14 and K6/K14 expression in *K14.cre/lsl.ROCK^{ef}/HK1.fos* and *HK1.fos* mice at 20 weeks of 4-HT treatment. (a) *K14.cre/lsl.ROCK^{ef}/HK1.fos* keratotic papilloma and (b) *HK1.fos* hyperplasia exhibit K1 expression in the supra-basal layers. (c) *K14.cre/lsl.ROCK^{ef}/HK1.fos* benign papilloma and (d) *HK1.fos* hyperplasia display K6 expression in all epidermal layers consistent with a typical K6 expression in response to hyperproliferation. (Scale bar: 100 μ m).

3.4.2 Expression of p53 and p21 in bi-genic ROCK/fos mice

Given the lack of malignant progression and the dominant keratosis in the papillomas, the expression profiles of p53 and p21 were determined by IHC analysis of *K14.cre/Isl.ROCK^{er}/HK1.fos* tumour histotypes. Both p53 and p21 are known for their tumour growth inhibitory function, and were shown to be fundamental in preventing conversion of both bi-genic *ras¹²⁷⁶/Δ5PTEN^{flx}* and *fos/Δ5PTEN^{flx}* tumours (Yao et al., 2006, 2008, Macdonald et al., 2014). Therefore, it was expected that both p53 and p21 would be strongly expressed at this benign stage.

As shown in figure 3.29, *K14.cre/Isl.ROCK^{er}/HK1.fos* papillomas expressed high p53 levels with intense distribution in all epidermal compartments including the proliferative basal layer keratinocytes (figure 3.29a,b), similar to its expression in *HK1.fos* epidermis (figure 3.29e). Moreover, both *K14.cre/Isl.ROCK^{er}/HK1.fos* (figure 3.29c,d) and *HK1.fos* (figure 3.29f) exhibited elevated and uniform expression of p21 throughout the epidermal layers. This finding was similar to the p53/p21 expression profiles observed in bi-genic *ROCK/ras¹²⁰⁵* during formation of benign papillomas. However, in this context and unlike the previous model where first p53 then followed by p21 expression became faded, persistent p53/p21 expression became elevated and resulted in a stable papilloma not prone to conversion, despite ROCK2 activation. Hence, both p53 and p21 act as pivotal targets to suppress malignant conversion in *K14.cre/Isl.ROCK^{er}/HK1.fos* benign tumours.

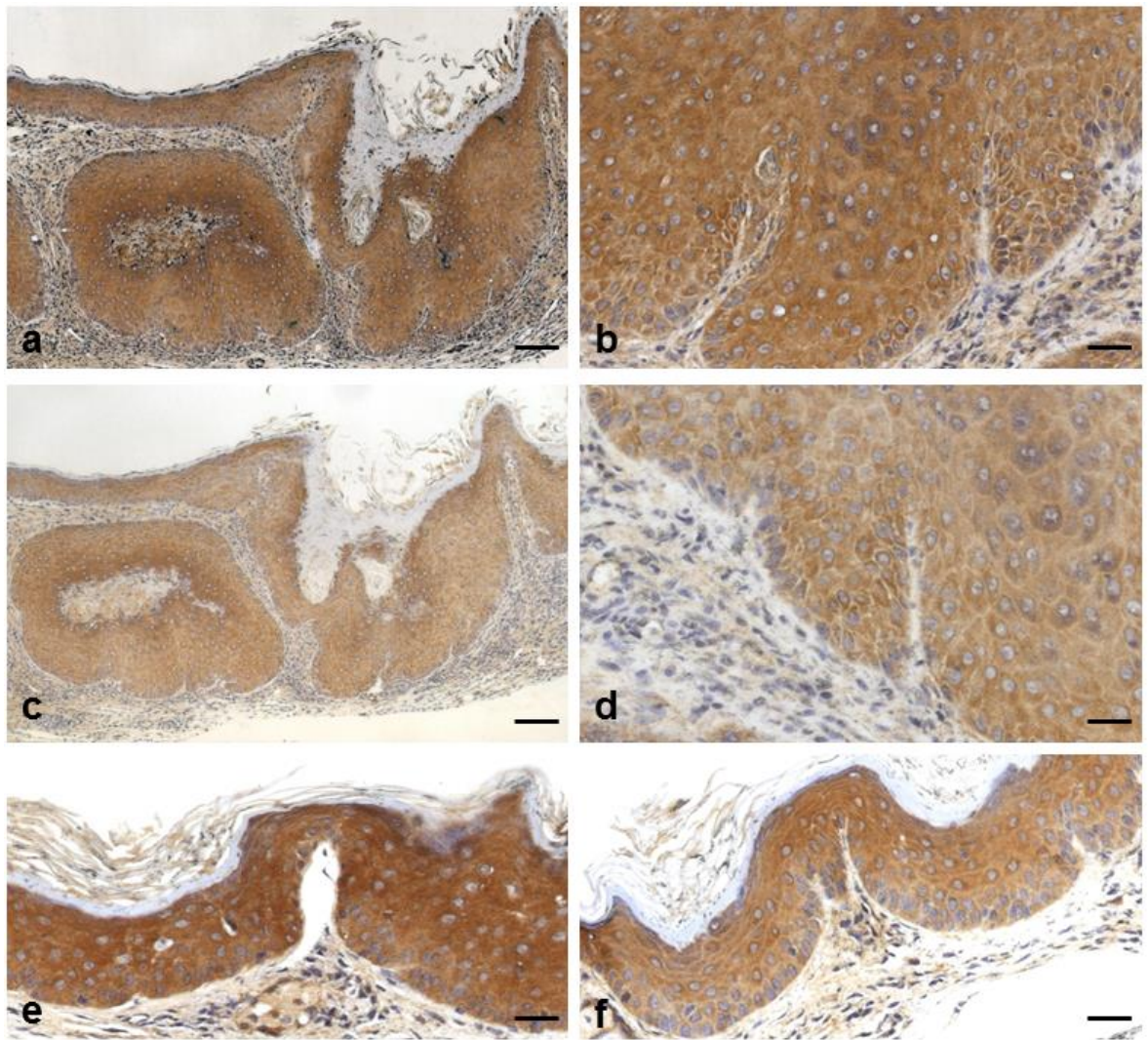


Figure 3.29 IHC analysis of p53 and p21 in RU486-/4-HT-treated *K14.cre/Isl.ROCK^{ef}/HK1.fos* and *HK1.fos* cohorts. (a) p53 is highly expressed throughout epidermal layers including (b) basal layers of *K14.cre/Isl.ROCK^{ef}/HK1.fos* benign papilloma histotypes. (c, d) Uniform expression of p21 in all epidermal layers of *K14.cre/Isl.ROCK^{ef}/HK1.fos* papilloma histotypes. (e) *HK1.fos* hyperplasia histotypes also exhibit strong expression of p53 and (f) p21 in all epidermal layers.

3.4.3 BrdU-labelling of bi-genic ROCK/fos mice

Skin biopsies were analysed for BrdU-labelling expression to assess proliferating cells in *K14.cre/Isl.ROCK^{er}/HK1.fos* mice. As expected, BrdU-positive cells (figure 3.30) showed more distribution in RU486-/4-HT-treated *K14.cre/Isl.ROCK^{er}/HK1.fos* benign tumours which indicated higher cell proliferation activity (22.1%) than fos hyperplasia (4-HT-treated and 4-HT-untreated *HK1.fos* hyperplasia: 15.2% and 14.8%; RU486-treated/4-HT-untreated *K14.cre/Isl.ROCK^{er}/HK1.fos* 14.5%). These findings indicate that cell proliferation rates increase as ROCK co-operates with fos in benign papilloma formation as compared to fos or ROCK/fos in the hyperplasia stage.

Higher levels of BrdU-labelling were displayed in bi-genic ROCK/fos benign papillomas. However, this proliferation rate was considerably lower in comparison to mitotic activity during bi-genic ROCK/ras¹²⁰⁵ papillomatogenesis which was almost three times higher and consistent with p53 loss that led to a papilloma prone to conversion. This lower level of proliferative activity also supports the idea that increased expression of p53 and p21 is instrumental in preventing conversion in bi-genic ROCK/fos papillomas.

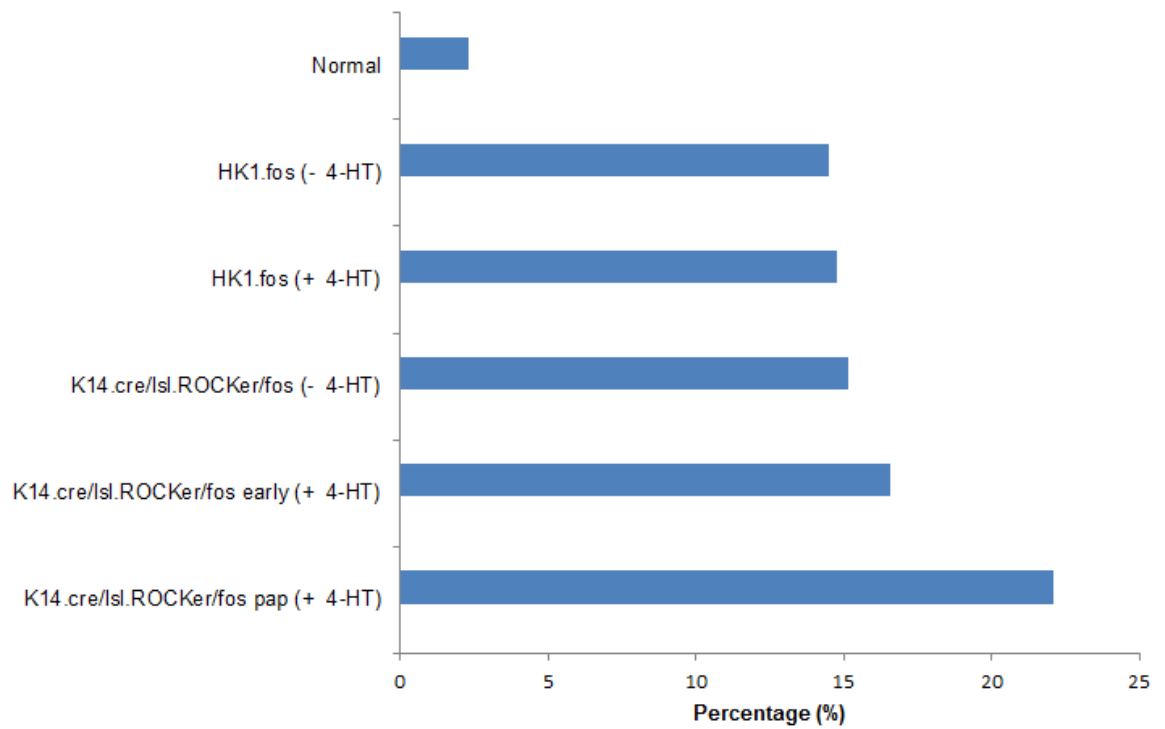


Figure 3.30 BrdU-labelling of bi-genic ROCK/fos carcinogenesis. Graph displays serial increases in cell proliferation activity upon conversion of hyperplasia to benign papilloma phenotypes in *K14.cre/lsl.ROCKer/HK1.fos* mice. (No significant difference between each cohort; $p > 0.05$).

3.4.4 Summary

Collectively, this study has shown for the first time that ROCK2 can act as an initiator in co-operation with fos oncogene activation and together their activation produce benign squamous papilloma histotypes. Since ROCK is well-known for its role during the late stage of cancer (Croft et al., 2004, Samuel et al., 2011), this finding is also a novel indicator of early co-operation between ROCK2 and fos activation in benign tumour formation. Moreover, in comparison to co-operation between activated ROCK and ras^{Ha}, bi-genic ROCK/fos mice did not achieve the context where papillomas are prone to convert to malignancy. The resistance in *K14.cre/lsl.ROCKer/HK1.fos* benign papillomas was associated with an increased, possibly premature expression of keratin K1, and compensatory p53 and p21 that supported formation of stable benign squamous papillomas, and limited further progression.

3.5 Co-operation of ROCK2 and *K14.cre/Δ5PTEN^{flox}* in transgenic mouse skin carcinogenesis

PTEN is one of the major tumour suppressor genes targets in cancer, thus its loss may be one of the key elements in tumourigenesis (Yao et al., 2006, 2008). It has been shown that inactivation of PTEN, particularly on exon 5 which encodes the phosphatase active site, is implicated in tumour formation (Suzuki et al., 2003, Freeman et al., 2006). Since PTEN negatively regulates the PI3K/AKT pathway, apparent differentiation activity may be induced to compensate for loss of PTEN as AKT is essential in proliferation (Suzuki et al., 2003). A long term goal of this study has been to model the effect of deregulated ROCK signalling alongside the PTEN/AKT pathway (Yao et al., 2006) as mediated by loss of PTEN regulation of AKT (Macdonald et al., 2014). As ROCK kinase is well-known for its role in actomyosin contraction which affects cellular tension and cytoskeletal organisation (Samuel et al., 2011, Rath and Olson, 2012); and PTEN has been associated with regulation of cytoskeleton proteins and adherens junctions (Subauste et al., 2005) prior to its more popular roles in interacting with p53 expression (Yao et al., 2006, 2008, Macdonald et al., 2014) . This made the study of the roles of ROCK activation with PTEN loss in carcinogenesis and epidermal differentiation a logical step.

In the past, *in vivo* models were unable to address these questions, yet evidence of a relationship between the Rho/ROCK signalling pathway and PTEN in the regulation of p-AKT levels was suggested by a single *in vitro* study (Li et al., 2005). However, this past study was performed on human embryonic kidney cells and did not specify whether it was ROCK1 or ROCK2. Furthermore, there is still a lack of evidence about the relationship between ROCK and PTEN through *in vivo*, thus, a co-operation study between ROCK2 activation and inactivation of PTEN activity was directly examined in this transgenic mouse model.

It is documented that PTEN shares a homology with tensin which is a cytoskeleton component (Li et al., 1997, Di Cristofano et al., 1998) and it is known that ROCK plays an essential role in the regulation of actin cytoskeleton. However, the implication of direct co-operation between ROCK2 activation and inactivation of

PTEN activity in multistage skin carcinogenesis remains unclear. Yao et al., (2006) demonstrated that inactivation of PTEN alone in the absence of chemical treatment or additional oncogenes resulted in mild epidermal hyperplasia and hyperkeratosis associated with Cowden disease, a familial cancer syndrome (Suzuki et al., 2003, Mao et al., 2004). Interestingly, co-operation between PTEN loss ($\Delta 5PTEN^{flx}$) and ras^{Ha} activation produced benign squamous papillomas without conversion (Yao et al., 2006), whilst co-operation between PTEN loss ($\Delta 5PTEN^{flx}$) and fos oncogene activation showed an alternative tumour formation which developed to a progressive keratoacanthoma (KA) (Yao et al., 2008). Therefore, the mechanistic consequences of co-operation between ROCK2 and PTEN loss ($\Delta 5PTEN^{flx}$) in early tumour formation will be examined and later, studies will progress to ROCK2 activation in bi-genic $ras/\Delta 5PTEN^{flx}$ and $fos/\Delta 5PTEN^{flx}$.

3.5.1 Confirmation of *Isl.ROCK^{er}* expression in bi-genic **ROCK/ $\Delta 5PTEN^{flx}$ mice**

As mentioned earlier, the new *Isl.ROCK^{er}* model was used in this study to ensure the same genes: $ROCK^{er}$ and $\Delta 5PTEN^{flx}$ were targeted by the K14.CreP vector in the epidermis and hair follicles following induction by RU486 treatment (Berton et al., 2000b). *K14.cre/Isl.ROCK^{er}/ $\Delta 5PTEN^{flx}$* mice were first analysed to verify the expression of the gfp-tag which is indicative of $ROCK^{er}$ transgene expression (EGFP). As shown in figure 3.31a, *K14.cre/Isl.ROCK^{er}/ $\Delta 5PTEN^{flx}$* skin demonstrated gfp expression in all epidermal layers including follicular areas as compared to no expression in *K14.cre/ $\Delta 5PTEN^{flx}$* mice (figure 3.31b). Therefore, this study confirmed $ROCK^{er}$ transgene expression in *K14.cre/Isl.ROCK^{er}/ $\Delta 5PTEN^{flx}$* mice.

To confirm that the *K14.cre/Isl.ROCK^{er}/ $\Delta 5PTEN^{flx}$* phenotype was due to activation of 4-HT treatment, analysis of p-Mypt1 which is a downstream substrate for ROCK was performed on the skin biopsies. As shown in figure 3.31c, p-Mypt1 was expressed throughout the epidermal layers of RU486-/4-HT-treated *K14.cre/Isl.ROCK^{er}/ $\Delta 5PTEN^{flx}$* mouse skin including the proliferative basal layer and hair follicles, consistent with the K14.CreP expression profile (Berton et al., 2000b). In contrast, p-Mypt1 expression appeared at very low levels in the mildly

hyperplastic RU486-/4-HT-treated *K14.cre/Δ5PTEN^{fix}* control epidermis (figure 3.31d). These findings showed that not only was the *ROCK^{er}* transgene expressed in all epidermal layers including hair follicles of the new *Isl.ROCK^{er}* model, but also confirmed the 4-HT activation of *K14.cre/Isl.ROCK^{er}/Δ5PTEN^{fix}* cohorts.

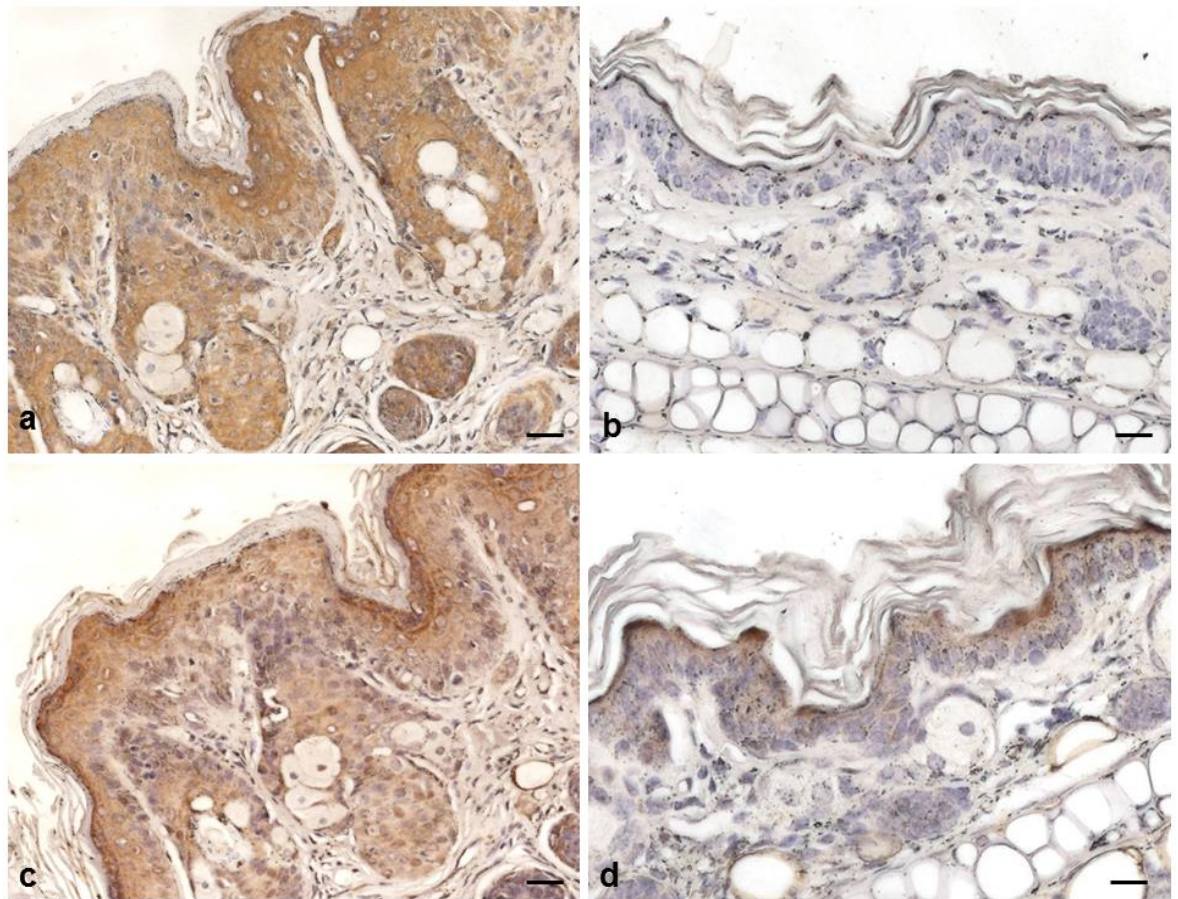


Figure 3.31 IHC analysis for the GFP-tagged ROCK^{er} transgene and p-Mypt1 of ROCK substrate. (a) Strong basal expression of exogenous ROCK^{er} in the keratinocyte cytoplasm of all epidermal layers including follicular areas of RU486-/4-HT-treated *K14.cre/lsI.ROCK^{er}/Δ5PTEN^{flx}* papillomatous hyperplasia. (b) No gfp expression in RU486-/4-HT-treated *K14.cre/Δ5PTEN^{flx}* line. (c) Elevated expression of Mypt1 phosphorylation in RU486-/4-HT-treated *K14.cre/lsI.ROCK^{er}/Δ5PTEN^{flx}* papillomatous hyperplasia including hair follicles compared to (d) weak p-Mypt1 expression in RU486-/4-HT-treated *K14.cre/Δ5PTEN^{flx}* hyperplasia.

3.5.2 ROCK2 co-operates with $\Delta 5PTEN^{fix}$ to elicit hyperplasia with papillomatous appearance

Transgenic mice expressing the new ROCK2 transgenic genotype, *Isl.ROCK^{er}* mice were crossed with *K14.cre/ $\Delta 5PTEN^{fix}$* lines to make sure that the same epidermal cells were being targeted as in the PTEN floxed model which requires the K14.creP regulator (Berton et al., 2000b). Cohorts (n=10) of new *K14.cre/Isl.ROCK^{er}/ $\Delta 5PTEN^{fix}$* and age-matched *K14.cre/ $\Delta 5PTEN^{fix}$* siblings were topically treated with RU486 on both ears to activate the cre and thus ablate the exon5 of PTEN and the transcriptional stop cassette for *Isl.ROCK^{er}* transgene expression. Subsequently, mice were treated with 4-HT 3 times per week to activate the ROCK^{er} function in the epidermis, for an eventual 7 months. Each bi-genic control genotype (n=5) received identical RU486/4-HT treatment for up to 27 weeks; with a cohort (n=5) of *K14.cre/Isl.ROCK^{er}/ $\Delta 5PTEN^{fix}$* controls receiving RU486 but ethanol alone.

Both RU486-/4-HT-treated *K14.cre/Isl.ROCK^{er}/ $\Delta 5PTEN^{fix}$* and *K14.cre/ $\Delta 5PTEN^{fix}$* transgenic mice had skin thickening with mild keratosis as early as 10 to 12 weeks but these remained relatively unchanged on week 27th (figure 3.32a,b). However, no tumours appeared at any time unlike bi-genic ROCK/ras¹²⁰⁵ and ROCK/fos mice where tumours appeared by 12–18 weeks. All control cohorts, 4-HT-untreated *K14.cre/Isl.ROCK^{er}/ $\Delta 5PTEN^{fix}$* or *K14.cre/ $\Delta 5PTEN^{fix}$* exhibited similar phenotypes with no tumours produced up to 7 months (figure 3.32c,d), a result consistent with the *K14.ROCK^{er}* genotypes and earlier *K14.cre/ $\Delta 5PTEN^{fix}$* studies (Yao et al., 2006, 2008).

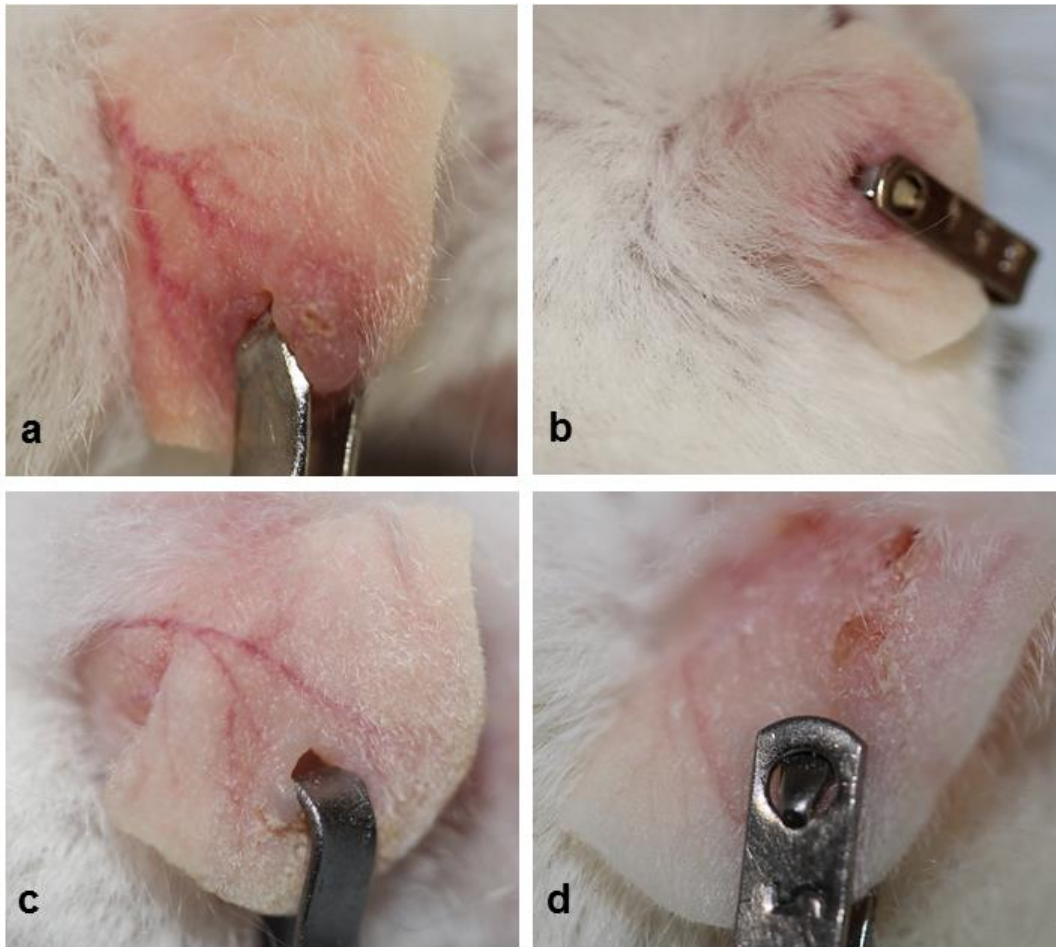


Figure 3.32 Phenotypes of *K14.cre/Isl.ROCK^{er}/Δ5PTEN^{fix}* and *K14.cre/Δ5PTEN^{fix}* mice at 27 weeks treatment. (a) RU486-/4-HT-treated *K14.cre/Isl.ROCK^{er}/Δ5PTEN^{fix}* exhibit thickened ear with small protrusion. (b) RU486-/4-HT-treated *K14.cre/Δ5PTEN^{fix}* together with (c) RU486-treated/4-HT-untreated *K14.cre/Isl.ROCK^{er}/Δ5PTEN^{fix}* and (d) RU486-treated/4-HT-untreated *K14.cre/Δ5PTEN^{fix}* mice display scaly and slightly thickened ears.

Following initial RU486 treatments in week 1, and 27 weeks of 4-HT treatment, *K14.cre/Isl.ROCK^{er}/Δ5PTEN^{flx}* ear skin biopsies were shown histologically to have a more extensive epidermal hyperplasia, hyperkeratosis and papillomatous features with many folds (figure 3.33a) as compared to RU486-/4-HT-treated *K14.cre/Δ5PTEN^{flx}* cohorts; which showed a mild epidermal hyperplasia with a slightly folded appearance and mild keratosis as observed previously (figure 3.33b), and as observed in control RU486-treated/4HT-untreated *K14.cre/Isl.ROCK^{er}/Δ5PTEN^{flx}* and *K14.cre/Δ5PTEN^{flx}* cohorts (figure 3.33c,d). This finding suggests that at this stage, in the absence of ras^{Ha}-associated initiation or fos associated promotion, there appears to be little co-operation between ROCK and PTEN to drive papillomatogenesis in *K14.cre/Isl.ROCK^{er}/Δ5PTEN^{flx}* cohorts. However, there appears to be a synergism between these pathways in terms of increased proliferation and altered differentiation when compared to their single transgene littermates. This unique and unexpected finding from RU486-/4-HT-treated *K14.cre/Isl.ROCK^{er}/Δ5PTEN^{flx}* mice showed a distinctive opposite outcome when compared to the result from bi-genic ROCK/ras¹²⁰⁵ and ROCK/fos mice which resulted in tumour formation around 8-12 weeks. Moreover, *K14.cre/Isl.ROCK^{er}/Δ5PTEN^{flx}* histotypes showed little difference to the mild hyperplasia histotypes from ROCK activation alone and *K14.cre/Δ5PTEN^{flx}* mice.

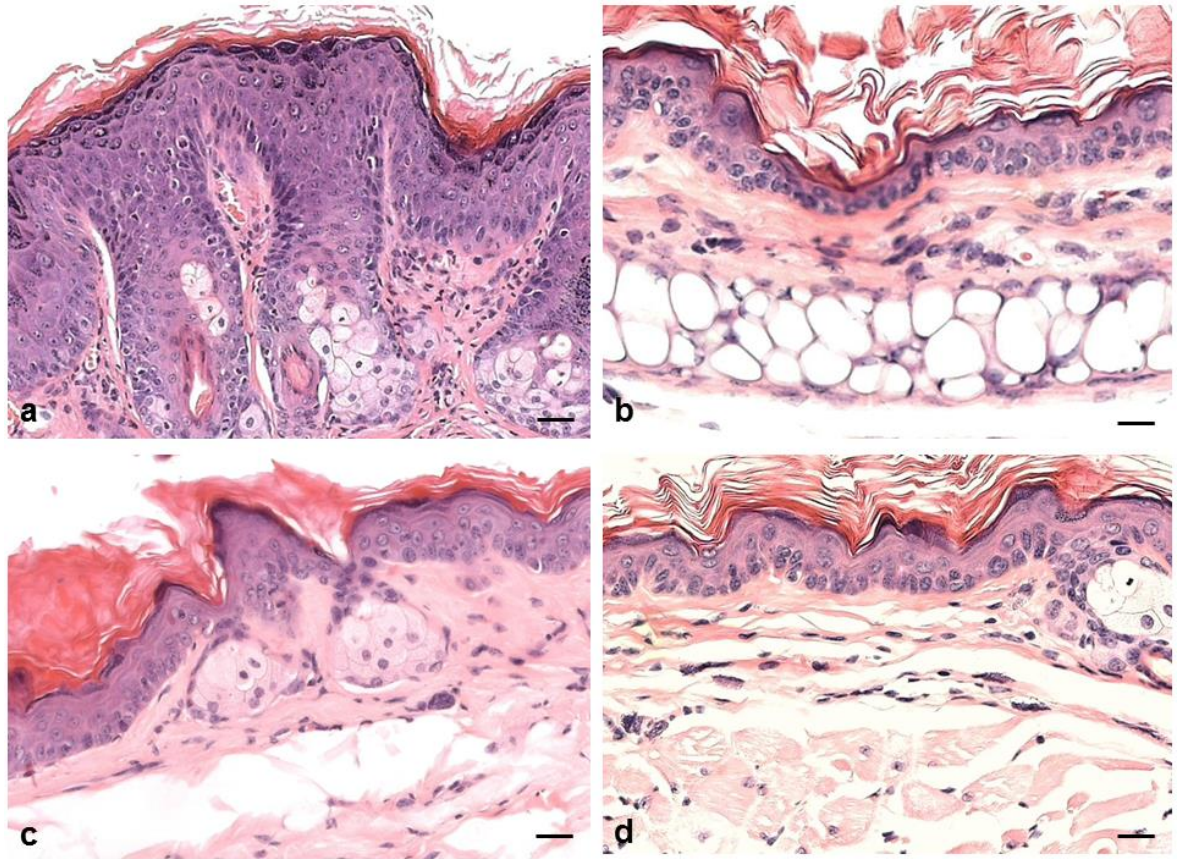


Figure 3.33 Histotype of *K14.cre/Isl.ROCK^{er}/Δ5PTEN^{flx}* and *K14.cre/Δ5PTEN^{flx}* mice at 27 weeks. (a) RU486-/4-HT-treated *K14.cre/Isl.ROCK^{er}/Δ5PTEN^{flx}* epidermis show hyperplasia with expanded epidermal compartments. (b) RU486-/4-HT-treated *K14.cre/Δ5PTEN^{flx}* mice; together with (c) RU486-treated/4-HT-untreated *K14.cre/Isl.ROCK^{er}/Δ5PTEN^{flx}* and (d) RU486-treated/4-HT-untreated *K14.cre/Δ5PTEN^{flx}* mice exhibit identical hyperplasia. (Scale bar: 100μm).

3.5.3 Expression of differentiation markers in bi-genic ROCK/ Δ 5PTEN^{flx}

Skin biopsies were analysed for the expression of the early differentiation markers keratin K1 and K6 to examine the effects of bi-genic ROCK/ Δ 5PTEN^{flx} in keratinocytes differentiation as no tumours resulted from this co-operation. K1, which is expressed in the supra-basal layer, is one of the earliest markers of differentiation whereas K6 is not expressed in the normal epidermis, except for the hair follicle, and its expression in the epidermis is associated with hyperproliferation or stress. Both K1 and K6 markers are counterstained with keratin K14 which represents the keratinocytes.

RU486-/4-HT-treated *K14.cre/Isl.ROCK^{er}/ Δ 5PTEN^{flx}* and *K14.cre/ Δ 5PTEN^{flx}* cohorts exhibited K1 expression in the supra-basal layers (figure 3.34a,b), however K1 expression in the *K14.cre/Isl.ROCK^{er}/ Δ 5PTEN^{flx}* epidermis appears to be stronger than typical K1 expression in hyperplasia (e.g. *HK1.fos* hyperplasia), due to thick basal layer (arrows) which suggests a high rate of proliferation (figure 3.34a), consistent with an increased mitotic index (below). In *K14.cre/Isl.ROCK^{er}/ Δ 5PTEN^{flx}* cohorts, K6 expression seems to appear in an atypical fashion with patchy expression in the thick hyperplastic layers (figure 3.34c) whereas no K6 expression was seen in the mild epidermal hyperplasia of *K14.cre/ Δ 5PTEN^{flx}* cohorts, and only appeared in the follicles (figure 3.34d). These findings suggest that co-operation between ROCK^{er} activation and PTEN loss (Δ 5PTEN^{flx}) can lead to changes in proliferation and differentiation activities leading to a greater degree of both hyperplasia and hyperkeratosis instead of papilloma formation.

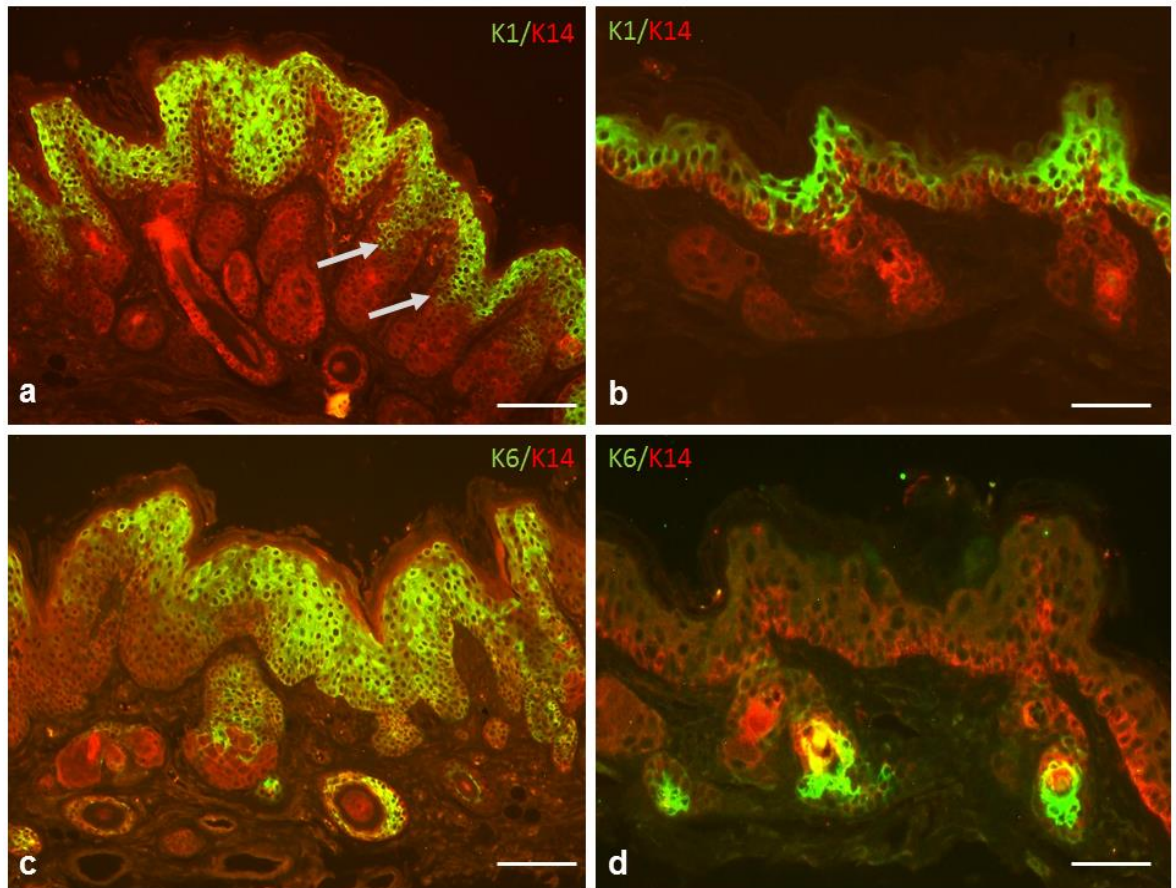


Figure 3.34 Immunofluorescence analysis of K1/K14 and K6/K14 expression at 27 weeks of 4-HT treatment. (a) RU486-/4-HT-treated *K14.cre/Isl.ROCK^{er}/Δ5PTEN^{flx}* epidermal hyperplasia shows a supra-basal K1 expression in folded papillomatous epidermal layers and appears delayed (arrows) due to thick proliferative basal layers. (b) RU486-/4-HT-treated *K14.cre/Δ5PTEN^{flx}* mild hyperplasia exhibits uneven green K1 expression in the supra-basal layer. (c) RU486-/4-HT-treated *K14.cre/Isl.ROCK^{er}/Δ5PTEN^{flx}* papillomatous hyperplasia shows patchy expression of K6. (d) RU486-/4-HT-treated *K14.cre/Δ5PTEN^{flx}* mild hyperplasia exhibits a usual lack of K6 expression except in the follicle areas. (Scale bar: 100μm).

3.5.4 Expression of p53, p21 and p-AKT1 in bi-genic ROCK/ Δ 5PTEN^{flx} mice

It is well documented that PTEN acts as negative regulator of AKT inhibiting phosphorylation of AKT (p-AKT) and this inactivation leads to apoptosis and cell death (Vasudevan et al., 2007). In addition, loss of PTEN regulation also has an impact on p53/p21 expression given that p-AKT activation typically leads to down-regulation of p53 by increasing MDM2, which is induced by p-AKT (Freeman et al., 2003, Suzuki et al., 2003), and thus facilitates tumourigenesis. As previously shown both p53 and p21 are compromised during multistage carcinogenesis studies with loss of p53 expression observed upon malignant conversion, followed by p21 loss when tumours progressed to aggressive carcinomas (Macdonald et al., 2014), and p53/p21 profiles in bi-genic ROCK/ras¹²⁰⁵ carcinomas concurred with this (above). In addition, both p53 and p21 are also known to prevent further tumour progression and this compensatory function has been demonstrated in all early bi-genic ROCK/ras¹²⁰⁵ papillomas; and as shown in bi-genic ROCK/fos tumours can prevent malignant conversion as these papillomas remain benign. These results were consistent with findings in previous studies involving PTEN mutation (Yao et al., 2006, 2008, Macdonald et al., 2014).

In this study, expression profiles of p53, p21 and p-AKT1 in *K14.cre/Isl.ROCK^{er}/Δ5PTEN^{flx}* hyperplastic histotypes were determined by IHC and IFC analysis. As hyperplastic *K14.cre/Isl.ROCK^{er}/Δ5PTEN^{flx}* cohorts resulted in changes in epidermal differentiation instead of tumour formation, it was anticipated that expression of p53 and p21 may be up regulated as previously observed in bi-genic ROCK/fos and ROCK/ras¹²⁰⁵ epidermis. For activated AKT, expression of p-AKT1 protein was chosen for analysis which is detectable and specific to skin instead of p-AKT2 protein which has not been detected in skin (below).

As shown in figure 3.35, surprisingly RU486-/4-HT-treated *K14.cre/Isl.ROCK^{er}/Δ5PTEN^{flx}* cohorts demonstrated patchy expression of p53 (figure 3.35a, b) and anomalous expression of p21 (figure 3.35d, e). Similarly, mildly hyperplastic *K14.cre/Δ5PTEN^{flx}* epidermis also displayed uneven and weak expression of both p53 and p21 (figure 3.35c, f) at this stage. This anomalous

expression of both p53 and p21 in *K14.cre/Isl.ROCK^{er}/Δ5PTEN^{flx}* and *K14.cre/Δ5PTEN^{flx}* epidermis was unexpected and appeared to be in contrast to the uniform and elevated p53/p21 expression in benign tumour formation observed in bi-genic ROCK/ras¹²⁰⁵ and ROCK/fos benign papillomas (above). However, as shown in figure 3.35(d - box,e), there seem to be an elevated expression of p21 and this may suggest the limited expression of p-AKT1 in the same area of *K14.cre/Isl.ROCK^{er}/Δ5PTEN^{flx}* hyperplasia (figure 3.36a – box). Only low levels of p-AKT1 expression appeared in the proliferative basal layer of RU486-/4-HT-treated *K14.cre/Isl.ROCK^{er}/Δ5PTEN^{flx}* epidermis (figure 3.36a) and this also compared to a surprising lack of p-AKT1 expression in RU486-/4-HT-treated *K14.cre/Δ5PTEN^{flx}* hyperplasia (figure 3.34b). These interesting findings indicate that at this early stage, neither p53 nor p21 appear to be induced in *K14.cre/Isl.ROCK^{er}/Δ5PTEN^{flx}* and *K14.cre/Δ5PTEN^{flx}* epidermal hyperplasia. At this hyperplastic stage active proliferation and altered differentiation have been shown occur (K6 analysis - above), which perhaps implies limited expression of p-AKT1 and thus, a lack of oncogenic activity in the context of this mild hyperplasia insufficient to induce high levels of p53/p21 expression. Nonetheless, often the p21 expression profile increase with time and this may have contributed to the lack of papillomas; however, the conclusion remains that the oncogenic hits supplied by ROCK and PTEN are either redundant or need to be linked by deregulation of the MAPK pathway in terms of ras initiation, fos promotion or both.

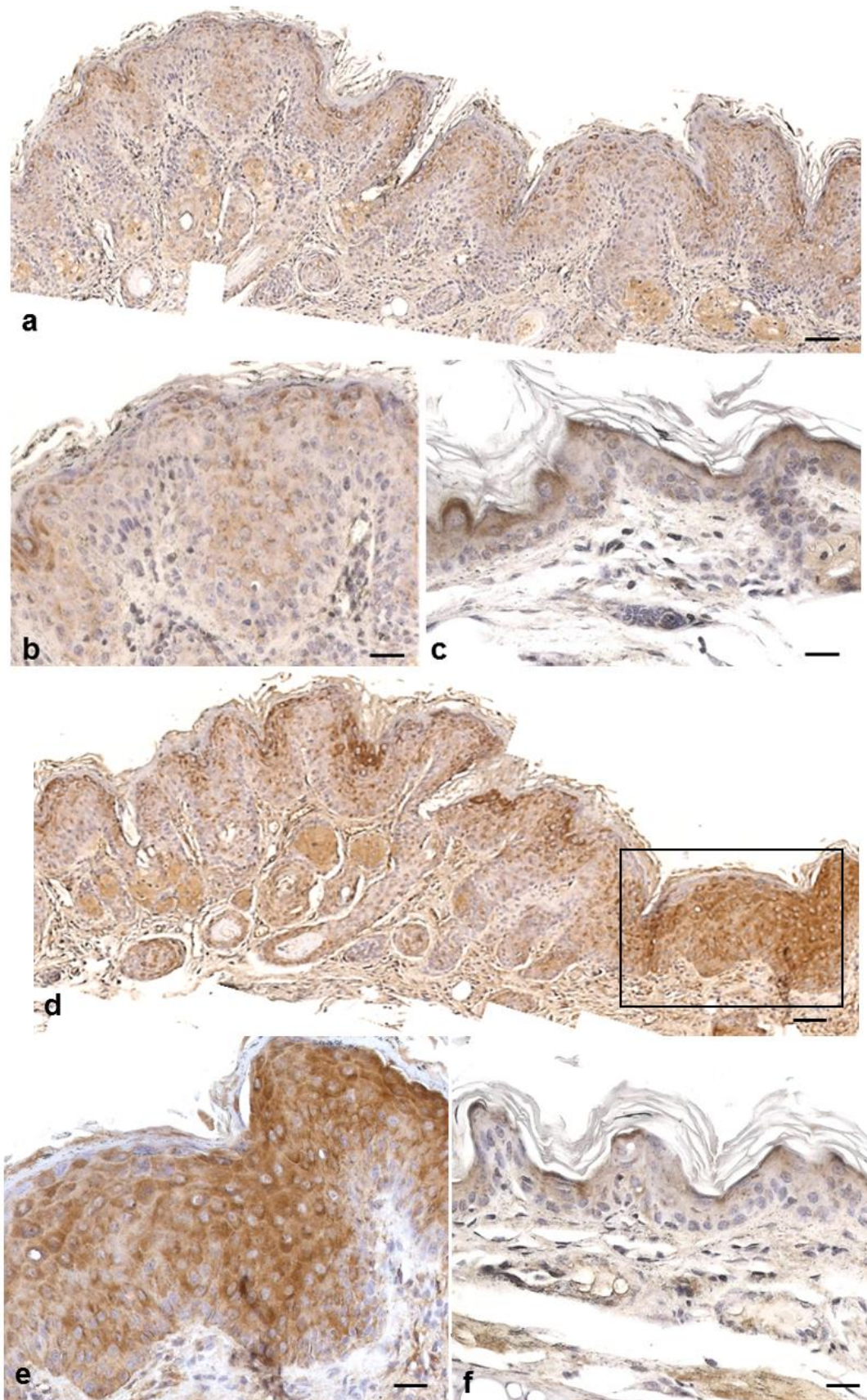


Figure 3.35 IHC analyses of p53 and p21. (a, b) RU486-/4-HT-treated *K14.cre/lsl.ROCK^{er}/Δ5PTEN^{flx}* papillomatous hyperplasia histotypes show uneven expression and sparse distribution of p53 in the epidermal layers. (c) Low level of p53 expression in the mildly hyperplastic RU486-treated/4-HT-treated *K14.cre/Δ5PTEN^{flx}* epidermis. (d) RU486-/4-HT-treated *K14.cre/lsl.ROCK^{er}/Δ5PTEN^{flx}* hyperplasia histotypes display anomalous expression of p21 in the

epidermal layer, though p21 expression appeared to be elevated in some areas (box). (e) Elevated p21 expression in RU486-/4-HT-treated *K14.cre/lsl.ROCK^{er}/Δ5PTEN^{flx}* hyperplasia may be the reason for the lack of p-AKT1 expression in the same area (figure 3.36a-box). (f) Higher magnification of RU486-treated/4-HT-treated *K14.cre/Δ5PTEN^{flx}* hyperplasia shows lack of p21 expression.

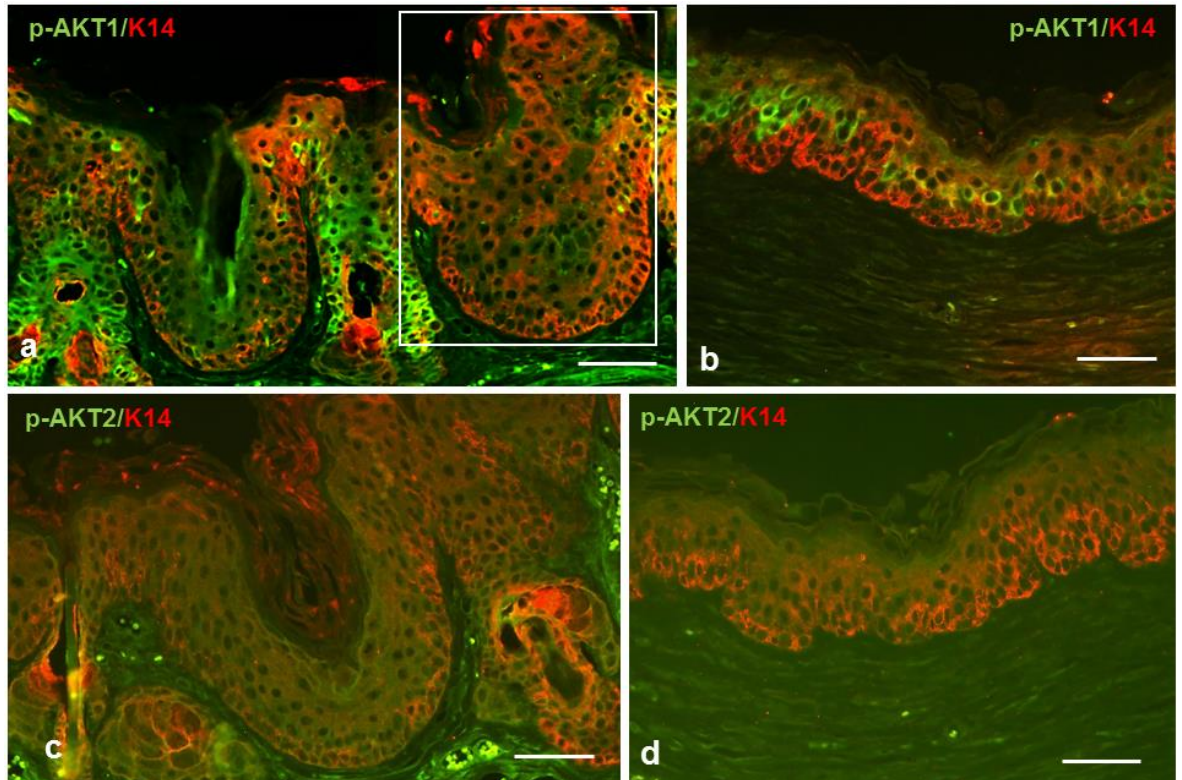


Figure 3.36 Immunofluorescence analysis of p-AKT1. (a) RU486-/4-HT-treated *K14.cre/lsl.ROCK^{er}/Δ5PTEN^{flx}* folded hyperplasia exhibits little expression of p-AKT1 which is limited to the proliferative basal layer. However, in the box area (elevated p21) shows no expression of p-AKT1, suggesting suppression by p21. (b) RU486-treated/4-HT-treated *K14.cre/Δ5PTEN^{flx}* display supra-basal expression of p-AKT1 in the epidermal hyperplasia histotypes. (c) RU486-/4-HT-treated *K14.cre/lsl.ROCK^{er}/Δ5PTEN^{flx}* and (d) RU486-treated/4-HT-treated *K14.cre/Δ5PTEN^{flx}* exhibit no expression of p-AKT2 which is not specific to skin unlike p-AKT1.

3.5.5 BrdU-labelling of bi-genic ROCK/ Δ 5PTEN^{flx} mice

Analysis of BrdU-labelling was performed on *K14.cre/Isl.ROCK^{er}/Δ5PTEN^{flx}* epidermis as a measure of cell proliferation activity. As shown in figure 3.37, BrdU-labelling of papillomatous hyperplasia from RU486-/4-HT-treated *K14.cre/Isl.ROCK^{er}/Δ5PTEN^{flx}* epidermis showed three times more proliferating cells (64.2%) than in mildly hyperplastic *K14.cre/Δ5PTEN^{flx}* epidermis (RU486-/4-HT-treated and RU486-treated/4-HT-untreated *K14.cre/Δ5PTEN^{flx}* cohorts: 18.2% and 20%; RU486-treated/4-HT-untreated *K14.cre/Isl.ROCK^{er}/Δ5PTEN^{flx}* 18.6%). Moreover, IFC analysis demonstrated groups of BrdU-labelled cells scattered in the proliferative basal layers of the *K14.cre/Isl.ROCK^{er}/Δ5PTEN^{flx}* epidermis (figure 3.37a) as compared to that of BrdU-labelled cells in control *K14.cre/Δ5PTEN^{flx}* epidermis (figure 3.37b). This finding indicates that although an elevated level of p21 expression (figure 3.35d-box, e) that downregulates p-AKT1 (figure 3.36a – box), and the lack of p53 expression (figure 3.35a) together with some p-AKT1 expression in the basal layer (figure 3.36a) may induce the significant increase in proliferative activity in *K14.cre/Isl.ROCK^{er}/Δ5PTEN^{flx}* papillomatous hyperplasia. This too may cause feedback loops that inhibited papilloma formation.

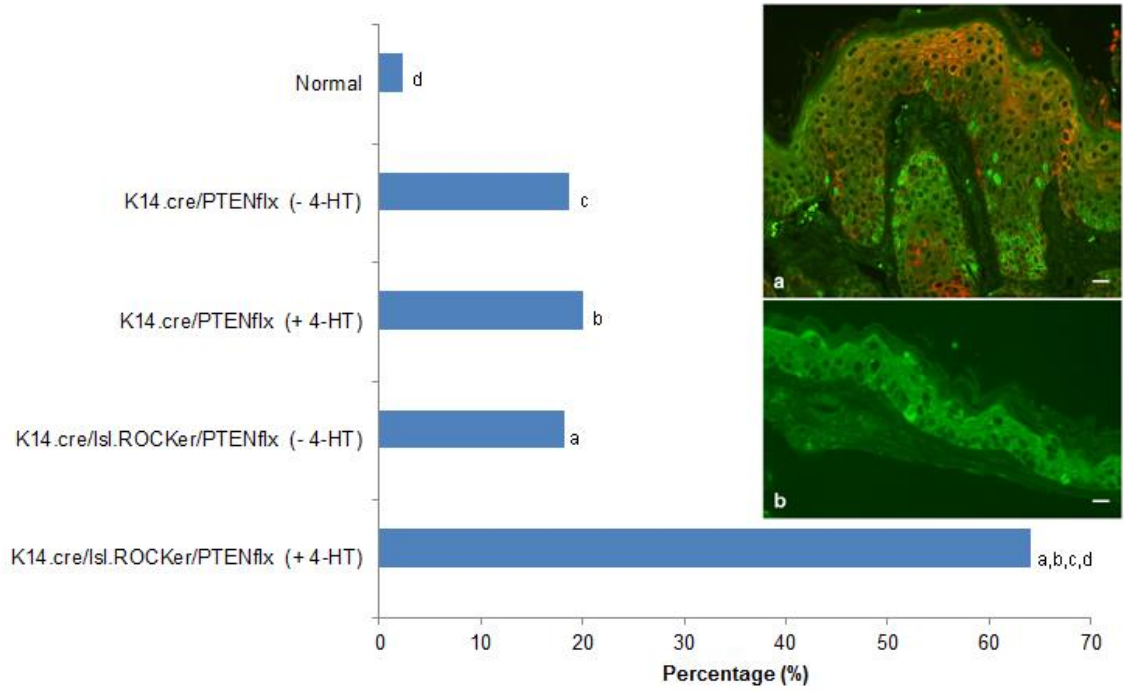


Figure 3.37 BrdU-labelling of bi-genic ROCK/ Δ 5PTEN^{flx} carcinogenesis. The graph displays cell proliferation activity in RU486-/4-HT-treated bi-genic ROCK/ Δ 5PTEN^{flx} mice that is significant and three times higher than that from Δ 5PTEN^{flx} mice (with or without 4-HT-treatment). (a,b,c,d : significant difference between *K14.cre/Isl.ROCK^{er}/Δ5PTEN^{flx}* (+ 4-HT) and each cohort; $p < 0.05$).

(a) RU486-/4-HT-treated *K14.cre/Isl.ROCK^{er}/Δ5PTEN^{flx}* epidermis exhibits a high number of BrdU-labelled keratinocytes in proliferative basal layers compared to (b) low numbers of BrdU-labelled cells in mildly hyperplastic epidermis of RU486-/4-HT-treated *K14.cre/Δ5PTEN^{flx}*. (Scale: 100 μm).

3.5.6 Summary

Bi-genic ROCK/ Δ 5PTEN^{fix} synergism showed little appearance of tumour formation even with continuous treatment for 7 months. Instead, alteration in both epidermal proliferation and differentiation appeared as shown by a delay in K1 expression due to increased thickness in the proliferative basal layers together with anomalous expression of K6. Nonetheless, in this study, the K6 expression in *K14.cre/lsl.ROCK^{er}/Δ5PTEN^{fix}* cohorts was elevated as compared to lack of K6 expression in Δ 5PTEN^{fix} hyperplasia, matched by the folded hyperplasia and much thicker appearance in bi-genic ROCK/ Δ 5PTEN^{fix}. This finding is consistent with the high proliferation rates from BrdU data.

In addition, low and patchy expression of p53 and p21 in bi-genic ROCK/ Δ 5PTEN^{fix} compared to a strong and uniform p53/p21 expression profile in bi-genic ROCK/fos papillomas indicate that p53 and p21 are not responsible for the lack of tumour formation. On the other hand, phosphorylated AKT which could contribute to tumorigenesis by its cell growth and cell survival functions may be accountable for the lack of tumour formation as it exhibited little expression. However, the areas of patchy p-AKT1 expression in RU486-/4-HT-treated *K14.cre/lsl.ROCK^{er}/Δ5PTEN^{fix}* folded hyperplasia were accompanied by an increased p21 expression which may suppress the p-AKT1 oncogenic functions; as observed in tri-genic ras/fos/ Δ 5PTEN^{fix} models (Greenhalgh, - manuscript in preparation, per communication with Greenhalgh). Furthermore, deregulation of PTEN has been associated with hyperkeratosis such as in Cowden's disease and is implicated in premature keratinocyte differentiation (Yao et al., 2008), which suggests that ROCK2 acts as a weak partner in co-operation with Δ 5PTEN^{fix} compared to its novel early co-operation with the fos oncogene in the initiation of papillomatogenesis.

3.6 Analysis of ROCK2 activation *in vitro*: effects on differentiation not carcinogenesis.

Earlier results successfully demonstrated co-operation between ROCK and each of the *ras/fos/Δ5PTEN^{fix}* transgenes *in vivo*. Several interesting features came to light, one of which was the surprising lack of co-operation with *Δ5PTEN^{fix}* and the unusual expression of various differentiation markers, such as keratin K6. In addition, the ROCK family has been demonstrated to effect and regulate keratinocytes differentiation (McMullan et al., 2003, Lock and Hotchin, 2009) and some of the first IHC staining experiments suggested that both ROCK1 and 2 were predominantly expressed in differentiated supra-basal cells; a finding consistent with roles in epidermal integrity and barrier functions. Therefore, this study now aimed to establish primary transgenic mouse keratinocyte cultures to mimic the *in vivo* model in order to understand further the role of ROCK2 in epidermal differentiation and proliferation.

Keratinocytes undergo different stages of growth in the formation of an epidermis and keratinocytes differentiation can be modelled *in vitro* by altering the calcium concentration in the medium. Through *in vitro* analysis, expression of keratin markers related to keratinocytes proliferation and differentiation can be analysed such as keratin K14 in the proliferative keratinocytes, keratin K1 expressed in the early stages of terminal differentiation as keratinocytes fully commit to the differentiation process following exposure to increased calcium, and keratin K6 which is often associated with hyperproliferation and wounding *in vivo* (Schermer et al., 1989, Rothnagel et al., 1999) and also with a highly stressed epidermis such as transgenic expression of TGFβ1 (Sellheyer et al., 1993) which inhibited neonatal keratinocyte proliferation but induced dermal fibroblast proliferation.

Employing standard protocols (Hennings et al., 1980, Yuspa et al., 1980) modified to prevent spontaneous transformation (Greenhalgh et al., 1989), primary keratinocytes were isolated from transgenic neonatal mouse skin and both differentiation and proliferation activities were monitored by switching to different calcium concentrations in the culture medium (Hennings et al., 1980). Calcium (Ca^{2+}) concentrations are a critical factor in primary keratinocytes culture, low calcium medium (0.05 mM) maintains a proliferative basal cell population whereas

switching to higher calcium concentration (> 0.10 mM) was classically employed to induce keratinocyte differentiation (Hennings et al., 1980, Yuspa et al., 1980); and later a staggered switch to 0.10 mM from 24 hours then to 0.15 mM was found to enhance expression of early differentiation markers such as K1 (Greenhalgh et al., 1989, Rothnagel et al., 1993).

3.6.1 Establishment of primary transgenic mouse keratinocyte culture

In order to investigate differentiation and proliferation activities, primary keratinocytes isolated from transgenic neonatal mouse skin were grown in DMEM medium containing 10% commercial keratinocyte growth medium (KGM), 10% chelexed fetal calf serum (FCS) and 10% fibroblast conditioned media with a calcium concentration of 0.05 mM (low Ca^{2+} medium) and plated out at 5×10^6 primary keratinocytes per 60mm dish in 5ml medium. As demonstrated in figure 3.38, at 48 hours in low Ca^{2+} medium (0.05 mM), primary keratinocytes isolated from *K14.cre/Isl.ROCK^{er}* transgenic mice grew uniformly and had a typical cobblestone appearance. There was little difference in the cell growth profiles between *K14.cre/Isl.ROCK^{er}* cells supplemented with 4-HT (10^{-9} M) (figure 3.38a) and RU486-treated/4-HT-untreated (10^{-9} M) *K14.cre/Isl.ROCK^{er}* cells (figure 3.38b).

Terminal differentiation was induced by adding medium containing first 0.10 mM for 24 hours and then 0.15 mM Ca^{2+} for 48 hours. *K14.cre/Isl.ROCK^{er}* keratinocytes with or without 4-HT in 0.10 mM Ca^{2+} demonstrated the typical signs of stratification and spaces between cells became apparent after 24 hour incubation (figure 3.38 c,d). Significant changes in cells appearance were noted and many cells sloughed off during the differentiation to form squames or cornified envelopes displayed in the cells supplemented with 0.15 mM Ca^{2+} after 48 hours (figure 3.38 e,f). However, again there were no obvious changes in the cell morphology to suggest an effect of additional ROCK2 activation in these *K14.cre/Isl.ROCK^{er}* cells.

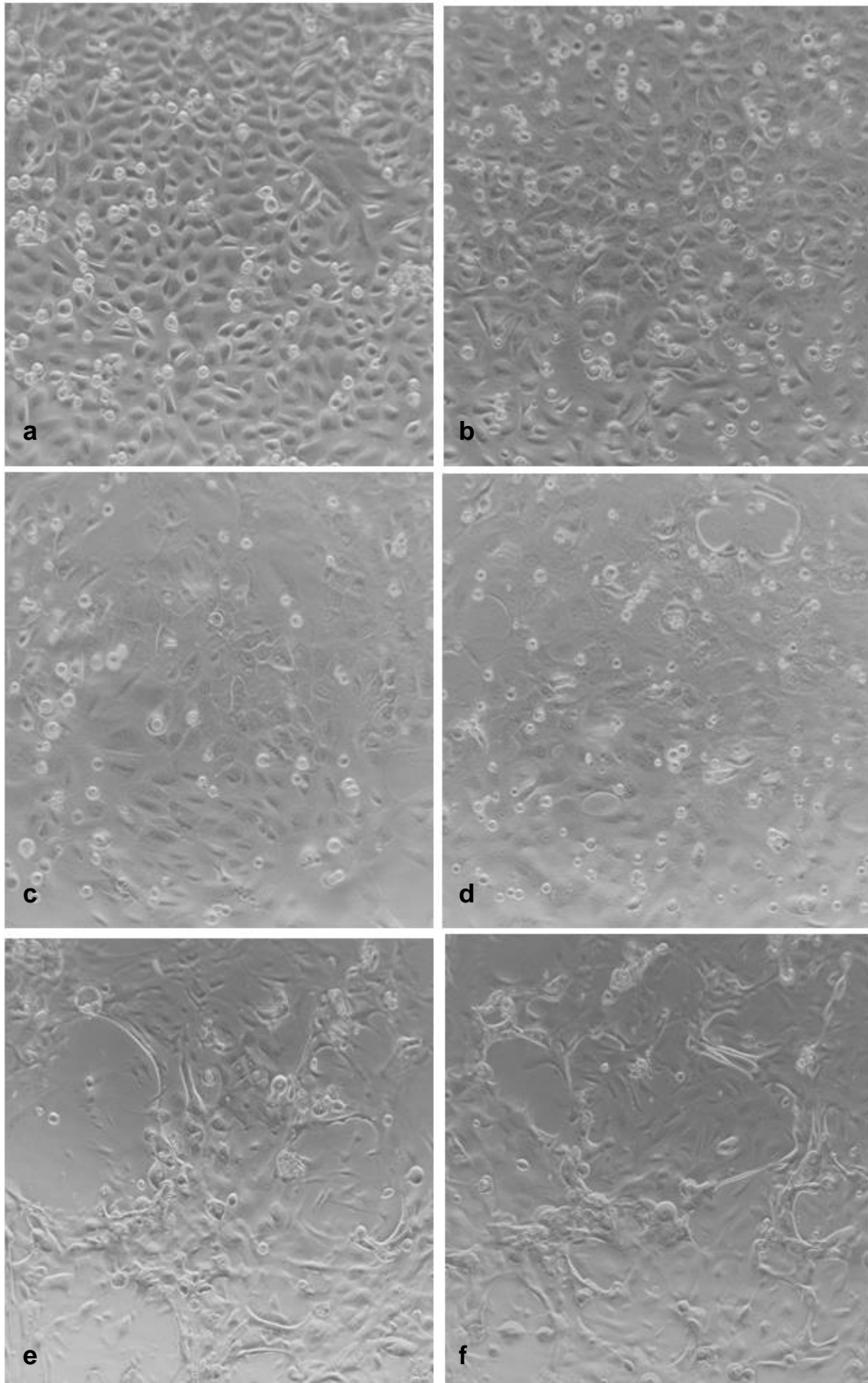


Figure 3.38 Morphology of primary *K14.cre/Sl.ROCK^{er}* keratinocytes in medium containing different calcium concentrations. (a, b) Primary keratinocytes 2 days after plating in 0.05 mM, low calcium media: (a) supplemented with (RU486-) 4-HT and (b) without 4-HT/with RU486. Cells were switched to 0.10 mM Ca²⁺ (c) with (RU486-) 4-HT and (d) without 4-HT/with RU486, which became less bright and lost the cobblestone appearance; continued to second switch 0.15 mM Ca²⁺ (e) with (RU486-) 4-HT and (f) without 4-HT/with RU486 where keratinocytes displayed the typical stratification and sloughing of cells into the medium.

In the next experiment, primary keratinocytes isolated from newborn *K14.cre/Isl.ROCK^{er}/HK1.fos* and *K14.cre/Isl.ROCK^{er}/Δ5PTEN^{fix}* mice were plated in medium supplemented with different calcium concentrations to investigate their differentiation and potential transformation due to resistance to Ca²⁺-induced terminal differentiation *in vitro* (Strickland et al., 1988, Greenhalgh et al., 1989, Morgan et al., 1992). Here, both bi-genic ROCK/fos (figure 3.39) and ROCK/Δ5PTEN^{fix} (figure 3.40) keratinocytes rapidly reached confluency in low Ca²⁺ media (0.05mM) compared to *K14.cre/Isl.ROCK^{er}* alone or non-transgenic normal ICR cultures. Although no formal growth curves were performed, in these bi-genic cultures, many individual rounded cells were seen floating in low Ca²⁺ medium due to this confluency and limited space for cells to grow. Following the staggered switch to 0.15mM Ca²⁺, these bi-genic keratinocytes rapidly changed morphology and differentiation to form several distinct layers (figure 3.39 b,d,f and figure 3.40 b,d,f). However, this may be due to the low Ca²⁺ medium observations that suggested an increased plating efficiency, may lead to a more rapid or intense response to the Ca²⁺ challenge. Few other differences were observable between treated bi-genic versus non-transgenic or untreated controls keratinocytes. Neither *K14.cre/Isl.ROCK^{er}*, *HK1.fos* nor *K14.cre/Isl.ROCK^{er}/fos* expression elicit classical keratinocyte transformation, as determined by resistance to Ca²⁺ induced terminal differentiation following extensive culture over a 6 weeks period (Strickland et al., 1988, Greenhalgh et al., 1989, Morgan et al., 1992). This *in vitro* result would be consistent with the earlier *in vivo* findings given that neither fos nor ROCK2 activation gave rise to malignant tumours in the absence of ras activation and that bi-genic ROCK/Δ5PTEN^{fix} seemed to be redundant perhaps representing a similar oncogenic 'hit' as with Δ5PTEN^{fix} which just altered the keratinocyte differentiation programme. Hence, to confirm these observations, western analysis (below) was performed.

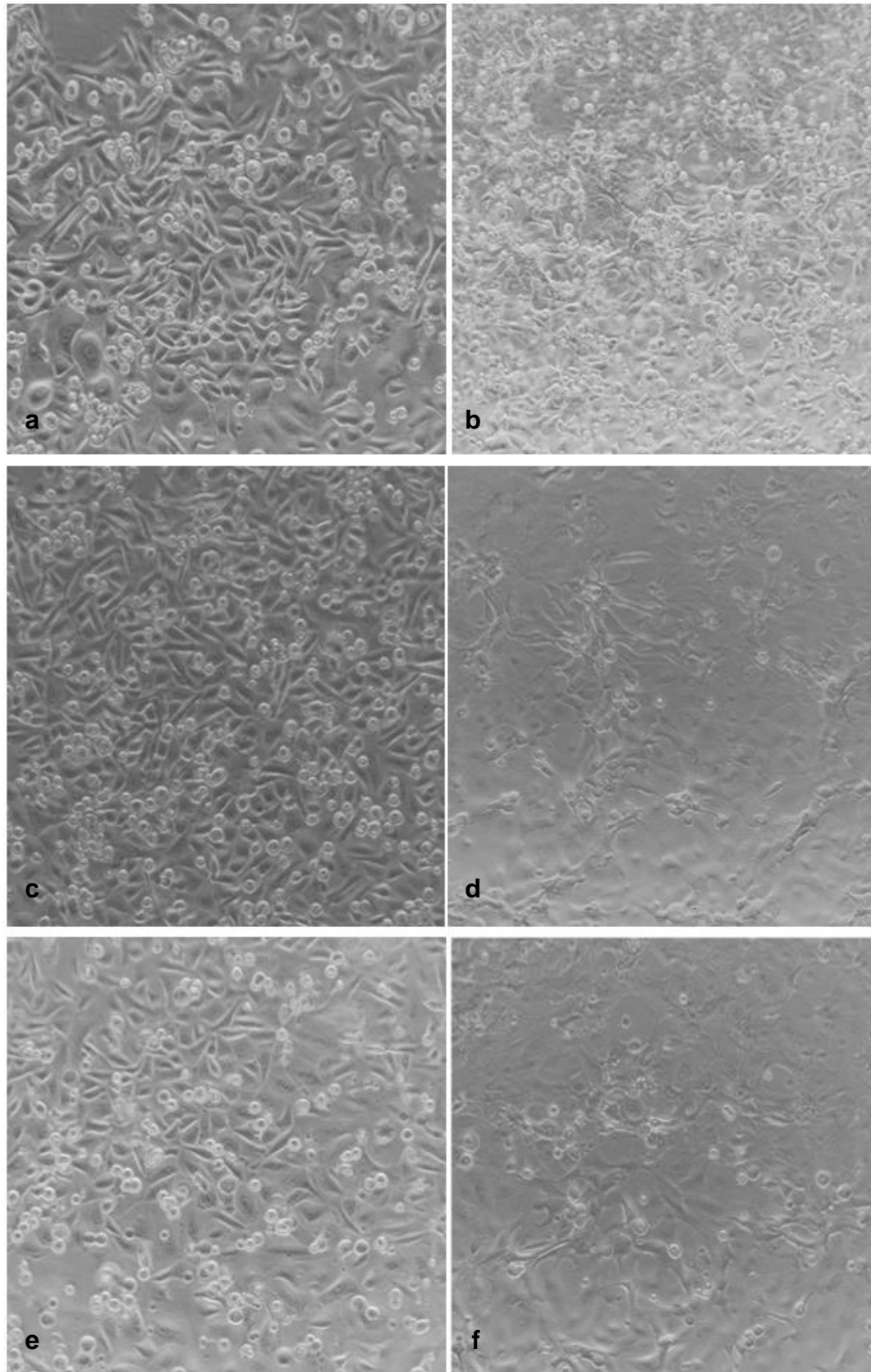


Figure 3.39 Morphology of *K14.cre/Isl.ROCK^{er}/HK1.fos* mouse keratinocytes in medium containing different calcium concentrations. Cells were maintained in low Ca^{2+} medium (0.05mM) (left) for 3 days and switched to high Ca^{2+} medium (0.15mM) (right) for 24 to 48 hours.

[(a, b) RU486-/4-HT-treated *K14.cre/Isl.ROCK^{er}/HK1.fos* cells; (c, d) 4-HT-untreated/RU486-treated *K14.cre/Isl.ROCK^{er}/HK1.fos* cells; (e, f) 4-HT-treated *HK1.fos* cells].

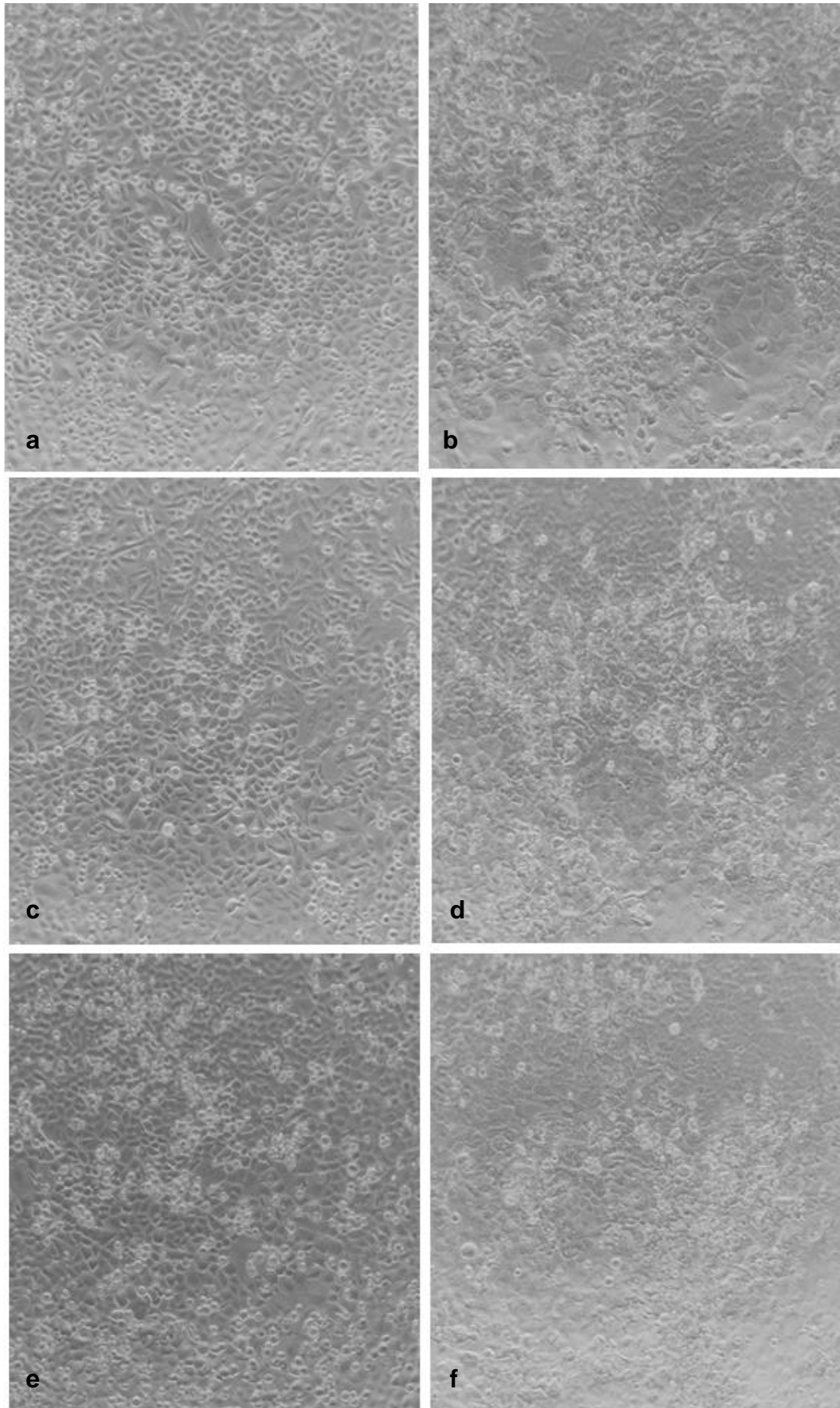


Figure 3.40 Morphology of *K14.cre/Isl.ROCK^{er}/Δ5PTEN^{flx}* mouse keratinocytes in medium containing different calcium concentrations. Cells were maintained in low Ca^{2+} medium (0.05mM) (left) for 3 days and switched to high Ca^{2+} medium (0.15mM) (right) for 24 to 48 hours. [(a, b) RU486-/4-HT-treated *K14.cre/Isl.ROCK^{er}/Δ5PTEN^{flx}* cells; (c, d) 4-HT-untreated/RU486-treated *K14.cre/Isl.ROCK^{er}/Δ5PTEN^{flx}* cells; (e, f) RU486-/4-HT-treated *K14.cre/Δ5PTEN^{flx}* cells].

One unfortunate observation was that neither primary bi-genic *K14.cre/Isl.ROCK^{er}/HK1.ras¹²⁷⁶* nor *HK1.ras* (line 1276 and 1205) alone keratinocytes could be maintained in culture; even after multiple attempts. Typically within 24 hours of plating, the majority of cells had either failed to attach or had attached but remained rounded. The cells quickly become senescent as early as day 3, before the induction of high calcium concentration (figure 3.41). This finding suggests that due to the hyperplastic nature of a ras^{Ha} epidermis, cells detached in this early growth by trypsinisation died and /or could not be cultured due to the oncogenic ras induction of cellular senescence (Yaswen and Campisi, 2007).

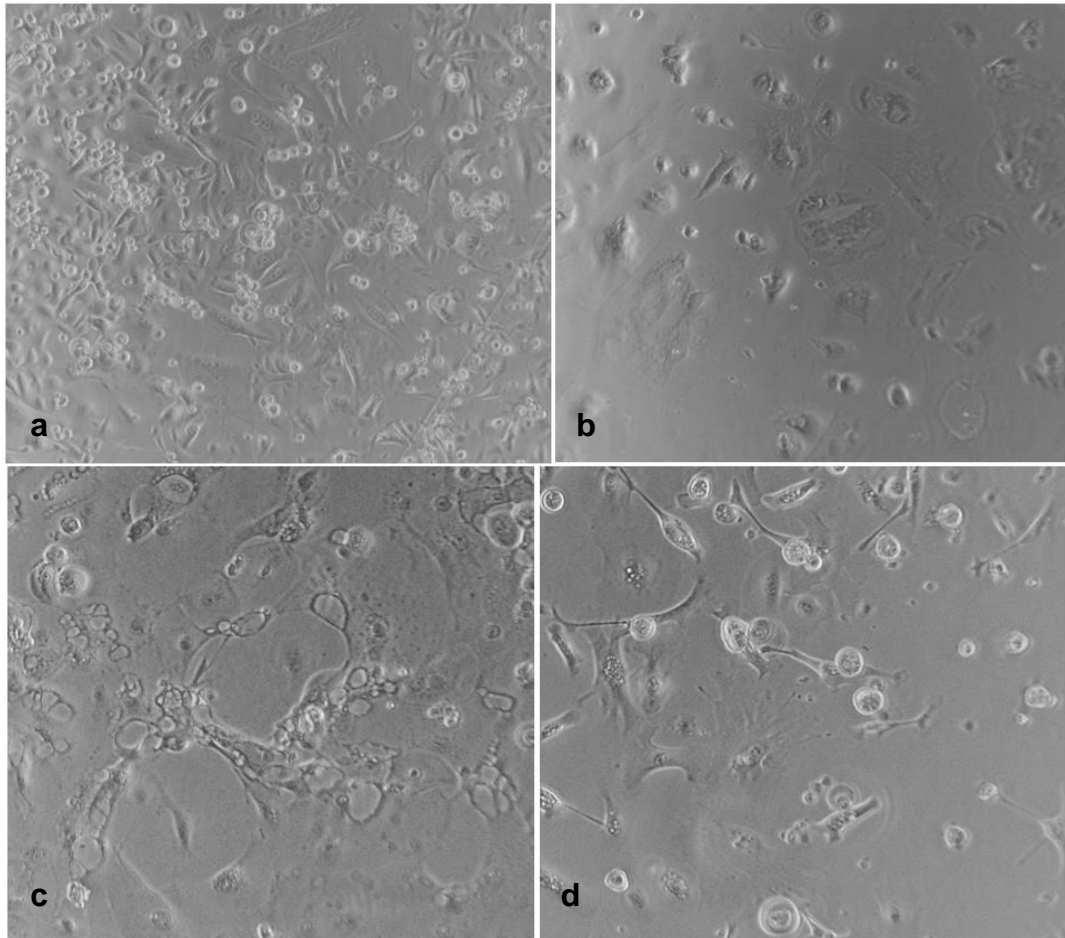


Figure 3.41 Morphology of primary *K14.cre/Isl.ROCK^{er}/HK1.ras¹²⁷⁶* mouse keratinocytes. (a) Several primary *K14.cre/Isl.ROCK^{er}/HK1.ras¹²⁷⁶* keratinocytes failed to attach after 24 hour of plating. (b) RU486-/4-HT-treated *K14.cre/Isl.ROCK^{er}/HK1.ras¹²⁷⁶*, (c) 4-HT-treated *HK1.ras¹²⁷⁶* and (d) RU486-treated/4-HT-untreated *K14.cre/Isl.ROCK^{er}/HK1.ras¹²⁷⁶* cells became senescent on day 3 in low Ca^{2+} medium.

3.6.2 Expression of keratinocyte differentiation markers *in vitro*

As outlined above, *in vivo* both *K14.cre/Isl.ROCK^{er}* and /or $\Delta 5PTEN^{flx}$ expression appeared to alter keratinocyte differentiation in terms of atypical keratin K6 expression and, for $\Delta 5PTEN^{flx}$ early anomalous keratin K1 expression in the basal layer. This led to speculation that these two insults may exert a similar effect as surprisingly, relatively little co-operation was observed in the bi-genic ROCK/ $\Delta 5PTEN^{flx}$ cohorts. Furthermore, a previous report demonstrated that ROCK2 knockdown inhibited terminal differentiation in the HaCat human keratinocyte cell line (Lock and Hotchin, 2009) and again this led to speculation that the odd keratin K6 result may also reflect a response to anomalous ROCK2 activation that instigated the differentiation pathways rather than proliferation signals; or it may be that given the extra or increased intra-cellular tension provided by ROCK2 activation via MLC, that stress response keratin such as K6 or early differentiation keratins such as K1 were altered.

In this *in vitro* study, keratinocytes from the *K14.cre/Isl.ROCK^{er}* model were used to compare results on the differentiation changes *in vivo* due to co-operation of bi-genic ROCK/*fos* and ROCK/ $\Delta 5PTEN^{flx}$. As shown in figure 3.42, western analysis demonstrated that *K14.cre/Isl.ROCK^{er}* (n= 3) is activated and expressed more upon induction by RU486/4-HT treatment in both low and high calcium conditions. From western analysis, RU486-/4-HT-treated *K14.cre/Isl.ROCK^{er}* primary keratinocytes showed increased MLC phosphorylation (ROCK substrate) particularly in the RU486-/4-HT-treated *K14.cre/Isl.ROCK^{er}* cells in low Ca²⁺ medium (figure 3.42: L+ versus L). Whilst in high Ca²⁺ medium, the high levels of endogenous MLC phosphorylation produced on induction of differentiation were increased again in 4-HT-treated cells (figure 3.42: H+ versus H). These data are consistent with previous findings from Samuel et al., (2009, 2011) with the increased MLC phosphorylation in RU486-/4-HT-treated *K14.cre/Isl.ROCK^{er}* cells comparable to the levels in high calcium medium and consistent with ROCK2 roles in differentiation. To assess this possibility, further western analysis was performed to assess keratin K1 and K6 expression in cultured *K14.cre/Isl.ROCK^{er}* primary keratinocytes.

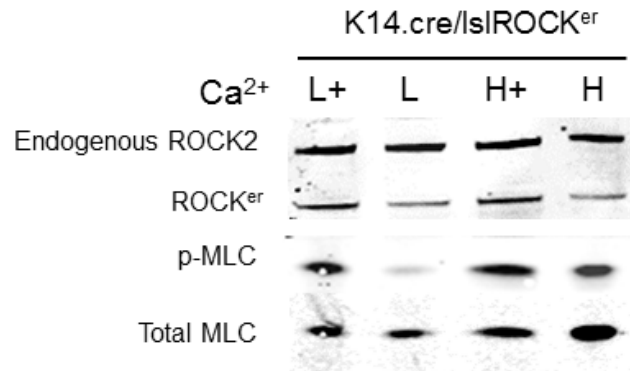
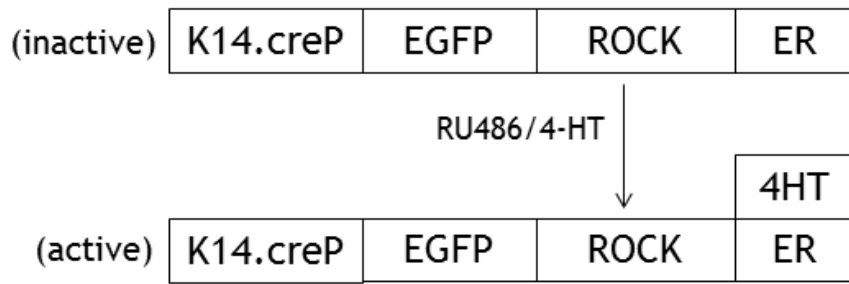


Figure 3.42 *K14.cre/IsI.ROCK^{er}* is activated after RU486-/4-HT treatment. Western blot shows endogenous ROCK, ROCK^{er} transgene, phosphorylated MLC and total MLC in *K14.cre/IsI.ROCK^{er}* primary keratinocytes. Similar levels of ROCK^{er} expression were determined after treatment with 4-HT as compared to 4-HT-untreated. Increased expression of phosphorylated MLC in both low and high Ca²⁺ medium treated with 4-HT was also observed. (L: low calcium; L+: low calcium with 4-HT; H: high calcium; H+: high calcium with 4-HT).

Next, western analysis was performed to assess K1 and K6 expression in cultured *K14.cre/Isl.ROCK^{er}* primary keratinocytes. Confluent dishes of transgenic and normal keratinocytes were cultured in low Ca^{2+} for 3 days with or without RU486/4-HT treatment and a cohort switched for 24 hours into 0.10mM Ca^{2+} and then 0.15 mM Ca^{2+} for a second 48 hours. Normal keratinocytes proliferate in low Ca^{2+} conditions expressing typical markers such as K14 and K5, together with the hyperproliferative keratin K6. Upon induction of high Ca^{2+} (0.15 mM), these keratin markers persist due to their stability and are joined by early markers of differentiation such as keratin K1 and K10, and their expression increases maximally if pre-incubation at an intermediate Ca^{2+} concentration of 0.10 mM for 24 hours is applied when primary keratinocytes adopt a spinous cell morphology (above).

As shown in figure 3.43(a), western analysis of normal ICR keratinocytes exhibit this K1/K6 profile in the presence or absence of 4-HT. K1 is often detected in low Ca^{2+} keratinocytes as they naturally differentiate and this level varies from batch to batch. In this primary culture, there was a higher degree of K1 expression but this increased in high Ca^{2+} appeared as routinely observed. K6 expression is also high in these low cells Ca^{2+} as expected and is detectable in high Ca^{2+} due to the general stability of keratin proteins. Interestingly, primary keratinocytes isolated from *K14.cre/Isl.ROCK^{er}* did not show this standard K1/K6 profile (figure 3.43b). Instead, keratin K1 expression was increased in low Ca^{2+} medium after treatment with 4-HT (figure 3.43b – box) as compared to untreated group (a result that parallels to the MLC phosphorylation – above). This result was repeated several times and was consistent with the overall observation that there appeared to be an increased stratification of *K14.cre/Isl.ROCK^{er}* cultured in high calcium with more squames and floating cornified envelope cells in the media; all indicative of an elevated level of differentiation.

This increased keratin K1 expression may indicate a role for ROCK2 in keratinocyte differentiation in primary cultures concurs with a previous study that reported reduced differentiation following ROCK2 knockdown in the human keratinocyte cell line, HaCat (Lock and Hotchin, 2009). Further supporting this idea, *K14.cre/Isl.ROCK^{er}* cells exhibited very low levels of the hyperproliferative, wound/stress-associated keratin K6 (figure 3.43b – box), again consistent with an increased shift towards differentiation rather than proliferation *in vitro*. These

results are consistent with that observed *in vivo*, as IFC analysis also found patchy K6 expression in hyperplastic *K14.cre/lsl.ROCK^{er}* histotypes. Therefore, these data support the idea that alterations in keratinocyte differentiation are mediated by ROCK2 signalling activation, suggesting important roles for ROCK family members in maintenance of epidermal homeostasis.

When the same analysis was performed on primary *K14.cre/lsl.ROCK^{er}/Δ5PTEN^{flx}* and *K14.cre/lsl.ROCK^{er}/fos* keratinocytes, several differences became more apparent. In these bi-genic keratinocytes, both expression of additional *HK1.fos* or *Δ5PTEN^{flx}* in activated *K14.cre/lsl.ROCK^{er}* keratinocytes rescued their K6 expression profiles (figure 3.43c,e (box) – middle and lower panels). For *K14.cre/lsl.ROCK^{er}/fos* keratinocytes, this result was consistent with the uniform keratin K6 expression data observed *in vivo*; whilst keratin K6 expression in *K14.cre/lsl.ROCK^{er}/Δ5PTEN^{flx}* hyperplasia remained only patchy and this may be due to the complex situation found in mutated PTEN keratinocytes and subsequent AKT deregulation.

Whilst *K14.cre/lsl.ROCK^{er}/HK1.fos* and *HK1.fos* appeared to restore the normally low levels of *in vitro* keratin K1 expression in low Ca²⁺ medium, this increased on a staggered switch to high Ca²⁺ medium; the same was not observed in *K14.cre/lsl.ROCK^{er}/Δ5PTEN^{flx}* and *K14.cre/Δ5PTEN^{flx}* keratinocytes. Here, keratin K1 expression occurred in exactly the opposite pattern to what would be expected. A unique and novel K1 expression was noticed in both *K14.cre/lsl.ROCK^{er}/Δ5PTEN^{flx}* and *K14.cre/Δ5PTEN^{flx}* keratinocytes which showed little K1 expression in high Ca²⁺ medium but high levels in low Ca²⁺ medium (figure 3.43c,d – middle panel). Further, it appears that activated ROCK2 expression again contributed to this mainly *Δ5PTEN^{flx}* associated result, via increased keratin K1 expression in 4-HT-treated low Ca²⁺ medium, but it is also noted that K1 levels are lesser in *K14.cre/lsl.ROCK^{er}/Δ5PTEN^{flx}* versus *K14.cre/Δ5PTEN^{flx}* keratinocytes independent of 4-HT treatment; and this keratin K1 observation is unclear. Nonetheless, this finding of reduced keratin K1 expression *in vitro* correlates with earlier immunofluorescence data where a delay in supra-basal K1 expression appeared in *K14.cre/lsl.ROCK^{er}/Δ5PTEN^{flx}* papillomatous hyperplasia consistent with the increases in the proliferative basal layer compartment.

However, this finding may also be due to the difference in p-AKT function *in vivo* versus *in vitro*. The idea in brief, being that one major AKT function in the epidermis is its supra-basal expression to prevent p53-mediated induction of widespread apoptosis, a counter-productive feature in a tissue evolved for barrier maintenance (Calautti et al., 2005, Macdonald et al., 2014). This provides times for keratinocytes to commit to the terminal differentiation programme. As outlined elsewhere, basal p53/p21 expression appears as a ready response to prevent anomalous AKT expression in the basal layers and basal p21 expression is known to accelerate commitment to differentiation in basal cells (Devgan et al., 2006); hence anomalous basal layer keratin K1 expression appears in *K14.cre/Δ5PTEN^{flx}* hyperplasia (Greenhalgh, – manuscript in preparation). But conversely, p21 actually inhibits differentiation in the later stages of terminal differentiation of the supra-basal/granular layers (Devgan et al., 2006). Thus, collectively, this K1 oddity in *K14.cre/Isl.ROCK^{er}/Δ5PTEN^{flx}* and *K14.cre/Δ5PTEN^{flx}* keratinocytes may derive in part from the fact that in low calcium medium, anomalous expression of AKT may paradoxically induced a feedback that express markers of early stage differentiation programme; leading to anomalous expression of a keratin associated with the keratinocyte commitment to differentiate (e.g. keratin K1). Whilst in high calcium, p-AKT expression returns to its oncogenic role and inhibits differentiation at a stage where now a p21 response also inhibits differentiation. This is still unclear, but what is clear is that this phenotype is mediated by PTEN not ROCK2 and the latter still exerts a slight increase in K1 expression in 4-HT-treated *K14.cre/Isl.ROCK^{er}/Δ5PTEN^{flx}* keratinocytes cultured in low calcium. Furthermore, as keratin K1 is significantly reduced in high calcium medium and expression of ROCK2 in this *K14.cre/Isl.ROCK^{er}/Δ5PTEN^{flx}* was insufficient to rescue the K1 expression profile, yet it appeared to increase K1 in low calcium, again suggests that these two molecules have close links in the regulation of keratinocyte terminal differentiation.

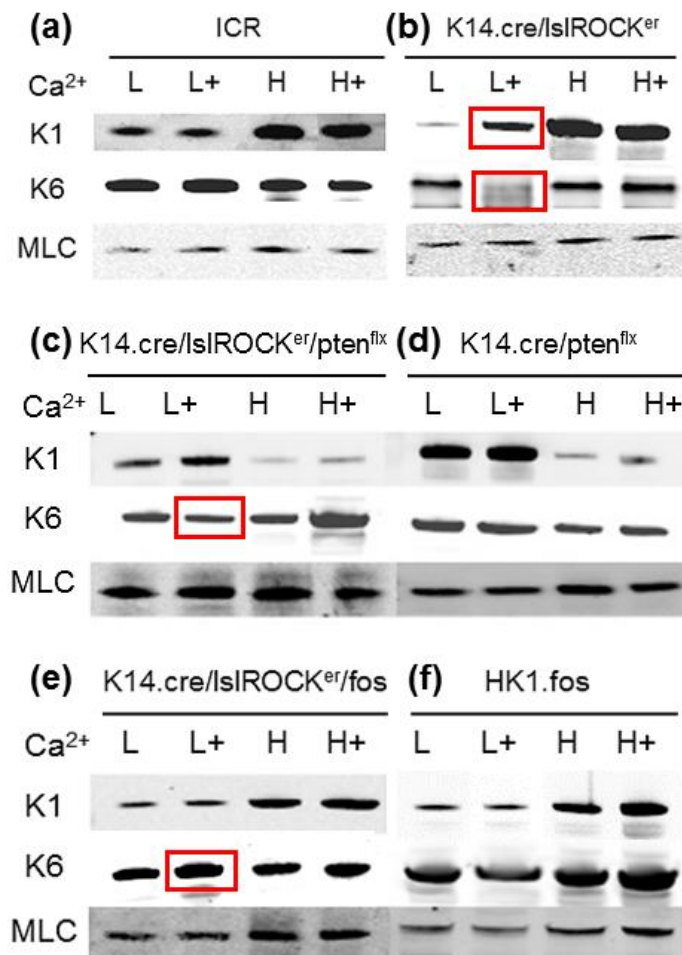


Figure 3.43 Western analysis of K1 and K6 differentiation marker expression in primary keratinocytes.

Top panel: (a) (left) Keratin K1 expression in normal ICR keratinocytes showed typical elevated expression when switched from culture in low (L, L+) to high calcium medium (H, H+). Keratin K6 expression is high in low calcium proliferative conditions and is stable, thus it also appears in high calcium too.

(b) (Right): ROCK2 activation induces more K1 expression in low calcium medium with 4-HT (box) (L+ versus L); and K1 appears increased further when switched to high calcium medium (H, H+). Interestingly, anomalous low levels of K6 expression appear upon ROCK2 activation in low calcium medium (box) (L+ versus L) consistent with *in vivo* observations of roles of ROCK2 activation in alteration of differentiation markers.

Middle panel: (K1) Keratin K1 expression was altered being low in the high calcium medium of both (c) *K14.cre/Isl.ROCK^{er}/Δ5PTEN^{flx}* and (d) *K14.cre/Δ5PTEN^{flx}* keratinocytes. This may suggest that due to inactivation of PTEN activity leading to more activated AKT. This mediated more oncogenic proliferation, which counteract the calcium-induced differentiation.

(K6) However, *in vitro* combination of $\Delta 5PTEN^{flx}$ deregulation to activated ROCK2 has rescued keratin K6 expression (box); and this too was observed *in vivo*.

Bottom panel: In both (e) *K14.cre/Isl.ROCK^{er}/HK1.fos* and (f) *HK1.fos* keratinocytes expression of fos restore the correct normal expression profile of keratin K1 in both low and high calcium medium and bi-genic ROCK/fos keratinocytes also restored typical K6 expression (box), similar to typical K1/K6 expression profiles as in normal non-transgenic ICR keratinocytes.

Total MLC served as a loading control. (L: low calcium; L+: low calcium with 4-HT; H: high calcium; H+: high calcium with 4-HT).

3.6.3 Summary

This study has demonstrated both changes in morphology *in vitro* and atypical expression of standard proliferation and differentiation markers when *K14.cre/Isl.ROCK^{er}*, *K14.cre/Isl.ROCK^{er}/Δ5PTEN^{flx}* and *K14.cre/Isl.ROCK^{er}/fos* primary keratinocytes were cultured in low calcium conditions and challenged to differentiate by increasing calcium. However, both *K14.cre/Isl.ROCK^{er}/ras¹²⁷⁶* and *HK1.ras¹²⁷⁶* keratinocytes (figure 3.41) could not be cultured and failed to survive after approximately day 2 to 3. This was probably due to the nature of ras^{Ha} activation (both line 1276 and 1205) which may have affected the ability of the keratinocytes to attach to the culture surface from which they easily became detached leading to their terminal differentiation, similar to a programme of oncogene induced senescence (Yaswen and Campisi, 2007).

The data from this study showed that overall transgenic primary keratinocytes maintained their growth in low calcium before undergoing differentiation following a high calcium switch. However in repeated western analysis an altered differentiation profile was found in 4-HT-treated primary *K14.cre/Isl.ROCK^{er}* cultures with respect to both keratin K1 and K6 expression. Whilst the expected high keratin K1 expression in *K14.cre/Isl.ROCK^{er}* keratinocytes appeared upon increased calcium, elevated K1 expression also appeared in low calcium medium (with 4-HT). This premature K1 expression was consistent with previous *in vitro* studies, where in a reverse of this model, ROCK2 knockdown suppressed terminal differentiation (Lock and Hotchin, 2009). In addition, the lack of K6 expression upon ROCK2 activation in low calcium medium again, showed that ROCK2 activation alters expression of hyperproliferative or stress associated keratin markers and this further supports significant roles for ROCK2 in differentiation. These roles appeared to be consistent with *in vivo* analysis where low levels and patchy expression of keratin K6 markers were seen in *K14.cre/Isl.ROCK^{er}* hyperplasia.

In addition, both *K14.cre/Isl.ROCK^{er}/Δ5PTEN^{flx}* and *K14.cre/Δ5PTEN^{flx}* keratinocytes showed an unexpected and reduced keratin K1 expression in high calcium medium; and in this genetic context, this unusual K1 inhibition in high calcium was not demonstrated in low calcium medium as both

K14.cre/Isl.ROCK^{er}/Δ5PTEN^{flx} and *K14.cre/Δ5PTEN^{flx}* keratinocytes exhibited very unusual and increased levels of K1 in low calcium medium. This finding seemed to be tailored with the keratinocytes morphology (figure 3.40) in 0.15mM Ca²⁺, which was not completely differentiated when compared to other transgenic keratinocyte morphology in the same conditions and cultured at the same time (figure 3.38 and 3.39).

It is that this observation is linked to PTEN phenotypes rather than those of ROCK, and more experiments are required, however the analysis demonstrates a difference between *in vitro* vs *in vivo*. For instance, in respect to K6 expression, as shown earlier, the *in vivo* loss of K6 in Δ5PTEN^{flx} hyperplasia was completely reversed in the *in vitro* situation, and this may depend upon the altered AKT roles that mediate a response in culture against the whole animal. In the *K14.cre/Δ5PTEN^{flx}* epidermis, p-AKT1 expression is selective and typically confined to supra-basal layers, but *in vitro*, it is expressed all the time (Yao et al., 2006), thus inducing proliferation and this restores K6 expression in low calcium. Hence, K6 expression was rescued in both *K14.cre/Isl.ROCK^{er}/Δ5PTEN^{flx}* and *K14.cre/Δ5PTEN^{flx}* keratinocytes. In high calcium medium, these oncogenic activities of AKT may inhibit differentiation as manifest by a lack of K1 regardless of ROCK status. But, this apparently conflicts with induction of K1 in low calcium medium. Here, the answer may lie in the fact that normally AKT expression is supra-basal and counters p53, so that terminal differentiation (not apoptosis) is the outcome (Calautti et al., 2005, Yao et al., 2008, Macdonald et al., 2014). Thus, in the *in vitro* context, *K14.cre/Isl.ROCK^{er}/Δ5PTEN^{flx}* and *K14.cre/Δ5PTEN^{flx}* keratinocytes cultured in low calcium medium respond to AKT by anomalous expression of early differentiation markers (keratin K1). Furthermore, adding *HK1.fos* activation to cultured ROCK2 keratinocytes was shown to rescue the normally strong K6 expression profile and here, K1 expression also returned to normal and remained unaltered in 4-HT-treated or untreated bi-genic keratinocytes from *K14.cre/Isl.ROCK^{er}/fos* and *HK1.fos* genotypes. Collectively, these data suggest that whilst ROCK2 alters differentiation in some instances, fos activation exerts a more dominant nature in terms of differentiation.

In experiments designed to assess whether ROCK2, bi-genic ROCK/Δ5PTEN^{flx} or ROCK/fos could induced immortalisation or transformation, these *in vitro* data showed that none of the transgenic primary keratinocytes possessed the classic

resistance to high Ca^{2+} indicative of a malignant phenotype (Morgan et al., 1992) by producing colonies following 4 to 5 weeks culture in high calcium medium; a result consistent with the *in vivo* findings. Although none of the transgenic primary keratinocytes showed signs of transformation, cell lines of ROCK2, bi-genic ROCK/ $\Delta 5\text{PTEN}^{\text{flx}}$ and ROCK/fos were successfully established by the end of this approach which will be valuable for future studies (see appendix A).

3.7 Co-operation of ROCK2, *HK1.ras* and *HK1.fos* in transgenic mouse skin carcinogenesis

A major goal of this study was to assess ROCK2 activation in skin carcinogenesis and mimic the two-stage DMA/TPA studies performed earlier on *K14.ROCK^{er}* mice (Samuel et al., 2011) with a view to identifying the co-operating genes and determining at which stage ROCK2 becomes active and causal. Subsequently, experiments would begin to analyse the downstream mechanisms and establish a stage-specific tumour archive for this and future studies. Earlier, bi-genic ROCK/*ras*¹²⁰⁵ studies showed that co-operation appeared to centre on conversion from benign papillomas to carcinoma, and this required wound-associated promotion to achieve the correct papilloma context for ROCK causality. Excitingly, for the first time, co-operation between *fos* and ROCK2 activation in bi-genic ROCK/*fos* revealed a novel early co-operation in benign papilloma formation, a result consistent with ROCK being a downstream effector of *ras* signalling and possibly performing an initiating role for co-operation with *fos*. However, again in this benign ROCK/*fos* context, no conversion was observed in the absence of *ras* activation suggesting its requirement or that of another similar event. This would be consistent to some extent with the lack of tumours produced by TPA promotion alone controls in the two-stage *K14.ROCK^{er}* chemical carcinogenesis studies (Olson, - unpublished data).

As outlined in the introduction, the early *ras*^{Ha}/*fos* models were initially considered to mimic two-stage chemical carcinogenesis (Greenhalgh and Yuspa, 1988, Greenhalgh et al., 1990); consistent with a lack of tumours in *ras*-infected *c-fos* knockout mice (Saez et al., 1995). Bi-genic *HK1.ras*¹²⁷⁶/*fos* mice exhibited co-operation during papillomatogenesis but instead of malignancy, this model produced persistent papillomas with no sign of regression (Greenhalgh et al., 1993c); possibly due to elevated p53/p21 (Macdonald et al., 2014). However, the lack of spontaneous tumour progression exhibited by *HK1.ras*¹²⁷⁶/*fos* papillomas (Greenhalgh et al., 1996) makes them ideal to study the requirements for malignant conversion.

Previously, as reported by Greenhalgh et al., (1993c), mice from *HK1.fos* line 488 crossed with *HK1.ras* lines 1205 exhibited a degree of co-operation resulting in

numerous tumours and this tumour burden was deemed far too excessive for UK animal experimentation. Fortunately, the majority of mice from *HK1.fos*⁴⁸⁸ bred with *HK1.ras*¹²⁷⁶ survived, and co-operation typically produced bi-lateral benign squamous papillomas on both ears regardless of the wound promotion stimulus, together with increased skin hyperplasia and hyperkeratosis giving a scruffy appearance. Therefore, inducible ROCK^{er} activation was assessed in *HK1.ras*¹²⁷⁶/*HK1.fos* transgenic mice to study this tri-genic synergism and to compare these tri-genic mice with two tri-genic (PTEN models) where the *K14.cre/Isl.ROCK*^{er} line was employed (below).

3.7.1 ROCK2 co-operates with *HK1.ras/fos* to elicit malignant progression

In repeat experiments, 6-7 week old *K14.cre/Isl.ROCK*^{er}/*ras*¹²⁷⁶/*fos* mice (cohorts of 10) were treated with RU486 for 1 week to ablate the stop cassette, and express ROCK^{er} in all epidermal layers and hair follicles, then, activated by treatment with 4-HT 3 times per week. Appropriate control cohorts (5 per genotype): *HK1.ras*¹²⁷⁶/*fos* received 4-HT treatment without RU486, or RU486 and ethanol alone for control *K14.cre/Isl.ROCK*^{er}/*ras*¹²⁷⁶/*fos* were included. At 13 weeks of continuous 4-HT treatment, *K14.cre/Isl.ROCK*^{er}/*ras*¹²⁷⁶/*fos* mice exhibited quite large tumours (figure 3.44a,b) in both ears. These tumours were keratotic, pale and relatively flattened compared to tri-genic ROCK/*ras*¹²⁰⁵/ Δ 5PTEN^{het} tumours (below) that appeared more rounded and red. The increased keratosis reflected alterations in differentiation elicited by ROCK2 and fos co-operation (above). However, these tumours approached the Home Office UK limits, therefore these mice were not maintained for periods longer than 16 weeks. In contrast, all sibling control groups of 4-HT-treated *HK1.ras*¹²⁷⁶/*fos* (figure 3.44c,d) and RU486-treated/4-HT-untreated *K14.cre/Isl.ROCK*^{er}/*ras*¹²⁷⁶/*fos* (figure 3.44e,f) mice displayed mainly thickened ears at this stage with some showing the early formation of smaller keratotic tumours, typical of previous *HK1.ras*¹²⁷⁶/*fos* at three months (Greenhalgh et al., 1993c).

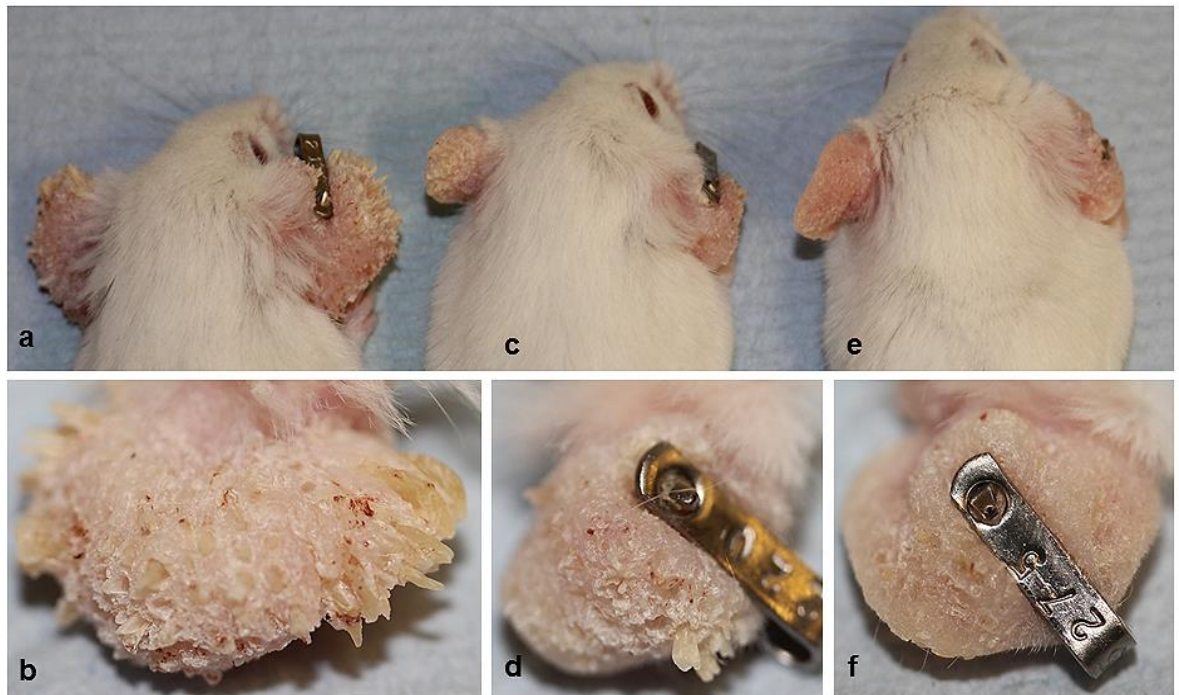


Figure 3.44 Phenotypes of *K14.cre/Isl.ROCK^{er}/ras¹²⁷⁶/fos* transgenic mice at 13 weeks. (a, b) RU486-/4-HT-treated tri-genic *ROCK/ras¹²⁷⁶/fos* mice exhibit large tumours with a keratotic appearance. (c, d) 4-HT-treated *HK1.ras¹²⁷⁶/fos* and (e, f) RU486-treated/4-HT-untreated *K14.cre/Isl.ROCK^{er}/ras¹²⁷⁶/fos* mice appear to show the formation of early keratotic tumours.

Interestingly, as shown in figure 3.45, *K14.cre/lsl.ROCK^{er}/ras¹²⁷⁶/fos* histopathology often comprised a mixed histotypes of both papilloma and well-differentiated carcinoma, and also showed that an epidermal nest of more aggressive SCC (figure 3.45a - arrow) had begun to infiltrate the dermal areas. This suggests that ROCK2 not only induced malignant conversion in the context of a late stage *ras¹²⁷⁶/fos* papilloma, but possibly has begun to accelerate invasion and malignant progression from wdSCC to SCC (figure 3.45a). Moreover, at higher magnification, in these SCC malignant areas, the tissue architecture became disoriented, with gaps between the tumour keratinocyte populations, giving a sponge-like feature (figure 3.45b). This may reflect a failure in cell-cell adhesion as these keratinocytes became increasingly mobile and invasive, or speculatively, this feature may possibly relate to brittle nature of these tumours due to increased ROCK-mediated stiffness (Samuel et al., 2011), as it was noticed, anecdotally, that these tumour sections were oddly prone to ripping during the H&E histology processing (yet, not to the same degree as observed in the final model of *ROCK/ras¹²⁰⁵/Δ5PTEN^{het}* pdSCCs – below). At this time, bi-genic *HK1.ras¹²⁷⁶/fos* histopathology remained as that of benign papillomas that exhibited well-ordered differentiation under higher magnification (figure 3.45c-f), with expanded epidermal layers given the *ras* roles in proliferation and *fos* associated with differentiation.

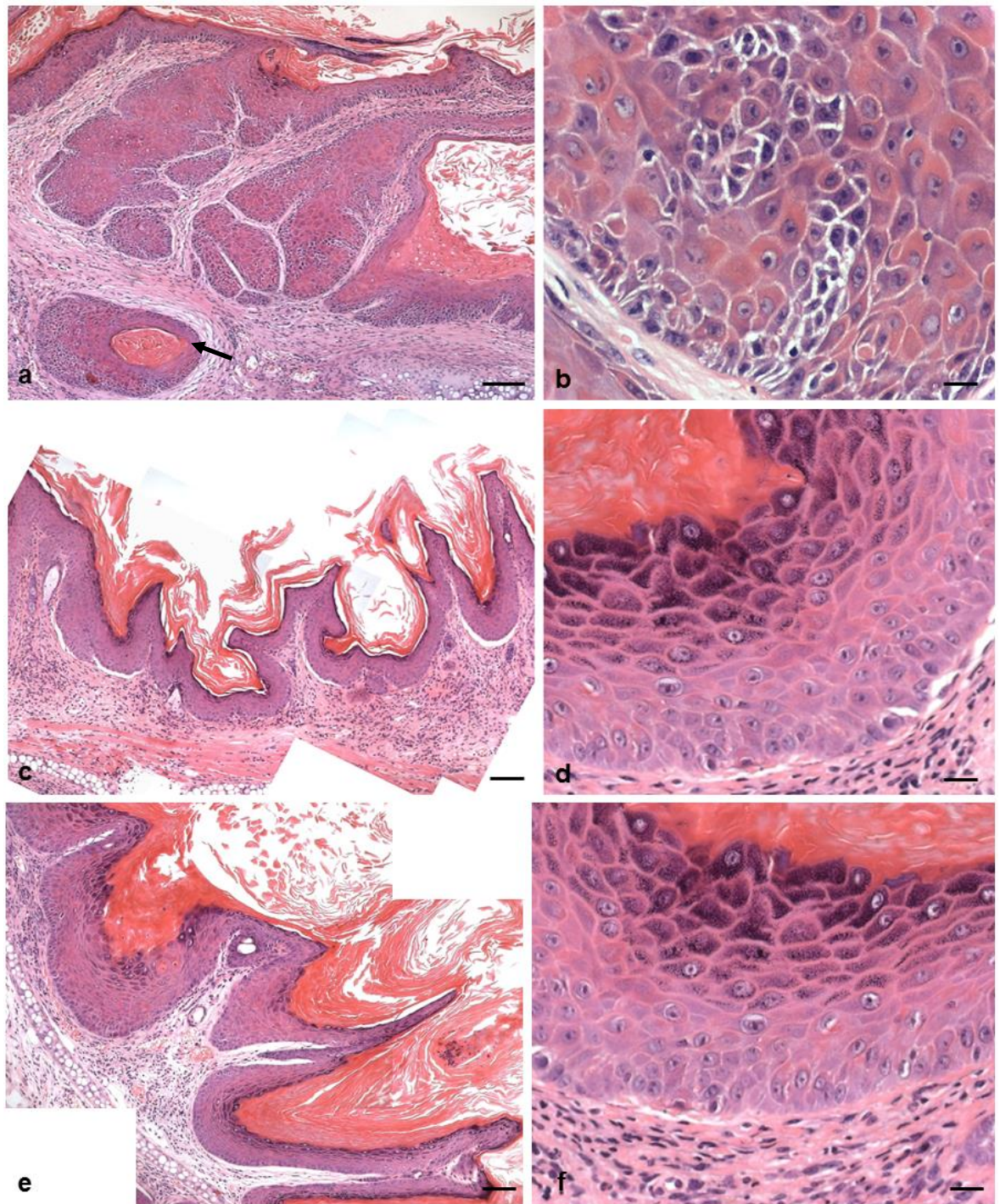


Figure 3.45 Histopathology of *K14.cre/Isl.ROCK^{er}/ras¹²⁷⁶/fos* and *HK1.ras¹²⁷⁶/fos* tumours at 13 weeks. (a) RU486-/4-HT-treated tri-genic *ROCK/ras¹²⁷⁶/fos* epidermis exhibits a mixed histotype of papilloma and wdscc with nests of more aggressive SCC (arrows). (b) At higher magnification, RU486-/4-HT-treated *K14.cre/Isl.ROCK^{er}/ras¹²⁷⁶/fos* carcinoma shows an increasingly disorganised basal layer with sponge-like gaps appearing between cells. (c) Low and (d) higher magnification of 4-HT-treated *HK1.ras¹²⁷⁶/fos* papilloma histotypes show an organised basal layer. (e) Low and (f) higher magnification of RU486-treated/4-HT-untreated *K14.cre/Isl.ROCK^{er}/ras¹²⁷⁶/fos* epidermis also exhibit a similar organised benign papilloma histotypes. (Scale bar: 100µm in a,c,e; 50µm in b,d,f).

3.7.2 Expression of differentiation markers in tri-genic ROCK/ras¹²⁷⁶/fos

Tumour biopsies were routinely analysed for the expression of the early differentiation marker, keratin K1 to confirm the malignant conversion and /or assess what stage this tri-genic co-operation had achieved, together with keratin K6 the standard epidermal hyperproliferation marker. As shown in figure 3.46a, K1 (green) expression was reduced upon malignant conversion and the retained K1 expression in tri-genic ROCK/ras¹²⁷⁶/fos papilloma gradually disappeared (figure 3.46a – box) as tri-genic ROCK/ras¹²⁷⁶/fos wdSCCs achieved a more aggressive SCC malignancy (figure 3.46b). In contrast, K1 expression remained ordered and was expressed normally in the supra-basal layers of *HK1.ras¹²⁷⁶/fos* benign papilloma histotypes (figure 3.46c) showing that differentiation remained relatively undisturbed in this benign tumour context. Analysis of K6 in RU486-/4-HT-treated *K14.cre/Isl.ROCK^{er}/ras¹²⁷⁶/fos* mixed tumour histotype demonstrated a uniform expression in all epidermal layers (figure 3.46d) showing that ras/fos signalling returned expression of this hyperproliferation keratin. Control *HK1.ras¹²⁷⁶/fos* papillomas also showed strong K6 expression throughout epidermal keratinocytes (figure 3.46e).

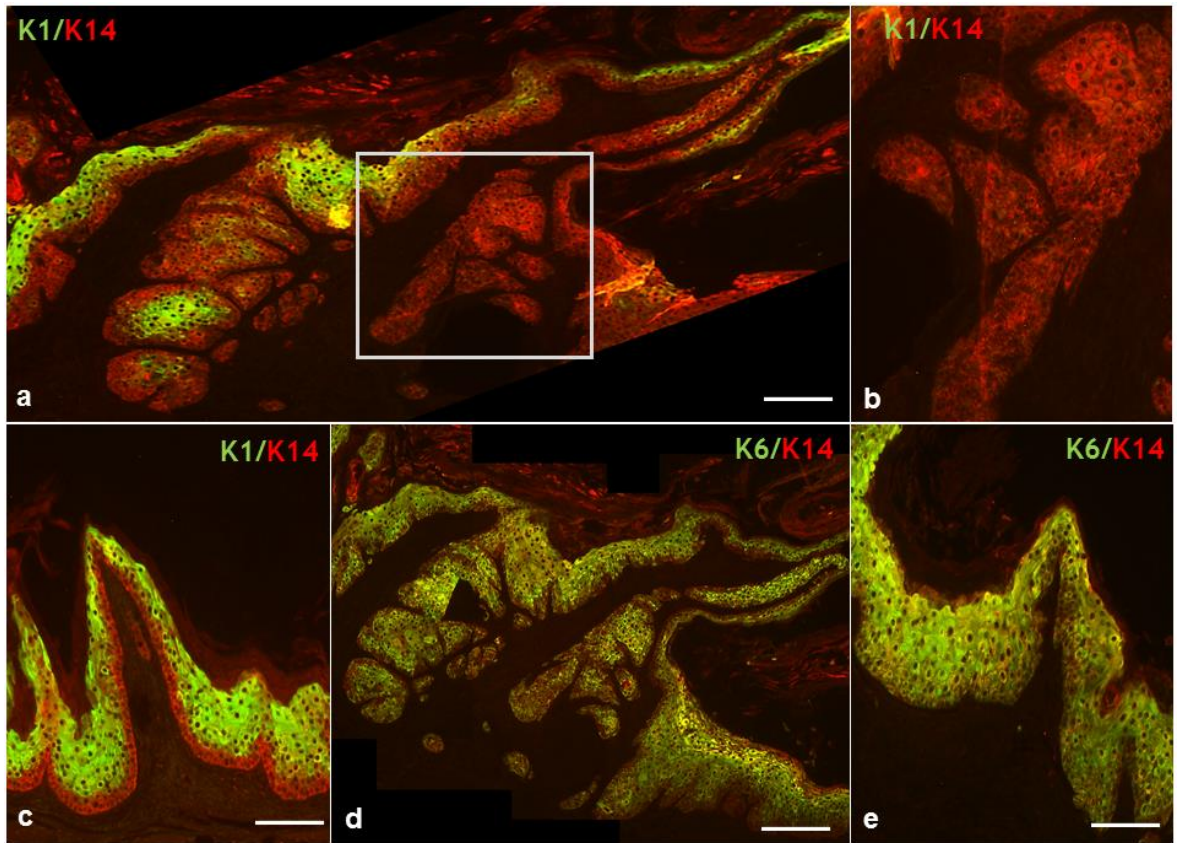


Figure 3.46 Immunofluorescence analysis of K1/K14 and K6/K14 expression in RU486-/4-HT-treated *K14.cre/Isl.ROCK^{er}/ras¹²⁷⁶/fos* tumours at 13 weeks. (a) *K14.cre/Isl.ROCK^{er}/ras¹²⁷⁶/fos* tumours display K1 expression which is being lost on progression from wdSCC to aggressive SCC (box). (b) At higher magnification, the SCC area shows complete loss of K1 expression. (c) 4-HT-treated *HK1.ras¹²⁷⁶/fos* papillomas show strong K1 expression in the supra-basal layers consistent with a typical benign papilloma histotype. (d) Strong and uniform K6 expression in all epidermal layers appears in *K14.cre/Isl.ROCK^{er}/ras¹²⁷⁶/fos* mixed histotype and (e) *HK1.ras¹²⁷⁶/fos* papilloma. (Scale bar: 100µm).

3.7.3 Expression of p53 and p21 in tri-genic ROCK/ras¹²⁷⁶/fos mice

As a routine part of tumour analysis in this model, the expression profiles of tumour suppressor genes, p53 and p21 were analysed in *K14.cre/Isl.ROCK^{er}/ras¹²⁷⁶/fos* histotypes. It was anticipated that p53 expression would be depleted consistent with malignant progression in tri-genic *ROCK^{er}/ras¹²⁷⁶/fos* histotypes; although in a similar approach, large *HK1.fos/Δ5PTEN^{flx}* tumours exhibited unexpectedly high levels of p53 and this was the first indications that *fos/Δ5PTEN^{flx}* tumours had progressed to keratoacanthoma and not SCC (Yao et al., 2008). As shown in figure 3.47a, composite micrographs of tri-genic ROCK/ras¹²⁷⁶/fos mixed tumours showed that the protective, high level p53 expression appearing in all epidermal compartments of the papilloma histotypes (as determined in K1 analysis of serial sections), had gradually decreased and became lost in the areas of wdSCC or SCC nests histotype (figure 3.47a - box); as clearly demonstrated at higher magnification (figure 3.47b). In contrast, *HK1.ras¹²⁷⁶/fos* papilloma demonstrated a strong expression of p53 in all epidermal layers (figure 3.47c) which is consistent with their lack of spontaneous progression to malignancy.

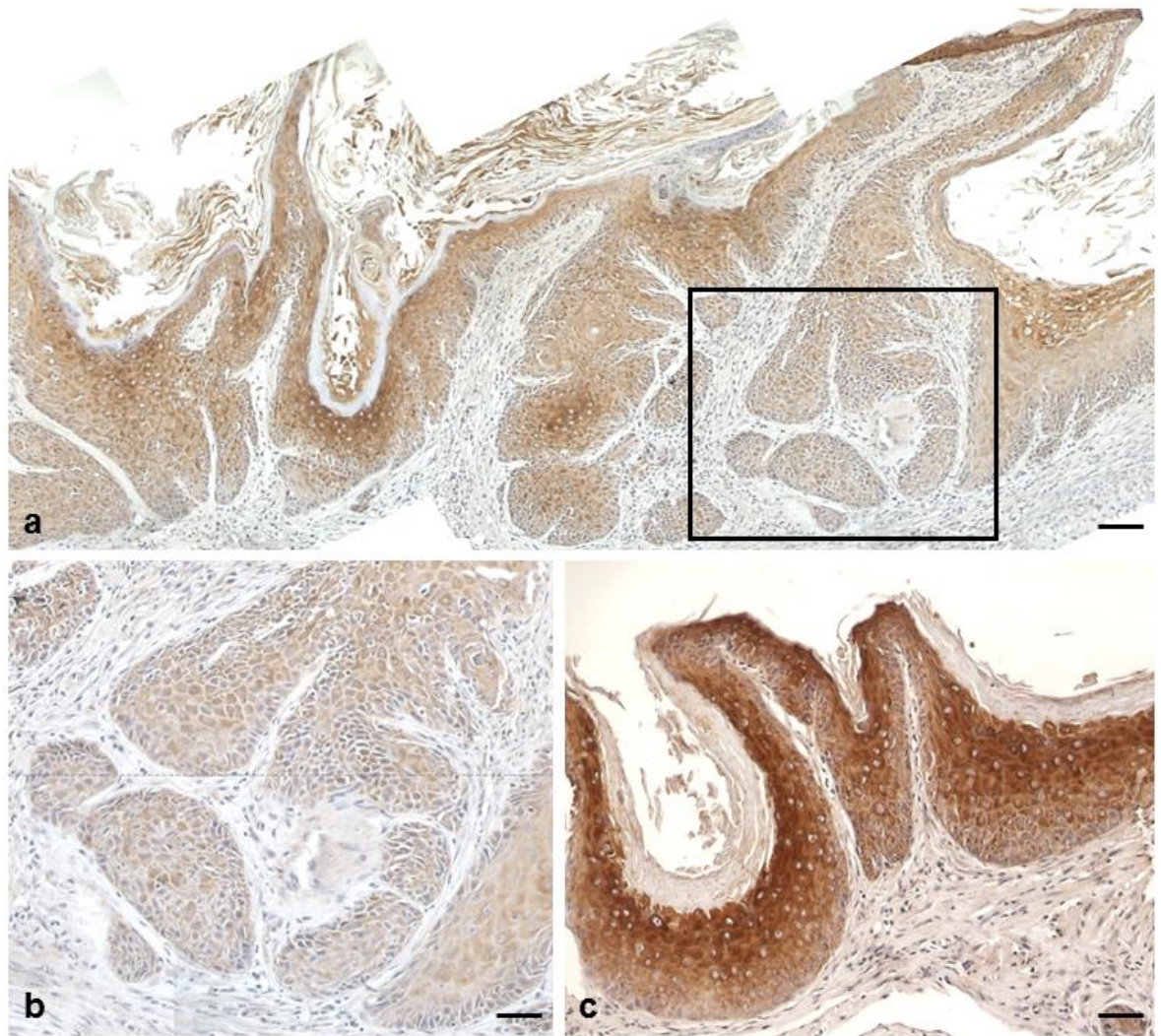


Figure 3.47 IHC analysis of p53 expression in malignant RU486-/4-HT-treated *K14.cre/lsl.ROCK^{e1}/ras¹²⁷⁶/fos* histotypes. (a) Composite micrograph shows p53 expression fading from pre-malignant to malignant areas. (b) High magnification of malignant area shows expression of p53 becoming gradually lost. (c) Benign papilloma of 4-HT-treated *HK1.ras¹²⁷⁶/fos* histotype exhibit elevated p53 expression. (Scale bar: a: 150 μ m; b-c: 100 μ m).

Analysis of p21 expression, normally considered a downstream effector of p53, proved to be more interesting, as its expression can be either dependent or independent of p53 (Ng et al., 1999). Previously, persistent p21 expression in the basal layer was shown to be a significant response to p53 loss in tri-genic $ras^{1276}/fos/\Delta 5PTEN^{flx}$ models (Macdonald et al., 2014), although not to the high levels observed in papillomas on cessation of 4-HT in bi-genic $ROCK/ras^{1205}$ mice (above). Here, in this IHC analysis, whilst p53 expression became reduced and eventually disappeared during malignant progression, p21 expression remained persistent in both papillomas and carcinomas of tri-genic $ROCK/ras^{1276}/fos$ mixed histotypes (figure 3.48a). At higher magnification, persistent p21 expression was still observed in p53/K1 negative areas of wdSCC and SCC nests (figure 3.48b).

In a subtle contrast, in $HK1.ras^{1276}/fos$ papillomas, p21 expression became elevated (figure 3.48c) along with strong p53 expression in all supra-basal layers, however p21 expression was often reduced in the basal layer. This would be consistent with a reduced level of differentiation exerted by ras^{1276}/fos co-operation as p21 was associated with increased differentiation (Topley et al., 1999, Devgan et al., 2006) as observed in bi-genic $fos/\Delta 5PTEN^{flx}$ mice (Yao et al., 2008) and this also suggests that, as found for previous tri-genic $ras^{1276}/fos/\Delta 5PTEN^{flx}$ tumours, p21 expression becomes basal and protective once p53 has become reduced or lost in the basal layer (Macdonald et al., 2014). This feature of elevated p21 levels following conversion may also contribute to the predominance of wdSCCs and limited progression. This may also be due to the lack of p-AKT1 observed in the tri-genic $ROCK/ras^{1276}/fos$ pathway (below); and which became a recurrent theme in this ROCK2 mediated progression mechanism. Thus, these results indicate that upon malignant progression in tri-genic $ROCK/ras^{1276}/fos$ synergism, p53 expression became lost whilst p21 levels persisted.

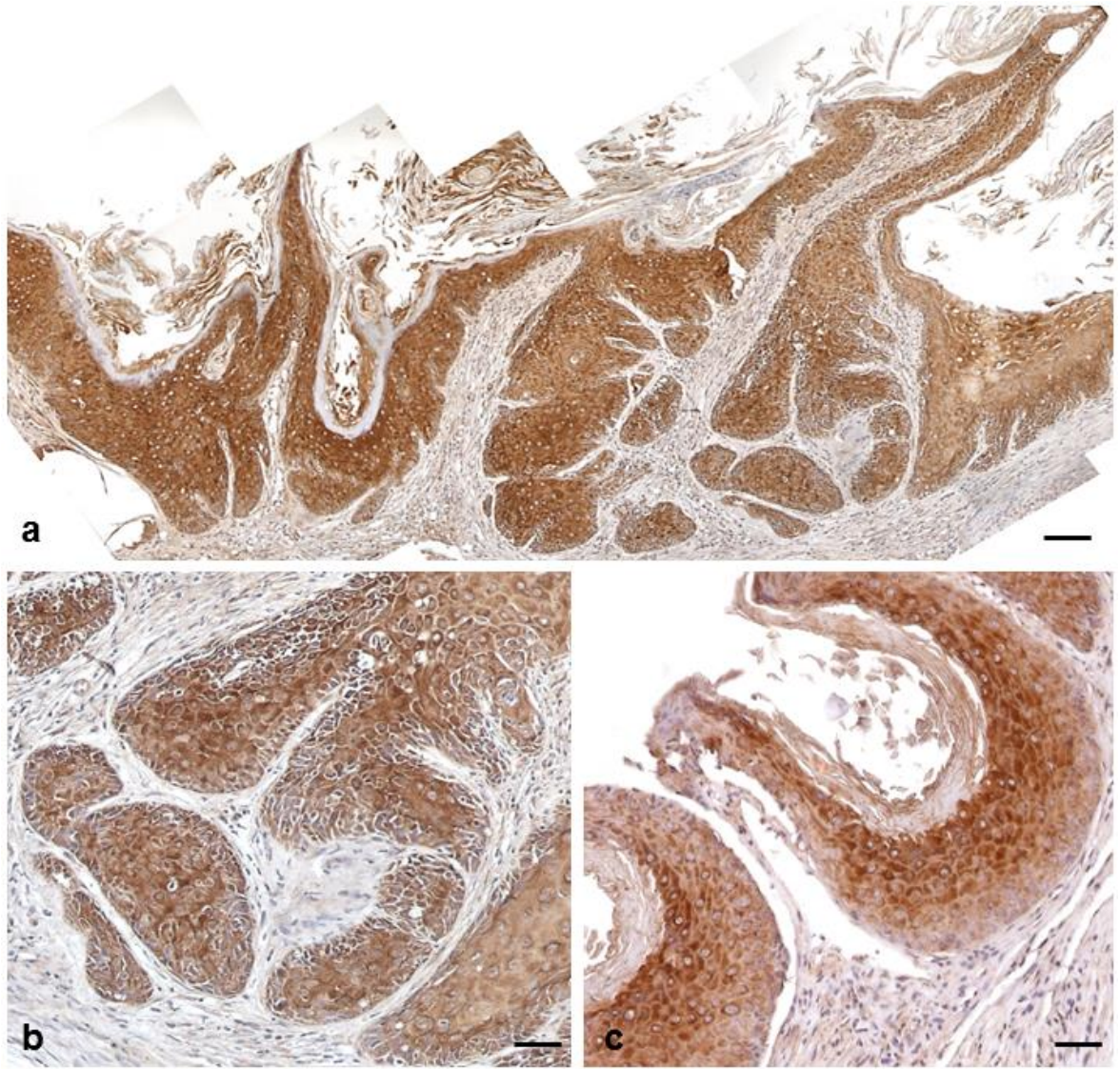


Figure 3.48 IHC Analysis of p21 expression in RU486-/4-HT-treated *K14.cre/Isl.ROCK^{er}/ras¹²⁷⁶/fos* malignant histotypes. (a) Composite micrograph shows strong and elevated p21 expression. (b) High magnification of malignant area showing p21 expression that remained persistent in both nucleus and cytoplasm. (c) Benign papilloma of 4-HT-treated *HK1.ras¹²⁷⁶/fos* histotype exhibits a delayed, supra-basal p21 expression. (Scale bar: a: 150 μ m; b-c: 100 μ m).

Next, p-AKT1 expression was analysed in *K14.cre/Isl.ROCK^{er}/ras¹²⁷⁶/fos* using immunofluorescence. Previously, in bi-genic *fos/Δ5PTEN^{flx}* models (Yao et al., 2008), it was theorised that compensatory p53 and p21 expression inhibited AKT activity and in tri-genic *ras¹²⁷⁶/fos/PTEN^{flx}* models (Macdonald et al., 2014), loss of p53 expression may have contributed to the persistence of p21 in order to combat the threat of activated AKT (Macdonald et al., 2014, Greenhalgh, – manuscript in preparation). Hence, to assess the role of PTEN/AKT signalling in this context, the expression of activated AKT1 and AKT2 were assessed.

In *K14.cre/Isl.ROCK^{er}/ras¹²⁷⁶/fos* epidermis and tumours, p-AKT2 was not expressed (not shown) which is again consistent with the earlier finding that p-AKT2 was not expressed in bi-genic *ROCK/Δ5PTEN^{flx}* hyperplasia (above). However interestingly, as shown in figure 3.49(a,b), little to no expression of p-AKT1 appeared in *K14.cre/Isl.ROCK^{er}/ras¹²⁷⁶/fos*, even with loss of p53. In addition, p-AKT1 was not detectable in *HK1.ras¹²⁷⁶/fos* benign papilloma (figure 3.49c) consistent with strong p53/p21 expression profiles that halted the p-AKT1 activities in bi-genic *fos/Δ5PTEN^{flx}* mice (Yao et al., 2008). Thus, this finding indicates that malignancy in *K14.cre/Isl.ROCK^{er}/ras¹²⁷⁶/fos* does not appear to involve the p-AKT signalling pathway. This was assessed again (below) to compare with the previous study by Macdonald et al., (2014), where expression of p-AKT, in theory, was mediated by loss of exon5 PTEN in *ras¹²⁷⁶/fos/Δ5PTEN^{flx}* models and this helped drive malignant progression.

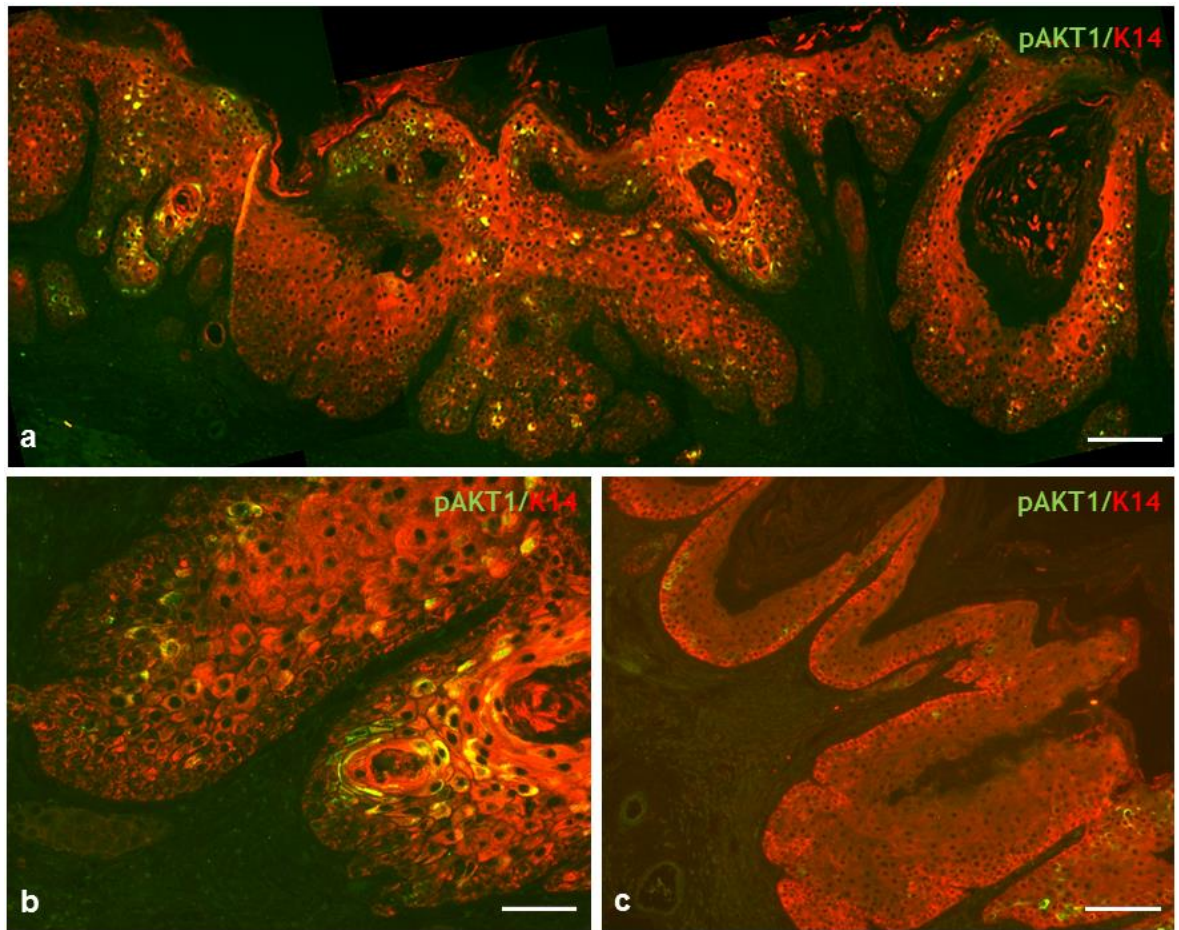


Figure 3.49 Immunofluorescence analysis of p-AKT1 expression in RU486-/4-HT-treated *K14.cre/Isl.ROCK^{er}/ras¹²⁷⁶/fos* malignant histotypes. (a) Lack of p-AKT1 expression is displayed in a composite micrograph of *K14.cre/Isl.ROCK^{er}/ras¹²⁷⁶/fos* mixed papilloma and wdSCC histotypes. (b) Little to no p-AKT1 expression is seen in high magnification of *K14.cre/Isl.ROCK^{er}/ras¹²⁷⁶/fos* wdSCC histotype. (c) 4-HT-treated *HK1.ras¹²⁷⁶/fos* benign papilloma histotype p-AKT1 expression is undetectable perhaps due to high p53/p21 expression profiles. (Scale bar: a: 150µm; b: 50µm; c: 100µm).

3.7.4 BrdU-labelling of tri-genic ROCK/ras¹²⁷⁶/fos tumours

Analysis of cell proliferation rates was carried out using BrdU-labelling. As shown in figure 3.50, RU486-/4-HT-treated *K14.cre/Isl.ROCK^{er}/ras¹²⁷⁶/fos* wdSCCs/SCCs possessed higher cell proliferation rates (69.5%, figure 3.50a) compared to bi-genic ras¹²⁷⁶/fos papillomas (4-HT-treated and 4-HT-untreated *HK1.ras¹²⁷⁶/fos* cohorts: 37.5% (figure 3.50b) and 35.6%; RU486-treated/4-HT-untreated *K14.cre/Isl.ROCK^{er}/ras¹²⁷⁶/fos* 38.6%). These findings demonstrate that as tri-genic ROCK/ras¹²⁷⁶/fos undergo malignant progression, higher cell proliferation rates were recorded in comparison to bi-genic ras¹²⁷⁶/fos synergism which still remained benign papillomas. IFC analysis showed that the increased numbers in BrdU-labelled keratinocytes was not only confined to basal layer but also appeared in the supra-basal layer. Furthermore, this significant increase in proliferation rates in *K14.cre/Isl.ROCK^{er}/ras¹²⁷⁶/fos* malignancy corresponds to loss of p53 expression (figure 3.47b).

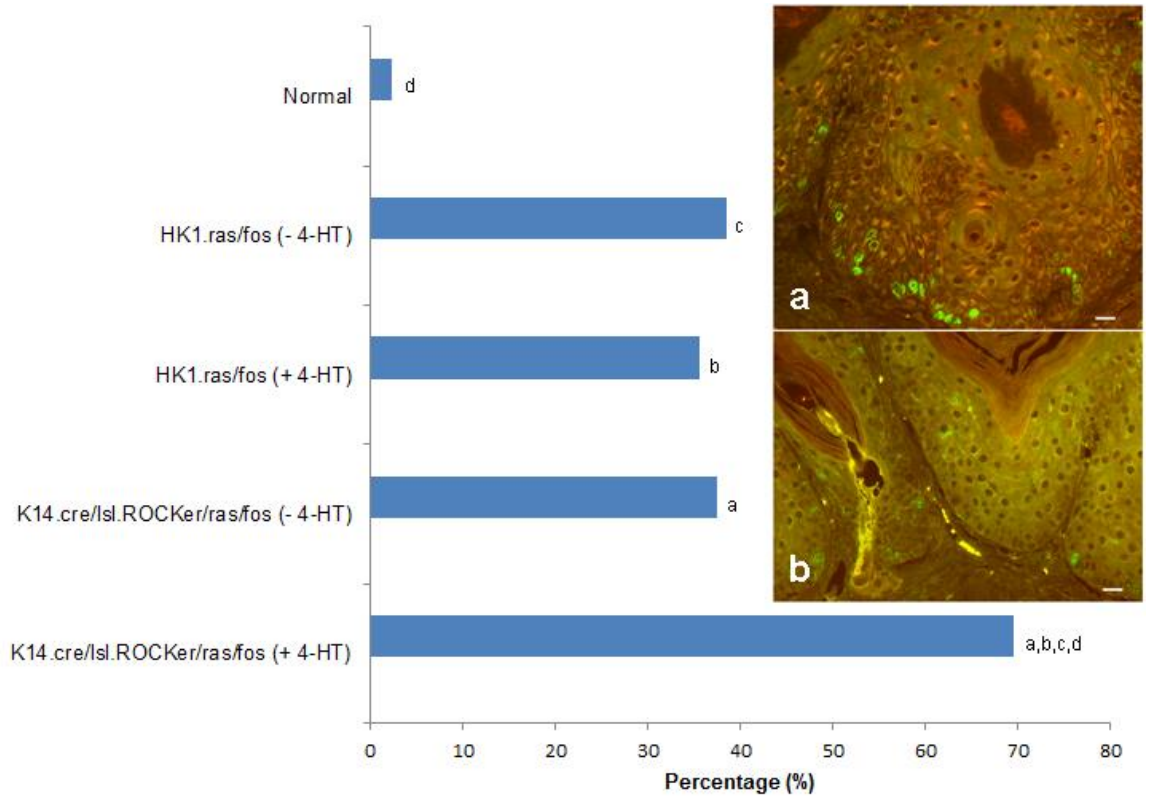


Figure 3.50 BrdU-labelling of tri-genic ROCK/ras¹²⁷⁶/fos carcinogenesis. Graph displays increased cell proliferation activity in RU486-/4-HT-treated *K14.ROCK^{er}/ras¹²⁷⁶/fos* wdSCC/SCC compared to bi-genic ras¹²⁷⁶/fos papillomas. (a,b,c,d : Significantly difference between *K14.cre/Isl.ROCK^{er}/ras¹²⁷⁶/fos* (+ 4-HT) and all transgenic cohorts; $p < 0.05$). (a) RU486-/4-HT-treated *K14.cre/Isl.ROCK^{er}/ras¹²⁷⁶/fos* wdSCC histotype show high BrdU-labelling compared to (b) low BrdU-labelling in 4-HT-treated *HK1.ras¹²⁷⁶/fos* benign papilloma histotype. (Scale: 50 μ m).

3.7.5 Summary

Collectively, this tri-genic synergism of *K14.cre/lsl.ROCK^{er}/ras¹²⁷⁶/fos* produced conversion to carcinoma in 100% of animals. These findings indicate that the consequence of activated ROCK expression in co-operation with *ras¹²⁷⁶/fos* is to achieve malignant transformation and progression; whereas tumours in bi-genic ROCK/fos (or *HK1.ras¹²⁷⁶/fos*) mice remained benign papillomas and ROCK/*ras¹²⁷⁶* mice exhibited hyperplasia. Furthermore, this study showed that *K14.cre/lsl.ROCK^{er}/ras¹²⁷⁶/fos* tumours produced a mixed histotype of papilloma and wdSCC/SCC by 13-14 weeks, as confirmed by loss of keratin K1 expression in the SCC histotype and consistent with p53 loss together with the significant increase in proliferation rates from Brdu-labelling analysis. However, this malignant histotype was mainly limited to a wdSCC with only nests of more aggressive SCC. This may have been due to the persistent p21 expression that still remained strong in all tri-genic ROCK/*ras¹²⁷⁶/fos* tumour tissues, despite p53 loss that limit or protect the tissue from further progression. Interestingly these tumours showed lack of p-AKT1 expression despite loss of p53 expression in the *K14.cre/lsl.ROCK^{er}/ras¹²⁷⁶/fos* carcinoma area (wdSCC progression to SCC). This may indicate that p-AKT1 was not involved in progression in this tri-genic ROCK/*ras¹²⁷⁶/fos* model, an idea supported by the lack of p-AKT1 expression in *HK1.ras¹²⁷⁶/fos* benign papillomas that may be due to strong p53/p21 expression profiles. Thus, this suggests that ROCK inhibitors may be a good idea for cancer treatment where ras/MAPK signalling drives tumour progression, rather than targeting anti p-AKT as these tumours still continue to progress even in the absence of p-AKT expression.

3.8 Co-operation of ROCK2, *HK1.fos* and *K14.cre/Δ5PTEN^{flx}* in transgenic mouse skin carcinogenesis

In the bi-genic model, activated ROCK2 and *fos* oncogene co-operation resulted in highly keratotic, benign papilloma formation but unlike bi-genic ROCK/*ras*¹²⁰⁵, no conversion was observed. Nonetheless, these data revealed a novel co-operation between ROCK and *fos* signalling deregulation, but now in the early stages of carcinogenesis where ROCK, being downstream of *ras* may substitute for its initiation role. In addition to this finding, which appears to be the first to describe such early roles, the previous sections also showed that ROCK2-mediated carcinogenesis in a bi-genic cohort required additional events, such as both *ras*^{Ha} for initiation and then wounding or constitutive *fos*-mediated promotion to achieve highly keratotic papillomas. This was also anticipated for co-operation with *Δ5PTEN^{flx}* mutation and subsequent loss of p-AKT regulation; but this was not the case as very little synergism was observed in *K14.cre/Isl.ROCK^{er}/Δ5PTEN^{flx}* cohorts. Hence, the co-operation to achieve even a benign tumour by ROCK2 activation appeared to be specific to deregulation of the MAPK pathway and the lack of p-AKT expression in tri-genic ROCK/*ras*¹²⁷⁶/*fos* mice (above) also suggested that the PTEN/PI3K/AKT pathway was not involved in ROCK2 mediated tumour mechanisms. This seemed unlikely, and instead it may be that the appropriate contexts were not supplied in the *K14.cre/Isl.ROCK^{er}/Δ5PTEN^{flx}*, either due to a similarity in oncogenic insults resulting in redundancies or compensatory responses such as p53/p21 expression. Alternatively, the roles for PTEN mutation may have quite different outcomes depending upon context, as when introduced into the *HK1.fos* model (Yao et al., 2008), keratoacanthomas were produced giving a less aggressive scenario than that observed following TPA promotion (c-*fos* activated) of *HK1.ras*¹²⁷⁶/*Δ5PTEN^{flx}* cohorts which gave pdSCCs (Yao et al., 2006).

The co-operation between *HK1.fos* and inactivation of PTEN mediated AKT regulation following topical RU486 treatment (*K14.cre/Δ5PTEN^{flx}*) had resulted in keratoacanthoma (KA) formation (Yao et al., 2008). In this context, no evidence of malignancy was recorded due to sudden compensatory p53 and p21 expression

that diverted proliferative papilloma keratinocytes into a dead-end programme of terminal differentiation; resulting in huge amounts of keratosis and classic KA formation (Yao et al., 2008). Co-operation between *K14.cre/Isl.ROCK^{er}* and $\Delta 5PTEN^{flx}$ was also implicated in an increased degree of epidermal differentiation instead of tumour formation, as demonstrated by an anomalous lack of K6 expression and the appearance of K1 in low calcium culture conditions. In this instance even with the promotion from wounding, their synergism appeared almost redundant; suggesting some similar functions in epidermal homeostasis.

Thus, given this background, generation of these *K14.cre/Isl.ROCK^{er}/fos/ $\Delta 5PTEN^{flx}$* cohorts in essence to assess whether additional mutation events in ROCK2 signalling would change the outcome from KA to SCC, and if so, would allow investigation of how (and when) the protective p53/p21 expression was circumvented. Alternatively, in the context of papillomatogenesis as in ROCK/fos signalling, so, would this tri-genic ROCK/fos/ $\Delta 5PTEN^{flx}$ synergism remain redundant and still produce papillomas; yet to be determined via p53/p21 profiles and AKT status.

3.8.1 ROCK2 co-operates with *HK1.fos/ $\Delta 5PTEN^{flx}$* to produce malignant progression to SCC not keratoacanthomas.

To analyse tri-genic ROCK/fos/ $\Delta 5PTEN^{flx}$ synergism in multistage carcinogenesis, these cohorts exploited the RU486-inducible *K14.cre/Isl.ROCK^{er}* transgenic line in order to hit the same keratinocyte populations as that of $\Delta 5PTEN^{flx}$ driven by *K14.creP* promoter in transgenic mice expressing activated fos (*HK1.fos*). In repeat experiments, 10 individual *K14.cre/Isl.ROCK^{er}/fos/ $\Delta 5PTEN^{flx}$* transgenic mice at 6-7 week old were treated with RU486 in the week 1 to ablate the stop cassette to express *Isl.ROCK^{er}* transgene and ablate exon5 PTEN to induce loss of AKT regulation ($\Delta 5PTEN^{flx}$). Then, routine 4-HT treatments, 3x per week maintained an activated ROCK^{er} transgene with appropriate controls: *K14.cre/fos/ $\Delta 5PTEN^{flx}$* (n= 5) receiving RU486 and 4-HT whilst *K14.cre/Isl.ROCK^{er}/fos/ $\Delta 5PTEN^{flx}$* controls (n= 5) receiving RU486 alone.

Excitingly, at only 9 weeks of 4-HT treatment, tri-genic *K14.cre/Isl.ROCK^{er}/fos/ $\Delta 5PTEN^{flx}$* mice had formed large tumours on both the

tagged and untagged ears as compared to control cohorts (figure 3.51a-g); a result again consistent with the promotion stimulus received from *HK1.fos*. The ears possessed a very thick keratotic phenotype but with a pale appearance (figure 3.51 a,b) and without the large keratin structures that typified KA formation (later) (figure 3.51g) (Yao et al., 2008). At this time, both RU486-/4-HT-treated *K14.cre/fos/Δ5PTEN^{flx}* and RU486-treated/4-HT-untreated *K14.cre/Isl.ROCK^{ex}/fos/Δ5PTEN^{flx}* control mice displayed thickened ears only, and possibly the early beginning that eventually develop into KAs (figure 3.51 c-f).

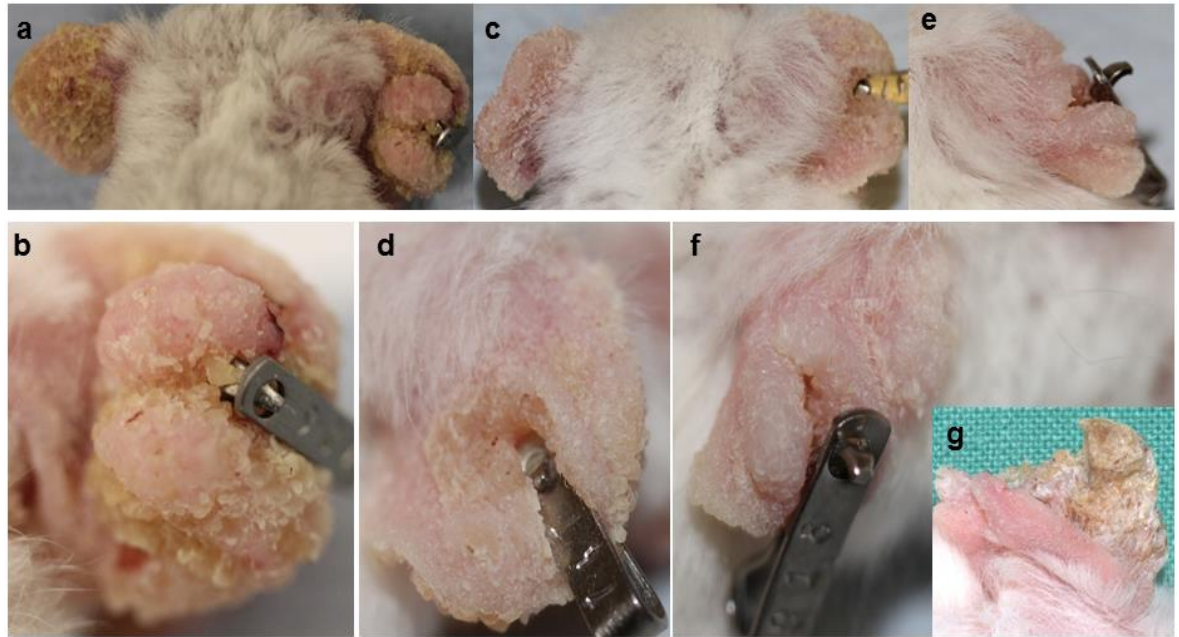


Figure 3.51 Phenotypes of *K14.cre/lsl.ROCK^{er}/fos/Δ5PTEN^{flx}* transgenic mice at approximately 9 weeks. (a, b) RU486-/4-HT-treated tri-genic *ROCK/fos/Δ5PTEN^{flx}* mice exhibit large tumours with keratotic appearance. (c, d) RU486-/4-HT-treated *K14.cre/fos/Δ5PTEN^{flx}* and (e, f) RU486-treated/4-HT-untreated *K14.cre/lsl.ROCK^{er}/fos/Δ5PTEN^{flx}* mice display thickened keratotic ears with early sign of KA formation; (g) But not the overt obvious KAs seen in older RU486-treated *K14.cre/fos/Δ5PTEN^{flx}*.

Due to this rapid growth and tumour size, most *K14.cre/Isl.ROCK^{er}/fos/Δ5PTEN^{fix}* mice underwent biopsy as early as 9 weeks. These phenotypes now suggest a significant co-operation that has bridged any gaps in carcinogenesis between tri-genic ROCK/fos/Δ5PTEN^{fix} mice in terms of a massive degree of both proliferation and differentiation. Most importantly, the outcome was very different to the KAs exhibited in *K14.cre/fos/Δ5PTEN^{fix}* co-operation reported by Yao et al., (2008) and also the mechanism observed in tri-genic ROCK/ras¹²⁷⁶/fos (above). In addition, the histopathology of *K14.cre/Isl.ROCK^{er}/fos/Δ5PTEN^{fix}* tumours also reflected an antagonism between keratinocyte proliferation and differentiation that gave rise to a very confused differentiation pattern.

At only 9 weeks of 4-HT treatment, a typical *K14.cre/Isl.ROCK^{er}/fos/Δ5PTEN^{fix}* tumour showed a massive keratosis possibly associated with *K14.cre/fos/Δ5PTEN^{fix}* synergism (Yao et al., 2008) and /or bi-genic ROCK/fos co-operation (above), but now all tumours exhibited malignant conversion to a wdSCC histotype. In addition, the benign areas comprised a mix of highly keratotic papilloma pathology (as determined by K1 expression) and carcinoma histotypes (figure 3.52a) as they possessed a very confused pattern of keratinocyte differentiation, with granular cells in the proliferative basal layer (most likely malignant keratinocytes in the upper layers, as demonstrated by differentiation and BrdU labelling - below) and this was similar to that early papillomatous KA histotypes exhibited by *K14.cre/fos/Δ5PTEN^{fix}* (Yao et al., 2008). This odd degree of anomalous differentiation gave a question to an initial impression that this wdSCC; as KAs and SCCs are often confused. However, the rapid nature of their growth, the increased areas of non-keratosis and the analysis of p53/p21 status below are consistent with malignant conversion to wdSCC, plus the appearance again of ripped sections (figure 3.52c – red arrow) and mitotic cells.

At higher magnification (figure 3.52 b,c), while the layers of keratinocytes in these areas of wdSCC looked massively disorganised and the multiple layers of proliferative cells possessed patches of micro-acanthosis (typified by strands of K1 expression; below (figure 3.53)) and micro-cysts (figure 3.52b,c – black arrows), with some intercellular gaps between the malignant keratinocytes, these areas showed a rip in this tissue (figure 3.52c – red arrow). A similar disorganised histopathology was also exhibited by *K14.cre/fos/Δ5PTEN^{fix}* keratotic papillomas, here with more significant hyperkeratosis and pre-mature differentiation that

offered cornified cells embedded in very prominent granular layers and growth of micro-cysts in the epidermal layers (figure 3.52d,e - arrows). However, these pre-malignant histotypes possessed fewer proliferative layers and were devoid of invasive areas, mitotic figures, the unique intercellular gap and possessed clear differences in terms of differentiation markers.

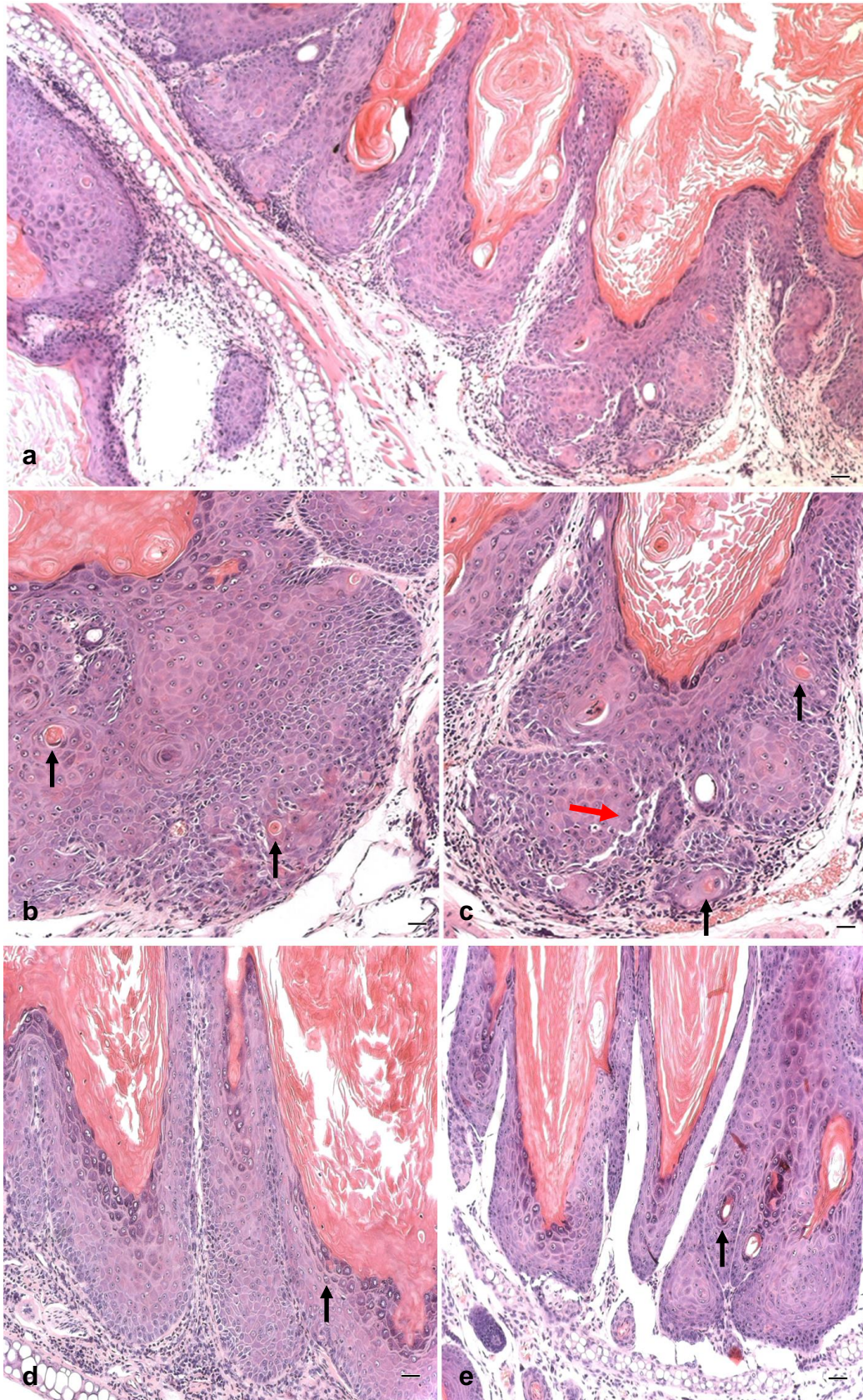


Figure 3.52 Histotypes of *K14.cre/Isl.ROCK^{er}/fos/Δ5PTEN^{flx}* biopsies at 9 weeks. (a) RU486-/4-HT-treated *K14.cre/Isl.ROCK^{er}/fos/Δ5PTEN^{flx}* biopsy shows mixed histotypes of papilloma and SCC with massive keratosis. (b, c) At higher magnification, tri-genic *ROCK/fos/Δ5PTEN^{flx}* areas of both wdSCC and SCC exhibit highly disorganisation in epidermal architecture, prominent intercellular gaps (red arrow) and appearance of micro-cysts (black arrows). (d) RU486-treated/4-HT-untreated *K14.cre/Isl.ROCK^{er}/fos/Δ5PTEN^{flx}* and (e) RU486-/4-HT-treated *K14.cre/fos/Δ5PTEN^{flx}* biopsies display hyperkeratotic papilloma histotypes with irregular differentiation giving rise to micro-cysts formation (arrows). (Scale bar: 150µm in a; 50µm in b,c; 100µm in d,e).

3.8.2 Expression of tumour progression marker keratin K1 in tri-genic ROCK/fos/ Δ 5PTEN^{flx} carcinogenesis

The loss of keratin K1 has been an essential indicator of tumour progression to malignancy and progression to aggressive SCC in this model. In addition, in previous *K14.cre/fos/ Δ 5PTEN^{flx}* studies (Yao et al., 2008), K1 expression was employed in a more conventional manner and used as an indicator of keratinocyte differentiation. Indeed, the very odd K1 expression in the basal layers of pre-KA papillomas was amongst the first indications that the sudden appearance of compensatory p53 and p21 in *K14.cre/fos/ Δ 5PTEN^{flx}* KAs (Yao et al., 2008) led to a highly confused state of premature differentiation or supra-basal proliferation, as now also observed histologically in *K14.cre/Isl.ROCK^{er}/fos/ Δ 5PTEN^{flx}* tumours.

Therefore, whilst immunofluorescence analysis of keratin K1 was mainly performed to confirm progression of *K14.cre/Isl.ROCK^{er}/fos/PTEN^{flx}* wdSCC histotypes (figure 3.53), it was recognised that in certain instances, K1 was expressed in an anomalous fashion; e.g. in the microcysts that formed in response to these anomalous differentiation signals. This is shown in figure 3.53a, where reduced K1 (green) expression was demonstrated in tri-genic ROCK/fos/ Δ 5PTEN^{flx} mixed histotypes upon transformation of keratotic papillomas to wdSCC and subsequently to more aggressive SCC. However, consequently here in these *K14.cre/Isl.ROCK^{er}/fos/ Δ 5PTEN^{flx}* wdSCC/SCC tumours, at higher magnification, K1 expression became lost upon progression but could remain in patches of anomalous differentiation exhibiting the normal intense green staining in the areas of microcysts (figure 3.53b). These islands were often surrounded by yellow due to reduced K1 in wdSCC or by red in SCC based on the keratin K14 (red) counterstain. Thus, this staining pattern again confirms malignant conversion and progression to wdSCC and SCC due to the tri-genic synergism. However, this staining pattern also possessed similarities to the premature differentiation that switched progression to KA (not SCC) in bi-genic fos/ Δ 5PTEN^{flx} shown by Yao et al., (2008) and thus, prompted analysis of markers of late stage differentiation: filaggrin and loricrin in this study. Indeed in the 4-HT-treated *K14.cre/fos/ Δ 5PTEN^{flx}* keratotic papillomas, all controls exhibited strong K1 expression that remained intact and uniform in the supra-basal layer (figure 3.53

c), similar to K1 expression in RU486-treated/4-HT-untreated *K14.cre/Isl.ROCK^{er}/fos/Δ5PTEN^{flx}* histotype (not shown). Note that this strong supra-basal K1 expression in control bi-genic *fos/Δ5PTEN^{flx}* was displayed at 9 weeks and it was shown in the previous study (Yao et al., 2008) that K1 expression appeared in the basal layer of later KAs in bi-genic *fos/Δ5PTEN^{flx}*. In addition, in these tri-genic tumours, the typical K6 expression profiles were restored and strong K6 expression now appeared in uniform throughout the epidermal compartments in RU486-/4-HT-treated *K14.cre/Isl.ROCK^{er}/fos/Δ5PTEN^{flx}* and *K14.cre/fos/Δ5PTEN^{flx}* tumours (figure 3.53d,e).

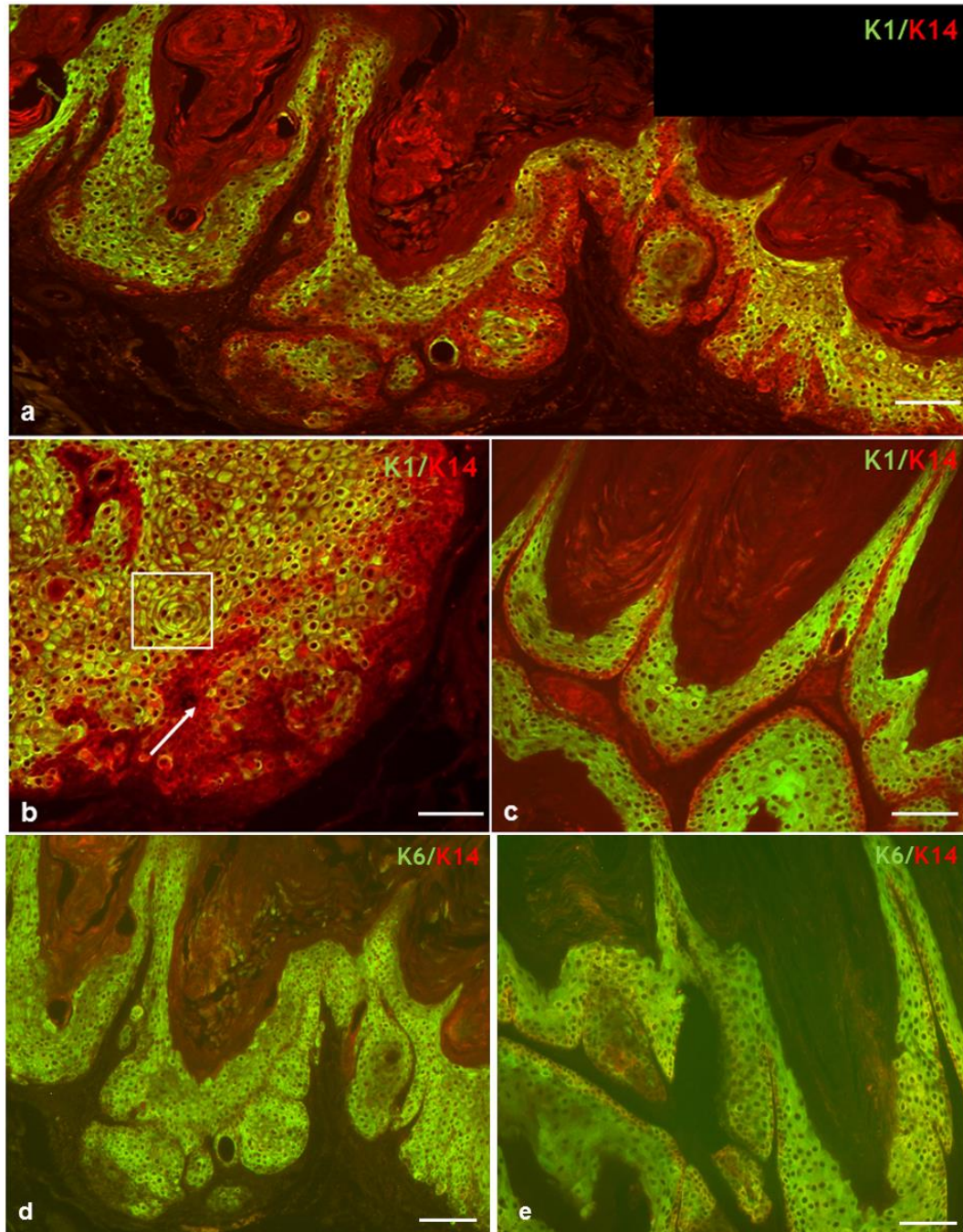


Figure 3.53 Immunofluorescence analysis of K1/K14 and K6/K14 expression in *K14.cre/Isl.ROCK^{er}/fos/Δ5PTEN^{fix}* carcinogenesis. (a) Tri-genic ROCK/fos/Δ5PTEN^{fix} tumours exhibit reduced K1 (green) expression that became gradually lost together with elevated yellow colour upon progression to SCC. (b) Higher magnification of a wdSCC/SCC area of *K14.cre/Isl.ROCK^{er}/fos/Δ5PTEN^{fix}* has a band of K1 expression in an overtly K1 negative area (arrow) and an oval expression pattern highlighting a microcyst (box). (c) RU486-/4-HT-treated *K14.cre/fos/Δ5PTEN^{fix}* keratotic papilloma showed strong K1 expression in supra-basal layers. (d) RU486-/4-HT-treated of *K14.cre/Isl.ROCK^{er}/fos/Δ5PTEN^{fix}* and (e) *K14.cre/fos/Δ5PTEN^{fix}* display K6 expression in all epidermal compartments. (Scale bar: 100μm in a,c,d,e; 50μm in b).

3.8.3 Expression of late differentiation markers filaggrin and loricrin in tri-genic ROCK/fos/ Δ 5PTEN^{flx} carcinogenesis

To investigate the status of later markers of terminal differentiation, a double-labelled IFC analysis of filaggrin and loricrin was performed (Yao et al., 2008). Typically expression of loricrin appears in the granular layer and is one of the most common proteins in these upper layers (Hohl et al., 1991). Whilst filaggrin migrates from granular layer to the upper cornified layer (Rothnagel and Steinert, 1990, Steven et al., 1990). It is worth noting that, here, both loricrin and filaggrin are regulated by c-fos possessing three AP1 binding sites (Yuspa, 1994, Mehic et al., 2005) and both proteins are essential for epidermal barrier maintenance. Indeed, reduction in the levels of filaggrin has been shown to compromise the cornified layers and in some individuals, this leads to eczema (McLean, 2011). Typically in skin carcinogenesis, as in most malignancies, there is a trend towards less differentiation and thus, loss of both filaggrin and loricrin expression is a common event and for filaggrin expression to be lost quite early in both hyperplasia and papillomas (Yao et al., 2006, 2008). Since both *K14.cre/Isl.ROCK^{er}/fos/ Δ 5PTEN^{flx}* and *K14.cre/fos/ Δ 5PTEN^{flx}* produced keratotic papillomas with a very odd confused keratinocyte differentiation histotypes, the expression of loricrin and filaggrin was investigated in this tri-genic ROCK/fos/ Δ 5PTEN^{flx} tumour progression mechanism and compared to the p53/p21 and p-AKT expression profiles.

K14.cre/Isl.ROCK^{er}/fos/ Δ 5PTEN^{flx} wdSCC/SCC histotypes showed a complete loss of filaggrin expression (figure 3.54a), but had persisted in the earlier biopsies consistent with the degree of papilloma keratosis. The loss of filaggrin expression indicates less differentiation upon progression to malignancy in tri-genic ROCK/fos/ Δ 5PTEN^{flx} synergism and this contrasted to the KAs observed previously (Yao et al., 2008). Conversely, filaggrin expression in *K14.cre/fos/ Δ 5PTEN^{flx}* keratotic papilloma (early, pre-KA) histotype appeared strong in most supra-basal layers as opposed to being restricted to the granular layer; which again suggests premature differentiation (figure 3.54b). In comparison, filaggrin expression was confined to the upper granular layers in typical control cohorts; e.g. *K14.cre/Isl.ROCK^{er}/fos* papilloma (figure 3.54c), *HK1.fos* hyperplasia (figure 3.54d), *K14.cre/Isl.ROCK^{er}/ Δ 5PTEN^{flx}* papillomatous-

like hyperplasia (figure 3.54e), *K14.cre/Δ5PTEN^{flx}* mild hyperplasia (figure 3.54f) and *K14.cre/Isl.ROCK^{er}* hyperplasia (figure 3.54g). However, filaggrin was difficult to detect in normal ICR histotypes due to the thin nature of normal murine epidermis (figure 3.54h).

These findings relating to filaggrin expression in controls (figure 3.54c-g) are consistent with limited tumour progression as mentioned in earlier results; which is mostly due to p53/p21 responses. Of note, these new findings demonstrated that filaggrin expression in activated ROCK hyperplasia (figure 3.54g) appeared stronger than in $\Delta 5PTEN^{flx}$ hyperplasia (figure 3.54f), which is again consistent with ROCK roles and links in the barrier of an epidermis. As mentioned earlier, the literature clearly shows that ROCK2 provides the tensile strength to epidermis (Samuel et al., 2011).

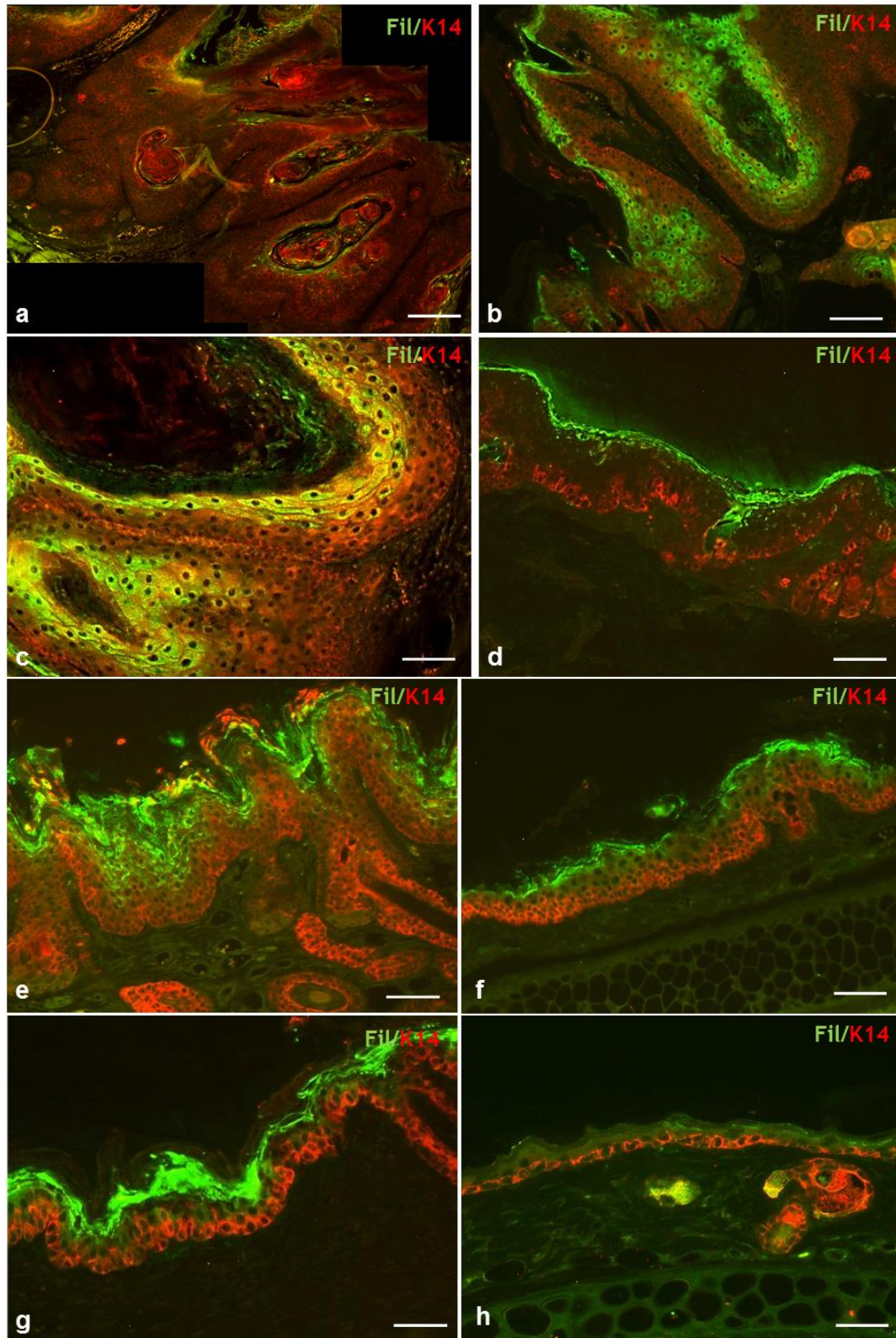


Figure 3.54 Immunofluorescence analysis of filaggrin/K14 expression in RU486-/4-HT-treated *K14.cre/Isl.ROCK^{er}/fos/Δ5PTEN^{flx}* tumours. (a) Filaggrin expression disappeared upon malignant progression in tri-genic *ROCK/fos/Δ5PTEN^{flx}* wdSCC/SCC. (b) RU486-/4-HT-treated *K14.cre/fos/Δ5PTEN^{flx}* early KA exhibits high level of filaggrin expression in supra-basal layers indicating active premature differentiation. (c) Filaggrin expression remained persisted in RU486-/4-HT-treated *K14.cre/Isl.ROCK^{er}/fos* papilloma, (d) 4-HT-treated *HK1.fos* hyperplasia, (e) RU486-/4-HT-treated *K14.cre/Isl.ROCK^{er}/Δ5PTEN^{flx}* papillomatous-like hyperplasia, (f) RU486-/4-HT-treated *K14.cre/Δ5PTEN^{flx}* hyperplasia, and (g) RU486-/4-HT-treated *K14.cre/Isl.ROCK^{er}* hyperplasia in granular and cornified layers. (h) Filaggrin was hardly detected in normal non-transgenic ICR histotype due to layer being one cell thick. (Scale bar: a,b,d-h: 100μm; c: 50μm).

Analysis of loricrin protein in *K14.cre/Isl.ROCK^{er}/fos/Δ5PTEN^{flx}* tumours also demonstrated a lower level of expression compared to age-matched *K14.cre/fos/Δ5PTEN^{flx}* control cohorts in which it disappeared upon malignant conversion prior to progression to SCC (figure 3.55a). This result was typical of progression in this model and contrasted to the premature loricrin expression found in the supra-basal layers of *K14.cre/fos/Δ5PTEN^{flx}* keratotic papilloma (figure 3.55b). This would support the idea that initially, in pre-malignant stages where both p53/p21 are expressed, the overlay of bi-genic ROCK/fos signalling inducing proliferation to the differentiation stimulus, plus ROCK/Δ5PTEN^{flx} gave rise to this confused keratinocyte differentiation pattern. Hence, in highly keratotic papillomas in the context of tri-genic *K14.cre/Isl.ROCK^{er}/fos/Δ5PTEN^{flx}*, this resulted in tumours prone to conversion due to additional ROCK2 activities. Whereas in the context of bi-genic *K14.cre/fos/Δ5PTEN^{flx}* tumours the continuous p53/p21 response led to a stall in progression, where continuous papilloma proliferation now gives rise to the excess differentiation leading to the keratosis of classic KAs. In control mice, loricrin expression remained confined to an expanded granular layer in cohorts of *K14.cre/Isl.ROCK^{er}/fos* papilloma (figure 3.55c). Whilst in *HK1.fos* hyperplasia (figure 3.55d), *K14.cre/Isl.ROCK^{er}/Δ5PTEN^{flx}* papillomatous-like hyperplasia (figure 3.55e), *K14.cre/Δ5PTEN^{flx}* mild hyperplasia (figure 3.55f) and *K14.cre/Isl.ROCK^{er}* hyperplasia (figure 3.55g), loricrin remained restricted to a relatively normal granular layer which coincided with their lack of tumour progression. As found similar to filaggrin (above), loricrin was also difficult to detect in a normal epidermal histotype of this non-transgenic ICR mice (figure 3.55h).

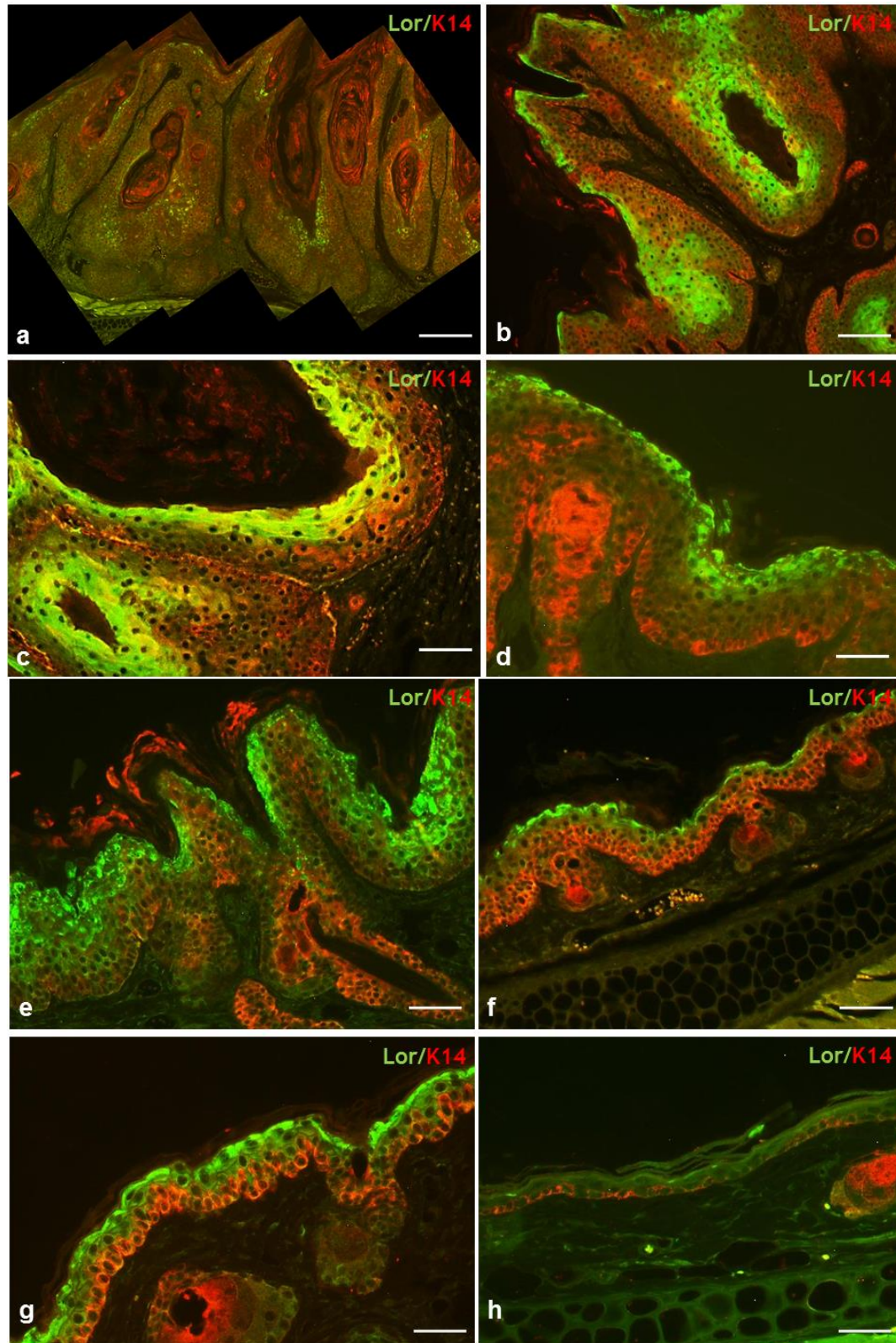


Figure 3.55 Immunofluorescence analysis of loricrin/K14 expression in RU486-/4-HT-treated *K14.cre/ls1.ROCK^{et}/fos/Δ5PTEN^{flx}* tumours. (a) Loricrin expression appears at a low level and is gradually lost in tri-genic *ROCK/fos/Δ5PTEN^{flx}* SCC. (b) RU486-/4-HT-treated *K14.cre/fos/Δ5PTEN^{flx}* keratotic papilloma exhibits a high level of loricrin in the supra-basal layer indicating atypical differentiation. (c) Loricrin expression remained confined in RU486-/4-HT-treated *K14.cre/ls1.ROCK^{et}/fos* papilloma, (d) 4-HT-treated *HK1.fos* hyperplasia, (e) RU486-/4-HT-treated *K14.cre/ls1.ROCK^{et}/Δ5PTEN^{flx}* hyperplasia; (f) RU486-/4-HT-treated *K14.cre/Δ5PTEN^{flx}* mild hyperplasia and (g) RU486-/4-HT-treated *K14.cre/ls1.ROCK^{et}* hyperplasia to the granular layer, indicative of limited tumour progression. (h) Loricrin was not detectable in normal, thin ICR epidermal layer (Scale bar: a,b,d-h: 100μm; c: 50μm).

3.8.4 Expression of p53 and p21 in tri-genic ROCK/fos/ Δ 5PTEN^{fix} tumours

The expression profiles of p53 and p21 tumour suppressor genes were analysed to determine their status in *K14.cre/Isl.ROCK^{er}/fos/ Δ 5PTEN^{fix}* tumours by IHC analysis. Since *K14.cre/Isl.ROCK^{er}/fos/ Δ 5PTEN^{fix}* tumours achieved malignant progression as confirmed by loss of K1, filaggrin and loricrin markers, it was expected that at least p53 expression may be down regulated as observed in other malignant histotypes from earlier models. Whereas in the *K14.cre/fos/ Δ 5PTEN^{fix}* model, both p53 and p21 were not expressed in early hyperplasia, their expression became elevated and appeared in basal layers in the overt KAs following GSK3 β inactivation (Yao et al., 2008). Interestingly, p53 expression, which was quite strong in the *K14.cre/Isl.ROCK^{er}/fos/ Δ 5PTEN^{fix}* hyperplasia and keratotic papillomas, faded and became lost upon malignant progression (figure 3.56a). Furthermore, at higher magnification (figure 3.56b), p53 expression had completely disappeared on progression to *K14.cre/Isl.ROCK^{er}/fos/ Δ 5PTEN^{fix}* SCCs. In contrast, a typical *K14.cre/fos/ Δ 5PTEN^{fix}* KA histotype showed strong and uniform p53 expression throughout the epidermal compartments (figure 3.56c). Again, it was noted that wdSCC and particularly SCC areas exhibited clear rips in the tumour tissue (figure 3.56a) suggesting a brittle nature possibly caused by ROCK2 mediated increased tissue stiffness and this was less prominent in the benign areas.

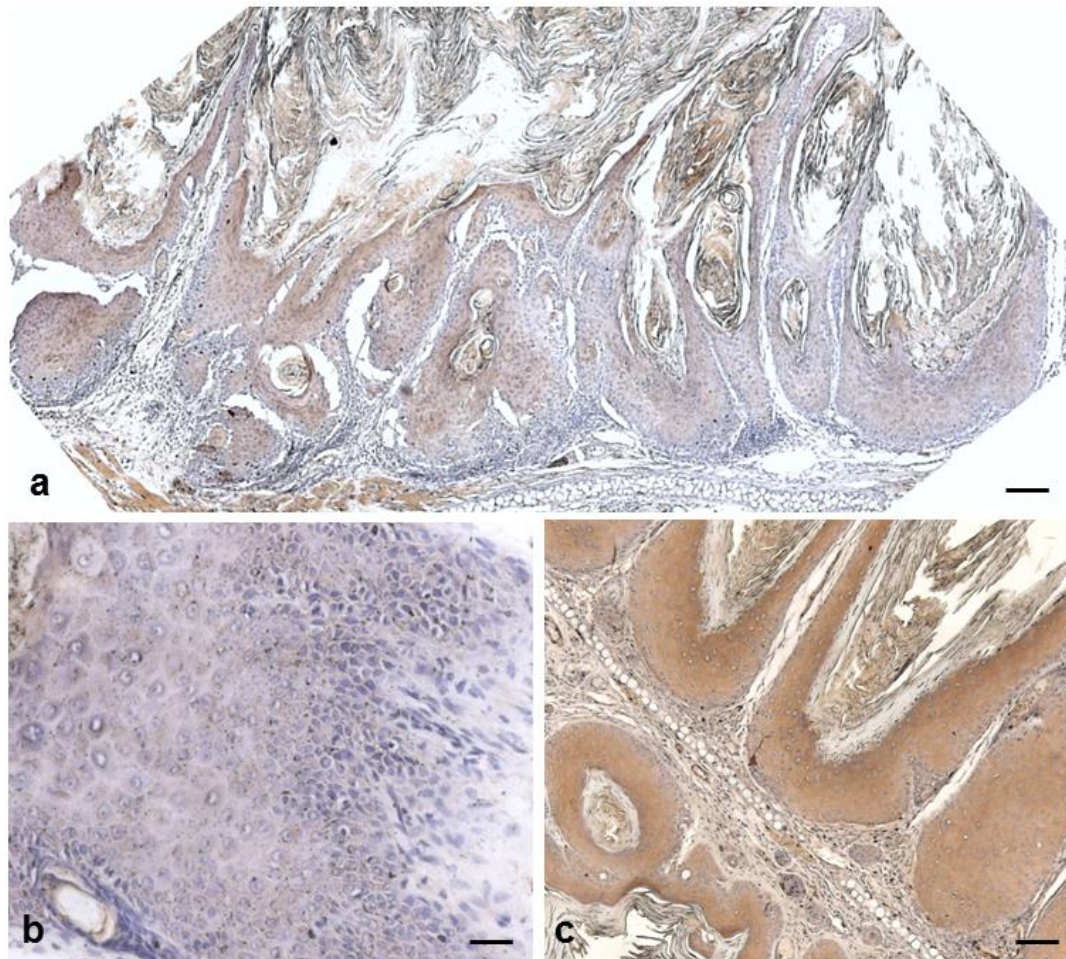


Figure 3.56 IHC analysis of p53 expression in RU486-/4-HT-treated *K14.cre/lsl.ROCK^{er}/fos/Δ5PTEN^{flx}* tumours. (a) Composite micrograph shows diminishing p53 expression in the late stage papilloma areas and faded in the wdSCC/SCC histotypes. (b) High magnification of *K14.cre/lsl.ROCK^{er}/fos/Δ5PTEN^{flx}* SCC area (from box) exhibits complete loss of p53 expression. (c) RU486-/4-HT-treated *K14.cre/fos/ΔPTEN^{flx}* keratotic papilloma displays strong p53 expression in all epidermal layers. (Scale bar: a: 150μm; b: 50μm; c: 100μm).

While p53 expression reduced and disappeared as *K14.cre/Isl.ROCK^{er}/fos/Δ5PTEN^{fix}* tumours became malignant, analysis of p21 which is an effector of p53 function remained expressed (figure 3.57a). Not only was p21 expression persistent in the areas of keratin K1 loss (wdSCC/SCC histotype), p21 expression also appeared to increase based on the IHC staining upon p53 loss. This too was observed in tri-genic ROCK/ras¹²⁷⁶/fos model (above) and also in tri-genic ras/fos/Δ5PTEN^{fix} study (Macdonald et al., 2014) suggesting that persistent p21 expression is a major response to p53 loss. At higher magnification in such overt and highly invasive SCC areas, p21 expression appeared cytoplasmic and peri-nuclear; and also began to fade particularly in the proliferative fingers of invasive basal layer SCC keratinocytes (figure 3.57b). Over careful analysis of repeated biopsies, serial sections showed that the areas of wdSCC possessed significant p21 expression and sometimes a reasonable amount of residual but supra-basal p53. This suggests that reduction of p21 protection is a potential for further progression, and that this invasive mechanism was possibly enhanced by ROCK2 activation in conjunction with AKT activation; an idea clearly supported in the *K14.cre/Isl.ROCK^{er}/ras¹²⁷⁶/Δ5PTEN^{fix}* model given the degree of progression to pdSCC histotypes observed (below).

In contrast, comparison of aged-matched sibling controls 4-HT-treated *K14.cre/fos/PTEN^{fix}* or 4-HT-untreated *K14.cre/Isl.ROCK^{er}/fos/Δ5PTEN^{fix}* keratotic papillomas displayed increasing levels of p21 expression which in much later overt KAs (Yao et al., 2008), showed intense and uniform p21 expression in all epidermal keratinocytes (figure 3.57c). The initial lack of p53 or p21 was observed in bi-genic ROCK/Δ5PTEN^{fix} mice (above) and previously in pre-neoplastic bi-genic fos/Δ5PTEN^{fix} (Yao et al., 2008); and this p21 increase appeared to counter any Δ5PTEN^{fix} mediated AKT expression, also giving rise to patchy p-AKT1 expression in bi-genic ROCK/Δ5PTEN^{fix} mice. Whilst in bi-genic fos/Δ5PTEN^{fix} mice, this persistent high level of p21 prevented progression to SCC and also limited keratinocyte proliferation alongside p53 in these fos/Δ5PTEN^{fix} tumours as determined by Brdu-labelling.

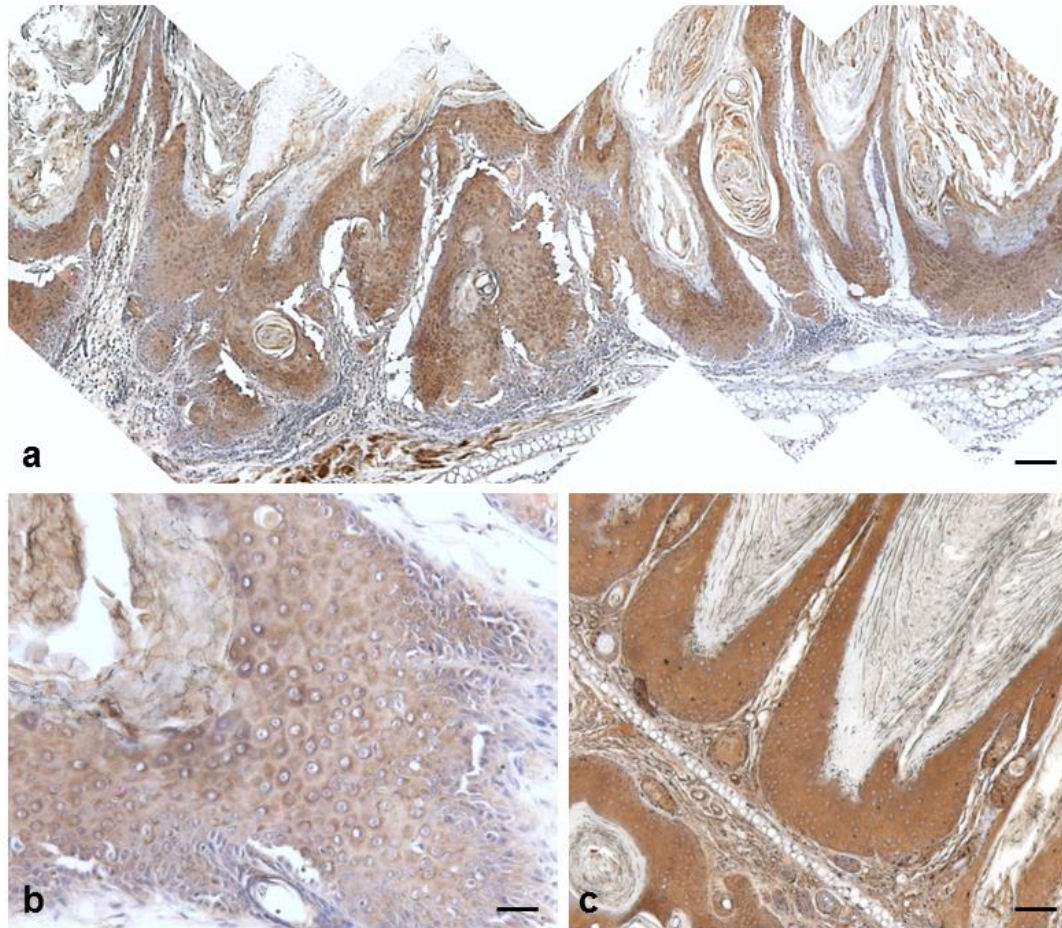


Figure 3.57 IHC analysis of p21 expression in RU486-/4-HT-treated *K14.cre/Isl.ROCK^{et}/fos/Δ5PTEN^{flx}* tumours. (a) Composite micrograph shows that p21 expression remained intact in all epidermal compartments. (b) High magnification of more aggressive SCC area shows p21 expression is reduced and appears in a more cytoplasmic and peri-nuclear manner, and has begun to fade particularly in the epidermal basal layer. (c) RU486-/4-HT-treated *K14.cre/fos/Δ5PTEN^{flx}* keratotic papilloma exhibits strong and uniform p21 expression. (Scale bar: a: 150μm; b: 50μm; c: 100μm).

3.8.5 BrdU-labelling of tri-genic ROCK/fos/ Δ 5PTEN^{fix} mice

Next, cell proliferation activity was analysed by positive BrdU-labelling in epidermal cells of *K14.cre/Isl.ROCK^{er}/fos/ Δ 5PTEN^{fix}* tumours. As shown in figure 3.58, RU486-/4-HT-treated *K14.cre/Isl.ROCK^{er}/fos/ Δ 5PTEN^{fix}* wdSCC/SCC histotypes have significantly higher proliferation rates and higher BrdU-labelling that scattered throughout all epidermal layers (89.1%, figure 3.58a) than bi-genic *fos/ Δ 5PTEN^{fix}* keratotic papilloma histotypes (RU486-/4-HT-treated and RU486-treated/4-HT-untreated *K14.cre/fos/ Δ 5PTEN^{fix}* cohorts: 34.1%, figure 3.58b and 34.7%; RU486-treated/4-HT-untreated *K14.cre/Isl.ROCK^{er}/fos/ Δ 5PTEN^{fix}* 32.1%). This finding is consistent with increased proliferation activity upon malignant progression in *K14.cre/Isl.ROCK^{er}/fos/ Δ 5PTEN^{fix}* SCC coinciding with loss of filaggrin and loricrin, together with p53 loss. Moreover, this BrdU-labelling finding demonstrated a large difference between *K14.cre/Isl.ROCK^{er}/fos/ Δ 5PTEN^{fix}* SCC and *K14.cre/fos/ Δ 5PTEN^{fix}* KA histotypes reported by Yao et al., (2008), where a much lower mitotic index in the KA histotypes due to strong expression of p53 and p21 together with loricin and filaggrin was observed.

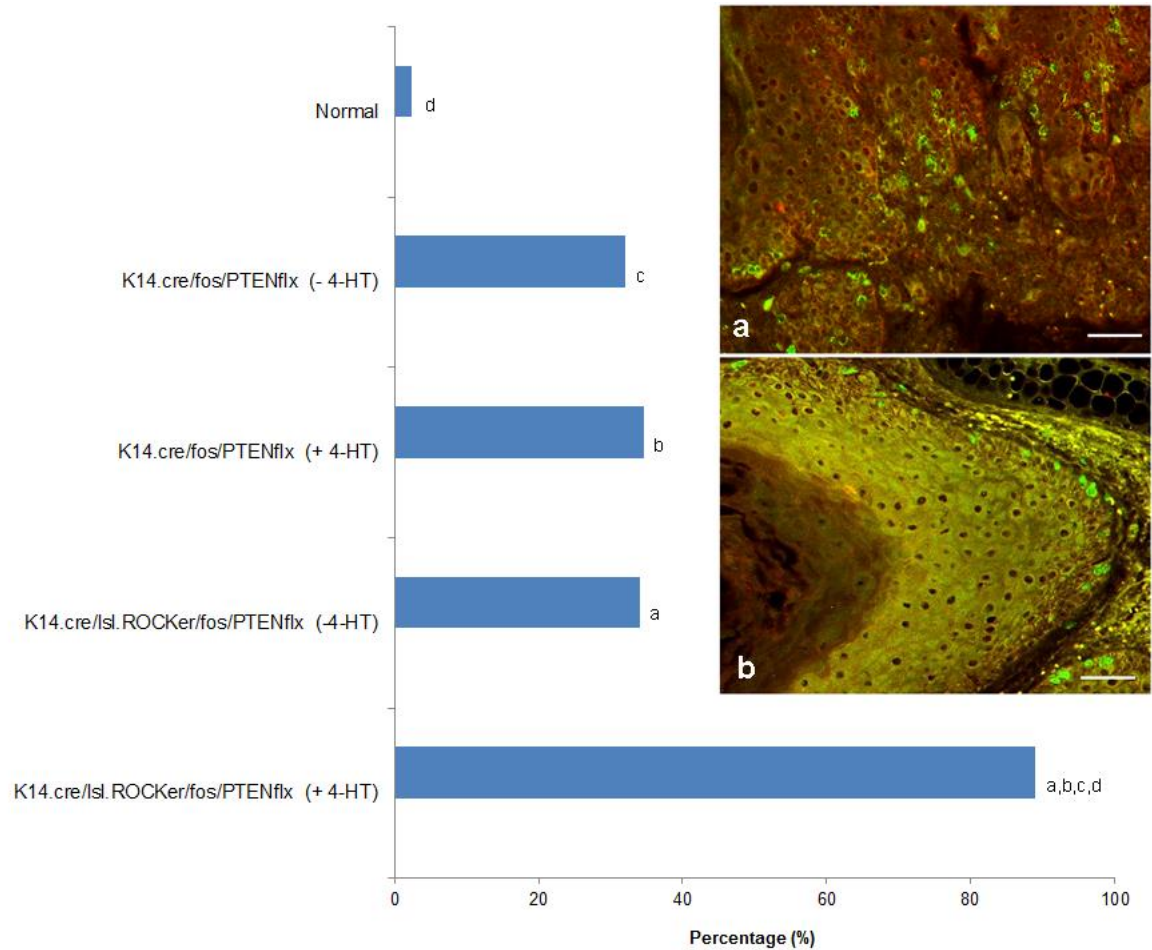


Figure 3.58 BrdU-labelling of RU486-/4-HT-treated $K14.cre/lsl.ROCK^{er}/fos/\Delta 5PTEN^{flx}$ carcinogenesis. Graph displays high cell proliferation activity in tri-genic ROCK/fos/ $\Delta 5PTEN^{flx}$ tumours compared to bi-genic fos/ $\Delta 5PTEN^{flx}$ keratotic papillomas. (a,b,c,d : Significantly difference between $K14.cre/lsl.ROCK^{er}/fos/PTEN^{flx}$ (+ 4-HT) and each cohort; $p < 0.05$).

(a) RU486-/4-HT-treated $K14.cre/lsl.ROCK^{er}/fos/\Delta 5PTEN^{flx}$ SCC histotype showed high BrdU-labelling that scattered throughout epidermal layers, compared to (b) low levels of BrdU-labelled cells in RU486-/4-HT-treated bi-genic fos/ $\Delta 5PTEN^{flx}$ keratotic papilloma and the BrdU-labelling remained confined to basal layers. (Scale: 50 μ m).

3.8.6 Expression of p-AKT1 in tri-genic ROCK/fos/ Δ 5PTEN^{fix} tumours

K14.cre/Isl.ROCK^{er}/fos/ Δ 5PTEN^{fix} tumours were next analysed for AKT activation status since it is well known that PTEN acts as the inhibitory antagonist for AKT in the PTEN signalling pathway. Thus, it was logical to predict that AKT activation would be a significant contributor to tri-genic ROCK/fos/ Δ 5PTEN^{fix} carcinogenesis; as opposed to its absence in the tri-genic ROCK/ras¹²⁷⁶/fos model (above). As shown in figure 3.59, double-labelled IFC analysis of p-AKT1 against a K14 counterstain showed elevated levels of expression in *K14.cre/Isl.ROCK^{er}/fos/ Δ 5PTEN^{fix}* SCCs compared to a complete lack of p-AKT1 expression (strong p53/p21 expression) in the *K14.cre/fos/ Δ 5PTEN^{fix}* keratotic papilloma histotype (figure 3.59(a,b) versus c). However, this p-AKT expression profile remained quite patchy; and showed a low level of expression in the p53/p21 positive areas of papilloma. Furthermore, in areas of high premature keratin K1 expression, the (confused) micro-cysts also displayed p-AKT1 expression in their mini-suprabasal layers. This latter feature was consistent with the finding that normally AKT is activated in the supra-basal epidermis to halt p53-mediated apoptosis and maintain barrier function (Calautti et al., 2005).

Hence, these data indicate that increasing p-AKT1 expression in tri-genic ROCK/fos/ Δ 5PTEN^{fix} carcinomas is possibly mediated by reduced p53/p21 expression and this is consistent with increased proliferation rates from Brdu-labelling data (figure 3.58); whereas the patchy areas of p-AKT1 expression may derive from residual p53 and strong p21 expression to induce differentiation. Further, in this study, following p53 loss, p21 expression appears to be increased in the basal layers of wdSCCs. This may explain why p-AKT1 remained essentially confined in supra-basal, until basal layer p21 expression faded in the SCCs. Thus, at this point, increased p-AKT1 expression may co-operate with ROCK2 roles in the later stages of carcinogenesis and this might drive malignant progression to give increased levels of SCC invasion; an idea that was again suggested by the tri-genic ROCK/ras¹²⁰⁵/ Δ 5PTEN^{het} model (below) which exhibited very rapid progression to pdSCCs in a matter of weeks.

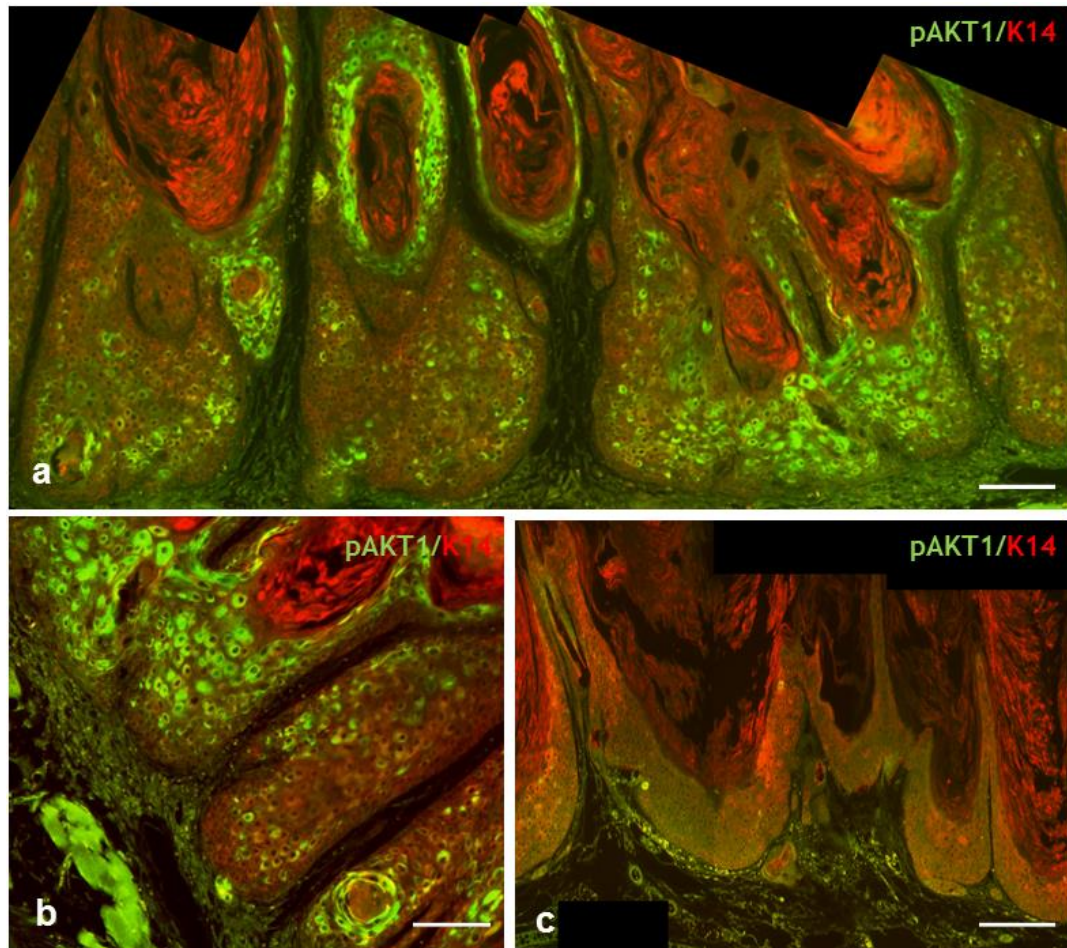


Figure 3.59 Immunofluorescence analysis of p-AKT1 expression. (a,b) RU486-/4-HT-treated *K14.cre/Isl.ROCK^{er}/fos/Δ5PTEN^{fix}* wdSCC/SCC histotypes show elevated p-AKT1 expression in both cytoplasm and nucleus. (c) RU486-/4-HT-treated *K14.cre/fos/Δ5PTEN^{fix}* keratotic papilloma displays a complete lack of p-AKT1 expression. (Scale bar: 100μm: a,c; 50μm: b).

3.8.7 Summary

These data indicate that tri-genic ROCK^{er}/fos/ Δ 5PTEN^{fix} synergism successfully converted papillomas to SCC as early as 9 weeks, and diverted tumourigenesis away from a KA outcome, back to the pathway outcome of a wdSCC and further progression to overt SCC. This result was similar to that found for additional ras^{Ha} activation in fos/ Δ 5PTEN^{fix} mice (Macdonald et al., 2014); although in ras/fos/ Δ 5PTEN^{fix} models, papillomatogenesis was more rapid and tumours were less keratotic. Here, in this current tri-genic model, malignant conversion was again consistent with the loss of K1 and p53 in all epidermal layers. This loss of p53 is likely to be the factor that prevented a KA outcome and progression thus switching back to carcinogenesis, suggesting that ROCK2 activation dictated the route of progression after keratotic papilloma formation, possibly due to its co-operation with *HK1.fos* in papillomatogenesis as a substitute for ras^{Ha} activation. In this study, tri-genic ROCK/fos/ Δ 5PTEN^{fix} mice also displayed a persistent p21 profile, and some indication of an increase in wdSCCs upon p53 loss; although not to the very intense levels observed following cessation of 4-HT in bi-genic ROCK/ras¹²⁰⁵ carcinomas where massive p21 expression was associated with the outgrowth of benign papillomas. Further, in bi-genic ROCK/ras¹²⁰⁵, p21 expression was lost on progression to pdSCCs and this feature began to appear in these tri-genic ROCK/fos/ Δ 5PTEN^{fix} SCCs which exhibited reduced p21 that was lost in the basal layer. It is this loss of p21 in the basal layers which appeared to follow the complete loss of p53 in all epidermal layers that may reflect the appearance of elevated p-AKT1 expression and thus aid further tumour progression via co-operation with the ROCK activation which is known to be highly associated in late stage of carcinogenesis (Croft et al., 2004, Samuel et al., 2011). On the other hand, one difference between the previous study of tri-genic ras/fos/ Δ 5PTEN^{fix} (Macdonald et al., 2014) and this current tri-genic ROCK/fos/ Δ 5PTEN^{fix} model was the continuation of the disturbed epidermal architecture that is a common feature in bi-genic fos/ Δ 5PTEN^{fix} which was noted in the tri-genic ROCK/fos/ Δ 5PTEN^{fix} tumours.

Interestingly, as observed in both bi-genic fos/ Δ 5PTEN^{fix} and 4-HT-untreated *K14.cre/lsf.ROCK^{er}/fos/ Δ 5PTEN^{fix}* tumour controls, the conflicting proliferation versus proliferation signals in the tri-genic ROCK/fos/ Δ 5PTEN^{fix} cohorts gave a

confused differentiation and little apoptosis. Hence, the default position for skin keratinocytes is not apoptosis but terminal differentiation to avoid progression from early stages if possible and in this study, highly keratotic papillomas were produced which resembled early KAs. Indeed, the main reason for a lack of KA formation in *K14.cre/fos/PTEN^{flx}* histotypes was because in the previous study (Yao et al., 2008), the mice were kept on procedure for 5 to 6 months for KAs to form; compared to this study where all mice were kept for just over 2 months.

3.9 Analysis of the co-operation between ROCK2 and ras^{Ha} activation, and loss of PTEN regulation in transgenic mouse skin carcinogenesis

In the previous sections, results in the *K14.cre/PTEN^{flx}* background demonstrated that 4-HT-activated ROCK^{er}, together with loss of PTEN-mediated AKT regulation, showed little co-operation; with no evidence of tumour formation even after 7 months. In these experiments, the ROCK2 transgenic lines (*K14.cre/lsl.ROCK^{er}* and *K14.ROCK^{er}*) instead displayed an altered epidermal differentiation in terms of keratin K6 and K1 expression, and possibly suggested a premature basal layer commitment to terminal differentiation, mediated by initial $\Delta 5$ PTEN mutation and again altered by ROCK2 co-expression over time in the context of a hyperplastic epidermis. Moreover, this lack of tumours contrasted with *K14.cre/PTEN^{flx}* co-operation with *HK1.ras¹²⁷⁶* which demonstrated papillomatogenesis and showed no sign of malignant conversion unless treated with TPA (to activate c-fos) (Yao et al., 2006), a result now consistent with malignant conversion observed in the tri-genic *HK1.ras/fos/ $\Delta 5$ PTEN^{flx}* model (Macdonald et al., 2014). In comparison, co-operation between ROCK^{er} and *HK1.ras* line 1205 did achieve malignant conversion, and this appeared dependent upon the promotion stimulus received from wounding, similar to co-operation in *HK1.ras* line 1276, which required constitutive promotion from additional *HK1.fos* to achieve conversion (above). In all these previous models, the majority of mice exhibited well-differentiated SCCs with the occasional mix of more aggressive SCCs, and this was likely due to persistent p21 following loss of p53, possibly antagonising p-AKT1 in a compensatory response to inhibit the early stages of malignant progression.

With time in *K14.ROCK^{er}/HK1.ras¹²⁰⁵* tumours, it appeared that exogenous ROCK2 could drive progression to overt SCC/pdSCC histotypes and once this was achieved, exogenous ROCK2 appeared no longer necessary. Therefore, this ultimate tri-genic genotype was geared to assess whether ROCK2 co-operation with *HK1.ras¹²⁷⁶* (and later with *HK1.ras¹²⁰⁵*) but now in the context of mutated PTEN, could achieve an accelerated malignant progression to elicit SCC/pdSCC mediated by an overlay of ROCK/ras¹²⁷⁶ and a $\Delta 5$ PTEN^{flx}- mediated loss of AKT

regulation and to investigate the mechanism to assess whether this combination overcame the compensatory p53/p21 responses.

3.9.1 ROCK2 co-operates with *HK1.ras*¹²⁷⁶/ Δ 5PTEN^{flx} to elicit malignant progression

In initial experiments, very few tri-genic *K14.cre/Isl.ROCK^{er}/ras*¹²⁰⁵/ Δ 5PTEN^{flx} mice survived as the *HK1.ras*¹²⁰⁵/ Δ 5PTEN^{flx} co-operation gave an increased epidermal hyperplasia that resolved into a severe hyperkeratosis at day 8 to 10, deemed too excessive for further experimentation. This has been observed in earlier *HK1.ras* genotypes and thus *HK1.ras*¹²⁰⁵ has not been used, e.g. in *HK1.fos* co-operation (Greenhalgh et al., 1993a,c). Thus in this study, experiments employed the lesser *HK1.ras*¹²⁷⁶ line that has already successfully been bred with inducible *Isl.ROCK^{er}* mice in the ROCK/*ras*¹²⁷⁶/*fos* model (above), which also facilitated breeding and provided additional comparison controls. Nonetheless, as these ROCK/*ras*¹²⁷⁶/ Δ 5PTEN^{flx} phenotypes (and ideas regarding the underlying mechanism) developed, experiments returned to assessment of PTEN loss in the original ROCK/*ras*¹²⁰⁵ system, but employing mice heterozygous for the Δ 5PTEN allele (*K14.cre/Isl.ROCK^{er}/ras*¹²⁰⁵/ Δ 5PTEN^{het}). Therefore, in tri-genic ROCK/*ras*/ Δ 5PTEN^{flx} synergism, inducible *Isl.ROCK^{er}* activation was examined in transgenic mice expressing activated *HK1.ras*¹²⁷⁶ and *K14.cre/ Δ 5PTEN^{flx}*. In repeat experiments, age-matched sibling cohorts of 5 to 6 week old *K14.cre/Isl.ROCK^{er}/ras*¹²⁷⁶/ Δ 5PTEN^{flx} (n= 10) were treated with RU486 at week 1 to ablate the stop cassette in *Isl.ROCK^{er}* transgene and express ROCK^{er}, and to induce PTEN mutation (Δ 5PTEN^{flx}). Subsequent topical treatment with 4-HT to activate ROCK^{er} transgene followed three times per week from the second week, with controls receiving either RU486 or ethanol alone.

At 22 weeks of 4-HT treatment, *K14.cre/Isl.ROCK^{er}/ras*¹²⁷⁶/ Δ 5PTEN^{flx} mice had displayed only the typical thickened ears observed in bi-genic mice and only now for the first time, exhibited signs of tumour formation (figure 3.60a,b) as compared to the lack of tumours in either ROCK/*ras*¹²⁷⁶ or ROCK/ Δ 5PTEN^{flx} cohorts (above). However, it was noted that these tumours were now independent of wound promotion, as they appeared on both tagged and untagged ears of the tri-genic ROCK/*ras*/ Δ 5PTEN^{flx} mice virtually simultaneously. Conversely, at this same time

point, RU486-/4-HT-treated $K14.cre/ras^{1276}/\Delta 5PTEN^{fix}$ and RU486-treated/4-HT-untreated $K14.cre/Isl.ROCK^{er}/ras^{1276}/\Delta 5PTEN^{fix}$ control mice (n = 6 per cohort) showed only the mild keratotic appearance of their parental bi-genic genotypes (Yao et al., 2006) regardless of ear tagging (figure 3.60c-f). In contrast to tumours observed in bi-genic $ROCK/ras^{1205}$ models, all 100% of $K14.cre/Isl.ROCK^{er}/ras^{1276}/\Delta 5PTEN^{fix}$ mice only developed this keratotic frill-like structure appearing at each edge of the ears (figure 3.60a,b) suggested a lack of co-operation and prompted early termination of the experiments. This was a premature decision as following histological analysis a clear synergism had indeed developed; hence, why final experiments were prompted to return to co-operation with activated (original) $K14.ROCK^{er}$ genotypes but now in the $HK1.ras^{1205}/\Delta 5PTEN^{het}$ background.

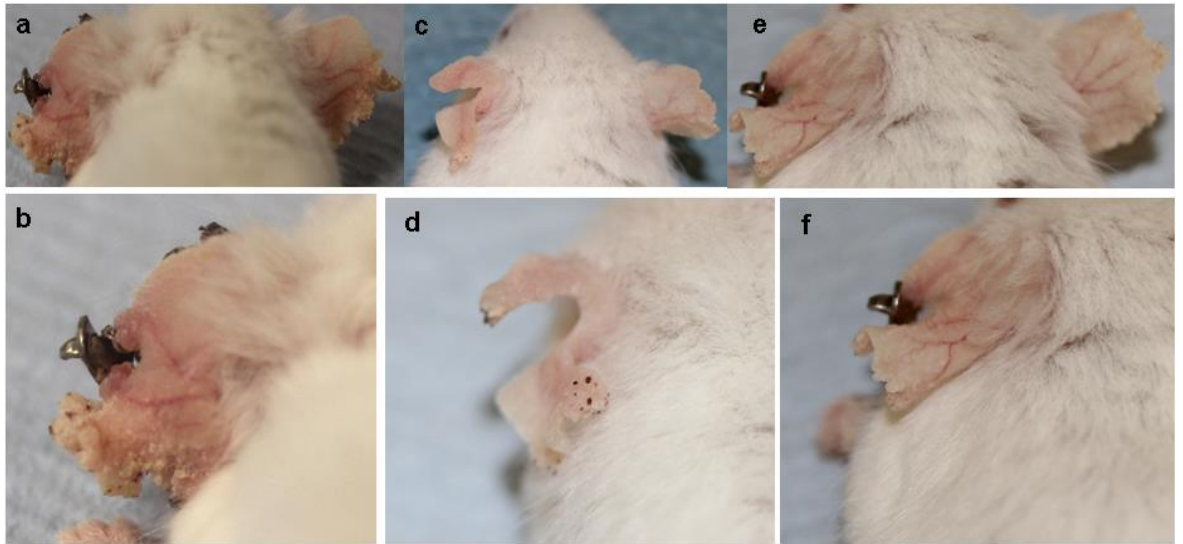


Figure 3.60 Phenotypes of *K14.cre/Isl.ROCK^{er}/ras¹²⁷⁶/Δ5PTEN^{flx}* transgenic mice at 22 weeks. (a, b) RU486-/4-HT-treated *K14.cre/Isl.ROCK^{er}/ras¹²⁷⁶/Δ5PTEN^{flx}* mice show early formation of tumour with keratotic phenotypes. (c, d) RU486-/4-HT-treated *K14.cre/ras¹²⁷⁶/Δ5PTEN^{flx}* and (e, f) RU486-treated/4-HT-untreated *K14.cre/Isl.ROCK^{er}/ras¹²⁷⁶/Δ5PTEN^{flx}* mice display thickened ear and mild keratotic phenotypes.

Given the relative lack of large tumours at 22 weeks, there was a total surprise at the unexpected malignant histotype produced by these smaller and highly keratotic appearing lesions. Here remarkably, the histopathology of *K14.cre/Isl.ROCK^{er}/ras¹²⁷⁶/Δ5PTEN^{flx}* ear biopsies at 22 weeks 4-HT treatment showed that these lesions had transformed to malignancy (figure 3.61a). Moreover, despite their small size, at higher magnification, *K14.cre/Isl.ROCK^{er}/ras¹²⁷⁶/Δ5PTEN^{flx}* tumours actually possessed an aggressive SCC histotype (figure 3.61b), and in many areas of a wdSCC the histotype exhibited an increasing disorganisation to the surrounding epidermal architecture (figure 3.61c). Furthermore, these tri-genic SCC keratinocytes appeared to infiltrate into the dermis in tight finger-like projections (figure 3.61b), which may indicate the onset to a rapid progression to highly invasive pdSCC as observed following the spontaneous malignant progression mechanism in the bi-genic *ROCK/ras¹²⁰⁵* models at 16/18 weeks. Thus, ROCK2 in this context may aid in both the conversion of benign tumours and also to drive the early mechanism of malignant progression. The question remained as to why it took until 22 weeks for this to occur? The answer again may be due to the persistence of p53/p21 expression and AKT status (investigated below). In contrast, control RU486-/4-HT-treated *K14.cre/ras¹²⁷⁶/Δ5PTEN^{flx}* (figure 3.61d,e) and RU486-treated/4-HT-untreated *K14.cre/Isl.ROCK^{er}/ras¹²⁷⁶/Δ5PTEN^{flx}* (figure 3.61f,g) biopsies showed a hyperplasia histotype as seen previously with well-organised epidermal layers at this stage.

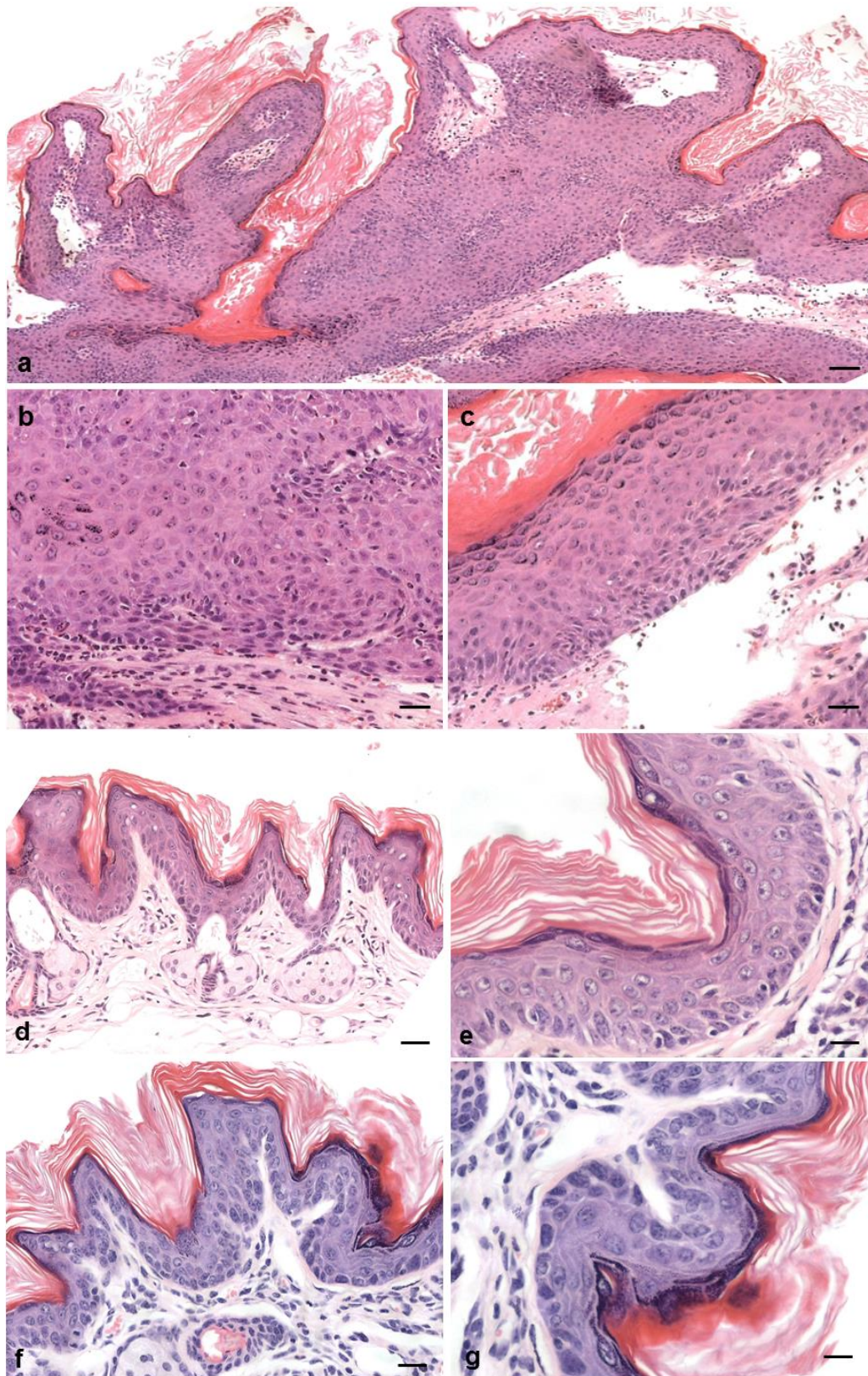


Figure 3.61 Histotypes of RU486-/4-HT-treated *K14.cre/Isl.ROCK^{er}/ras¹²⁷⁶/Δ5PTEN^{flx}* biopsies at 22 weeks. (a) Composite micrograph of tri-genic *ROCK/ras/Δ5PTEN^{flx}* biopsy shows SCC histotype with rapid disorganisation in all layers of the surrounding epidermis. (b) At higher magnification, *K14.cre/Isl.ROCK^{er}/ras¹²⁷⁶/Δ5PTEN^{flx}* carcinoma exhibits finger-like projection that may imply a progression to highly invasive pdSCC. (c) Whilst higher magnification at *K14.cre/Isl.ROCK^{er}/ras¹²⁷⁶/Δ5PTEN^{flx}* wdSCC areas exhibit disorganised basal layers. (d) RU486-/4-HT-treated *K14.cre/ras¹²⁷⁶/Δ5PTEN^{flx}* and (e, f) RU486-treated/4-HT-untreated *K14.cre/Isl.ROCK^{er}/ras¹²⁷⁶/Δ5PTEN^{flx}* histopathologies display similar hyperplasia histotypes and well-ordered epidermal architecture at higher magnification. (Scale bar: 150µm in a; 100µm in b, c, d, f; 50µm in e, g).

3.9.2 Expression of tumour progression marker keratin K1 in **ROCK/ras¹²⁷⁶/Δ5PTEN^{flx}** carcinogenesis

Routine analysis of keratin K1 expression was now of more significant interest given the small tumour size achieved at 22 weeks. As shown in composite micrographs of *K14.cre/Isl.ROCK^{er}/ras¹²⁷⁶/Δ5PTEN^{flx}* tumours (figure 3.62a), despite their size and keratotic appearance, K1 (green) expression had virtually disappeared in the areas of SCC confirming both conversion and malignant progression to this more aggressive histotype; compared to the areas of wdSCC (figure 3.62a(box),b) where K1 expression still appeared, but as ever, was becoming gradually reduced. In control cohorts, both RU486-/4-HT-treated *K14.cre/ras¹²⁷⁶/PTEN^{flx}* and RU486-treated/4-HT-untreated *K14.cre/Isl.ROCK^{er}/ras¹²⁷⁶/Δ5PTEN^{flx}* biopsies displayed hyperplasia with strong K1 expression, that remained confined to supra-basal layers (figure 3.62 c,d), thus with little changes to the ordered nature of differentiation in this context.

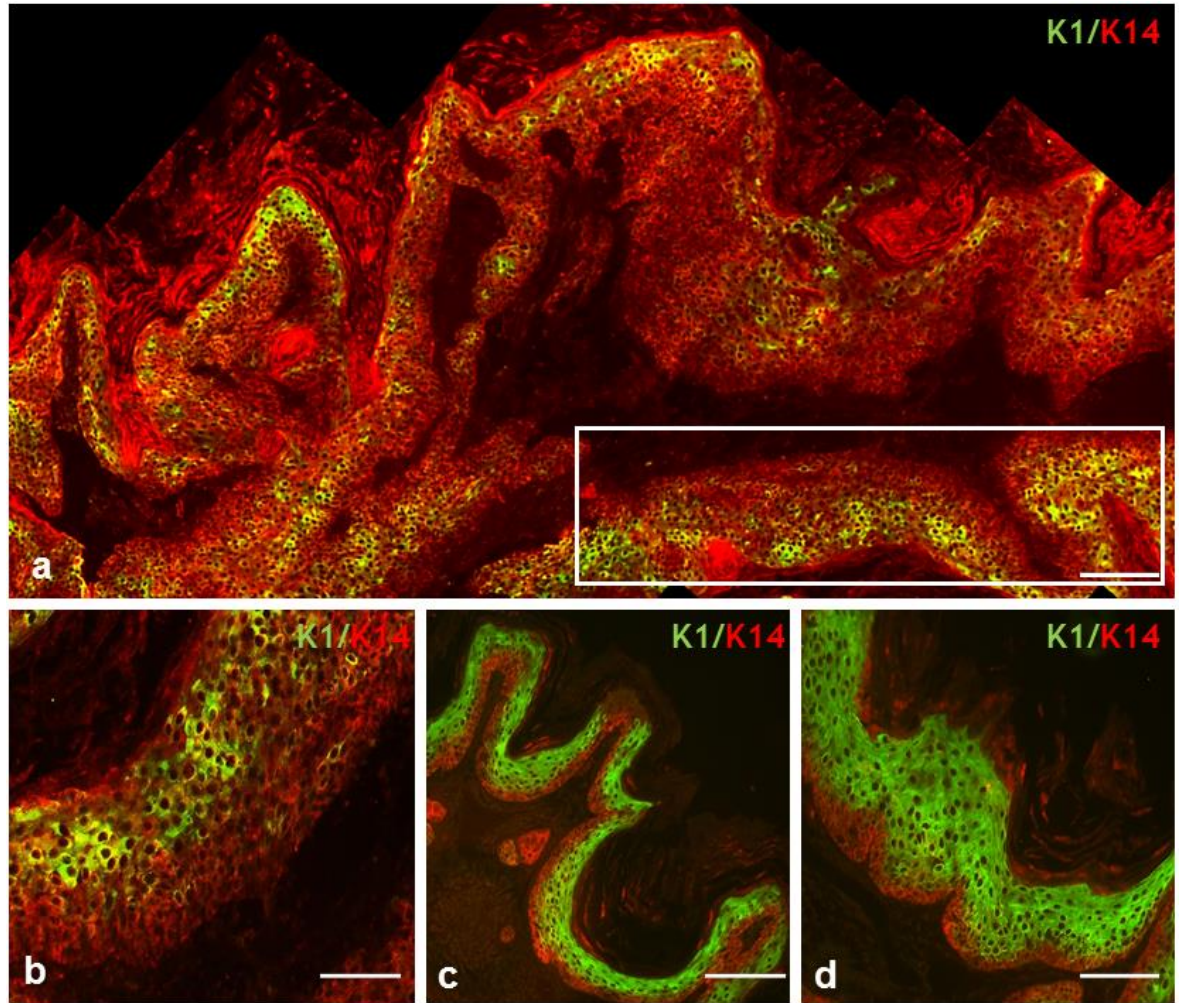


Figure 3.62 Immunofluorescence analysis of K1/K14 expression at 22 weeks. (a) Composite micrograph of RU486-/4-HT-treated *K14.cre/lsI.ROCK^{er}/ras¹²⁷⁶/Δ5PTEN^{flx}* cohort showed K1 expression disappeared on progression to carcinoma indicating many areas of aggressive SCC and possible progression to invasive pdSCC. (b) High magnification at tri-genic *ROCK^{er}/ras¹²⁷⁶/Δ5PTEN^{flx}* wdSCC areas (figure 3.62a-box) showed reduced K1 expression. (c) In comparison, keratin K1 expression appear strong and uniform in supra-basal layer of RU486-/4-HT-treated *K14.cre/ras¹²⁷⁶/Δ5PTEN^{flx}* and (d) RU486-treated/4-HT-untreated *K14.cre/lsI.ROCK^{er}/ras¹²⁷⁶/Δ5PTEN^{flx}* papillomatous hyperplasia histotypes. (Scale bar: a: 150μm, b: 50μm; c,d: 100μm).

3.9.3 Expression of p53 and p21 in tri-genic ROCK/*ras*¹²⁷⁶/ Δ 5PTEN^{flx} mice

The expression profiles of tumour suppressor genes p53 and p21 were routinely analysed in these malignant *K14.cre/lsl.ROCK^{er}/ras¹²⁷⁶/ Δ 5PTEN^{flx}* tumours. Consistent with earlier finding involving either bi-genic or tri-genic models, composite micrographs of *K14.cre/lsl.ROCK^{er}/ras¹²⁷⁶/ Δ 5PTEN^{flx}* wdSCCs/SCCs displayed a loss of p53 expression (figure 3.63a) and at higher magnification of the SCC area demonstrated that p53 had completely disappeared throughout epidermal layers (figure 3.63b). Whilst p53 expression in the *K14.cre/lsl.ROCK^{er}/ras¹²⁷⁶/ Δ 5PTEN^{flx}* wdSCC area also showed disappearance and has totally disappeared at this stage (figure 3.63a(box),c) consistent with other wdSCC histotypes from earlier cohorts (e.g. ROCK/*ras*¹²⁰⁵). However, *K14.cre/ras¹²⁷⁶/ Δ 5PTEN^{flx}* hyperplasia showed strong p53 expression in all epidermal layers (figure 3.63d), as observed in all bi-genic benign papillomas, e.g. *HK1.ras¹²⁷⁶/fos* (above).

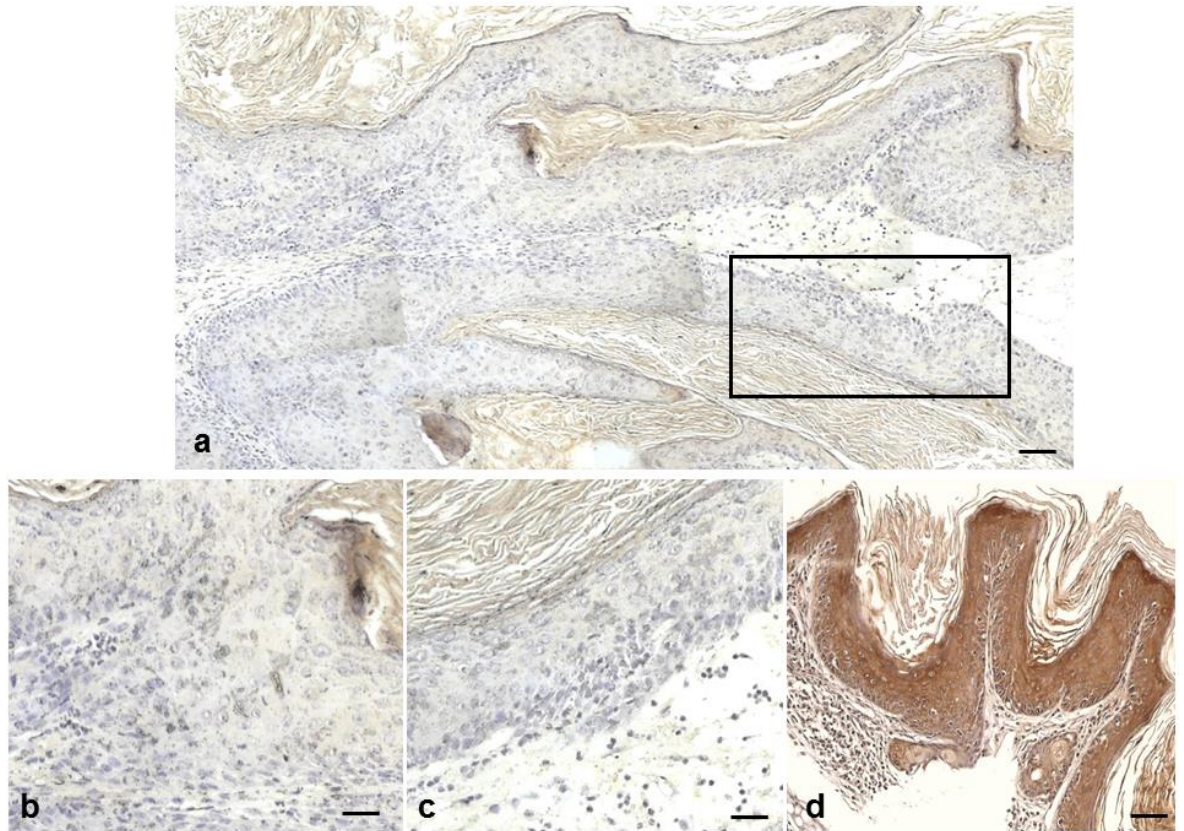


Figure 3.63 IHC analysis of p53 expression. (a) Composite micrograph of RU486-/4-HT-treated *K14.cre/Isl.ROCK^{er}/ras¹²⁷⁶/Δ5PTEN^{flx}* wdSCC/SCC shows no p53 expression in a uniform manner. (b) At higher magnification, p53 expression disappeared throughout epidermal layers in the SCC areas; and also (c) in the wdSCC area (box). (d) RU486-/4-HT-treated *K14.cre/ras¹²⁷⁶/Δ5PTEN^{flx}* hyperplasia exhibits strong p53 expression in all epidermal layers that limited further tumour progression. (Scale bar: a: 150μm; b,c: 50 μm; d: 100μm).

In parallel to the loss of p53 expression upon malignant conversion in *K14.cre/Isl.ROCK^{er}/ras¹²⁷⁶/Δ5PTEN^{flx}* wdSCCs/SCCs, analysis of p21, which had persisted in all previous models of conversion (above), turned out to be completely lost also at this time point (figure 3.64a). Again, and unique to the tumour context produced by this tri-genic *ROCK^{er}/ras¹²⁷⁶/Δ5PTEN^{flx}* model, at higher magnification, all *K14.cre/Isl.ROCK^{er}/ras¹²⁷⁶/Δ5PTEN^{flx}* SCCs, exhibited an expanded invasive basal layer where p21 expression was completely absent (figure 3.64b). This contrasted to the more typical persistent profiles of basal layer p21 expression; which can become reduced or appear cytoplasmic (above). This finding was similar to a previous study of bi-genic *ras¹²⁷⁶/Δ5PTEN^{flx}* mice treated with TPA where analysis of papillomas and even hyperplasia revealed that p21 was eliminated as rapidly as p53 (Yao et al., 2006, Macdonald et al., 2014). Interestingly, this loss of basal p21 expression also appeared in the wdSCC area (figure 3.64a(box),c) and was weaker in the papilloma histotypes; where p21 became reduced or appeared cytoplasmic. Again, this finding was different from earlier cohorts of wdSCC histotypes where p21 expression still remained and was confined to the epidermal layers (e.g. *ROCK/ras¹²⁷⁶/fos*). Conversely, in *K14.cre/ras¹²⁷⁶/Δ5PTEN^{flx}* hyperplastic or benign control histotypes, p21 expression as expected showed strong and uniform expression in all epidermal compartments (figure 3.64d).

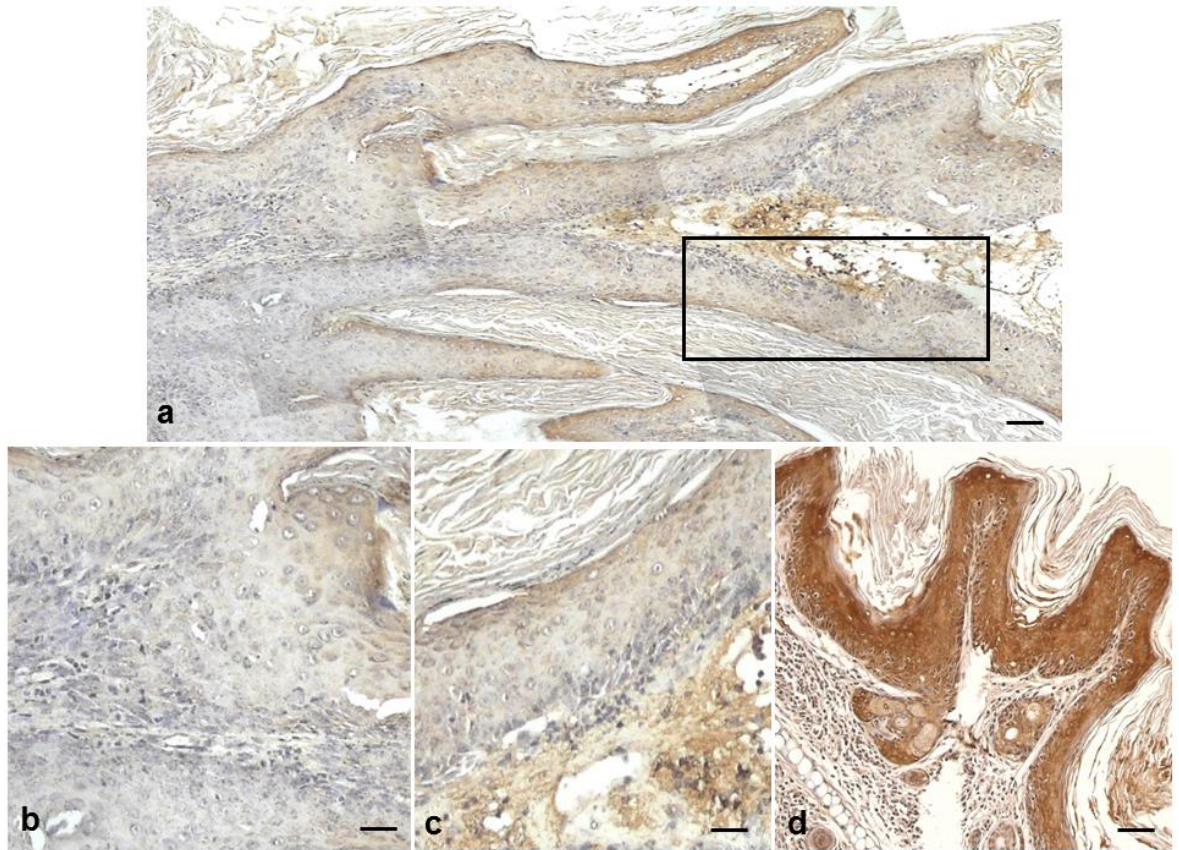


Figure 3.64 IHC analysis of p21 expression. (a) Composite micrograph of RU486-/4-HT-treated *K14.cre/lsl.ROCK^{er}/ras¹²⁷⁶/Δ5PTEN^{flx}* wdSCC/SCC shows p21 expression becomes faded and disappears in all epidermal compartments. (b) At higher magnification, p21 expression disappears throughout epidermal layers in the SCC area; and also (c) in the wdSCC area (figure 3.64a-box). (d) RU486-/4-HT-treated *K14.cre/ras¹²⁷⁶/Δ5PTEN^{flx}* hyperplasia exhibits strong and uniform p21 expression. (Scale bar: a: 150μm; b,c: 50 μm; d: 100μm).

3.9.4 BrdU-labelling of tri-genic ROCK/ras¹²⁷⁶/Δ5PTEN^{flx} tumours

BrdU-labelling analysis of cell proliferation rates was performed on tri-genic ROCK/ras¹²⁷⁶/Δ5PTEN^{flx} SCCs. As shown in figure 3.65, RU486-/4-HT-treated *K14.cre/lsl.ROCK^{er}/ras¹²⁷⁶/Δ5PTEN^{flx}* SCCs scored the highest cell proliferation rates (90.9%, figure 3.65a) recorded in this model (and also compared to other malignant histotypes in earlier models). In addition, the mitotic index in RU486-/4-HT-treated *K14.cre/lsl.ROCK^{er}/ras¹²⁷⁶/Δ5PTEN^{flx}* wdSCCs followed as the second highest in this model (62.2%, figure 3.65b). Conversely, low mitotic activity was observed in bi-genic ras¹²⁷⁶/Δ5PTEN^{flx} hyperplasia (RU486-/4-HT-treated and RU486-treated/4-HT-untreated *K14.cre/ras¹²⁷⁶/Δ5PTEN^{flx}* cohorts: 21.2%, figure 3.65c and 20%; RU486-treated/4-HT-untreated *K14.cre/lsl.ROCK^{er}/ras¹²⁷⁶/Δ5PTEN^{flx}* 16.4%). This data demonstrate that *K14.cre/lsl.ROCK^{er}/ras¹²⁷⁶/Δ5PTEN^{flx}* SCC has the highest proliferation index as compared to other malignancies from earlier results. In addition, this finding is consistent with synchronised loss of p53 expression followed by p21 in a similar manner to the tri-genic ROCK/ras¹²⁷⁶/Δ5PTEN^{flx} SCC. Moreover, as shown in figure 3.65(a,b) the BrdU-labelling was scattered throughout epidermal layers of RU486-/4-HT-treated *K14.cre/lsl.ROCK^{er}/ras¹²⁷⁶/Δ5PTEN^{flx}* wdSCC/SCC as compared to Brdu-labelling in RU486-/4-HT-treated *K14.cre/ras¹²⁷⁶/Δ5PTEN^{flx}* hyperplasia that remained in the basal layers (figure 3.65c).

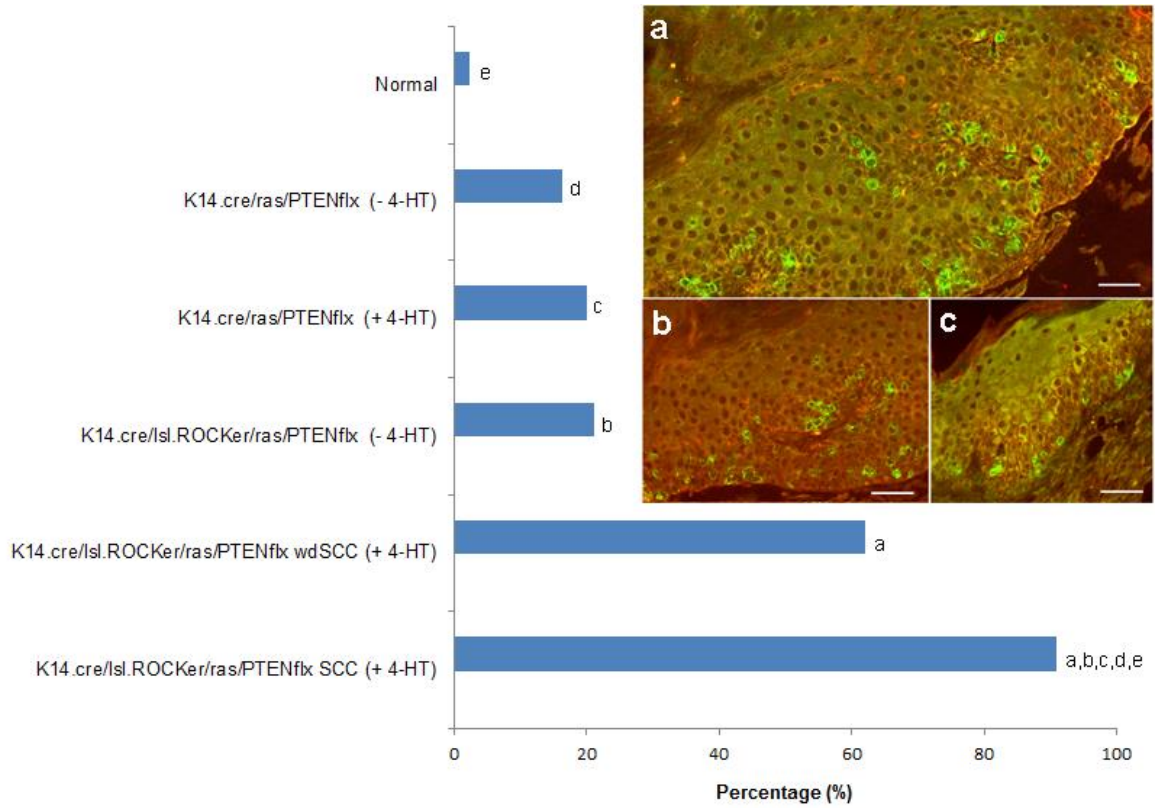


Figure 3.65 BrdU-labelling of *K14.cre/lsl.ROCK^{er}/ras¹²⁷⁶/Δ5PTEN^{flx}* carcinogenesis. Graph displays a rapid increase in cell proliferation activity in tri-genic *ROCK/ras¹²⁷⁶/Δ5PTEN^{flx}* SCC that is almost five times higher than bi-genic *ras¹²⁷⁶/Δ5PTEN^{flx}*. (a,b,c,d,e : Significantly difference between *K14.cre/lsl.ROCK^{er}/ras¹²⁷⁶/Δ5PTEN^{flx}* (+ 4-HT) and each cohort; $p < 0.05$).

(a) RU486-/4-HT-treated *K14.cre/lsl.ROCK^{er}/ras¹²⁷⁶/Δ5PTEN^{flx}* SCC histotype and (b) RU486-/4-HT-treated *K14.cre/lsl.ROCK^{er}/ras¹²⁷⁶/Δ5PTEN^{flx}* wdSCC histotype show high BrdU-labelling that is scattered throughout epidermal layers, compared to (c) low BrdU-labelling in RU486-/4-HT-treated bi-genic *ras¹²⁷⁶/Δ5PTEN^{flx}* hyperplasia histotype. (Scale: 50-100 μ m).

3.9.5 Expression of p-AKT1 in tri-genic ROCK/ras¹²⁷⁶/Δ5PTEN^{flx} tumours

The PTEN tumour suppressor gene is one of the most commonly mutated genes for tumour development, with a frequency that rivals that of p53 mutation (Wang et al., 2003, Yao et al., 2006, 2008). The main mutation in PTEN, often leads to a failure to regulate PI3K/AKT signalling pathways via inhibition of AKT activities through its dephosphorylation. Thus, in this Δ5PTEN^{flx} model, inactivation of this PTEN function via ablation of exon 5 contributes to the upregulation of AKT (Carnero and Paramio, 2014). Therefore, as above, IFC analysis of p-AKT1 expression was performed to investigate the association between the loss of PTEN phosphatase activity (Δ5PTEN^{flx}) in tri-genic ROCK/ras¹²⁷⁶/Δ5PTEN^{flx} synergism via analysis of the activated AKT1 (p-AKT1) expression profile.

In the previous chapters, AKT1 rather than AKT2 was shown to be the major AKT isoform expressed in the epidermis and was unexpectedly shown to be either inhibited in the presence of p53 and p21; or restricted to supra-basal layers even in malignant wdSCCs/SCCs via the persistence of p21 in the basal layer. As shown in figure 3.66a, analysis of p-AKT1 in this more aggressive tumour context showed very high levels of expression in *K14.cre/Isl.ROCK^{er}/ras¹²⁷⁶/Δ5PTEN^{flx}* SCC as compared to its expression in *K14.cre/ras¹²⁷⁶/Δ5PTEN^{flx}* hyperplasia (figure 3.66b). Further, this p-AKT1 expression appeared in all layers of these aggressive carcinomas including the basal layers and thus exhibited an expression profile reverse of the expression profiles of p53 and p21 observed in either *K14.cre/Isl.ROCK^{er}/ras¹²⁷⁶/Δ5PTEN^{flx}* or control *K14.cre/ras¹²⁷⁶/Δ5PTEN^{flx}* cohorts (figure 3.63, 3.64).

In addition, p-AKT1 expression was now also elevated in the *K14.cre/Isl.ROCK^{er}/ras¹²⁷⁶/Δ5PTEN^{flx}* wdSCC histotype (figure 3.66c) in the absence of persistent p21 suggesting that these tumours were now likely to progress. This was consistent with the data from papillomas and carcinomas analysed in the previous models, in which the low level of p-AKT1 or its supra-basal expression was associated with compensatory p53 and /or p21 expression in the proliferative basal layer keratinocytes. Thus, these data suggest that the loss or low levels of p53/p21 expression in the context of relatively small but

clearly aggressive *K14.cre/lsl.ROCK^{er}/ras¹²⁷⁶/Δ5PTEN^{flx}* wdSCCs/SCCs mediated an acceleration in malignant progression following conversion, driven in part by p-AKT1 expression.

This feature of p21/AKT antagonism in early stage malignancy has also been previously observed in *HK1.ras¹²⁷⁶/fos/Δ5PTEN^{flx}* mice (Greenhalgh, – manuscript in preparation). Therefore, it may be that AKT-mediated inhibition of the compensatory p21 subsequently facilitates the oncogenic functions of ROCK2 in driving the latter stages of carcinogenesis in this context, consistent with many reports on ROCK2 activities. These data are also consistent with a sudden burst of excessive proliferation in the tri-genic *ROCK/ras¹²⁷⁶/Δ5PTEN^{flx}* SCC histotypes as demonstrated by the finding of the highest proliferation rates to date from BrdU-labelling analysis (figure 3.65). Again, a result consistent with the invasive profiles induced by ROCK2 activation in co-operation with *ras¹²⁷⁶* activation and *Δ5PTEN^{flx}* loss.

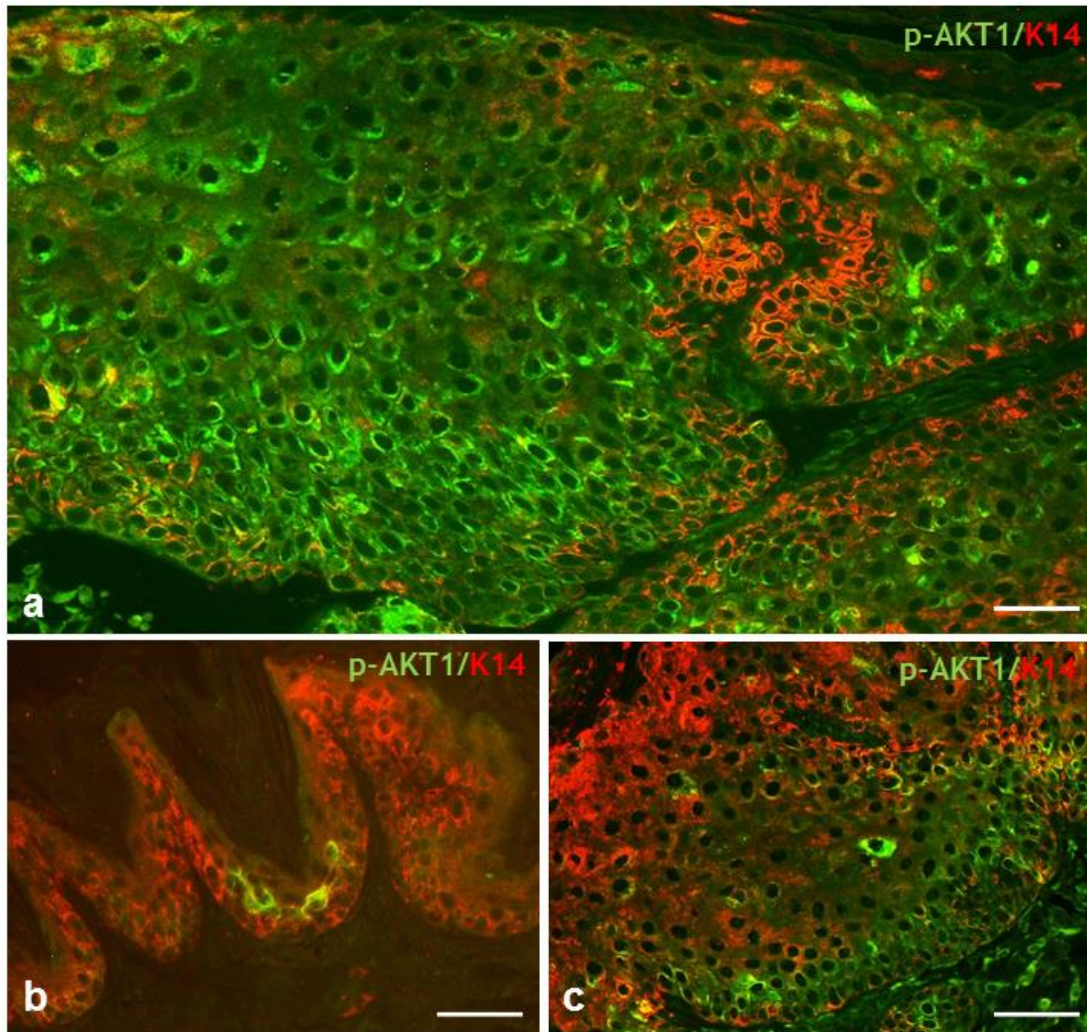


Figure 3.66 Immunofluorescence analysis of p-AKT1 expression in RU486-/4-HT-treated *K14.cre/Isl.ROCK^{er}/ras¹²⁷⁶/Δ5PTEN^{flx}* tumours. (a) *K14.cre/Isl.ROCK^{er}/ras¹²⁷⁶/Δ5PTEN^{flx}* SCC showed high level of cytoplasmic p-AKT1 expression in all epidermal layers compared to (b) little p-AKT1 expression in RU486-/4-HT-treated *K14.cre/ras¹²⁷⁶/Δ5PTEN^{flx}* hyperplasia. (c) Interestingly, elevated expression of p-AKT1 was displayed in RU486-/4-HT-treated *K14.cre/Isl.ROCK^{er}/ras¹²⁷⁶/Δ5PTEN^{flx}* wdSCC due to loss of p53/p21 expression. (Scale bar: a,c: 50μm; b: 100 μm).

3.9.6 ROCK2 rapidly elicits malignant conversion and progression to aggressive, poorly differentiated SCCs in co-operation with *HK1.ras*¹²⁰⁵/ Δ *5PTEN*^{het} mice

The surprising malignant nature of the histotypes produced from such overtly small tumours suggested that once a specific context of aggressive yet benign papilloma had been achieved [i.e. in this case not until 22 weeks of 4HT treatment in the *K14.cre/lsI.ROCK^{er}/ras¹²⁷⁶/ Δ 5PTEN^{flx}* model] ROCK2-induced conversion to malignancy. If so, it was theorised that the aggressive, and autonomous papillomas created by *HK1.ras*¹²⁰⁵ co-operation with heterozygous PTEN loss (Δ 5PTEN^{het}) (Yao et al., 2006) would provide this context. Thus, the original *K14.ROCK^{er}* transgene was employed and introduced into this heterozygous Δ 5PTEN^{het} background in order to compare the original bi-genic ROCK/*ras*¹²⁰⁵ observations of similar pdSCC formation in these two contexts.

Following the standard RU486 and 3x per week of 4-HT treatments, it became very clear that tumourigenesis in *K14.ROCK^{er}/HK1.ras*¹²⁰⁵/ Δ 5PTEN^{het} occurred rapidly (less than 3 weeks) and produced a completely different class of overt tumours. As shown in figure 3.67, typical RU486-treated *HK1.ras*¹²⁰⁵/ Δ 5PTEN^{het} (figure 3.67a - left) which required more than 3 months to reach the size of RU486-/4-HT-treated *K14.ROCK^{er}/HK1.ras*¹²⁰⁵/ Δ 5PTEN^{het} transgenic mouse tumours (figure 3.67a – middle and right), which had appeared very rapidly over the first 2 to 3 weeks and had to be sacrificed by 6-7 weeks due to their increasing size. Note also that the control mice (*HK1.ras*¹²⁰⁵/ Δ 5PTEN^{het}) exhibited a typical papilloma cluster, which could be large in size but were completely different from the SCCs in *K14.ROCK^{er}/HK1.ras*¹²⁰⁵/ Δ 5PTEN^{het} (figure 3.67a). Indeed the dissected papilloma cluster from control animals shows a typical cauliflower-like appearance (figure 3.67b), whereas the *K14.ROCK^{er}/HK1.ras*¹²⁰⁵/ Δ 5PTEN^{het} tumours are more uniform, less keratotic, well vascularised and possess a smooth, darker centre (figure 3.67c). This appearance was similar to the aggressive SCCs which rapidly appeared following TPA promotion of *HK1.ras*¹²⁷⁶/ Δ 5PTEN^{flx} mice (Yao et al., 2006). In comparison, RU486-treated/4-HT-untreated *K14.ROCK^{er}/HK1.ras*¹²⁰⁵/ Δ 5PTEN^{het} (figure 3.67d) and RU486-treated/4-HT-treated *HK1.ras*¹²⁰⁵/ Δ 5PTEN^{het} mice (figure 3.67e) at 14 weeks showed no differences in tumour phenotypes to those of control RU486-treated

HK1.ras¹²⁰⁵/Δ5PTEN^{het} mice (figure 3.67a - left). In addition, control cohorts of *K14.ROCK^{er}-K14.creP/Δ5PTEN^{het}* (*Δ5PTEN^{fix}*) and also showed that the original *K14.ROCK^{er}* transgenic line produced identical phenotypes either in homozygous or heterozygous *Δ5PTEN* backgrounds (figure 3.67f,g) to that of the new *Isl.ROCK^{er}* line studied above (in bi-genic *ROCK/Δ5PTEN^{fix}*).

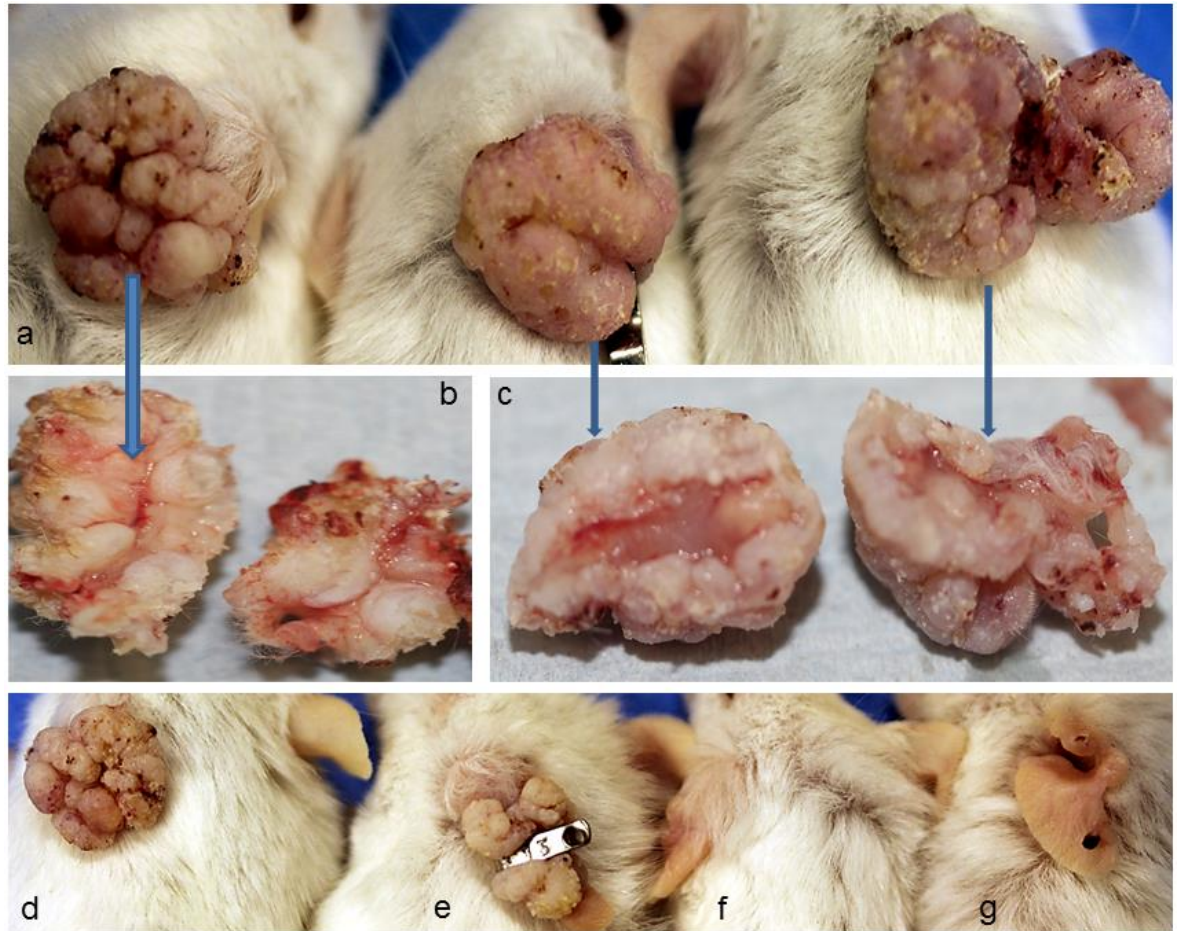


Figure 3.67 Rapid tumorigenesis developed in $K14.ROCK^{er}/HK1.ras^{1205}/\Delta 5PTEN^{het}$ transgenic mice. (a) Left: papilloma cluster on RU486-treated $HK1.ras^{1205}/\Delta 5PTEN^{het}$ at 14 weeks; versus Middle and Right: large and smooth SCCs produced in RU486-/4-HT-treated $K14.ROCK^{er}/HK1.ras^{1205}/\Delta 5PTEN^{het}$ mice at only 6 weeks. (b) Dissection of papilloma cluster compared to (c) individual halves of tri-genic $ROCK/ras^{1205}/\Delta 5PTEN^{het}$ mice reveal distinctly different architectures to their appearance consistent with a benign or malignant histotype. (d) Control genotypes at 14 weeks: RU486-treated/4-HT-untreated $K14.ROCK^{er}/HK1.ras^{1205}/\Delta 5PTEN^{het}$ and (e) RU486-treated/4-HT-treated $HK1.ras^{1205}/\Delta 5PTEN^{het}$ at 14 weeks show similar papilloma cluster appearance to RU486-treated $HK1.ras^{1205}/\Delta 5PTEN^{het}$ papilloma. (f) RU486-/4-HT-treated $K14.ROCK^{er}-K14.creP-\Delta 5PTEN^{het}$ and (g) RU486-/4-HT-treated $K14.ROCK^{er}-K14.creP-\Delta 5PTEN^{flx}$ mice display thickened ears and mild keratotic phenotypes.

The histotype confirmed the expected SCC histotypes (figure 3.68a-f and figure 3.69a-e) and these tumours exhibited large areas of aggressive pdSSCs and an odd feature manifested in their processing. In the areas of aggressive SSC/pdSSC, a unique ripping occurred during cutting of these sections (figure 3.68a-c – arrows); but this did not happen in the control tumours that were processed at the same time. Hence, it is tempting to conclude that these tumours were of a brittle nature and this phenotype was derived from an increased stiffness and rigidity mediated by ROCK2 signalling (Samuel et al., 2011). At higher magnification (figure 3.69a-e), areas of SCC and pdSSC not only manifest as being brittle and easily ripped on sectioning, but also contained numerous mitotic figures (figure 3.69 – circles) indicative of a rapid proliferation rate as observed in the tri-genic ROCK/ras¹²⁷⁶/Δ5PTEN^{flx} version. Also, many areas exhibited clear spaces between groups of basal layer SCC cells (figure 3.69e); a result also observed in the tri-genic ROCK/ras¹²⁷⁶/Δ5PTEN^{flx} model. Exactly what this spacing indicates is still unclear, but it may be a precursor necessary to facilitate increased cellular migration and invasive potential. In support of this idea, these spaces between cells are very clear and appear to be devoid of the typical intercellular projections that define the spinous layer and give it its integrity. This too would be consistent with the observation that this intercellular histotype was often separate to that of the brittle/ripped tissue (figure 3.69c,d versus figure 3.69e). This suggests that in one case ROCK2 is increasing tissue stiffness via actomyosin contraction, or changes in the extracellular matrix and tumours invade on a wide front (Samuel et al., 2011). On the other hand, ROCK2 mediated intracellular changes may facilitate cell motility (Croft et al., 2004), for rapid invasion via the finger-like projections observed in the tri-genic ROCK/ras¹²⁷⁶/Δ5PTEN^{flx} model (above) as shown in figure 3.68(b,f) and figure 3.69(a,b & d). These speculations have already been theorised in previous study of ROCK2-mediated carcinogenesis through tissue stiffness and may involve changes in β-catenin signalling (Samuel et al., 2011). If so, this would in turn affect adherens junctions such as E-cadherin (Holeiter et al., 2012), and thus may possibly account for the lack of spinous projections observed in this histotype suggesting a failure to form appropriate adherens junctions or desmosomes that maintain cellular integrity (Brandner et al., 2010, Simpson et al., 2011).

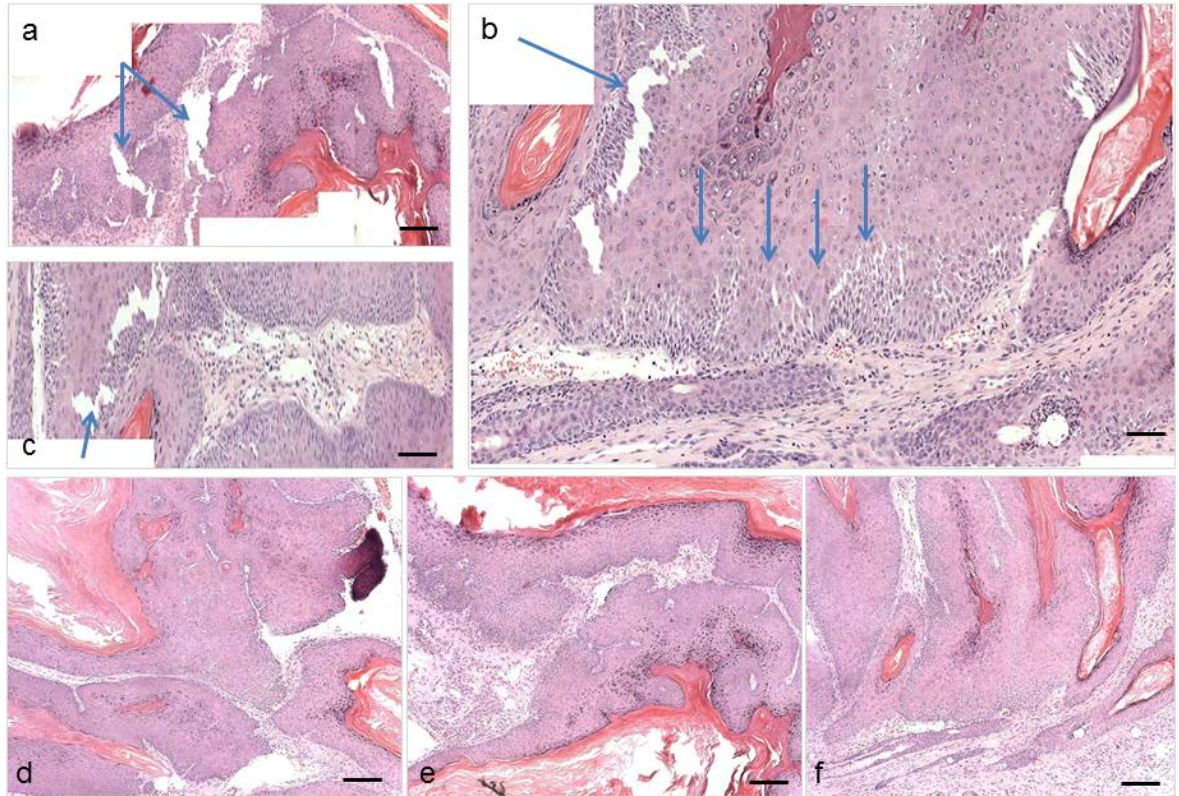


Figure 3.68 Histotypes of RU486-/4-HT-treated *K14.ROCK^{er}/HK1.ras¹²⁰⁵/Δ5PTEN^{het}* biopsies at 6 weeks. (a-f) Composite low magnification micrographs of tri-genic ROCK/*ras¹²⁰⁵/Δ5PTEN^{het}* biopsies show mainly SCC (a,c) and mainly pdSCC (b,d-f) histotypes with highly invasive cells. In addition, all these examples exhibited rips in the tissue sections (arrows) together with areas of disorganised basal layer cells. Serial sections from (a-c) [mouse 9423] were employed for p53 analysis and (d-f) [mouse 9422] were used to investigate p21 expression. (Scale bar: approx 200μm in a,d-f; approx 150μm in b,c).

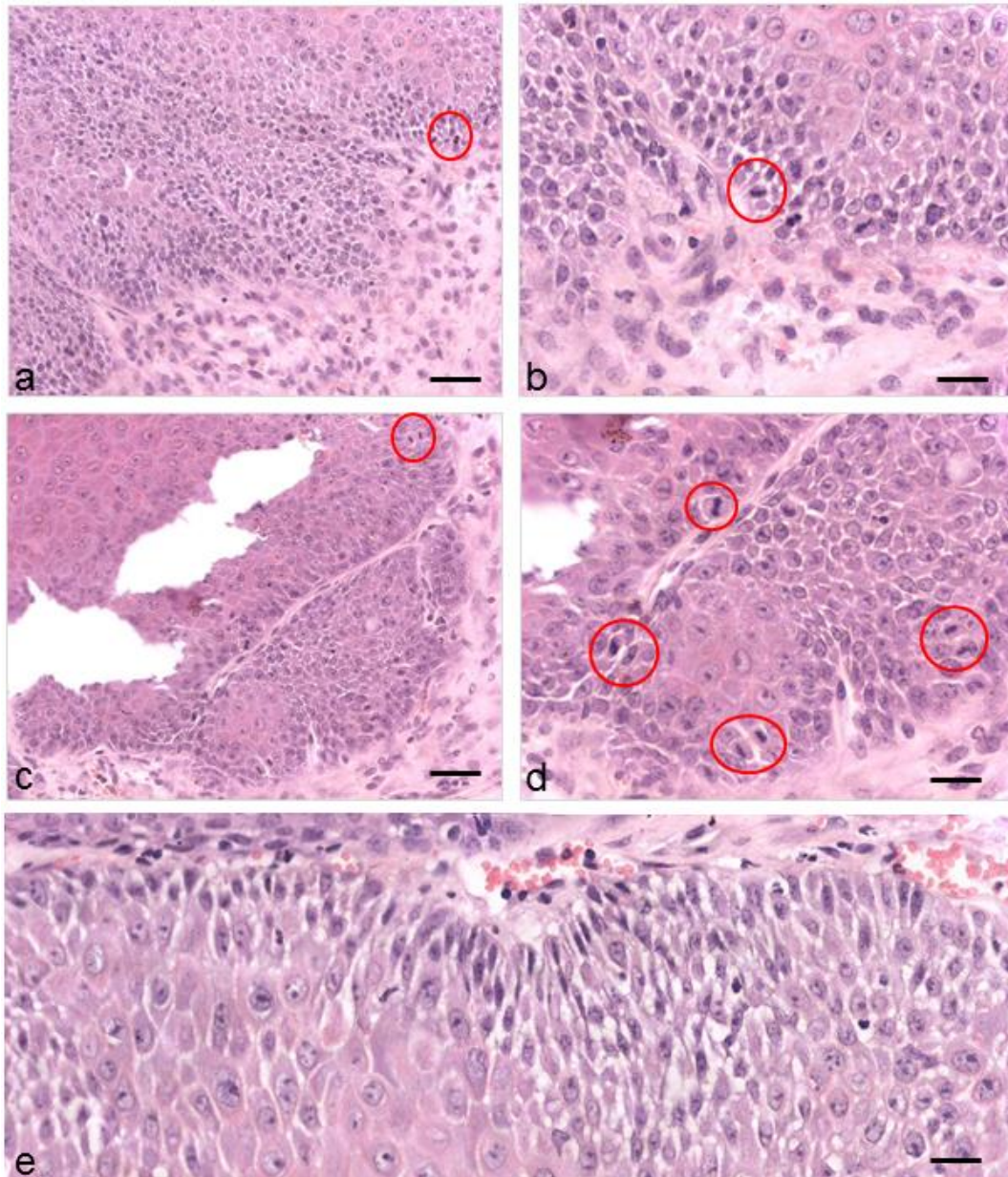


Figure 3.69 Histotypes of RU486-/4-HT-treated *K14.ROCK^{er}/HK1.ras¹²⁰⁵/Δ5PTEN^{het}* biopsies at 6 weeks. (a,b) At higher magnification, *K14.ROCK^{er}/HK1.ras¹²⁰⁵/Δ5PTEN^{het}* carcinomas exhibit highly invasive pdSCCs with numerous easily detected mitotic figures (circles). (c,d) This example of pdsc histotype shows that the ripped areas appeared to be separate to the disorganised basal layer shown in (e). Here there a fewer mitotic cells but the spaces between cells are very clear and appear to be devoid of the typical intercellular projections that define the spinous layer. (Scale bar:100μm in a,c; 50μm in b,d; 25μm e).

Experiments to the analysis of p53 and p21 status (figures 3.70 and 3.71) in this rapid carcinogenesis were carried out. As expected, all examples tested had lost the p53 tumour suppressor gene (figure 3.70a,b) and it was noted that in this context, areas of keratin K1-positive, late-stage papilloma had also already lost p53 expression by 5- 6 weeks (figure 3.70c-e). This was in contrast to control papilloma cohorts (not shown) where p53 expression was maintained in all epidermal layers (Macdonald et al., 2014).

A similar result was observed for p21 expression. Here in the RU486-/4-HT-treated ROCK/ras¹²⁰⁵/Δ5PTEN^{het} mouse tumour from 9422, p21 expression had appeared in the smaller areas of less aggressive histotypes (figure 3.71), unlike that for p53 loss, but as these papilloma/wdSCC rapidly progressed to SCC and pdSCC, any remaining p21 expression disappeared. However, just as observed in the ROCK/ras¹²⁷⁶/Δ5PTEN^{fix} version, and unlike progression in all the other contexts, here little or no persistent p21 expression appeared in the basal layers, with occasional supra-basal cells expressing barely detectable levels in the presence of numerous mitotic figures (figure 3.71e-g). This p53 and p21 result was again similar to the rapid carcinogenesis observed following TPA promotion of *HK1.ras¹²⁷⁶/Δ5PTEN^{fix}* mice (Yao et al., 2006, Macdonald et al., 2014), in which both p53 and p21 expression were lost, suggesting that neither had been expressed. Whereas in this tri-genic ROCK/ras¹²⁰⁵/Δ5PTEN^{het} carcinogenesis, whilst p53 was lost very early, it appears that there was an attempt at a compensatory p21 response; but this was lost/bypassed relatively quickly, thus leading to a rapid progression to aggressive carcinomas in these *K14.ROCK^{er}/HK1.ras¹²⁰⁵/Δ5PTEN^{het}* mice.

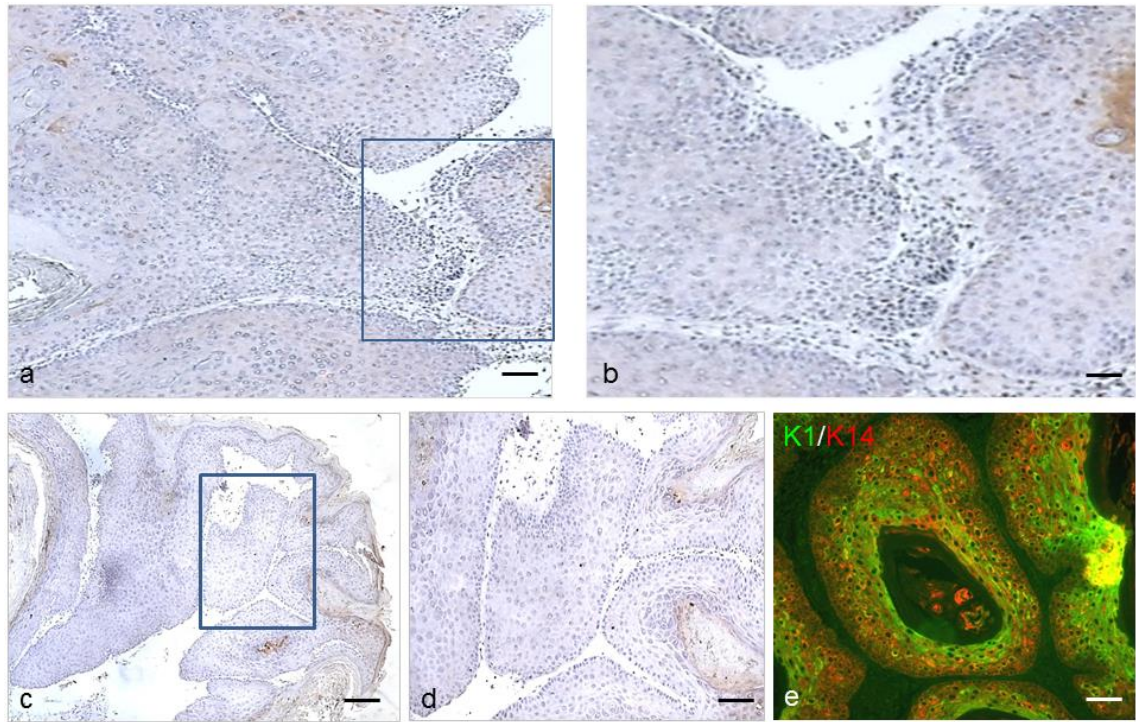


Figure 3.70 IHC analysis of p53 expression in *K14.ROCK^{er}/HK1.ras¹²⁰⁵/Δ5PTEN^{het}* carcinogenesis. (a) Low magnification composite micrograph of RU486-/4-HT-treated SCC and pdSCC (box) from mouse 9423 and (b) higher mag of boxed area, shows complete loss of p53 expression in a uniform manner. (c-e) Ear tumour from mouse 9423 also possessed some areas of late-stage papilloma which were also devoid of p53 despite these areas being K1 positive. (Scale bar: a: 150μm; b,d,e: 50 μm; c: 200μm).

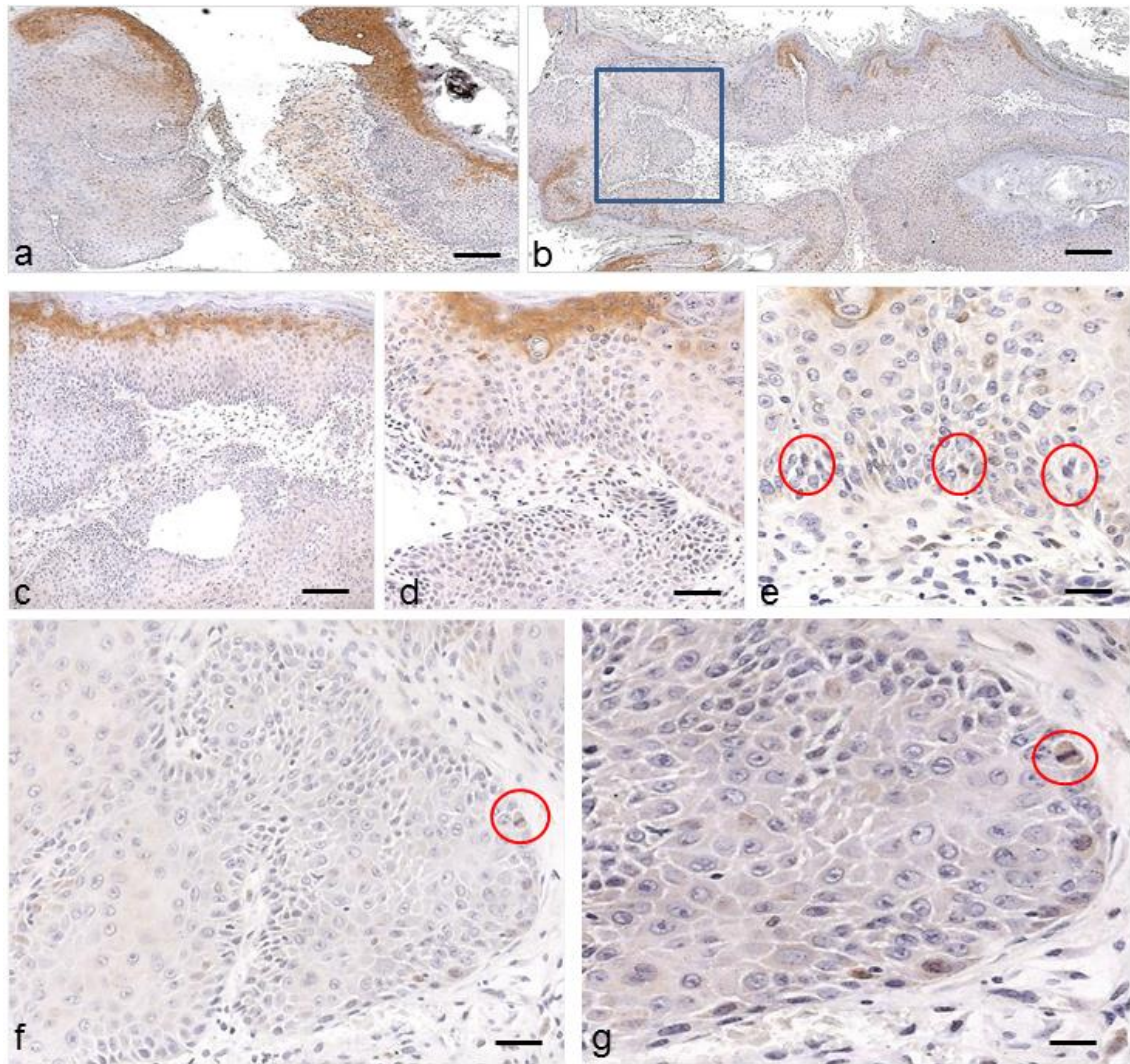


Figure 3.71 IHC analysis of p21 expression in *K14.ROCK^{er}/HK1.ras¹²⁰⁵/Δ5PTEN^{het}* carcinogenesis. (a, b) Low magnification composite micrograph of p21 expression in RU486-/4-HT-treated mouse tumour from 9422 shows p21 loss as papilloma/wdSCC progressed to larger areas of more uniform SCC with increased regions of pdSCC. (c) The remaining p21 expression in SCC remains localised to the keratotic layer of the wdSCC/SCC, disappears in SCC and no p21 expression was observed in the basal layers; whilst again a rip appeared in the SCC tumour tissue. (d, e) Higher magnification of this wdSCC/SCC area confirms p21 loss in the majority of keratinocytes with occasional supra-basal cells expressing just detectable low levels and numerous mitotic figures. (f, g) High magnification of the boxed area (from b) again confirms uniform loss of p21 in this SCC/pdSCC (K1 negative - see below); with very faint staining observed in some mitotic figures (circles). (Scale bars: a,b: 200 μm; c: 100 μm; d,e,f: 50 μm; g: 25 μm).

Therefore, given the data from above, the status of activated AKT1 was also assessed. As shown in figure 3.72(a,b), p-AKT1 expression followed the similar outline as observed earlier in tri-genic ROCK/ras¹²⁷⁶/Δ5PTEN^{flx} version; but here given the loss of both p53 and now the lack of persistent p21, the elevated p-AKT1 expression became rapidly uniform and also appeared in the basal layers of SCCs (p21-negative). This observation suggests that among the many progression pathways, in these aggressive tumours, the very rapid progression to SCC and appearance of pdSCC, may be driven by basal layer ROCK2 and (sporadic) basal ras^{Ha} activation in co-operation with Δ5PTEN-associated p-AKT1 activation. This happened in the context where malignant conversion had been achieved and mediated by ROCK2 and *HK1.ras*¹²⁰⁵ co-operation as observed in the spontaneous progression pathways of the original bi-genic ROCK/ras¹²⁰⁵ model (above).

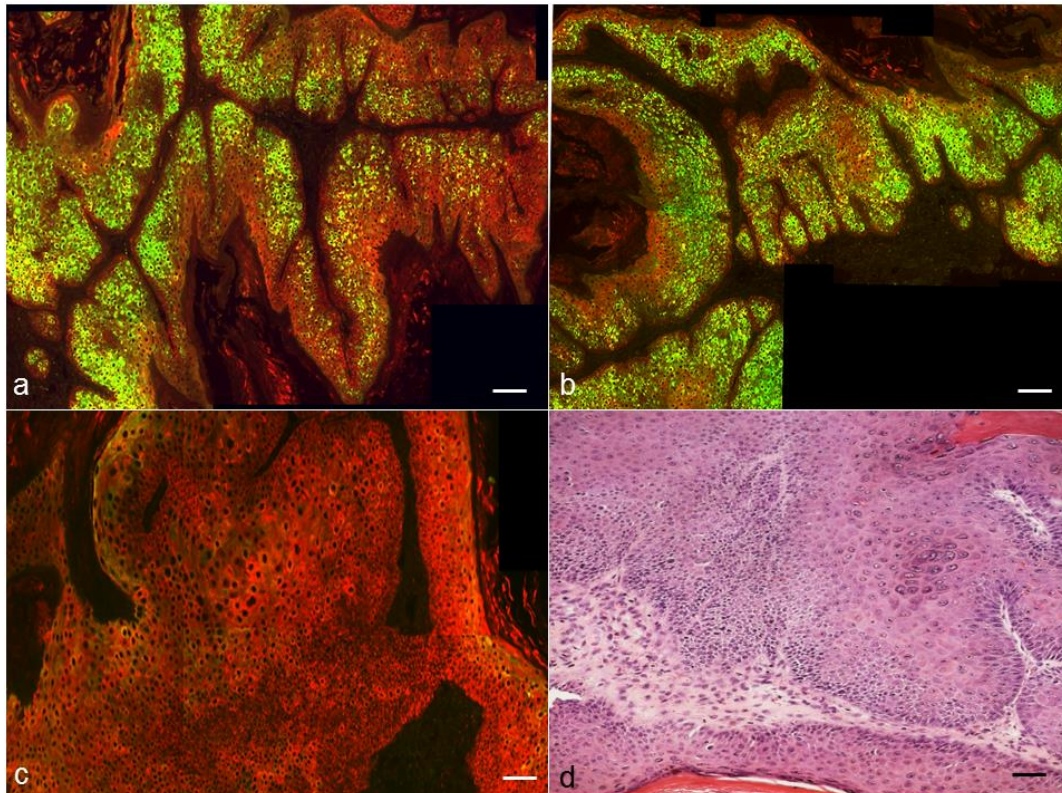


Figure 3.72 Immunofluorescence analysis of p-AKT1 and keratin K1 expression in *K14.ROCK^{er}/HK1.ras¹²⁰⁵/Δ5PTEN^{het}* carcinogenesis. (a) Activated p-AKT1 expression in a late stage papilloma/SCC area of mouse tumour 9423 and (b) SCC area of tumour 9422 shows increasing expression throughout epidermal layers. (c) Typical uniform loss of keratin K1 expression in SCC/pcSCC in a serial section of the (d) tumour 9422 SCC/pdSCC (Scale bars: a,b: 150 μm; c,d: 100 μm).

3.9.7 Summary

In this study, inducible ROCK2 activation showed direct co-operation with $ras^{1276}/\Delta 5PTEN^{flx}$ in malignant conversion and progression (at 22 weeks) supported by loss of keratin K1, p53 and p21, together with strong basal expression of p-AKT1. Moreover, epidermal architecture of *K14.cre/Isl.ROCK^{er}/ras¹²⁷⁶/Δ5PTEN^{flx}* SCC/pdSCC appeared massively disorganised with finger-like projections into the dermis making it difficult to distinguish each epidermal layer. Intriguing finding from this tri-genic ROCK/ $ras^{1276}/\Delta 5PTEN^{flx}$ study was shown on the tumour phenotypes. Even though tri-genic ROCK/ $ras^{1276}/\Delta 5PTEN^{flx}$ mice gave no large tumours in comparison to the massive tumour size from other tri-genic models (e.g. tri-genic ROCK/ ras^{1276}/fos and ROCK/ $fos/\Delta 5PTEN^{flx}$ mice); yet the tumours have shown a very progressive malignancy. Another important feature from this study was the contrast between these tri-genic mice to the bi-genic $ras^{1276}/\Delta 5PTEN^{flx}$ mice which showed hyperplasia histotypes only at this time point due to persistent p53/p21 expression profiles. Whereas during co-operation of ROCK2 activation in a context of $ras^{1276}/\Delta 5PTEN^{flx}$, once the hyperplastic histotype had been bypassed; presumably by p53 loss, these tiny tumours rapidly progressed to SCCs, accompanied by loss of p21 and increased AKT expression. Thus, these data indicated a significant role of ROCK2 in malignant conversion and progression when both MAPK kinase signalling and PTEN/PI3K/AKT signalling combined.

This conclusion proved to be correct in experiments investigating the co-operation between ROCK2 and $ras^{1205}/\Delta 5PTEN^{het}$ using the original bi-genic ROCK/ ras^{1205} model. Here, even with a normal PTEN allele, rapid papillomatogenesis occurred in tri-genic ROCK/ $ras^{1205}/\Delta 5PTEN^{het}$ mice, and this study has not only demonstrated the important role of ROCK2 in malignant conversion but also in malignant progression; as these tumours rapidly progressed to pdSCC as early as 6 weeks. Further, both p53/p21 expressions in this tri-genic ROCK/ $ras^{1205}/\Delta 5PTEN^{het}$ model disappeared early in a similar pattern to that seen in the tri-genic ROCK/ $ras^{1276}/\Delta 5PTEN^{flx}$ model, where total loss of p53 in SCC/pdSCC expression followed by gradual loss of p21 from late stage papillomas prior to complete loss of p21 expression in the SCC/pdSCC areas was observed. Thus, the loss of p53/p21 along with strong and basal expression of p-

AKT1 in tri-genic ROCK/ras¹²⁰⁵/Δ5PTEN^{het} model is consistent to a previous study by Yao et al., (2006) upon TPA promotion in bi-genic ras¹²⁷⁶/Δ5PTEN^{flx} mice. In addition, one important observation in this tri-genic ROCK/ras¹²⁰⁵/Δ5PTEN^{het} model is the appearance of several rips/broken areas in the aggressive SCC/pdSCC areas. Since ROCK2 activation in this tri-genic ROCK/ras¹²⁰⁵/Δ5PTEN^{het} model showed the most severe malignancy to date, the rip/broken tissue observation may imply that activated ROCK2 contributed to an increase tissue stiffness during tumourigenesis (Samuel et al., 2011) and thus, these fixed sections became brittle, harder to cut and this feature manifests in the SCC areas of H&E sections.

Chapter 4 – Discussion

4.1 ROCK2 activation in transgenic mouse skin carcinogenesis

Carcinogenesis is a complex process that evolves through different stages of tumour development. From a clinician's point of view, the conversion of benign tumours to malignancy and further progression to metastasis are the most significant stages for cancer patients and thus understanding the cancer pathogenesis is essential in this context. One of the most successful models used to study the multistage mechanism in carcinogenesis is the mouse skin model of two-stage chemical carcinogenesis, which allows the exploration of the mechanisms of tumour progression using DMBA to initiate and TPA to promote (Yuspa et al., 1991). Through development of transgenic mice, the initiation and promotion steps of DMBA and TPA have been mimicked in many skin models typically with the introduction of activated oncogene ras^{Ha} , the oncogene activated most following DMBA treatment (Balmain and Pragnell, 1983, Balmain et al., 1984, Roop et al., 1986) and addition of fos oncogene activation (Greenhalgh et al., 1993b), a major facet of TPA promotion (Schlingemann et al., 2003). With the respect to ras^{Ha} activation acts an initiator of carcinogenesis and fos activation as a promoter, and when driven by a HK1 promoter modified to express in proliferative basal layers (Greenhalgh et al., 1993a), HK1.ras/fos co-operation gave benign papillomas without a spontaneous malignancy (Greenhalgh et al., 1993c, 1996). This stability of phenotype enabled analysis of malignant conversion such as co-operation with inducible PTEN loss at exon 5 which deregulated AKT activity (Macdonald et al., 2014).

Therefore, with the main aim to identify the specific stage of tumour events, combination of well characterised mutations that signify some of the most altered interacting signalling pathways in carcinogenesis has been chosen. In this study, inducible ROCK2 activation was introduced into a transgenic mouse skin model in co-operation with ras^{Ha} and /or fos oncogene activation and inducible PTEN tumour suppressor gene loss. This has been employed to identify ROCK2 activation roles in producing benign tumours, driving conversion to malignancy and

/or promoting further progression to aggressive tumours; and at the same time investigated the involvement of ROCK2 in the process of normal epidermal differentiation. In addition, this study also introduced the latest and unpublished *Isl.ROCK^{er}* model that is driven by the universal CAG promoter following cre mediated ablation of stop cassette and is conditionally activated by 4-HT regulation (Samuel et al., 2009a). This *Isl.ROCK^{er}* model offered ROCK expression in the same target cells to the PTEN ablation at exon 5 by K14.creP, which is in the proliferative keratinocytes (Berton et al., 2000b).

These studies commenced with an initial analysis of the original transgenic mouse model of ROCK activation (*K14.ROCK^{er}*) (Samuel et al., 2009a) to show that 4-HT treatment produced the same phenotypes in the background strain of ICR mice employed in the HK1 models (Greenhalgh et al., 1993a-c). Accordingly, *K14.ROCK^{er}* mice resulted in epidermal hyperplasia but no tumour formation, and gave identical results in terms of GFP analysis that confirm its expression in each epidermal layer and phosphorylated Mypt (p-Mypt1) expression to confirm ROCK activation mediated by 4-HT (Samuel et al., 2009a, 2011). Given the hyperplasia histotypes produced by *K14.ROCK^{er}* mice in this study, it appeared to be very similar to the hyperplasia formed by young *HK1.ras* or *HK1.fos* mice prior to papilloma formation in terms of e.g keratin K1 differentiation marker expression (Greenhalgh et al., 1993a,b). However, *K14.ROCK^{er}* hyperplasia also expressed changes in e.g keratin K6, which appeared unique to ROCK deregulation and this may reflect ROCK2 functions in actomyosin contraction that seems to affect the cellular composition. This finding also echoed a previous observation that PTEN mice exhibited a very unusual lack of this hyperproliferative associated keratin in their hyperplasia (Yao et al., 2006); whereas typically K6 is strong and uniform in epidermal hyperplasia (Greenhalgh et al., 1993a,b). This suggests links and similarities between deregulation of the ROCK2 and PTEN signalling systems in an epidermis that may be accountable for an apparent lack of synergism in papillomatogenesis and thus effects in differentiation were explored in vivo and in vitro (below).

In addition, these studies also employed a new ROCK2 transgenic line, *Isl.ROCK^{er}*. This line which is a 4-HT-inducible ROCK^{er} transgene driven by a generic CAG promoter was designed using the cre/loxP system, and following cre recombinase activity to ablate a series of stop cassette in a target gene. Thus,

depending upon which promoter drives the regulator of cre expression, now ROCK^{er} can be expressed in most cell types and not just the epithelia. Therefore, these *Isl.ROCK^{er}* mice were mainly chosen so that the identical keratinocytes would express ROCK^{er} in the same keratinocyte populations when crossed into the *K14.creP/Δ5PTEN^{flx}* genotype and mice were treated with RU486 to translocate cre activity from the cytoplasm to the nucleus following dimerization of the progesterone ligand binding domain (Berton et al., 2000b). Thus, a series of experiments were conducted to establish this *Isl.ROCK^{er}* genotype into the K14.creP background and assess the phenotypes produced in *K14.cre/ Isl.ROCK^{er}* genotype and compare to the original *K14.ROCK^{er}* model (Samuel et al., 2009a). In both strains, phenotypes from these studies were identical, and as for the *K14.ROCK^{er}* in ICR mice, RU486/4-HT treatments in *K14.cre/ Isl.ROCK^{er}* genotypes again demonstrated that ROCK2 activation produced an identical skin thickening associated with keratinocyte hyperplasia identical to that of previous studies (Samuel et al., 2009a, 2011), but no tumour formation at this stage.

Previously, a study by Berton et al., (2000b) has crossed K14.creP mice with mice carrying a similar reporter construct (CAG-CAT-Z reporter gene) to that of the CAG-*Isl.ROCK^{er}* construct. Despite K14 expression in all epidermal compartments including hair follicles and stem cells following RU486 mediated cre activity, CAG driven β-gal expression showed expression only in the differentiated supra-basal layers. Thus, even though the clear hyperplasia histotypes has been produced by *K14.cre/Isl.ROCK^{er}* cohorts in the beginning of this study, given an unexpected lack of bi-genic ROCK/Δ5PTEN^{flx} co-operation, concerns existed that *Isl.ROCK^{er}* transgene may be expressed from a similar CAG promoter and would follow the same expression, and also be limited in the supra-basal layers. This proved to be unfounded, as again in an identical fashion to *K14.ROCK^{er}* mice, uniform expression of GFP and p-Mypt1 appeared throughout epidermal layers, including hair follicles in *K14.cre/Isl.ROCK^{er}* epidermal hyperplasia (and in *K14.cre/Isl.ROCK^{er}/Δ5PTEN^{flx}* mice) and thus have answered these concerns.

Now that the activated ROCK transgenic mice have been characterised and found to be consistent in phenotypes and histotypes to that observe previously (Samuel et al., 2009a, 2011). Hence, this study proceeds to assess the co-operation of ROCK with ras and /or fos oncogenes activation employed in the HK1 models (*HK1.ras*, *HK1.fos*). Thus, several questions were posed given the previous

DMBA/TPA chemical carcinogenesis study on ROCK2 (Samuel et al., 2011). It was anticipated that ROCK2 would co-operate with ras^{Ha} which is the well-known oncogene that acts as an initiator in the multistage carcinogenesis model; but the question is at what stage that ROCK2 becomes causal? Yet, there is still lack of evidence on the effect of either DMBA or TPA alone on ROCK2 in carcinogenesis. In addition, given the 2 types of *HK1.ras* lines in this study where *HK1.ras*¹²⁷⁶ line is insensitive to wound promotion whilst *HK1.ras*¹²⁰⁵ line produces papillomatogenesis in response to wound promotion; thus this allows this study to test whether ROCK2 activation would co-operate with ras^{Ha} and if so, as a converter or promoter?. Further, in co-operation study between ROCK2 and fos activation, this would testify the ROCK2 ability as an initiator since fos activation is a constitutive promoter. In addition, as targeting several pathways in combination offers potential insight for most cancer therapies, thus co-operation between ROCK2 and PTEN in this study would introduce the link between AKT pathway and MAPK deregulation.

ROCK expression has shown high expression in human cutaneous SCC (Ibbetson et al., 2013) complies with the roles of ROCK in late cancer event (Croft et al., 2004). This observation is also consistent to the introduction analysis of each tumour stage of *ras/fos/ΔPTEN*^{fix} transgenic mouse skin carcinogenesis (Macdonald et al., 2014), which displayed an elevated expression of both ROCK1 and ROCK2 upon poor prognosis of tumours. Moreover, it was revealed that both ROCK1 and ROCK2 expression became greater in all epidermal compartments of wdSCCs and SCCs, but expression was lesser in papillomas and remained confined to supra-basal layers. Thus, one of many questions to be addressed in this study was aimed to answer whether ROCK2 can be the causal to drive the malignant conversion prior to its more familiar roles in malignant progression. Hence, this led to the first co-operation study between ROCK2 and ras^{Ha} activation. Previous studies have shown the effect of two-stage chemical carcinogenesis (DMBA/TPA) on ROCK^{er} mice (Samuel et al., 2011) which resulted in increased number of SCCs. Therefore, it was logical to assume that ROCK2 could co-operate with ras^{Ha} , but no directed evidence existed until now in this new HK1 study. Furthermore, a result found by induction of DMBA alone on ROCK^{er} mice revealed no tumour formation (Olson, - unpublished data), a result that has now been answered in this study by the need for promotion (e.g. wounding or fos promotion). Indeed, the fact that both activated ras^{Ha} and fos mimics the

DMBA/TPA carcinogenesis as activated ras^{Ha} induced initiation and activated fos induced promotion (Greenhalgh and Yuspa, 1988, Greenhalgh et al., 1990, Greenhalgh et al., 1993a-c), thus, the co-operation between ROCK2 and ras^{Ha} and /or fos was not only mimicked chemical carcinogenesis models (Samuel et al., 2011, Balmain and Yuspa, 2014), but also revealed the stages when oncogenic ROCK2 activation can actually contribute, now including the early stage of carcinogenesis.

4.2 Co-operation of ROCK2 and *HK1.ras* in transgenic mouse skin carcinogenesis

In this study, the direct co-operation between ROCK and ras has identified the important roles of ROCK to drive malignant conversion of benign tumours, as activated *HK1.ras*¹²⁰⁵ alone controls produced papillomas only without malignant conversion in 100% of animals. Indeed, when activated *HK1.ras*¹²⁰⁵ developed a papilloma, bi-genic ROCK/ras¹²⁰⁵ cohorts at the same time (8 weeks) have already showed a sign of papilloma progression; given the reduced keratin K1 expression. This then continued on carcinoma conversion to wdSCCs/SCCs, with all animals exhibiting wdSCC histotypes upon additional treating time (until 12 weeks), whilst *HK1.ras*¹²⁰⁵ tumours remained as benign papillomas. This intriguing finding has confirmed the roles of ROCK2 activation in conversion but with the necessary addition of wounding which in this context was required to facilitate the formation of appropriate papillomas before activated ROCK2 becomes causal and convert these late-stage papillomas to malignant tumours. Although there are few studies that have reported the link between ras and Rho/ROCK pathway (Olson et al., 1998, Sahai et al., 2001), and since ROCK is a downstream effector of RhoA is considered as a member of the Ras superfamily, this interaction between ROCK and ras is predictable. Yet, it was possible that these roles were redundant in benign upon the same pathway, but now are proven to be additive. However, this co-operation did require the correct papilloma context prior to the direct co-operation between ROCK2 and ras^{Ha} and now this study has shown that ROCK2 plays its roles as a converting agent. In addition, expression of ROCK^{er} transgene and its substrate, p-Mypt1 appeared in all epidermal compartments and together with tenascin C expression which became elevated upon malignancy. Since it is transpired that high expression of tenascin C is linked to poor prognosis (Dang et

al., 2006, Orend and Chiquet-Ehrismann, 2006) and it is also highly expressive in solid malignant tumours (Orend and Chiquet-Ehrismann, 2006, Midwood and Orend, 2009). Thus, these data suggest that it is the increased in stiffness mediated by ROCK activation which aids in conversion as well as in progression.

Analysis of p53 and p21 proved to be very informative regarding the underlying mechanism. Besides, p53 expression that became gradually lost in all epidermal layers typically prior to and definitely following malignant conversion at 12 weeks, a major finding was that this p53 loss was countered by p21 expression that remained confined in all epidermal layers to suppress further malignant progression (Efeyan et al., 2007, Macdonald et al., 2014). Since p21 acts as an important component for p53 in tumour suppression, study has shown significant depletion in tumour suppression in the super-p53 mice but in the absence of p21 expression (Efeyan et al., 2007). This was demonstrated by continuous malignant progression in bi-genic ROCK/ras¹²⁰⁵ to pdSCC histotypes with loss of both p53/p21 expressions at 16 weeks. Moreover, it has also been reported by Yao et al., (2006) that the loss of both p53 and p21 expression in bi-genic ras¹²⁷⁶/Δ5PTEN^{flx} after TPA induction lead to pdSCCs formation, showing their potency as tumour suppressor genes. In contrast, therefore in the absence of 4-HT, bi-genic ROCK/ras¹²⁰⁵ stayed as benign papillomas and showed no sign of conversion as observed in ras^{Ha} (Greenhalgh et al., 1993a) due to strong expression of both p53 and p21.

Several intriguing findings in this current study emerged from cessation of 4-HT treatments. One showed that the bi-genic ROCK/ras¹²⁰⁵ wdSCCs/SCCs continued to pdSCCs even without exogenous ROCK (cessation of 4-HT). Here at this stage, p21 expression was lost in the invasive pdSCC areas at 16 weeks, but in the wdSCC area, p21 expression persisted; consistent with the data that appeared at 12 weeks. This persistence plus the altered disturbed basal layers observed in these wdSCC histotypes suggests that at this stage, malignancy depended on exogenous ROCK being a downstream regulator of ras and when both are activated, it provides more proliferation and a benefit for tumour progression (Molina and Adjei, 2006). The lack of requirement for exogenous ROCK in the pdSCCs may be due to the levels of endogenous ROCK which took control in continuous progressive SCC and this idea was not unexpected since it is well-known that high expression of ROCK (1 and 2) occurred correlated to poor

prognosis of tumours (Croft et al., 2004, Samuel et al., 2011). Samuel et al., (2011) have also shown that high expression of endogenous ROCK was demonstrated in almost all cases of human SCCs, coincided with high levels of ROCK (1 and 2) displayed in tri-genic ras/fos/ Δ 5PTEN^{flx} carcinomas. Therefore, this suggests that once tumours achieved progressive carcinomas, thus, it is possible that the additional exogenous ROCK activity is no longer considered as a rate limiting factor.

At the same time, this study found a remarkable tumour growth and larger rather than smaller tumour size in bi-genic ROCK/ras¹²⁰⁵ mice after the cessation of 4-HT. Indeed the fact that this new tumour growth turned out to be a late stage papilloma would suggest that ROCK was required for maintaining malignancy, but this sudden massive tumour growth was accompanied by K1 expression and also a very rare intense expression of p21 in all epidermal compartments that may sustain these papillomas from conversion. Previous study has shown that RhoA, the upstream regulator of ROCK was responsible to suppress the p21 expression in ras transformed cells (Sahai et al., 2001). Since RhoA-induced transformed cells (NIH3T3 fibroblasts) required ROCK signalling to establish and maintain the transformation (Sahai et al., 1999), thus, in this study where there is no exogenous ROCK activity due to cessation of 4-HT may implicate in the p21 expression. However, Sahai et al., (2001) have shown that ROCK activation which was required for RhoA-induced ras-transformed cells showed no responsibility in regulating p21 levels. Further, turned out that ERK/MAPK signalling down-regulated ROCK(1 and 2) activity in the RhoA-induced ras-transformed cells (Sahai et al., 2001). Thus, these observations may suggest two potential possibilities. First, ROCK was required to maintain malignancy, and the highly intense p21 level in bi-genic ROCK/ras¹²⁰⁵ after cessation of 4-HT was due to induction by ERK/MAPK signalling from ras oncogene activation. Second, it is also possible that after cessation of 4-HT, the rapid growth of late stage papilloma were maintained in a benign state due to this novel and rare intense of p21 expression. This was highly expressed presumably to compensate for the lack of p53 expression which did not appear to be restored and at the same time suppress further progression, as observed previously in tri-genic ras/fos/ Δ 5PTEN^{flx} mice (Macdonald et al., 2014). On the other hand, the additional tumour growth and size in the bi-genic ROCK/ras¹²⁰⁵ mice after cessation of 4-HT leads to an idea of anti tumour effect of 4-HT which inhibits the formation of papilloma subtype in certain

contexts. Thus, cessation of 4-HT allowed this odd, p53 negative intense p21 expression tumours to develop. However, this is still unclear since data showed that *HK1.ras*¹²⁰⁵ tumours remained benign papillomas with or without induction of 4-HT.

Furthermore, this study also indicated that the promotion stimulus received from wounding is required to develop a mature or appropriate papilloma before ROCK2 driven malignancy started to happen. In both bi-genic ROCK/*ras*¹²⁰⁵ and *HK1.ras*¹²⁰⁵ mice, benign papillomas developed at the ear tag in response to wound promotion and would regress upon loss of ear tag (no promotion). Even if loss of tag on bi-genic ROCK/*ras*¹²⁰⁵ mice occurred in the early period when only a small proper papilloma developed, tumours remained benign and failed to convert to malignancy. Thus, the tagged ear was responsible to create a wounding environment that established mature papilloma formation where ROCK^{er} expression achieved malignancy; a result confirmed by bi-genic ROCK/*ras*¹²⁷⁶ experiments that failed to produce tumours as *HK1.ras*¹²⁷⁶ mice are insensitive to wound promotion. Subsequently, given that *HK1.ras*¹²⁰⁵ remained benign papillomas, this study shows direct co-operation between ROCK2 and *ras*^{Ha} activation in facilitating tumour conversion into the beginning of the malignant stages with the presence of wound promotion; thus this study has assessed the co-operation between ROCK2 and fos activation which can mimic the TPA promotion to observe ROCK2 potential as an initiator.

4.3 Co-operation of ROCK2 and *HK1.fos* in transgenic mouse skin carcinogenesis

The next bi-genic line in this study is ROCK/*fos* which has shown novel direct co-operation between ROCK and fos activation in early stage of carcinogenesis with benign squamous papillomas formation. Interestingly, as reported in previous study, initially *HK1.fos* activation produced slow development of phenotype and resulted in hyperplasia/hyperkeratosis after a period of 4 to 6 months (Greenhalgh et al., 1993b). Moreover, to date there is still no definite answer whether ROCK2 activation can co-operate with fos in carcinogenesis. Adding to the fact that transcription factor fos regulates differentiation and proliferation (Basset-Seguin et al., 1990, Saez et al., 1995, Mehic et al., 2005). Since c-fos expression is not only

limited to the basal layers (Basset-Seguín et al., 1990) but it is also expressed in the supra-basal layers (Fisher et al., 1991, Mehic et al., 2005), thus, it is thought that fos plays an important role to switch the state between differentiation and proliferation. Fisher et al., (1991) have shown that sudden burst of massive c-fos expression in late stage differentiation just before cornification and cell death which linked the roles of fos in keratinization thus associated with keratosis feature. Since fos oncogene is highly targeted upon TPA induction, thus makes fos activation mimic the promotion stage (Dotto et al., 1986). Further, expression of v-fos driven by HK1 construct resulted in both hyperplasia and hyperkeratosis and required long period before benign papillomas appeared (Greenhalgh et al., 1993b). Moreover, v-fos gene (Curran et al., 1984) is stable and potentiates all of c-fos activities (Greenhalgh and Yuspa, 1988, Greenhalgh et al., 1990). It is also known that fos is a major transcription factor target for the ras/MAPK signalling pathway (Greenhalgh and Yuspa, 1988, Greenhalgh et al., 1990) thus given the co-operation observed between ROCK2 and fos activation above, and the previous studies on ras and fos synergisms (Greenhalgh et al., 1993c). This has led to the idea that links may exist between deregulated ROCK2 and fos functions, given that ROCK is considered to be an effector of ras signalling elements and to date, there is still lack of study on direct co-operation between fos and ROCK2 activation and what would be the final outcome from this co-operation? As ROCK is a late stage event driving malignant conversion, so, the question lies on would ROCK2 and fos synergism be too distant in the context of oncogenic insults, giving a lack of tumours, or be redundant in outcome as observed in bi-genic ROCK/ Δ 5PTEN^{flx} (below). In this context, could ROCK2 acts even earlier as a weak initiator for constitutive fos promotion, as the fos oncogene mimics the promotion stage in multistage cancer model (Greenhalgh and Yuspa, 1988, Greenhalgh et al., 1990) and ROCK2 is typically thought to becomes active in later stage of cancer (Croft et al., 2004, Samuel et al., 2011). This study has demonstrated for the first time that ROCK2 contributes in the early stage of cancer as an initiator to induce benign papilloma formation in co-operation with fos. Initially, when *HK1.fos* mice developed hyperplasia and hyperkeratosis histotypes, bi-genic ROCK/fos mice at this period (12 weeks) also resulted in hyperplasia/hyperkeratosis, except it is much thicker with acanthosis appearance which have expanded stratum spinosum layer. Then, continued on benign papilloma formation at 18 weeks as shown by strong K1 expression in supra-basal layer, whilst *HK1.fos* mice still remained as hyperplastic/hyperkeratotic. This novel

data showed ROCK2 activation possessed as an initiator and thus confirmed ROCK2 roles in the early stage of tumourigenesis. Though previous study has shown the link between ROCK and fos where ROCK activation induced the transcriptional activity of c-fos serum response element in fibroblasts through in vitro study (Chihara et al., 1997). Yet, it was not in the context of multi-stage cancer events and now this study has revealed the importance role of ROCK2 as an initiator. Thus, data showed different roles of ROCK2 with each ras and fos; hence, co-operation between ROCK2 and ras/fos (below) would be beneficial to match the link between each gene.

One major and remarkable feature to the results in this novel bi-genic ROCK/fos activation model was the complete lack of malignant conversion. This happened in 100% of all animals created to date (> 50 if include the later bi-genic control cohorts in a variety of aged matched tri-genic siblings from different transgenic lines over a 2 year period). None of the mice exhibited even the signs of a potential for additional progression as late as 20 weeks unlike that observed in bi-genic ROCK/ras¹²⁰⁵ papillomas by approximately 8 to 10 weeks (e.g. reduced K1 expression). In addition, though bi-genic ROCK/fos benign papillomas showed an increased in the proliferation rates via Brdu analysis, yet it was considered low when compared to the bi-genic ROCK/ras papillomas (eight weeks). Thus, this intrigues a question of what was preventing the conversion to malignancy?, was it simply due to the context of correct papilloma had not been reached? Or was the wound promotion not sufficient and may need an additional event.

Hence, another recurrent theme appearing in all the skin models to date was the compensatory roles of p53 and p21 (Yao et al., 2006,2008, Macdonald et al., 2014) and it has been highlighted in respect to p21 expression in the cessation of 4-HT study on bi-genic ROCK/ras¹²⁰⁵ synergism (above). Yet, this bi-genic ROCK/fos model did not elicit the keratoacanthoma (KA) tumours of bi-genic fos/ Δ 5PTEN^{flx} where p53 and p21 expression were delayed and only expressed in overt benign tumours which is in the keratotic KA histotypes (Yao et al., 2008); whilst in bi-genic ROCK/ras¹²⁰⁵, p53/p21 expression seemed to appear relatively quickly. Further, analysis of p53/p21 expression profiles in bi-genic ROCK/fos cohorts showed high levels of p53 and p21 expression which appeared relatively early. In this study, both p53 and p21 expression remained strong over all the time periods analysed in ROCK/fos papillomas and just as observed in bi-genic

ras/Δ5PTEN^{flx} model (Yao et al., 2006, Macdonald et al., 2014) where both expression appeared to prevent further tumour progression. Indeed, bi-genic *HK1.ras/fos* control papillomas also possessed elevated p53/p21 profiles consistent with their lack of malignant progression (below). These data is in contrast to bi-genic ROCK/*ras¹²⁰⁵* tumours, where p53 loss in early malignant conversion and then trailed by p21 loss from the highly invasive pdSCC histotypes. This strong expression of both p53 and p21 in all epidermal layers of bi-genic ROCK/*fos* tumours is similar to the p53/p21 expression profiles in *HK1.ras¹²⁰⁵* tumours that remained benign; and indeed were prone to regression in the absence of wound or *fos* promotion. Initially, this study found that the phenotype for *K14.cre/Isl.ROCK^{er}/HK1.fos* tumours at 20 weeks was relatively similar to the phenotype of *HK1.fos/PTEN^{flx}* tumours, where both set of papillomas appeared highly keratotic (Yao et al., 2008). However, with time in this *HK1.fos/PTEN^{flx}* context, papillomas progressed to a KA histotype. In this alternate mechanism, the timing of p53/p21 expression was quite different and these highly keratotic KAs subsequently possessed with a unique premature expression of K1 in the basal layer which indicated acceleration in differentiation (Yao et al., 2008) geared to counter the excessive proliferation. Whilst the typical supra-basal expression of keratin K1 in bi-genic ROCK/*fos* and p53/p21 clearly demonstrated a different mechanism of papillomatogenesis which had a greater similarity to bi-genic ROCK/*ras¹²⁰⁵* papilloma formation. In addition, the uniform expression of keratin K6 in all epidermal layers of bi-genic ROCK/*fos* tumours gave a different result to the low level and patchy expressions of K6 in ROCK hyperplastic histotypes. This demonstrates that *fos* expression over rides the ROCK2 activation-mediated changes in K6 and this is consistent with the finding from *in vitro* studies. Here, keratin K6 expression was rescued back in 4-HT-treated of bi-genic ROCK/*fos* low Ca^{2+} medium similar to its expression in normal keratinocytes when compared to no expression of K6 in 4-HT-treated of *K14.cre/Isl.ROCK^{er}* (low Ca^{2+} medium). Thus, this K6 expression in bi-genic ROCK/*fos* tumours which is similar to a typical K6 expression in *HK1.ras* and *HK1.fos* hyperplasia (Greenhalgh et al., 1993a,b) may reflect in the differentiation and proliferation activities by both ROCK and *fos* activation, and it is possible that the differentiation activity induced by ROCK2 alone in terms of K6 expression were over-ridden upon co-operation with *fos* activation given its major responsibilities in keratinocyte differentiation (Mehic et al., 2005). However, this study showed that the papilloma context in bi-

genic ROCK/fos was insufficient to convert to malignancy thus required an additional mutation which link to tri-genic co-operation studies (below).

4.4 Co-operation of ROCK2 and *K14.cre/Δ5PTEN^{flx}* in transgenic mouse skin carcinogenesis

In contrast to bi-genic ROCK/ras and ROCK/fos studies, the third bi-genic ROCK/Δ5PTEN^{flx} model in this study failed to show evidence of tumour formation; yet showed its co-operation in epidermal differentiation. The majority of mutation studies on PTEN are widely focused on its role in tumour suppression via interactions with e.g. p53 and proliferation (Freeman et al., 2003) and the failure to regulate AKT (Mayo and Donner, 2002). However, not all roles leading to tumour formation which is p53/AKT related (Yao et al., 2006, 2008, Macdonald et al., 2014). An often neglected series of PTEN studies show that in some cancers, such as prostate cancer and lymphoma, disruption of cytoskeleton proteins and adherens junctions appear to be a significant component following PTEN mutation (Subauste et al., 2005). As loss of adherens junctions typically occurs in tumour cells and studies by Subauste et al., (2005) have shown that disruption in adherens junctions can suppress the level of PTEN protein expression. In addition, it is transpired that loss of PTEN induced migration activity independent of AKT and involved a complex with focal adhesion kinase (FAK) pathway (Yamada and Araki, 2001). Thus, in theory, this role of PTEN has a linkage to the role of ROCK in regulating adherens junctions (Sahai and Marshall, 2002) that may be essential in the context of cytoskeleton remodelling and cell adhesion (Holeiter et al., 2012) which help mediate carcinogenesis. Therefore, the lack of tumours in this bi-genic ROCK/Δ5PTEN^{flx} model may be due to a redundancy effect between ROCK and PTEN at this initiation stage that gives a weak oncogenic hit to the epidermal layers. Hence, the response results in epidermal hyperplasia/hyperkeratosis only; yet the changes to proliferative give a folded papillomatous appearance even at almost seven months instead of tumour formation.

These data clearly support a need for more potent, additional events perhaps needed to overcome important compensatory responses to ROCK/Δ5PTEN^{flx} induced hyperplasia in this case such as p53 and p21; and this reflects the importance of ROCK and PTEN to epidermal physiology. On the other hand, this

result may be technical, as here ROCK2 expression in ROCK/ Δ 5PTEN^{flx} mice is driven by CAG promoter, thus lack of tumours may be an old report that CAG promoter may be off in the proliferative basal layers (Berton et al., 2000b). This concern was eliminated as analysis of both GFP and p-Mypt1 in bi-genic ROCK/ Δ 5PTEN^{flx} displayed strong expression throughout epidermal layers including hair follicles, consistent with the expression in *K14.cre/lsl.ROCK^{er}* hyperplasia histotypes outlined above. Thus, these two hits may again be similar in terms of carcinogenesis. As previous studies implicate Δ 5PTEN^{flx} in changes to epidermal differentiation, they also found that it acts as a weak initiator for TPA promotion (e.g. fos activation) leading to tumour (KA) formation, but after long latency period (> 20 weeks) (Yao et al., 2006). ROCK2 activation only resulted in hyperplasia, thus, these data combined suggest this bi-genic ROCK/ Δ 5PTEN^{flx} model indicate that ROCK cannot act as a weak initiator in co-operation with Δ 5PTEN^{flx} compared to its co-operation with fos.

This is also reflecting in the expression profiles of both p53 and p21 in ROCK/ Δ 5PTEN^{flx} cohorts. As demonstrated in bi-genic ROCK/fos benign papillomas, high expression profiles of p53/p21 throughout epidermal layers became the reason for lack of malignant conversion (Yao et al., 2006, 2008). Interestingly, when compared to these ROCK/ Δ 5PTEN^{flx} cohorts, this study found low and patchy expression of both p53 and p21 appeared in the hyperplastic histotypes which indicate an inhibition of papilloma formation. However, it may not be as straight forward as it seems. Whilst both p53 and p21 are important tumour suppressor genes, previous study by Greenhalgh et al., (1996) showed a very odd and paradox effect of p53 loss on papillomatogenesis, where *HK1.ras¹²⁰⁵/p53* knockout mice failed to produce any tumours and their bi-genic epidermis stayed hyperplastic which implicates the importance and requirement of p53 for papilloma formation in some cases. On the other hand, it was expected that p-AKT1 would display a high level of expression due to inactivation of PTEN's ability to dephosphorylate AKT (Suzuki et al., 2003, Freeman et al., 2006). Here, surprisingly p-AKT1 showed only low and patchy expression in the bi-genic ROCK/ Δ 5PTEN^{flx} hyperplasia which would also contribute to the lack of tumours. Nevertheless, through careful observation, as noted in the p53/p21 expression profiles of ROCK/ Δ 5PTEN^{flx} hyperplasia, in the area of p53 loss, p21 showed strong expression leading to low level of p-AKT1 in the specific area. Thus, this lack of tumours in bi-genic ROCK/ Δ 5PTEN^{flx} cohorts may be accountable from the

elevated level of p21 expression either counterbalancing AKT activation or preventing its expression; a recurrent theme in this model discussed further below.

In addition, the complex roles in epidermal differentiation may be associated in this context too, as in formation of KAs in *fos/Δ5PTEN^{flx}* mice that showed lack of p53 and p21 expression during papilloma formation and expressed elevated AKT activation (Yao et al., 2008). This situation reversed once GSK3β inactivation achieved a certain level when p53 expression followed by p21 appeared and AKT was evicted from the basal layer and expression reduced, thus keratinocytes switched from proliferation to differentiation giving keratosis that highlights KAs (Yao et al., 2008). In this study, bi-genic *ROCK/Δ5PTEN^{flx}* hyperplasia possessed this potent compensatory response of patchy p53 and an elevated p21 countered the oncogenic p-AKT1 returning it to supra-basal expression. Both these profiles would not only prevent papillomatogenesis but would alter keratinocyte differentiation. Despite the absence of tumours in bi-genic *ROCK/Δ5PTEN^{flx}*, the hyperplastic histotypes in *K14.cre/Isl.ROCK^{er}/Δ5PTEN^{flx}* model were completely different to the hyperplastic in *ROCK2* activation and *PTEN^{flx}*. In addition, anomalous K1 expression by an expansion of proliferative basal layers, together with low level of K6 expression and patchy in the bi-genic *ROCK/Δ5PTEN^{flx}* papillomatous hyperplasia may reflect in both proliferation and differentiation on the epidermal layers. It may be that epidermal hyperproliferation in bi-genic *ROCK/Δ5PTEN^{flx}* as signified by the increased in mitotic index, was countered by an accelerated differentiation activity via *ROCK2* and *Δ5PTEN^{flx}* which may be the clues for lack of tumours similar to the switch to KAs (not SCCs) formation in *fos/Δ5PTEN^{flx}* mice (Yao et al., 2008).

Nonetheless, data showed that bi-genic *ROCK/Δ5PTEN^{flx}* required an additional event such as *fos* activation; whilst earlier data in this study has shown that bi-genic *ROCK/fos* model also required additional mutation for conversion and for bi-genic *ROCK/ras*, the correct context of wound promotion that prepared proper papilloma formation was essential before malignant conversion. Therefore, this investigation proceeds with tri-genic co-operation studies (below) in similar context of bi-genic tumours and at the same time matches a possible connection between *ras/MAPK/fos* and /or *PTEN/AKT* pathways with *ROCK2* activation in tumour formation.

4.5 Analysis of ROCK2 activation *in vitro*: effects on differentiation not carcinogenesis.

Given the lack of tumours in *K14.cre/Isl.ROCK^{er}/Δ5PTEN^{flx}*, primary keratinocytes were established to address changes in differentiation, or transformation by increasing calcium concentrations (Hennings et al., 1980) and assessing if they grew in high calcium conditions (Morgan et al., 1992). Thus, primary transgenic mouse keratinocytes were established from bi-genic *K14.cre/Isl.ROCK^{er}/fos* and *K14.cre/Isl.ROCK^{er}/Δ5PTEN^{flx}* or *K14.cre/Isl.ROCK^{er}* keratinocytes and challenged with different concentrations of calcium to differentiate or grow in high calcium media. Their responses were compared to control *HK1.fos* and *K14.cre/Δ5PTEN^{flx}* via western analysis. Unfortunately, *K14.cre/Isl.ROCK^{er}/ras¹²⁷⁶* and *HK1.ras* keratinocytes failed to grow in this study due to oncogene ras induced senescence. Interestingly, keratin K1 expression which is normally weak in low calcium medium appeared at high expression levels in activated *K14.cre/Isl.ROCK^{er}* keratinocytes, whilst the hyperproliferative keratin K6 in the same condition showed abnormally low levels of expression. These data suggest that ROCK2 is involved in keratinocyte differentiation. This idea is supported by previous studies of ROCK2 knockdown in HaCat cells which showed reduced differentiation (Lock and Hotchin, 2009). Therefore, these previous studies, as well as this *in vitro* study have highlighted the roles of ROCK2 activation in keratinocyte differentiation which is an important component in epidermal homeostasis. Moreover, given that ROCK expression which typically appeared in supra-basal layers *in vivo*, as shown in *ras/fos/Δ5PTEN^{flx}* hyperplastic and papillomas histotypes, but in the *in vitro* context, when ROCK activity was forced to express in low calcium medium, it affects the increased levels of early K1 expression which associated with ROCK2 functions in differentiation.

Intriguingly, keratin K1 status appeared completely reversed in both *K14.cre/Isl.ROCK^{er}/Δ5PTEN^{flx}* and *K14.cre/Δ5PTEN^{flx}* keratinocytes giving high levels in low calcium medium but low levels of K1 expression in high calcium medium, which is in sharp contrast to typical K1 expression in normal keratinocytes. Typically in normal mouse keratinocytes, K1 appeared in a higher degree of expression upon induction of high calcium as keratinocytes naturally differentiate. This unique low level of K1 expression in high calcium medium could

correspond to the delay in K1 expression given the increased in basal layers observed in hyperplastic *K14.cre/Isl.ROCK^{er}/Δ5PTEN^{flx}* and the later *K14.cre/Δ5PTEN^{flx}* histotypes due to an increase in keratinocyte proliferation. One thing is clear is that inactivation of PTEN phenotypes is linked to this observation. It may be due to activated AKT activity that alter the keratinocyte differentiation, since both *K14.cre/Isl.ROCK^{er}/fos* and *HK1.fos* keratinocytes showed the typical fashion of K1 expression similar to normal keratinocytes. Moreover, this is still in speculation since it is concern that the outcome from *in vitro* may not be the same as *in vivo*. One possibility is that in the *K14.cre/Δ5PTEN^{flx}* epidermis, p-AKT expression is selective and typically observed in supra-basal layers compared to p-AKT expression in *K14.cre/Δ5PTEN^{flx}* keratinocytes culture where it is expressed all the time (Yao et al., 2006). Thus, it is speculate that high K1 expression in the low calcium media of both *K14.cre/Isl.ROCK^{er}/Δ5PTEN^{flx}* and *K14.cre/Δ5PTEN^{flx}* keratinocytes may be due to activated AKT mediating proliferation that was countered by more keratinocyte differentiation leading to K1 expression. Therefore, this may explains for the higher expression of the differentiation keratin K1 in low calcium medium of both *K14.cre/Isl.ROCK^{er}/Δ5PTEN^{flx}* and *K14.cre/Δ5PTEN^{flx}* keratinocytes. Whilst, in the context of high calcium medium, these data suggest that activated AKT is now a potent oncogenic insult, thus induce inhibition of differentiation as reflected by the low levels of K1 expression in both *K14.cre/Isl.ROCK^{er}/Δ5PTEN^{flx}* and *K14.cre/Δ5PTEN^{flx}* keratinocytes. Thus, this may explains that the appearance of both *K14.cre/Isl.ROCK^{er}/Δ5PTEN^{flx}* and *K14.cre/Δ5PTEN^{flx}* keratinocytes were not fully deteriorated even after induction of second high calcium switch (0.15 mM) compared to other transgenic keratinocytes in the same condition.

At the same time, the elevated of K1 expression in low calcium medium which indicates the roles of ROCK2 in differentiation activity was accompanied by lack of K6 expression in the same condition upon ROCK2 activation. This is consistent with early findings of low levels and patchy of K6 expression in *K14.cre/Isl.ROCK^{er}* hyperplasia histotypes, despite the fact that K6 marker is typically express strongly in response to hyperproliferation or wounding (Schermer et al., 1989). On the other hand, keratin K6 expression in low calcium medium was notably restored in *K14.cre/Isl.ROCK^{er}/fos* and *K14.cre/Isl.ROCK^{er}/Δ5PTEN^{flx}* keratinocytes parallel to K6 expression in normal keratinocytes. For *K14.cre/Isl.ROCK^{er}/fos* keratinocytes, this outcome is consistent with strong and uniform K6 expression accompanied by

hyperproliferation or in response to wounding in *K14.cre/Isl.ROCK^{er}/fos* benign papillomas. However, in *K14.cre/Isl.ROCK^{er}/Δ5PTEN^{flx}* and *K14.cre/Δ5PTEN^{flx}* keratinocytes, again, restored K6 expression may be responsive to p-AKT-mediated proliferation activity as it is expressed all the time (Yao et al., 2006). Nonetheless, none of the bi-genic keratinocytes showed resistance to high calcium which is a classic indicator of malignant transformation (Morgan et al., 1992) and this outcome is in accordance to the *in vivo* data where there is no evidence of malignancy in *K14.cre/Isl.ROCK^{er}*, *K14.cre/Isl.ROCK^{er}/fos* and *K14.cre/Isl.ROCK^{er}/Δ5PTEN^{flx}* mice.

4.6 Co-operation of ROCK2, *HK1.ras* and *HK1.fos* in transgenic mouse skin carcinogenesis

A major goal of this study was to assess ROCK2 activation in skin carcinogenesis via a mimic of the two-stage DMBA/TPA studies performed earlier on *K14.ROCK^{er}* mice with a view to identifying the co-operating genes, determine at which stage the 4-HT-activated ROCK2 becomes causal and investigate the subsequent progression mechanism. As outlined in the introduction, the bi-genic *ras^{Ha}/fos* model is a mimic of the two-stage chemical carcinogenesis model (Greenhalgh and Yuspa, 1988, Greenhalgh et al., 1990) where *in vitro* co-operation resulted in malignancy; whereas in transgenic mice *HK1.ras¹²⁷⁶/fos* produced a persistent papillomas with no sign of regression (Greenhalgh et al., 1993c); a result now attributed to elevated compensatory p53/p21 profiles (Macdonald et al., 2014). The initial bi-genic ROCK/*ras¹²⁰⁵* studies found that co-operation mainly centred on the conversion stage from papilloma to carcinoma context. This apparently required wound-associated promotion to achieve the correct papilloma context for ROCK causality; which then drove malignant progression to the point where the spontaneous progression momentum no longer required exogenous ROCK^{er}. Excitingly, bi-genic ROCK/*fos* revealed for the first time a novel early co-operation between ROCK2 and *fos* in benign papilloma formation. Thus, this finding was consistent with ROCK being a downstream effector of ras signalling; possibly performing an initiating role for co-operation with *fos*, similar but less potent to that observed in *HK1.ras¹²⁷⁶/fos* mice (Greenhalgh et al., 1993c). However, no malignant conversion was observed in the bi-genic ROCK/*fos* context. These data also suggest that ras activation was required to achieve the correct papilloma

context that facilitated causal roles for ROCK in conversion and tested in the tri-genic ROCK/ras¹²⁷⁶/fos models and compared with ROCK/fos and ROCK/ras carcinogenesis involving mutant PTEN and deregulation of AKT signalling.

Remarkably, all tri-genic lines (ROCK/ras¹²⁷⁶/fos, ROCK/fos/ Δ 5PTEN^{flx} and ROCK/ras¹²⁷⁶/ Δ 5PTEN^{flx} (and ROCK/ras¹²⁰⁵/ Δ 5PTEN^{het})) resulted in a synergism that directly led to malignancy in 100% of animals. Here, in the first tri-genic *K14.cre/lsl.ROCK^{er}/ras¹²⁷⁶/fos* model, activated ras^{Ha} provides the initiation step and activated fos oncogene provides the promotion; thus co-operation of both oncogenes with ROCK2 activation then resulted in direct malignancy conversion but progression was still relatively limited and this tri-genic synergism achieved mainly wdSCC and SCC histotypes. This study was originally tailored to mimic the previous study by Samuel et al., (2011) where *K14.ROCK^{er}* mice were induced with both DMBA/TPA resulted in increased carcinomas. This tri-genic ROCK/ras¹²⁷⁶/fos synergism also gave a similar conclusion of malignant conversion and also identified that a specific context of papillomas had to develop since there was lack of papillomatogenesis in bi-genic ROCK/ras¹²⁷⁶ mice; whilst both bi-genic ROCK/fos and ras¹²⁷⁶/fos (Greenhalgh et al., 1993c) developed benign papillomas with no sign of malignant conversion. Furthermore, although in this ROCK/ras¹²⁷⁶/fos model, both ras and fos appeared to provide the initiation and promotion elements (which mimic the DMBA/TPA carcinogenesis), but following ROCK2-mediated conversion, the tumours appeared mainly as wdSCCs with some progression of SCC nests histotypes.

In comparison, the other two tri-genic (with PTEN) models demonstrated more aggressive SCC histotypes consistent with deregulation of both MAPK kinase and PTEN/AKT signalling in co-operation with ROCK2 activation; a result similar to TPA promotion of bi-genic ras¹²⁷⁶/ Δ 5PTEN^{flx} mice (Yao et al., 2006). This difference was due to strong and persistent expression of p21 in all epidermal compartments of ROCK/ras¹²⁷⁶/fos tumours in comparison to the other two tri-genic models. Moreover, though p53 appeared faded, and is typically associated with reduced expression in late-stage papillomas (Macdonald et al., 2014). Whilst some traces of residual p53 expression were noted in the supra-basal layers, it was the high levels of basal p21 expression in the wdSCC/SCC histotypes that appears to inhibit the early stages of malignant progression. This compensatory

p53/p21 expression followed the same pattern in the previous tri-genic $ras^{1276}/fos/\Delta 5PTEN^{flx}$ carcinogenesis where p21 showed strong expression in the basal layer upon p53 loss that delays tumour progression through differentiation activity (Macdonald et al., 2014).

This study proves that ROCK2 activation plays a key role in the malignant transformation; although it is undeniable that there is no tumour growth in *HK1.ras¹²⁷⁶* mice without fos promotion (Greenhalgh et al., 1993c) as confirmed in bi-genic ROCK/ ras^{1276} and the need for wounding in ROCK/ ras^{1205} cohorts. This model also identifies the role for ROCK as a malignant converter in bi-genic ras^{1276}/fos mice since these tumours still remained benign papillomas (Greenhalgh et al., 1993c) and this was due to strong p53/p21 expression (Macdonald et al., 2014) before ROCK2 activation managed to turn to carcinomas; as discussed above in bi-genic ROCK/ ras^{1205} co-operation studies. Here, in tri-genic ROCK/ ras^{1276}/fos a similar compensatory p21 expression limited early stage progression, but given the goal to contrast with other tri-genic (with PTEN) models, AKT was investigated and these data showed that the lack of aggressive SCCs may be due to a lack of AKT deregulation. This proved to be a major difference in the models and shows the consequences of MAPK and PTEN/AKT in conjunction with ROCK mediated progression. This again has consequences for therapies and makes ROCK as a good dual target where both MAPK and AKT are disrupted.

One more interesting outcome in this tri-genic ROCK/ ras^{1276}/fos model was analysis of AKT signalling, as here, the tri-genic histotypes exhibited no activated p-AKT1 expression even in the areas with p53 loss. Following malignant transformation in tri-genic ROCK/ ras^{1276}/fos mice, and histotypes confirmed by routine loss of keratin K1/p53 expression in the wdSCC/SCC area, thus it was expected that there would be high expression of activated AKT. It is known that there is an interrelationship between p53 and AKT roles in cell death versus cell growth that commonly being disrupted during cancer; as p53 can essentially trigger PTEN suppressor gene expression leading to deactivation of AKT activity (Haupt et al., 2003). Whilst in reverse, activated AKT can activate MDM2 activity and degrade p53 to promote proliferation and cell survival (Mayo and Donner, 2002, Haupt et al., 2003). Therefore, from the evidence of no p-AKT1 expression, this study indicates that the malignancy transformation in tri-genic ROCK/ ras^{1276}/fos model appeared to have a unique lack of a link to p-AKT

activation in the presence of a fully functional PTEN tumour suppressor gene. This result is unclear, and may be due to the significant levels of p21 expression observed, or that p-AKT1 is unnecessary in this context of malignant progression mediated by ROCK/ras¹²⁷⁶/fos co-operation. In a tri-genic study on ras¹²⁷⁶/fos/ Δ 5PTEN^{flx} mice, increasing levels of p-AKT expression appeared following inactivation of PTEN activity and upon loss of p53/p21 expression in aggressive SCCs (Greenhalgh, – manuscript in preparation). However, in papillomatogenesis and malignant conversion, it was mTOR activation that appeared to drive the mechanism and supercede by AKT on progression of wdSCC to SCC (Greenhalgh, - manuscript in preparation).

These observations again highlight the differences and similarities involving these pathways and that the context produced by differing mutations is important to the final outcome. Thus, this study shows that the interaction between ROCK and ras/MAPK signalling pathway essentially provides the correct papilloma context where ROCK2 activation contributes to the later stages of carcinogenesis. These data are important to the design of new therapeutic targets, in particular this study designed to find an Achilles Heel to counter ras-mediated carcinogenesis. As to date, there are still continuous studies to find a clinically-approved way to inhibit ras in context of cancer therapy. Therefore, this study suggests that targeting ROCK2 signalling could be an effective approach to target ras signalling since ROCK acting downstream of ras family, not only functions as an initiator in papillomatogenesis alongside fos activation, but also act as a key role in malignant conversion and progression. Moreover, based on data below, it appears that ROCK plays a primary role in malignant progression to quite aggressive carcinomas when both MAPK and AKT signalling are disrupted.

4.7 Co-operation of ROCK2, *HK1.fos* and *K14.cre/ Δ 5PTEN^{flx}* in transgenic mouse skin carcinogenesis

In the bi-genic models, activated ROCK^{er} and fos co-operation resulted in highly keratotic, benign papilloma formation, but unlike bi-genic ROCK/ras¹²⁰⁵, no malignant conversion was observed. These data revealed a novel early co-operation between ROCK and fos signalling deregulation in papillomatogenesis

where ROCK2, being downstream of ras, may substitute an initiation role. In addition, the tri-genic ROCK/ras¹²⁷⁶/fos section also demonstrated that ROCK2-mediated carcinogenesis required the late stage autonomous papilloma context supplied by *HK1.ras*¹²⁷⁶/fos synergism, but only achieved a limited progression to wdSCC/SCC; possibly due to elevated p21 and the surprising lack of AKT activation. Given that very little synergism was observed in *K14.cre/Isl.ROCK^{er}/Δ5PTEN^{flx}* cohorts and this lack of AKT in tri-genic ROCK/ras¹²⁷⁶/fos models, these data suggested that ROCK2 activation appeared to be a specific partner in crime to deregulation of the MAPK; and that the PTEN/PI3K/AKT pathway was not involved in ROCK mediated mechanisms. If so, this would have serious implications for the design of new therapies. This seemed unlikely, and as observed above, a simple explanation was that the appropriate context was not achieved in this tri-genic context; as observed by *K14.cre/Isl.ROCK^{er}/Δ5PTEN^{flx}* synergism, either due to redundancies or compensatory responses such as rapid elevation of p53/p21 expression or a lack of AKT activation. As noted for *K14.ROCK^{er}/HK1.ras*¹²⁰⁵ co-operation, a significant oncogenic gap exists between event supplied by PTEN mutation at the initiation stage and roles for ROCK activation at the later stages of carcinogenesis.

Further, it was possible that PTEN mutation may drive a different mechanism of carcinogenesis, as discovered when introduced into the *HK1.fos* model resulting in KAs (Yao et al., 2008). In this fos/Δ5PTEN^{flx} context, no evidence of malignancy was recorded due to GSK3β inactivation; which induced a compensatory p53/p21 expression that had been previously missing in the early hyperplasia, a result different to these ROCK2 models here, and this expression of p53/p21 diverted proliferative papilloma keratinocytes into programme of terminal differentiation and keratosis/KA formation (Yao et al., 2008). Indeed, this roles of GSK3β would be of major interest to these studies given the putative interactions of ROCK signalling with β-catenin (Samuel et al., 2011) which is a prime degradation target of GSK3β (Ghosh and Altieri, 2005). Also, *K14.cre/Isl.ROCK^{er}/Δ5PTEN^{flx}* co-operation already identified changes in epidermal differentiation *in vivo* and *in vitro* (lack of K6 /premature K1) that are consistent with an inhibition of early neoplasia.

Hence, given this background from the bi-genic synergisms of ROCK/ras¹²⁰⁵ and ROCK/fos to tri-genic ROCK/ras¹²⁷⁶/fos model, the data demonstrated that the deregulation of MAPK signalling pathway appears to be a crucial partner for

ROCK2-mediated tumourigenesis. If so, generation of these *K14.cre/Isl.ROCK^{er}/fos/Δ5PTEN^{fix}* cohorts in essence assessed whether additional mutation events in ROCK signalling coupled to addition of deregulated AKT signalling would change the outcome from KA to SCC; and if so, this allowed investigation of how (and when) the protective p53/p21 expression was circumvented. Indeed, it seems that PTEN/PI3K/AKT pathway is a weak target for co-operation with ROCK2 activation since bi-genic ROCK/Δ5PTEN^{fix} showed no evidence in papillomatogenesis even after almost 7 months. However, it was possible that introduction of p-AKT1 expression in the tri-genic ROCK/fos/Δ5PTEN^{fix} model could be the facet that produce the correct context for malignant conversion mediated by ROCK.

This proved to be the case as *K14.cre/Isl.ROCK^{er}/fos/Δ5PTEN^{fix}* mice demonstrated rapid formation of overt keratotic papillomas that transformed to aggressive SCC as early as 9 weeks. This tri-genic synergism showed direct co-operation between ROCK2 activation and bi-genic fos/Δ5PTEN^{fix} to change the final outcome from KAs (Yao et al., 2008) to SCC. Moreover, whilst ROCK2 activation clearly acts as an initiator with fos papillomatogenesis, this study suggests that ROCK2 activation now also acts to transform the fos/Δ5PTEN^{fix} papillomas into a carcinoma in this tri-genic model (ROCK/fos/Δ5PTEN^{fix}). Thus in this sense, the outcome seems to be more similar to previous tri-genic ras¹²⁷⁶/fos/Δ5PTEN^{fix} synergism (Macdonald et al., 2014) and the outcome of tri-genic ROCK/ras¹²⁷⁶/fos (above). Here, a rapid increase in p53/p21 expression was displayed in the ROCK/fos/Δ5PTEN^{fix} earlier hyperplasias associated with loss of filaggrin and loricrin expression upon malignancy. This was very different pathway to that of KA formation in previous bi-genic fos/Δ5PTEN^{fix} mice (Yao et al., 2008) and suggests that the co-operation between ROCK and fos already locks in the final tumour outcome, but at this early stage as also observed in tri-genic ras¹²⁷⁶/fos/Δ5PTEN^{fix} wdSCCs, where it was p21 expression that limited further malignant progression (Macdonald et al., 2014).

However, in this study, the tri-genic ROCK/fos/Δ5PTEN^{fix} model managed to convert to wdSCC and also advanced to progressive SCC histotypes; and now it appears AKT activation is playing a role in driving this progression alongside ROCK activation. This mechanism involved loss of keratin K1 and p53 expression in late stage papillomas, and following conversion in

K14.cre/lsl.ROCK^{er}/fos/Δ5PTEN^{flx} mice, p21 expression had also become reduced and now became supra-basal in the more aggressive SCCs. Thus, the activated AKT may now freely function in these wdSCC/SCC basal layers to induce more proliferation as shown by Brdu-labelling and this in turn suggests a loss of cell cycle control adds to ROCK co-operation in altering tissue stiffness and driving further progression.

This latter idea is supported by the observation that tri-genic ROCK/fos/Δ5PTEN^{flx} tumours also displayed thick and invasive proliferative layers with some intercellular gaps that are among the distinguish features of malignant progression. Therefore, this tri-genic outcome is consistent with ROCK activity being associated with late stage carcinogenesis (Croft et al., 2004, Samuel et al., 2011, Morgan-Fisher et al., 2013) with now a clear role for its co-operation with deregulated PTEN/PI3K/AKT together with fos/MAPK. Further, as the tumours in tri-genic ROCK/fos/Δ5PTEN^{flx} appeared more aggressive than tri-genic ROCK/ras¹²⁷⁶/fos, this dual activation of PTEN/AKT and fos/MAPK pathways may provide a proliferative context where ROCK2 functions in induction of tissue stiffness may accelerate epidermal proliferation and tumour progression.

In addition, this ROCK2 activation mediated progression may be accompanied by changes in β-catenin transcriptional activity that adds to cell motility and stiffness (Kumper and Marshall, 2011, Samuel et al., 2011). If so, this increased tissue stiffness would also affect in changes of epithelial morphogenesis (Jaalouk and Lammerding, 2009), such as the gaps observed between SCC keratinocytes. Since it is become known that ROCK activation mediates actomyosin contraction which induce tissue stiffness (Kumper and Marshall, 2011, Samuel et al., 2011), a stiffer tissue associated with invasion phenotypes (Jaalouk and Lammerding, 2009), may be more brittle and easily fractures during histological processing. Thus, this would explain the odd rips notably displayed in the SCC areas together with some intercellular gaps in the epidermis which do not appeared in *fos/Δ5PTEN^{flx}* keratotic papillomas or in any early bi-genic ROCK/fos benign tumours. Therefore this indicates that in tumour morphogenesis, the increased tensile strength that emerges due to ROCK activation is also an important biomechanical feature to influence the status of tumourigenesis in addition to biochemical signals. Thus, the availability of these tumours (and also in those of

K14.cre/lsl.ROCK^{er}/ras¹²⁷⁶/Δ5PTEN^{flx} and *K14.ROCK^{er}/ras¹²⁰⁵/Δ5PTEN^{het}* genotypes) will greatly aid in the investigation of this progression mechanism.

The finding that tri-genic ROCK/fos/Δ5PTEN^{flx} co-operation produced SCCs was very different to the outcome of bi-genic fos/Δ5PTEN^{flx} synergism which progressed to KAs after 5 to 6 months (Yao et al., 2008). In this study, control fos/Δ5PTEN^{flx} mice were kept on procedure for 9 weeks only and thus, have yet to develop a KA histotype. Nonetheless, in terms of an altered differentiation profile, whilst the tri-genic mice shown few features of KA, they did display highly keratotic papillomas and some indications of pre-mature differentiation, e.g. formation of micro-cysts in the papillomas and wdSCCs. Further, in *K14.cre/lsl.ROCK^{er}/fos/Δ5PTEN^{flx}* tumours, there are some microcysts embedded in the epidermal layers due to this fos/Δ5PTEN^{flx}-associated anomalous differentiation (Yao et al., 2008). However, although both *K14.cre/lsl.ROCK^{er}/fos/Δ5PTEN^{flx}* and *K14.cre/fos/Δ5PTEN^{flx}* tumours have this anomalous differentiation feature, the tri-genic ROCK/fos/Δ5PTEN^{flx} mice did not exhibit the odd premature basal K1 expression (Yao et al., 2008), nor was tri-genic ROCK/fos/Δ5PTEN^{flx} differentiation accompanied by strong loricrin and filaggrin. These data again highlight that at quite early stages the progression mechanism had become quite different and also highlighted the difference between these two tumours highlighted that ROCK activation during papillomatogenesis may increase the chance of malignant outcome.

Moreover, in *K14.cre/lsl.ROCK^{er}/fos/Δ5PTEN^{flx}* tumours, although K1 expression persisted in the microcysts in response to the mixed proliferation/differentiation signals, rapid loss of K1, together with loss of loricrin and filaggrin was again displayed upon conversion to wdSCC and rapid progression to SCC. This loss of the later markers of terminal differentiation (loricrin and filaggrin) indicated an acceleration in keratinocyte proliferation possibly mediated by elevated AKT expression in conjunction MAP Kinase activation and this combination lead to the loss of compensatory p21 expression (Macdonald et al., 2014, Greenhalgh, - manuscript in preparation). In tri-genic ROCK/fos/Δ5PTEN^{flx} SCCs, the tumours demonstrated elevated p-AKT1 expression following loss of p53 expression and now p21 expression appeared more supra-basal. This observation is consistent with p53/p21 loss in tri-genic ras¹²⁷⁶/fos/Δ5PTEN^{flx} mice where aggressive SCCs first co-express p-AKT1 and p21 in basal layers, but in older SCCs, expression of

p-AKT increased whilst p21 expression disappears (Greenhalgh, – manuscript in preparation).

This finding was also observed to a greater degree in the ultimate tri-genic ROCK/ras/PTEN model; where it is consistent with low levels of p53/p21 status as in this study, supra-basal p-AKT1 expression became basal and upon loss of p21 expression accelerated SCC progression to pdSCCs. This is in sharp contrast to lack of p-AKT1 expression in tri-genic ROCK/ras¹²⁷⁶/fos model where only wdSCCs/SCCs resulted. Collectively, these observations imply that to the inactivation of PTEN activity and induction of AKT activity together with MAP Kinase deregulation, increases proliferation in this tri-genic ROCK/fos/ Δ 5PTEN^{fix} model where an overlay of ROCK mediated activities in for instance increasing tissue stiffness contributed to the progression (Kumper and Marshall, 2011, Samuel et al., 2011). This again suggest that ROCK may be a useful therapeutic target affecting both pathways (Downward, 2003, Rath and Olson, 2012) and in a final series of experiments, this idea of ROCK activity in tissue stiffness overlaid onto deregulated MAPK and PTEN/AKT was stringently tested in the more potent in tri-genic ROCK/ras/PTEN model.

4.8 Co-operation of ROCK2, *HK1.ras* and *K14.cre/ Δ 5PTEN^{fix}* in transgenic mouse skin carcinogenesis

As discussed above in a *K14.cre/ Δ 5PTEN^{fix}* background, ROCK activation showed little co-operation; with no evidence of tumour formation even after seven months. Whilst there were alterations in differentiation indicated by K1/K6 analysis, this combination appeared impotent or was subjected to the elevated compensatory p53/p21 and thus lacked of p-AKT expression. This lack of *K14.cre/Isl.ROCK^{er}/ Δ 5PTEN^{fix}* tumours also contrasted with previous *K14.cre/ Δ 5PTEN^{fix}* co-operation with *HK1.ras¹²⁷⁶* which demonstrated a regular papillomatogenesis but malignant conversion required TPA (to activate c-fos) to elicit a very rapid progression to malignancy (Yao et al., 2006). Here, following only 2-3 weeks of TPA promotion, both p53 and p21 were early casualties in this rapid malignant progression (Yao et al., 2006); a result again consistent with malignant conversion mechanism observed in the tri-genic ras¹²⁷⁶/fos/ Δ 5PTEN^{fix}

models (Macdonald et al., 2014). For comparison, co-operation between ROCK and *HK1.ras*¹²⁰⁵ did achieve malignant conversion, and this appeared dependent upon the promotion stimulus received from wounding. In all the previous ROCK models, the majority of mice exhibited wdSCCs with the occasional mix of more aggressive SCCs, and this was likely due to persistent p21 expression following loss of p53, possibly antagonising p-AKT1. Thus, this may suggest a common compensatory response to inhibit the early stages of malignant progression. However, as shown in *K14.ROCK^{er}/HK1.ras*¹²⁰⁵ mice, the tumours produced were prone to spontaneously progress (at 16 – 18 weeks) and it appeared that exogenous ROCK2 could drive the progression to pdSCC histotypes, but subsequent finding shows that once SCC histotype had been achieved, exogenous ROCK2 appeared no longer necessary; possibly given the elevated levels of endogenous ROCK (1 and 2) expressed upon malignant progression as displayed in the introduction (Samuel et al., 2011).

Therefore, this ultimate tri-genic genotype was geared to assess whether ROCK2 co-operation with *HK1.ras*¹²⁷⁶ (and later *HK1.ras*¹²⁰⁵) in the context of mutated PTEN, could achieve an accelerated malignant progression to elicit SCC/pdSCC. This would test the idea that the combination of ROCK/*ras*¹²⁷⁶ and a Δ 5PTEN^{flx}-mediated loss of AKT regulation overcame the compensatory p53/p21 responses. Indeed, this proved to be the case and also highlighted that once the appropriate context had been achieved, despite even taking a seriously long time to achieve a papilloma, malignant conversion and progression to aggressive SCC did not need large-sized tumours. Initially, in this final tri-genic model, ROCK2 co-operation had to be assessed in *ras*¹²⁷⁶/ Δ 5PTEN^{flx} as total loss of PTEN function in *HK1.ras*¹²⁰⁵ mice had proved to be too severe. Interestingly, not only was tri-genic ROCK/*ras*¹²⁷⁶/ Δ 5PTEN^{flx} synergism observed, but also this tri-genic model demonstrated that despite taking many weeks to achieve a papilloma, progression to SCC was rapid with a mix of pdSCC histotypes; which was one of the most aggressive histotypes produced when compared with other two tri-genic models (ROCK/*fos*/ Δ 5PTEN^{flx} and ROCK/*ras*¹²⁷⁶/*fos*). Although in the beginning, given the small size of tumours observed in these tri-genic ROCK/*ras*¹²⁷⁶/ Δ 5PTEN^{flx} mice compared to larger tumours produced in the other 2 tri-genic models, this histotype outcome was totally unexpected. Though, this outcome may be understandable due to lack of tumours in bi-genic ROCK/*ras*¹²⁷⁶ and ROCK/ Δ 5PTEN^{flx} mice.

It became very clear that even in these tiny tumours, activated ROCK2 triggered malignant conversion and promoted malignant progression to pdSCCs. Whereas, previous bi-genic $ras^{1276}/\Delta 5PTEN^{flx}$ models exhibited no evidence of malignancy, unless promoted with TPA (Yao et al., 2006), or had fos included but even here the tumour outcome was mainly wdSCC due to the p21/AKT interaction (Macdonald et al., 2014). In the tri-genic ROCK/ $ras^{1276}/\Delta 5PTEN^{flx}$ mice, malignant progression to pdSCC histotypes demonstrated numerous finger-like projections into the dermis, and was confirmed by complete keratin K1 loss. Moreover, despite their small size, these tri-genic tumours were accompanied by remarkable and complete loss of both p53/p21 expression. Also this was now coincided with increased p-AKT1 expression in all epidermal layers, and a massive BrdU labelling scattered throughout the tumour and indicated a massive increase in proliferation consistent with both p53 and p21 loss.

This early loss of both p53 and p21 may be the significant highlight that driving the difference in malignant progression between tri-genic ROCK/ $ras^{1276}/\Delta 5PTEN^{flx}$ models and other tri-genic models of this study. Interestingly, lack of p21 expression appeared even in the tri-genic ROCK/ $ras^{1276}/\Delta 5PTEN^{flx}$ wdSCC areas, following complete loss of p53. The most significant previous tri-genic observation closest to this tri-genic result was wdSCC progression to SCC of tri-genic ROCK/ $fos/\Delta 5PTEN^{flx}$ mice where p21 expression became supra-basal upon p53 loss, in which released p-AKT expression to drive progression to aggressive SCCs possibly in conjunction with ROCK2 activation. Thus, the p21 loss reflected strong and basal p-AKT1 expression and may help explain the development of the most aggressive carcinomas produced in this tri-genic model to date. This consistent finding of p-AKT1 expression even in $K14.cre/Isl.ROCK^{er}/ras^{1276}/\Delta 5PTEN^{flx}$ wdSCC basal histotypes induced more proliferation activity that coincided with total loss of p53 and p21 expression, compared to supra-basal p-AKT1 expression due to persisted p21 expression in $K14.cre/Isl.ROCK^{er}/fos/\Delta 5PTEN^{flx}$ tumours.

Further, it is intriguing that this tri-genic ROCK/ $ras^{1276}/\Delta 5PTEN^{flx}$ model was able to achieve pdSCC histotypes, yet, it took about 5 to 6 months of 4-HT treatment before an apparent instant malignant conversion and rapid progression to pdSCCs. This may imply a lack of sensitivity to promotion during the papillomatogenesis phase in this tri-genic model, as $HK1.ras$ line 1276 is insensitive to wound promotion (Greenhalgh et al., 1993a). This was shown in bi-

genic ROCK/ras¹²⁷⁶ mice, whereas in bi-genic ROCK/ras¹²⁰⁵ mice, wound promotion was essential to achieve a proper papilloma formation to form before conversion to malignancy was mediated by ROCK. Therefore, if this was correct, it was theorised that in additional tri-genic ROCK/ras¹²⁰⁵/Δ5PTEN^{het} models where *HK1.ras* line 1205 was sensitive to wound promotion (Greenhalgh et al., 1993a) would the large tumours produced be susceptible to malignant conversion. And if so, would they also exhibit a rapid progression to pdSCCs as observed at 16-18 weeks in bi-genic ROCK/ras¹²⁰⁵ mice (above) or as observed in TPA treated bi-genic ras¹²⁷⁶/Δ5PTEN^{fix} mice (Yao et al., 2006); where significant levels of endogenous ROCK (1 and 2) had been observed upon tumour progression as shown in the introduction.

Indeed, this proved to be the case as large tumours appeared in all tri-genic ROCK/ras¹²⁰⁵/Δ5PTEN^{het} mice which were obviously malignant whereas bi-genic ras¹²⁰⁵/Δ5PTEN^{het} mice produced clusters of autonomous papillomas (Yao et al., 2006). These tri-genic ROCK/ras¹²⁰⁵/Δ5PTEN^{het} tumours rapidly produced SCCs that had progressed to pdSCCs in just 4 to 6 weeks. Here, again these data prove the important roles of ROCK2 activation in both malignant conversion and progression. Further, this ROCK/ras¹²⁰⁵/Δ5PTEN^{het} synergism also resulted an immediate loss of both compensatory p53/p21 status; as observed in TPA-treated ras¹²⁷⁶/Δ5PTEN^{fix} experiments, which again gave increased p-AKT activity throughout the tumours, as observed in the complementary tri-genic ROCK/ras¹²⁷⁶/Δ5PTEN^{fix} model. Moreover, p53 loss had occurred even during late stage papilloma followed by supra-basal p21 expression, before both p53/p21 disappeared upon malignancy, and this highlights the remarkable rapid tumour progression in this tri-genic ROCK/ras¹²⁰⁵/Δ5PTEN^{het} model as compared to p53/p21 status in other malignancies from tri-genic ROCK/fos/Δ5PTEN^{fix} and ROCK/ras¹²⁷⁶/fos or bi-genic ROCK/ras¹²⁰⁵ models.

Furthermore, this feature of ripped tissue during histological processing of these ROCK/ras¹²⁰⁵/Δ5PTEN^{het} SCCs which also appeared in tri-genic ROCK/fos/Δ5PTEN^{fix} SCCs, that provides strong evidence that ROCK2 activation mediated an increased tissue stiffness and possibly mediated cell migration that gave rise to the intercellular gaps (Kumper and Marshall, 2011, Samuel et al., 2011). Although the appropriate mechano-analysis has yet to be performed (Samuel et al., 2011), the tenascin C data would seem to support this idea

together with data that have shown that ras oncogene mediated extracellular signal regulated kinase (ERK) activation can also induce tissue stiffness via increased cellular tension (Jaalouk and Lammerding, 2009). Thus, the link between ras/ERK and ROCK pathways-mediated tissue stiffness (Jaalouk and Lammerding, 2009) may lead to more malignant progression but it may be that ROCK roles involve cell-cell elements such as β -catenin activation (Samuel et al., 2011) or failure in E-cadherin signalling and disrupt adherens junctions, which may be accountable for the intercellular gaps leading to brittle/ripped tissues in this tri-genic ROCK/ras¹²⁰⁵/ Δ 5PTEN^{het} model. Therefore, these two tri-genic models: ROCK/fos/ Δ 5PTEN^{flx} and ROCK/ras¹²⁷⁶/ Δ 5PTEN^{flx} (and ROCK/ras¹²⁰⁵/ Δ 5PTEN^{het}) have proven the important relationships between ROCK2 activation and PTEN/PI3K/AKT and ras/MAPK/fos pathways in mediating tumourigenesis.

Chapter 5 – Conclusions and future studies

Collectively, this study identified direct co-operation between ROCK2 activation and ras, fos and /or PTEN-mediated loss of AKT regulation in multi-stage transgenic mouse skin carcinogenesis. Consistent with previous studies, ROCK2 activation is mainly associated with the later stages of carcinogenesis and acts to drive malignant progression. However, this study also demonstrates that ROCK2 is involved at the earlier stage of malignant conversion, one of the most important stages in clinical terms and also another important conclusion was that the final outcome depended on the co-operative partners. It was clear that the appropriate benign tumour context had to be achieved for ROCK2 co-operation and malignant conversion. Even in the novel findings where for the first time ROCK2 deregulation was shown to co-operate with fos and now produced tumours, these remained benign and showed no sign of conversion. In the absence of wound promotion, bi-genic ROCK/ras tumours did not achieve malignancy; thus the appropriate papilloma context had to be achieved before ROCK2 was able to drive malignant conversion and progression. Further, in the tissue context created by ROCK and PTEN deregulation, it appeared that this combination failed to achieve even a benign tumour, suggesting either redundancy or the necessary events to bridge the oncogene gap. Hence, introduction of MAP Kinase deregulation into ROCK/PTEN epidermis via either fos or ras activation quite rapidly produced aggressive SCCs; which in some contexts rapidly progressed to pdSCCs. In reverse, in the absence of PTEN/AKT deregulation, whilst ras and fos provide the appropriate papilloma context for ROCK causality in the conversion stage, the progression was limited to mainly wdSCCs and this was due to persistent p21 expression.

In the bi-genic models, malignant conversion in the ROCK/ras¹²⁰⁵ model was shown to be driven by ROCK2 activation but this required wound promotion. However, after the early stages of malignancy, it would appear that malignant progression occurred even without exogenous ROCK2 activation; possibly given the increased expression of endogenous ROCK upon malignant progression. Indeed, in the cessation experiments that this 4-HT-treated ROCK model is specifically designed to test, the results show that whilst exogenous ROCK2 was

required for conversion, once a SCC or pdSCC histotype was attained, exogenous ROCK2 was no longer rate limiting, and p21 was lost. However, the most astonishing result was the resultant rapid outgrowth of papilloma and the levels of p21 expression exhibited by these papillomas. That their histotype was benign papillomas would suggest that continuous exogenous ROCK activation was needed for conversion and to maintain a malignant histotype; i.e. these tumours were oncogene dependent. However, one additional conclusion suggested by these data may be that 4-HT treatment successfully inhibits the growth of a papilloma sub-type, which now appears and this type cannot convert, given the high levels of p21. Thus, in this context, ROCK2 may indirectly act earlier with ras in papillomatogenesis, and 4-HT actually selects for papillomas prone to conversion (but not in bi-genic ROCK/fos papillomas). Nonetheless, all these models show an important role for p21 in limiting carcinogenesis following p53 loss.

Here interestingly, the bi-genic ROCK/fos model showed a novel finding of ROCK2 activation as it possessed roles as an initiator in co-operation with fos activation to induce benign squamous papillomas. In comparison to papilloma formation in early bi-genic ROCK/ras¹²⁰⁵ (at eight weeks), this bi-genic ROCK/fos model showed no sign of conversion, and bi-genic ROCK/fos papillomas showed high level of compensatory p53/p21 expression when compared to bi-genic ROCK/ras¹²⁰⁵ papillomas. Unlike bi-genic ROCK/fos papillomas, in bi-genic ROCK/ras¹²⁰⁵ papillomas, p53 expression became lost allowing conversion followed by supra-basal p21 expression and loss of protection in the proliferative benign basal keratinocytes. Thus, these data showed the difference role of ROCK2 activation with each ras and fos in these early-stage cancer events; and that additional mutations are required to achieve malignancy which were assessed in the tri-genic synergism experiments.

Also, for the first time, a new *Isl.ROCK^{er}* model, designed to express from a universal promoter, was successfully employed in this study. These *K14.cre/Isl.ROCK^{er}/Δ5PTEN^{flx}* data possessed identical phenotypes and histotypes to the original *K14.ROCK^{er}* model upon activation by *K14.creP*. Thus, although some concerns existed regarding potential technical problems employing this *Isl.ROCK^{er}* model, yet, this concern was eliminated as GFP and p-Mypt1 expression were confirmed in all epidermal layers including hair follicles. Thus, the

fact that *K14.cre/Isl.ROCK^{er}/Δ5PTEN^{fix}* mice developed no obvious tumours over an extended period, demonstrated a requirement of additional mutation events to fill in the oncogenic gap in this bi-genic ROCK/Δ5PTEN^{fix} model. Thus, the lack of tumours in this bi-genic model may be due to the unexpected low levels of p-AKT which was a possible consequence of compensatory elevated p21 expression.

Alternatively, it may be due to a redundancy in the oncogenic hits supplied between ROCK and PTEN, as throughout these studies, one conclusion hinted by the data is that in epidermis, their roles in differentiation and barrier maintenance may be similar. Given that actomyosin contraction by ROCK activation mediated changes in adherens junction (Sahai and Marshall, 2002) and previous data suggest that PTEN plays an important role in cell-cell adhesion (Subauste et al., 2005) where both are linked to cell migration through focal adhesion kinase signalling. This idea is supported by bi-genic ROCK/Δ5PTEN^{fix} synergism that appeared to alter the keratinocyte differentiation instead of a commitment to papillomatogenesis. Thus, at 27 weeks, bi-genic ROCK/Δ5PTEN^{fix} hyperplasia showed a significant increase in mitotic index consistent with expansion of proliferative basal layers and delayed keratin K1 expression. However, at earlier times, this proliferation activity was possibly countered by an accelerated differentiation; mediated via ROCK2 and Δ5PTEN^{fix} interactions in differentiation that affected K1 and K6 expression *in vivo* and *in vitro*, and where p21-mediated down regulation of AKT at these early stages, might account for their lack of tumours.

Nonetheless, despite their lack of tumours, these *K14.cre/Isl.ROCK^{er}/Δ5PTEN^{fix}* mice proved to be very useful to investigate epidermal differentiation both *in vivo* and *in vitro*. Further, the *in vitro* data provided evidence that supports roles for both ROCK2 and PTEN that may be crucial in epidermal homeostasis. These roles that accelerate differentiation observed in *K14.cre/Isl.ROCK^{er}*, *K14.cre/Isl.ROCK^{er}/fos* and *K14.cre/Isl.ROCK^{er}/Δ5PTEN^{fix}* keratinocytes may also account for the lack of overt tumours, and this role would certainly influence these early stages of carcinogenesis. For instance, premature keratin K1 expression suggests a commitment to differentiation, whilst the lack of keratin K6 (associated with stress/hyperproliferation) suggests the changes induced by ROCK2 activation could influence the differentiation mechanism. This change in keratin K6 was not as dramatic as compared to complete absence that observed *in vivo* following

PTEN mutation, which may be a response to anomalous AKT expression in basal keratinocytes; but, this again suggests links between ROCK and PTEN in the response to anomalous proliferation signals and reinforces links between their roles in epidermal physiology. With time, this increased proliferation overtakes this effect on differentiation in bi-genic ROCK/ $\Delta 5PTEN^{flx}$ model, as does expression of fos in the bi-genic ROCK/fos models. Here, data showed that fos activation restores both keratin K6 and K1 expression closer to a normal profile in bi-genic ROCK/fos keratinocytes *in vitro* and *in vivo*, giving highly keratotic papillomas that echo the differentiation aspects; again consistent with fos roles as a master regulator of epidermal homeostasis. Furthermore, the keratinocyte cell lines that have established from neonatal *K14.cre/Isl.ROCK^{er}*, *K14.cre/Isl.ROCK^{er}/fos* and *K14.cre/Isl.ROCK^{er}/ $\Delta 5PTEN^{flx}$* cohorts will be useful for further in-depth investigations in this differentiation/proliferation mechanism.

Collectively, these bi-genic outcomes establish an early foundation status of ROCK2 activation in multi-stage carcinogenesis model compared to alternate systems; such as ROCK2 roles in malignant conversion (ROCK/ras¹²⁰⁵) prior to the more accepted roles in malignant progression. In addition, phosphorylation of Mypt1 by ROCK activation which increase actomyosin contraction, may promote tenascin C expression as shown in bi-genic ROCK/ras¹²⁰⁵ tumours. Whilst tenascin C shows high expression upon malignant progression (Dang et al., 2006) which is also consistent with ROCK activity in late cancer events (Croft et al., 2004, Samuel et al., 2011) thus this may provide an idea that there is a possible connection between tenascin C and β -catenin in the progression mechanism mediated by ROCK2 activation-induced tissue stiffness. Yet this is still unclear and will be further investigated in future studies. Also for the first time, ROCK2 activation acts early in formation of benign tumours and this mimics the initiation stage (ROCK/fos). Whilst the weak co-operation between ROCK and inducible PTEN loss in papillomatogenesis demonstrates the essential point that context is important to the eventual tumour outcome and requires multiple events.

Remarkably, all tri-genic models: *K14.cre/Isl.ROCK^{er}/ras¹²⁷⁶/fos*, *K14.cre/Isl.ROCK^{er}/fos/ $\Delta 5PTEN^{flx}$* , and *K14.cre/Isl.ROCK^{er}/ras¹²⁷⁶/ $\Delta 5PTEN^{flx}$* (and *K14.ROCK^{er}/ras¹²⁰⁵/ $\Delta 5PTEN^{het}$*) demonstrated direct co-operation of ROCK2 activation and ras, fos, and /or $\Delta 5PTEN^{flx}$ mutations in malignant conversion and /or malignant progression. Subsequently, analysis of the underlying mechanism in

this whole study shows the important relationship between p53 and p21 expression in different epidermal layers to the outcome of each model: either to obstruct malignant conversion, induce malignant progression; or influence in keratinocyte differentiation in response to ROCK2 activation targeting ras/MAPK/fos and /or PTEN/PI3K/AKT pathways. For instance, aggressive SCCs and invasive pdSCCs histotypes were produced in tri-genic ROCK/fos/ $\Delta 5$ PTEN^{fix} and ROCK/ras¹²⁷⁶/ $\Delta 5$ PTEN^{fix} (and ROCK^{er}/ras¹²⁰⁵/ $\Delta 5$ PTEN^{het}) models given the early p53 loss in papillomas, followed by p21 expression that became supra-basal and /or disappeared which resulted in elevated expression of p-AKT in the proliferative tumour cells. Thus, this shows the crucial impact between p21 and AKT in the tumour outcome. Hence, in comparison to tri-genic ROCK/ras¹²⁷⁶/fos model, little to no expression of p-AKT may be the reason of these tumours to remain as wdSCCs.

Moreover, these data also showed that the tumour outcome become aggressive SCCs/invasive pdSCCs histotypes when the roles of ROCK2-mediated increase in tissue stiffness was overlaid with both MAPK and PTEN/AKT pathways. This idea is supported by a comparison to malignant progression in previous tri-genic ras¹²⁷⁶/fos/ $\Delta 5$ PTEN^{fix} model which also had a dual target on both MAPK and PTEN/AKT, yet, tumours remained as wdSCCs due to the persistence of p21 expression (Macdonald et al., 2014). However, in these current tri-genic models, with ROCK2 activation which hit on both MAPK and PTEN/AKT, data showed a remarkable malignant progression in both tri-genic ROCK/fos/ $\Delta 5$ PTEN^{fix} and ROCK/ras¹²⁷⁶/ $\Delta 5$ PTEN^{fix} models. Furthermore, as shown in the latest tri-genic ROCK/ras¹²⁰⁵/ $\Delta 5$ PTEN^{het} model where rapid tumour progression occurred (at 5-6 weeks) was due to an immediate loss of p53, followed by supra-basal expression of p21 even at pre-malignant stage which promotes p-AKT expression. This was also observed previously in bi-genic ras¹²⁷⁶/ $\Delta 5$ PTEN^{fix} with induction of TPA promotion (Yao et al., 2006). Thus, again, this shows that targeting ROCK2 signalling acts as a potential Achilles heel in ras cancer therapy in a dual hit target for both ras/MAPK/fos and PTEN/PI3K/AKT.

Each bi-genic and tri-genic transgenic mouse model in this study has established a foundation to study ROCK-associated mechanism(s) that drives carcinogenesis through each specific stage. Thus, the mice and their tumours provide an archive useful for further analysis with variety of relevant targets that can widen the

mechanism pathways. For example: β -catenin and GSK3 β which may have a connection in a later progression stage between ROCK2-mediated elevation in tissue stiffness and the loss of compensatory p53/p21 profiles (Yao et al., 2008, Samuel et al., 2011), NF κ B transcription factor which can be activated by RhoA/ROCK signalling (Perona et al., 1997, Benitah et al., 2003) during disruption of cell-cell adhesion mediated by cadherins leading to cell proliferation, invasion and migration (Cowell et al., 2009); and also future studies on the relationship between ROCK2 and FAK together with cadherins that may be accountable for the rip/broken tissues and intercellular gaps in the late stage of cancer. In addition to the *in vivo* models and their use in new breeding to create new genotypes, since several cell lines were established, future *in vitro* study will further investigate cell motility and cell adhesion assays together with western analysis to analyse effected targets.

Finally, these transgenic mouse models that provide a stable phenotype and have a connection with each stage-specific of cancer could be applicable to provide test animals to stringently assess new anti-cancer therapeutic agents *in vivo* prior to clinical trials which will contribute to the field of cancer research.

Appendix A

Cell lines of primary keratinocytes

Cell lines	Genotypes	Features
ROCK1.0	<i>K14.ROCK^{er}</i>	Fast-growing, not resistant to Ca ²⁺
K.ROCK1.0	<i>K14.cre/lsl.ROCK^{er}</i>	Fast-growing, not resistant to Ca ²⁺
K.ROCK1.0C	<i>K14.cre/lsl.ROCK^{er}</i>	Slow-growing, not resistant to Ca ²⁺
K.ROCK2.0	<i>K14.cre/lsl.ROCK^{er}</i>	Fast-growing, not resistant to Ca ²⁺
K.ROCK.FOS1.0	<i>K14.cre/lsl.ROCK^{er}/HK1.fos</i>	Fast-growing, not resistant to Ca ²⁺
Fos1.0C	<i>HK1.fos</i>	Slow-growing, not resistant to Ca ²⁺
K.ROCK.P10F	<i>K14.cre/lsl.ROCK^{er}/Δ5PTEN^{flx}</i>	Fast-growing, not resistant to Ca ²⁺
K.P10F	<i>K14.cre/Δ5PTEN^{flx}</i>	Fast-growing, not resistant to Ca ²⁺

Appendix B

Abstract/Publication	
<p>1. 2013 International Investigative Dermatology Meeting.</p>	<p>Inducible ROCK 2 activation increases primary keratinocyte differentiation but co-operates with ras^{Ha} activation in transgenic mouse skin carcinogenesis.</p> <p>Masre, S.F., Olson, M.F., and Greenhalgh, D.A. (2013) Inducible ROCK 2 activation increases primary keratinocyte differentiation but co-operates with ras^{Ha} activation in transgenic mouse skin carcinogenesis. <i>Journal of Investigative Dermatology</i>, 133(S1), S57-S57.(doi:10.1038/jid.2013.96)</p>
<p>2. XV World Congress on Cancers of The Skin, 2014.</p>	<p>ROCK-2 activation alters keratinocyte differentiation and initiates malignant conversion in ras/fos/PTEN^{null} transgenic mouse skin carcinogenesis</p> <p>Siti Masre¹ , Nicola Rath² , Michael Olson² , David Greenhalgh¹ , ¹ Dept. Of Dermatology, School of Medicine, MVLS Glasgow University, Glasgow Scotland, UK, ²Tumour Microenvironment Laboratory Beatson Institute for Cancer Research, Glasgow Scotland, UK.</p>
<p>3. American Association for Cancer Research, 2014.</p>	<p>Inducible ROCK2/ras^{Ha} cooperation requires wound promotion to achieve malignancy in transgenic mouse skin carcinogenesis, whereas inducible ROCK 2/PTEN loss fails to achieve benign papilloma. Siti F. Masre, Michael S. Samuel, Michael F. Olson, David A. Greenhalgh.</p>

List of references

- ABATE-SHEN, C., SHEN, M. M. & GELMANN, E. 2008. Integrating differentiation and cancer: The Nkx3.1 homeobox gene in prostate organogenesis and carcinogenesis. *Differentiation*, 76, 717-727.
- ABEL, E. L., DIGIOVANNI, J. & PENNING, T. M. 2011. Multistage Carcinogenesis. In: EL-DEIRY, W. (ed.) *Chemical Carcinogenesis*. Humana Press.
- AKHURST, R. J. & HATA, A. 2012. Targeting the TGFbeta signalling pathway in disease. *Nat Rev Drug Discov*, 11, 790-811.
- ALONSO, L. & FUCHS, E. 2003. Stem cells of the skin epithelium. *Proceedings of the National Academy of Sciences*, 100, 11830-11835.
- AMANO, M., CHIHARA, K., KIMURA, K., FUKATA, Y., NAKAMURA, N., MATSUURA, Y. & KAIBUCHI, K. 1997. Formation of actin stress fibers and focal adhesions enhanced by Rho-kinase. *Science*, 275, 1308-11.
- AMANO, M., FUKATA, Y. & KAIBUCHI, K. 2000. Regulation and functions of Rho-associated kinase. *Exp Cell Res*, 261, 44-51.
- AMANO, M., ITO, M., KIMURA, K., FUKATA, Y., CHIHARA, K., NAKANO, T., MATSUURA, Y. & KAIBUCHI, K. 1996. Phosphorylation and activation of myosin by Rho-associated kinase (Rho-kinase). *J Biol Chem*, 271, 20246-9.
- BAINES, A. T., XU, D. & DER, C. J. 2011. Inhibition of Ras for cancer treatment: the search continues. *Future Medicinal Chemistry*, 3, 1787-1808.
- BALMAIN, A. 1985. Transforming ras oncogenes and multistage carcinogenesis. *Br. J. Cancer*, 51, 1-7.
- BALMAIN, A. & PRAGNELL, I. B. 1983. Mouse skin carcinomas induced in vivo by chemical carcinogens have a transforming Harvey-ras oncogene. *Nature*, 303, 72-74.
- BALMAIN, A., RAMSDEN, M., BOWDEN, G. T. & SMITH, J. 1984. Activation of the mouse cellular Harvey-ras gene in chemically induced benign skin papillomas. *Nature*, 307, 658-660.
- BALMAIN, A. & YUSPA, S. H. 2014. Milestones in skin carcinogenesis: the biology of multistage carcinogenesis. *J Invest Dermatol*, 134, E2-7.
- BASSET-SEGUIN, N., ESCOT, C., BLANCHARD, J. M., KERAI, C., VERRIER, B., MION, H. & GUILHOU, J. J. 1990. High levels of c-fos proto-oncogene expression in normal human adult skin. *J Invest Dermatol*, 94, 418-22.
- BENITAH, S. A., VALERON, P. F. & LACAL, J. C. 2003. ROCK and nuclear factor-kappaB-dependent activation of cyclooxygenase-2 by Rho GTPases: effects on tumor growth and therapeutic consequences. *Mol Biol Cell*, 14, 3041-54.
- BERTON, T. R., WANG, X.-J., ZHOU, Z., KELLENDONK, C., SCHÜTZ, G., TSAI, S. & ROOP, D. R. 2000a. Characterization of an inducible, epidermal-specific knockout system: Differential expression of lacZ in different Cre reporter mouse strains. *genesis*, 26, 160-161.
- BERTON, T. R., WANG, X. J., ZHOU, Z., KELLENDONK, C., SCHUTZ, G., TSAI, S. & ROOP, D. R. 2000b. Characterization of an inducible, epidermal-specific knockout system: differential expression of lacZ in different Cre reporter mouse strains. *Genesis*, 26, 160-1.
- BOS, J. L. 1989. ras oncogenes in human cancer: a review. *Cancer Res*, 49, 4682-9.
- BRANDNER, J. M., HAFTEK, M. & NIESSEN, C. M. 2010. Adherens junctions, desmosomes and tight junctions in epidermal barrier function. *Open Dermatol J*, 4, 14-20.
- BRASH, D. E., RUDOLPH, J. A., SIMON, J. A., LIN, A., MCKENNA, G. J., BADEN, H. P., HALPERIN, A. J. & PONTÉN, J. 1991. A role for sunlight in skin cancer: UV-induced p53 mutations in squamous cell carcinoma. *Proc Natl Acad Sci U S A*, 88, 10124-10128.
- BROWN, K., BUCHMANN, A. & BALMAIN, A. 1990. Carcinogen-induced mutations in the mouse c-Ha-ras gene provide evidence of multiple pathways for tumor progression. *Proc Natl Acad Sci U S A*, 87, 538-42.
- BROWN, K., QUINTANILLA, M., RAMSDEN, M., KERR, I. B., YOUNG, S. & BALMAIN, A. 1986. v-ras genes from Harvey and BALB murine sarcoma viruses can act as initiators of two-stage mouse skin carcinogenesis. *Cell*, 46, 447-56.
- BYRNE, C., TAINSKY, M. & FUCHS, E. 1994. Programming gene expression in developing epidermis. *Development*, 120, 2369-2383.
- CALAUTTI, E., LI, J., SAONCELLA, S., BRISSETTE, J. L. & GOETINCK, P. F. 2005. Phosphoinositide 3-kinase signaling to Akt promotes keratinocyte differentiation versus death. *J Biol Chem*, 280, 32856-65.

- CANDI, E., SCHMIDT, R. & MELINO, G. 2005. The cornified envelope: a model of cell death in the skin. *Nat Rev Mol Cell Biol*, 6, 328-340.
- CARNERO, A. & PARAMIO, J. M. 2014. The PTEN/PI3K/AKT Pathway in vivo, Cancer Mouse Models. *Front Oncol*, 4, 252.
- CASTELLANO, E. & DOWNWARD, J. 2010. Role of RAS in the regulation of PI 3-kinase. *Curr Top Microbiol Immunol*, 346, 143-69.
- CASTELLANO, E. & DOWNWARD, J. 2011. RAS Interaction with PI3K: More Than Just Another Effector Pathway. *Genes & Cancer*, 2, 261-274.
- CHALHOUB, N. & BAKER, S. J. 2009. PTEN and the PI3-kinase pathway in cancer. *Annu Rev Pathol*, 4, 127-50.
- CHANG, F., STEELMAN, L. S., LEE, J. T., SHELTON, J. G., NAVOLANIC, P. M., BLALOCK, W. L., FRANKLIN, R. A. & MCCUBREY, J. A. 2003. Signal transduction mediated by the Ras/Raf/MEK/ERK pathway from cytokine receptors to transcription factors: potential targeting for therapeutic intervention. *Leukemia*, 17, 1263-93.
- CHIHARA, K., AMANO, M., NAKAMURA, N., YANO, T., SHIBATA, M., TOKUI, T., ICHIKAWA, H., IKEBE, R., IKEBE, M. & KAIBUCHI, K. 1997. Cytoskeletal Rearrangements and Transcriptional Activation of c-fos Serum Response Element by Rho-kinase. *Journal of Biological Chemistry*, 272, 25121-25127.
- COOPER, G. M. 2000. *The Cell: A Molecular Approach.*, Sinauer Associates.
- COWELL, C. F., YAN, I. K., EISELER, T., LEIGHTNER, A. C., DOPPLER, H. & STORZ, P. 2009. Loss of cell-cell contacts induces NF-kappaB via RhoA-mediated activation of protein kinase D1. *J Cell Biochem*, 106, 714-28.
- CRANE, A. & BHATTACHARYA, S. 2013. The Use of Bromodeoxyuridine Incorporation Assays to Assess Corneal Stem Cell Proliferation. In: WRIGHT, B. & CONNON, C. J. (eds.) *Corneal Regenerative Medicine*. Humana Press.
- CRISTOFANO, A. D., PESCE, B., CORDON-CARDO, C. & PANDOLFI, P. P. 1998. Pten is essential for embryonic development and tumour suppression. *Nat Genet*, 19, 348-355.
- CROFT, D. R. & OLSON, M. F. 2006. Conditional Regulation of a ROCK - Estrogen Receptor Fusion Protein. In: WILLIAM E. BALCH, C. J. D. & ALAN, H. (eds.) *Methods in Enzymology*. Academic Press.
- CROFT, D. R., SAHAI, E., MAVRIA, G., LI, S., TSAI, J., LEE, W. M. F., MARSHALL, C. J. & OLSON, M. F. 2004. Conditional ROCK activation *In vivo* induces tumor cell dissemination and angiogenesis. *Cancer Research*, 64, 8994-9001.
- CURRAN, T., MILLER, A. D., ZOKAS, L. & VERMA, I. M. 1984. Viral and cellular fos proteins: a comparative analysis. *Cell*, 36, 259-68.
- DANG, C., GOTTSCHLING, M., ROEWERT, J., FORSCHNER, T., STOCKFLETH, E. & NINDL, I. 2006. Tenascin-C patterns and splice variants in actinic keratosis and cutaneous squamous cell carcinoma. *Br J Dermatol*, 155, 763-70.
- DENG, T. & KARIN, M. 1994. c-Fos transcriptional activity stimulated by H-Ras-activated protein kinase distinct from JNK and ERK. *Nature*, 371, 171-5.
- DER, C. J., FINKEL, T. & COOPER, G. M. 1986. Biological and biochemical properties of human rasH genes mutated at codon 61. *Cell*, 44, 167-76.
- DEVGAN, V., NGUYEN, B. C., OH, H. & DOTTO, G. P. 2006. p21WAF1/Cip1 suppresses keratinocyte differentiation independently of the cell cycle through transcriptional up-regulation of the IGF-I gene. *J Biol Chem*, 281, 30463-70.
- DI CRISTOFANO, A., PESCE, B., CORDON-CARDO, C. & PANDOLFI, P. P. 1998. Pten is essential for embryonic development and tumour suppression. *Nat Genet*, 19, 348-55.
- DISEPIO, D., JONES, A., LONGLEY, M. A., BUNDMAN, D., ROTHNAGEL, J. A. & ROOP, D. R. 1995. The Proximal Promoter of the Mouse Loricrin Gene Contains a Functional AP-1 Element and Directs Keratinocyte-specific but Not Differentiation-specific Expression. *Journal of Biological Chemistry*, 270, 10792-10799.
- DOTTO, G. P., GILMAN, M. Z., MARUYAMA, M. & WEINBERG, R. A. 1986. c-myc and c-fos expression in differentiating mouse primary keratinocytes. *Embo j*, 5, 2853-7.
- DOWNWARD, J. 2003. Targeting RAS signalling pathways in cancer therapy. *Nat Rev Cancer*, 3, 11-22.
- DUFORT, C. C., PASZEK, M. J. & WEAVER, V. M. 2011. Balancing forces: architectural control of mechanotransduction. *Nat Rev Mol Cell Biol*, 12, 308-319.
- EFEYAN, A., ORTEGA-MOLINA, A., VELASCO-MIGUEL, S., HERRANZ, D., VASSILEV, L. T. & SERRANO, M. 2007. Induction of p53-dependent senescence by the MDM2 antagonist nutlin-3a in mouse cells of fibroblast origin. *Cancer Res*, 67, 7350-7.
- EL-DEIRY, W. S., TOKINO, T., VELCULESCU, V. E., LEVY, D. B., PARSONS, R., TRENT, J. M., LIN, D., MERCER, W. E., KINZLER, K. W. & VOGELSTEIN, B. 1993. WAF1, a potential mediator of p53 tumor suppression. *Cell*, 75, 817-25.

- FENG, J., ITO, M., KUREISHI, Y., ICHIKAWA, K., AMANO, M., ISAKA, N., OKAWA, K., IWAMATSU, A., KAIBUCHI, K., HARTSHORNE, D. J. & NAKANO, T. 1999. Rho-associated kinase of chicken gizzard smooth muscle. *J Biol Chem*, 1999 Feb 5;274(6):3744-52.
- FINKEL, M. P., BISKIS, B. O. & JINKINS, P. B. 1966. Virus induction of osteosarcomas in mice. *Science*, 151, 698-701.
- FISHER, C., BYERS, M. R., IADAROLA, M. J. & POWERS, E. A. 1991. Patterns of epithelial expression of Fos protein suggest important role in the transition from viable to cornified cell during keratinization. *Development*, 111, 253-8.
- FREEMAN, D., LESCHE, R., KERTESZ, N., WANG, S., LI, G., GAO, J., GROSZER, M., MARTINEZ-DIAZ, H., ROZENGURT, N., THOMAS, G., LIU, X. & WU, H. 2006. Genetic background controls tumor development in PTEN-deficient mice. *Cancer Res*. 2006 Jul 1;66(13):6492-6.
- FREEMAN, D. J., LI, A. G., WEI, G., LI, H. H., KERTESZ, N., LESCHE, R., WHALE, A. D., MARTINEZ-DIAZ, H., ROZENGURT, N., CARDIFF, R. D., LIU, X. & WU, H. 2003. PTEN tumor suppressor regulates p53 protein levels and activity through phosphatase-dependent and -independent mechanisms. *Cancer Cell*, 3, 117-30.
- FUCHS, E. 1990. Epidermal differentiation: the bare essentials. *J Cell Biol*, 111, 2807-14.
- FUCHS, E. 2007. Scratching the surface of skin development. *Nature*, 445, 834-842.
- FUCHS, E. 2008. Skin stem cells: rising to the surface. *J Cell Biol*, 180, 273-84.
- GHOSH, J. C. & ALTIERI, D. C. 2005. Activation of p53-dependent apoptosis by acute ablation of glycogen synthase kinase-3 β in colorectal cancer cells. *Clin Cancer Res*, 11, 4580-8.
- GLICK, A. B., SPORN, M. B. & YUSPA, S. H. 1991. Altered Regulation of TGF- β 1 and TGF- α in Primary Keratinocytes and Papillomas Expressing v-Ha-ras. *Molecular Carcinogenesis*, 4, 210-219.
- GREENHALGH, D., WANG, X., ECKHARDT, J. & ROOP, D. 1995. 12-O-tetradecanoylphorbol-13-acetate promotion of transgenic mice expressing epidermal-targeted v-fos induces rasHA-activated papillomas and carcinomas without p53 mutation: association of v-fos expression with promotion and tumor autonomy. *Cell Growth Differ*, 6, 579-586.
- GREENHALGH, D. A., QUINTANILLA, M. I., ORENGO, C. C., BARBER, J. L., ECKHARDT, J. N., ROTHNAGEL, J. A. & ROOP, D. R. 1993c. Cooperation between v-fos and v-ras^{HA} induces autonomous papillomas in transgenic epidermis but not malignant conversion. *Cancer Research*, 53, 5071-5075.
- GREENHALGH, D. A. & ROOP, D. R. 1994. Dissecting molecular carcinogenesis: development of transgenic mouse models by epidermal gene targeting. *Adv. Cancer Res.*, 64, 247-96.
- GREENHALGH, D. A., ROTHNAGEL, J. A., WANG, X. J., QUINTANILLA, M. I., ORENGO, C. C., GAGNE, T. A., BUNDMAN, D. S., LONGLEY, M. A., FISHER, C. & ROOP, D. R. 1993a. Induction of epidermal hyperplasia, hyperkeratosis, and papillomas in transgenic mice by a targeted v-Ha-ras oncogene. *Molecular Carcinogenesis*, 7, 99-110.
- GREENHALGH, D. A., ROTHNAGEL, J. A., WANG, X. J., QUINTANILLA, M. I., ORENGO, C. C., GAGNE, T. A., BUNDMAN, D. S., LONGLEY, M. A., FISHER, C. & ROOP, D. R. 1993b. Hyperplasia, hyperkeratosis and benign tumor production in transgenic mice by a targeted v-fos oncogene suggests a role for fos in epidermal differentiation and neoplasia. *Oncogene*, 8, 2145-2157.
- GREENHALGH, D. A., WANG, X.-J., DONEHOWER, L. A. & ROOP, D. R. 1996. Paradoxical Tumor Inhibitory Effect of p53 Loss in Transgenic Mice Expressing Epidermal-targeted v-rasHa, v-fos, or Human Transforming Growth Factor β . *Cancer Research*, 56, 4413-4423.
- GREENHALGH, D. A., WELTY, D. J., PLAYER, A. & YUSPA, S. H. 1990. Two oncogenes, v-fos and v-ras, cooperate to convert normal keratinocytes to squamous cell carcinoma. *Proc Natl Acad Sci U S A*, 87, 643-7.
- GREENHALGH, D. A., WELTY, D. J., STRICKLAND, J. E. & YUSPA, S. H. 1989. Spontaneous Ha-ras gene activation in cultured primary murine keratinocytes: consequences of Ha-ras gene activation in malignant conversion and malignant progression. *Mol Carcinog*, 2, 199-207.
- GREENHALGH, D. A. & YUSPA, S. H. 1988. Malignant conversion of murine squamous papilloma cell lines by transfection with the fos oncogene. *Mol Carcinog*, 1, 134-43.
- HANAHAH, D. 1988. Dissecting multistep tumorigenesis in transgenic mice. *Annu Rev Genet*, 22, 479-519.
- HAUPT, S., BERGER, M., GOLDBERG, Z. & HAUPT, Y. 2003. Apoptosis - the p53 network. *Journal of Cell Science*, 116, 4077-4085.
- HENNINGS, H., GLICK, A. B., LOWRY, D. T., KRSMANOVIC, L. S., SLY, L. M. & YUSPA, S. H. 1993. FVB/N mice: an inbred strain sensitive to the chemical induction of squamous cell carcinomas in the skin. *Carcinogenesis*, 14, 2353-8.

- HENNINGS, H., MICHAEL, D., CHENG, C., STEINERT, P., HOLBROOK, K. & YUSPA, S. H. 1980. Calcium regulation of growth and differentiation of mouse epidermal cells in culture. *Cell*, 19, 245-254.
- HENNINGS, H., SHORES, R., MITCHELL, P., SPANGLER, E. F. & YUSPA, S. H. 1985. Induction of papillomas with a high probability of conversion to malignancy. *Carcinogenesis*, 6, 1607-10.
- HOHL, D., MEHREL, T., LICHTI, U., TURNER, M. L., ROOP, D. R. & STEINERT, P. M. 1991. Characterization of human loricrin. Structure and function of a new class of epidermal cell envelope proteins. *J Biol Chem*, 266, 6626-36.
- HOLEITER, G., BISCHOFF, A., BRAUN, A. C., HUCK, B., ERLMANN, P., SCHMID, S., HERR, R., BRUMMER, T. & OLAYIOYE, M. A. 2012. The RhoGAP protein Deleted in Liver Cancer 3 (DLC3) is essential for adherens junctions integrity. *Oncogenesis*, 1, e13.
- HOLLANDER, M. C., BLUMENTHAL, G. M. & DENNIS, P. A. 2011. PTEN loss in the continuum of common cancers, rare syndromes and mouse models. *Nat Rev Cancer*, 11, 289-301.
- HOPKINS, B. D., HODAKOSKI, C., BARROWS, D., MENSE, S. M. & PARSONS, R. E. 2014. PTEN function: the long and the short of it. *Trends in Biochemical Sciences*, 39, 183-190.
- HORIUCHI, A., KIKUCHI, N., OSADA, R., WANG, C., HAYASHI, A., NIKAI, T. & KONISHI, I. 2008. Overexpression of RhoA enhances peritoneal dissemination: RhoA suppression with Lovastatin may be useful for ovarian cancer. 99, 2532-2539.
- HUNTER, T. 1991. Cooperation between oncogenes. *Cell*, 64, 249-270.
- IBBETSON, S. J., PYNE, N. T., POLLARD, A. N., OLSON, M. F. & SAMUEL, M. S. 2013. Mechanotransduction Pathways Promoting Tumor Progression Are Activated in Invasive Human Squamous Cell Carcinoma. *The American Journal of Pathology*, 183, 930-937.
- ILLA-BOCHACA, I. & MONTUENGA, L. M. 2006. The regenerative niche of the locust midgut as a model to study epithelial cell differentiation from stem cells. *J Exp Biol*, 209, 2215-23.
- ISHIZAKI, T., MAEKAWA, M., FUJISAWA, K., OKAWA, K., IWAMATSU, A., FUJITA, A., WATANABE, N., SAITO, Y., KAKIZUKA, A., MORII, N. & NARUMIYA, S. 1996. The small GTP-binding protein Rho binds to and activates a 160 kDa Ser/Thr protein kinase homologous to myotonic dystrophy kinase. *The EMBO Journal*, 15, 1885-1893.
- IZAWA, I., AMANO, M., CHIHARA, K., YAMAMOTO, T. & KAIBUCHI, K. 1998. Possible involvement of the inactivation of the Rho-Rho-kinase pathway in oncogenic Ras-induced transformation. *Oncogene*, 17, 2863-71.
- JAALOUK, D. E. & LAMMERDING, J. 2009. Mechanotransduction gone awry. *Nat Rev Mol Cell Biol*, 10, 63-73.
- KALININ, A. E., KAJAVA, A. V. & STEINERT, P. M. 2002. Epithelial barrier function: assembly and structural features of the cornified cell envelope. *Bioessays*, 24, 789-800.
- KAMAI, T., TSUJII, T., ARAI, K., TAKAGI, K., ASAMI, H., ITO, Y. & OSHIMA, H. 2003. Significant association of Rho/ROCK pathway with invasion and metastasis of bladder cancer. *Clin Cancer Res*, 9, 2632-41.
- KARNOUB, A. E. & WEINBERG, R. A. 2008. Ras oncogenes: split personalities. *Nat Rev Mol Cell Biol*, 9, 517-531.
- KELLENDONK, C., TRONCHE, F., MONAGHAN, A.-P., ANGRAND, P.-O., STEWART, F. & SCHÜTZ, G. 1996. Regulation of Cre Recombinase Activity by the Synthetic Steroid RU 486. *Nucleic Acids Research*, 24, 1404-1411.
- KIMMELMAN, A. C. 2015. Metabolic Dependencies in RAS-Driven Cancers. *Clinical Cancer Research*, 21, 1828-1834.
- KUMPER, S. & MARSHALL, CHRISTOPHERÂ J. 2011. ROCK-Driven Actomyosin Contractility Induces Tissue Stiffness and Tumor Growth. *Cancer Cell*, 19, 695-697.
- LANE, J., MARTIN, T. A., WATKINS, G., MANSEL, R. E. & JIANG, W. G. 2008. The expression and prognostic value of ROCK I and ROCK II and their role in human breast cancer. *Int J Oncol*, 33, 585-93.
- LEDER, A., PATTENGAL, P. K., KUO, A., STEWART, T. A. & LEDER, P. 1986. Consequences of widespread deregulation of the c-myc gene in transgenic mice: multiple neoplasms and normal development. *Cell*, 45, 485-95.
- LESCHER, R., GROSZER, M., GAO, J., WANG, Y., MESSING, A., SUN, H., LIU, X. & WU, H. 2002. Cre/loxP-mediated inactivation of the murine Pten tumor suppressor gene. *genesis*, 32, 148-149.
- LEUNG, T., CHEN, X. Q., MANSER, E. & LIM, L. 1996. The p160 RhoA-binding kinase ROK alpha is a member of a kinase family and is involved in the reorganization of the cytoskeleton. *Mol Cell Biol*, 16, 5313-27.
- LEUNG, T., MANSER, E., TAN, L. & LIM, L. 1995. A Novel Serine/Threonine Kinase Binding the Ras-related RhoA GTPase Which Translocates the Kinase to Peripheral Membranes. *Journal of Biological Chemistry*, 270, 29051-29054.

- LI, G., ROBINSON, G. W., LESCHE, R., MARTINEZ-DIAZ, H., JIANG, Z., ROZENGURT, N., WAGNER, K. U., WU, D. C., LANE, T. F., LIU, X., HENNIGHAUSEN, L. & WU, H. 2002. Conditional loss of PTEN leads to precocious development and neoplasia in the mammary gland. *Development*, 129, 4159-70.
- LI, J., YEN, C., LIAW, D., PODSYPANINA, K., BOSE, S., WANG, S. I., PUC, J., MILIAREISIS, C., RODGERS, L., MCCOMBIE, R., BIGNER, S. H., GIOVANELLA, B. C., ITTMANN, M., TYCKO, B., HIBSHOOSH, H., WIGLER, M. H. & PARSONS, R. 1997. PTEN, a Putative Protein Tyrosine Phosphatase Gene Mutated in Human Brain, Breast, and Prostate Cancer. *Science*, 275, 1943-1947.
- LI, Z., DONG, X., WANG, Z., LIU, W., DENG, N., DING, Y., TANG, L., HLA, T., ZENG, R., LI, L. & WU, D. 2005. Regulation of PTEN by Rho small GTPases. *Nat Cell Biol*, 7, 399-404.
- LITTLEWOOD, T. D., HANCOCK, D. C., DANIELIAN, P. S., PARKER, M. G. & EVAN, G. I. 1995. A modified oestrogen receptor ligand-binding domain as an improved switch for the regulation of heterologous proteins. *Nucleic Acid Res.*, 23, 1686-1690.
- LOCK, F. E. & HOTCHIN, N. A. 2009. Distinct roles for ROCK1 and ROCK2 in the regulation of keratinocyte differentiation. *PLoS One*, 4, e8190.
- MACDONALD, F. H., YAO, D., QUINN, J. A. & GREENHALGH, D. A. 2014. PTEN ablation in RasHa/Fos skin carcinogenesis invokes p53-dependent p21 to delay conversion while p53-independent p21 limits progression via cyclin D1/E2 inhibition. *Oncogene*, 33, 4132-4143.
- MAEHAMA, T. & DIXON, J. E. 1998. The tumor suppressor, PTEN/MMAC1, dephosphorylates the lipid second messenger, phosphatidylinositol 3,4,5-trisphosphate. *J Biol Chem*, 273, 13375-8.
- MALNOU, C. E., SALEM, T., BROCKLY, F., WODRICH, H., PIECHACZYK, M. & JARIEL-ENCONTRE, I. 2007. Heterodimerization with Jun family members regulates c-Fos nucleocytoplasmic traffic. *J Biol Chem*, 282, 31046-59.
- MAO, J. H., TO, M. D., PEREZ-LOSADA, J., WU, D., DEL ROSARIO, R. & BALMAIN, A. 2004. Mutually exclusive mutations of the Pten and ras pathways in skin tumor progression. *Genes Dev*, 18, 1800-5.
- MARSH, D. J., DAHIA, P. L., COULON, V., ZHENG, Z., DORION-BONNET, F., CALL, K. M., LITTLE, R., LIN, A. Y., EELES, R. A., GOLDSTEIN, A. M., HODGSON, S. V., RICHARDSON, A. L., ROBINSON, B. G., WEBER, H. C., LONGY, M. & ENG, C. 1998. Allelic imbalance, including deletion of PTEN/MMAC1, at the Cowden disease locus on 10q22-23, in hamartomas from patients with Cowden syndrome and germline PTEN mutation. *Genes Chromosomes Cancer*, 21, 61-9.
- MARSH, V., WINTON, D. J., WILLIAMS, G. T., DUBOIS, N., TRUMPP, A., SANSOM, O. J. & CLARKE, A. R. 2008. Epithelial Pten is dispensable for intestinal homeostasis but suppresses adenoma development and progression after Apc mutation. *Nat Genet*, 40, 1436-44.
- MAYO, L. D. & DONNER, D. B. 2002. The PTEN, Mdm2, p53 tumor suppressor-oncoprotein network. *Trends Biochem Sci*, 27, 462-7.
- MCCUBREY, J. A., STEELMAN, L. S., CHAPPELL, W. H., ABRAMS, S. L., WONG, E. W. T., CHANG, F., LEHMANN, B., TERRIAN, D. M., MILELLA, M., TAFURI, A., STIVALA, F., LIBRA, M., BASECKE, J., EVANGELISTI, C., MARTELLI, A. M. & FRANKLIN, R. A. 2007. Roles of the Raf/MEK/ERK pathway in cell growth, malignant transformation and drug resistance. *Biochimica et Biophysica Acta (BBA) - Molecular Cell Research*, 1773, 1263-1284.
- MCLEAN, W. H. I. 2011. The allergy gene: how a mutation in a skin protein revealed a link between eczema and asthma. *F1000 Medicine Reports*, 3, 2.
- MCMULLAN, R., LAX, S., ROBERTSON, V. H., RADFORD, D. J., BROAD, S., WATT, F. M., ROWLES, A., CROFT, D. R., OLSON, M. F. & HOTCHIN, N. A. 2003. Keratinocyte Differentiation Is Regulated by the Rho and ROCK Signaling Pathway. *Current Biology*, 13, 2185-2189.
- MEHIC, D., BAKIRI, L., GHANNADAN, M., WAGNER, E. F. & TSCHACHLER, E. 2005. Fos and jun proteins are specifically expressed during differentiation of human keratinocytes. *J Invest Dermatol*, 124, 212-20.
- MIDWOOD, K. S. & OREND, G. 2009. The role of tenascin-C in tissue injury and tumorigenesis. *Journal of Cell Communication and Signaling*, 3, 287-310.
- MIYAZAKI, K., KOMATSU, S. & IKEBE, M. 2006. Dynamics of RhoA and ROK1± translocation in single living cells. *Cell Biochemistry and Biophysics*, 45, 243-254.
- MOLINA, J. R. & ADJEI, A. A. 2006. The Ras/Raf/MAPK Pathway. *Journal of Thoracic Oncology*, 1, 7-9.
- MORGAN-FISHER, M., WEWER, U. M. & YONEDA, A. 2013. Regulation of ROCK Activity in Cancer. *Journal of Histochemistry & Cytochemistry*, 61, 185-198.
- MORGAN, D., WELTY, D., GLICK, A., GREENHALGH, D., HENNINGS, H. & YUSPA, S. H. 1992. Development of an in Vitro Model to Study Carcinogen-induced Neoplastic Progression of Initiated Mouse Epidermal Cells. *Cancer Research*, 52, 3145-3156.

- MORRIS, R. J. 2004. A perspective on keratinocyte stem cells as targets for skin carcinogenesis. *Differentiation*, 72, 381-386.
- MUELLER, B. K., MACK, H. & TEUSCH, N. 2005. Rho kinase, a promising drug target for neurological disorders. *Nat Rev Drug Discov*, 4, 387-398.
- MYERS, M. P., STOLAROV, J. P., ENG, C., LI, J., WANG, S. I., WIGLER, M. H., PARSONS, R. & TONKS, N. K. 1997. P-TEN, the tumor suppressor from human chromosome 10q23, is a dual-specificity phosphatase. *Proc Natl Acad Sci U S A*, 94, 9052-7.
- NAKAGAWA, O., FUJISAWA, K., ISHIZAKI, T., SAITO, Y., NAKAO, K. & NARUMIYA, S. 1996. ROCK-I and ROCK-II, two isoforms of Rho-associated coiled-coil forming protein serine/threonine kinase in mice. *FEBS Letters*, 392, 189-193.
- NG, I. O., LAM, K. Y., NG, M. & REGEZI, J. A. 1999. Expression of p21/waf1 in oral squamous cell carcinomas--correlation with p53 and mdm2 and cellular proliferation index. *Oral Oncol*, 35, 63-9.
- OLSON, M. F. 2008. Applications for ROCK kinase inhibition. *Current Opinion in Cell Biology*, 20, 242-248.
- OLSON, M. F., PATERSON, H. F. & MARSHALL, C. J. 1998. Signals from Ras and Rho GTPases interact to regulate expression of p21Waf1/Cip1. *Nature*, 394, 295-9.
- OLSON, M. F. & SAHAI, E. 2009. The actin cytoskeleton in cancer cell motility. *Clin. Exp. Metastasis*, 26, 273-287.
- OREND, G. & CHIQUET-EHRISMANN, R. 2006. Tenascin-C induced signaling in cancer. *Cancer Letters*, 244, 143-163.
- PAN, P., SHEN, M., YU, H., LI, Y., LI, D. & HOU, T. 2013. Advances in the development of Rho-associated protein kinase (ROCK) inhibitors. *Drug Discovery Today*.
- PATEL, R. A., FORINASH, K. D., PIREDDU, R., SUN, Y., SUN, N., MARTIN, M. P., SCHÄFFNERBRUNN, E., LAWRENCE, N. J. & SEBTI, S. D. M. 2012. RKI-1447 Is a Potent Inhibitor of the Rho-Associated ROCK Kinases with Anti-Invasive and Antitumor Activities in Breast Cancer. *Cancer Research*, 72, 5025-5034.
- PERONA, R., MONTANER, S., SANIGER, L., SANCHEZ-PEREZ, I., BRAVO, R. & LACAL, J. C. 1997. Activation of the nuclear factor-kappaB by Rho, CDC42, and Rac-1 proteins. *Genes Dev*, 11, 463-75.
- PIERCEALL, W. E., GOLDBERG, L. H., TAINSKY, M. A., MUKHOPADHYAY, T. & ANANTHASWAMY, H. N. 1991. Ras gene mutation and amplification in human nonmelanoma skin cancers. *Molecular Carcinogenesis*, 4, 196-202.
- QIU, R. G., CHEN, J., MCCORMICK, F. & SYMONS, M. 1995. A role for Rho in Ras transformation. *Proc Natl Acad Sci U S A*, 92, 11781-5.
- QUINTANILLA, M., BROWN, K., RAMSDEN, M. & BALMAIN, A. 1986. Carcinogen-specific mutation and amplification of Ha-ras during mouse skin carcinogenesis. *Nature*, 322, 78-80.
- RANSONE, L. J. & VERMA, I. M. 1990. Nuclear proto-oncogenes fos and jun. *Annu Rev Cell Biol*, 6, 539-57.
- RATH, N. & OLSON, M. F. 2012. Rho-associated kinase in tumorigenesis: re-considering ROCK inhibition for cancer therapy. *EMBO Rep.*, 13, 900-908.
- RIENTO, K. & RIDLEY, A. J. 2003. ROCKs: multifunctional kinases in cell behaviour. *Nat Rev Mol Cell Biol*, 4, 446-456.
- ROBERTS, P. J. & DER, C. J. 2007. Targeting the Raf-MEK-ERK mitogen-activated protein kinase cascade for the treatment of cancer. *Oncogene*, 26, 3291-310.
- ROOP, D. R., HUITFELDT, H., KILKENNY, A. & YUSPA, S. H. 1987. Regulated expression of differentiation-associated keratins in cultured epidermal cells detected by monospecific antibodies to unique peptides of mouse epidermal keratins. *Differentiation*, 35, 143-50.
- ROOP, D. R., LOWY, D. R., TAMBOURIN, P. E., STRICKLAND, J., HARPER, J. R., BALASCHAK, M., SPANGLER, E. F. & YUSPA, S. H. 1986. An activated Harvey ras oncogene produces benign tumours on mouse epidermal tissue. *Nature*, 323, 822-824.
- ROSSMAN, K. L., DER, C. J. & SONDEK, J. 2005. GEF means go: turning on RHO GTPases with guanine nucleotide-exchange factors. *Nat Rev Mol Cell Biol*, 6, 167-180.
- ROTHNAGEL, J. A., GREENHALGH, D. A., GAGNE, T. A., LONGLEY, M. A. & ROOP, D. R. 1993. Identification of a Calcium-Inducible, Epidermal-Specific Regulatory Element in the 3'-Flanking Region of the Human Keratin 1 Gene. *J Invest Dermatol*, 101, 506-513.
- ROTHNAGEL, J. A., SEKI, T., OGO, M., LONGLEY, M. A., WOJCIK, S. M., BUNDMAN, D. S., BICKENBACH, J. R. & ROOP, D. R. 1999. The mouse keratin 6 isoforms are differentially expressed in the hair follicle, footpad, tongue and activated epidermis. *Differentiation*, 65, 119-130.
- ROTHNAGEL, J. A. & STEINERT, P. M. 1990. The structure of the gene for mouse filaggrin and a comparison of the repeating units. *J Biol Chem*, 265, 1862-5.

- ROUTHIER, A., ASTUCCIO, M., LAHEY, D., MONFREDO, N., JOHNSON, A., CALLAHAN, W., PARTINGTON, A., FELLOWS, K., OUELLETTE, L., ZHIDRO, S., GOODROW, C., SMITH, A., SULLIVAN, K., SIMONE, P., LE, L., VEZULI, B., ZOHNI, M., WEST, E., GLIEASON, D. & BRYAN, B. 2010. Pharmacological inhibition of Rho-kinase signaling with Y-27632 blocks melanoma tumor growth. *Oncology Reports*, 23, 861-867.
- SAEZ, E., RUTBERG, S. E., MUELLER, E., OPPENHEIM, H., SMOLUK, J., YUSPA, S. H. & SPIEGELMAN, B. M. 1995. c-fos is required for malignant progression of skin tumors. *Cell*, 82, 721-732.
- SAHAI, E., ISHIZAKI, T., NARUMIYA, S. & TREISMAN, R. 1999. Transformation mediated by RhoA requires activity of ROCK kinases. *Current Biology*, 9, 136-145.
- SAHAI, E. & MARSHALL, C. J. 2002. ROCK and Dia have opposing effects on adherens junctions downstream of Rho. *Nat Cell Biol*, 4, 408-15.
- SAHAI, E. & MARSHALL, C. J. 2003. Differing modes of tumour cell invasion have distinct requirements for Rho/ROCK signalling and extracellular proteolysis. *Nat Cell Biol*, 5, 711-719.
- SAHAI, E., OLSON, M. F. & MARSHALL, C. J. 2001. Cross-talk between Ras and Rho signalling pathways in transformation favours proliferation and increased motility. *Embo j*, 20, 755-66.
- SAMUEL, MICHAEL S., LOPEZ, JOSE I., MCGHEE, EWAN J., CROFT, DANIEL R., STRACHAN, D., TIMPSON, P., MUNRO, J., SCHRÖDER, E., ZHOU, J., BRUNTON, VALERIE G., BARKER, N., CLEVERS, H., SANSOM, OWEN J., ANDERSON, KURT I., WEAVER, VALERIE M. & OLSON, MICHAEL F. 2011. Actomyosin-Mediated Cellular Tension Drives Increased Tissue Stiffness and β -Catenin Activation to Induce Epidermal Hyperplasia and Tumor Growth. *Cancer cell*, 19, 776-791.
- SAMUEL, M. S., MUNRO, J., BRYSON, S., FORROW, S., STEVENSON, D. & OLSON, M. F. 2009a. Tissue selective expression of conditionally-regulated ROCK by gene targeting to a defined locus. *Genesis*, 47, 440-6.
- SAMUEL, M. S., MUNRO, J., BRYSON, S., FORROW, S., STEVENSON, D. & OLSON, M. F. 2009b. Tissue selective expression of conditionally-regulated ROCK by gene targeting to a defined locus. *genesis*, 47, 440-446.
- SCHAUER, I. G., RESSLER, S. J. & ROWLEY, D. R. 2009. Keratinocyte-derived chemokine induces prostate epithelial hyperplasia and reactive stroma in a novel transgenic mouse model. *Prostate*, 69, 373-84.
- SCHERMER, A., JESTER, J. V., HARDY, C., MILANO, D. & SUN, T.-T. 1989. Transient synthesis of K6 and K16 keratins in regenerating rabbit corneal epithelium: keratin markers for an alternative pathway of keratinocyte differentiation. *Differentiation*, 42, 103-110.
- SCHLINGEMANN, J., HESS, J., WROBEL, G., BREITENBACH, U., GEBHARDT, C., STEINLEIN, P., KRAMER, H., FURSTENBERGER, G., HAHN, M., ANGEL, P. & LICHTER, P. 2003. Profile of gene expression induced by the tumour promotor TPA in murine epithelial cells. *Int J Cancer*, 104, 699-708.
- SELLHEYER, K., BICKENBACH, J. R., ROTHNAGEL, J. A., BUNDMAN, D., LONGLEY, M. A., KRIEG, T., ROCHE, N. S., ROBERTS, A. B. & ROOP, D. R. 1993. Inhibition of skin development by overexpression of transforming growth factor beta 1 in the epidermis of transgenic mice. *Proceedings of the National Academy of Sciences of the United States of America*, 90, 5237-5241.
- SHAULIAN, E. & KARIN, M. 2002. AP-1 as a regulator of cell life and death. *Nat Cell Biol*, 4, E131-E136.
- SHIMIZU, T., IHARA, K., MAESAKI, R., AMANO, M., KAIBUCHI, K. & HAKOSHIMA, T. 2003. Parallel coiled-coil association of the RhoA-binding domain in Rho-kinase. *J. Biol. Chem.*, 278, 46046-46051.
- SIMPSON, C. L., PATEL, D. M. & GREEN, K. J. 2011. Deconstructing the skin: cytoarchitectural determinants of epidermal morphogenesis. *Nature Reviews. Molecular Cell Biology*, 12, 565-580.
- SMEYNE, R. J., SCHILLING, K., ROBERTSON, L., LUK, D., OBERDICK, J., CURRAN, T. & MORGAN, J. I. 1992. fos-lacZ transgenic mice: mapping sites of gene induction in the central nervous system. *Neuron*, 8, 13-23.
- SOBINOFF, A. P., MAHONY, M., NIXON, B., ROMAN, S. D. & MCLAUGHLIN, E. A. 2011. Understanding the Villain: DMBA-Induced Preantral Ovotoxicity Involves Selective Follicular Destruction and Primordial Follicle Activation through PI3K/Akt and mTOR Signaling. *Toxicological Sciences*, 123, 563-575.
- SONG, M. S., SALMENA, L. & PANDOLFI, P. P. 2012. The functions and regulation of the PTEN tumour suppressor. *Nat Rev Mol Cell Biol*, 13, 283-296.

- STAMBOLIC, V., SUZUKI, A., DE LA POMPA, J. L., BROTHERS, G. M., MIRTSOS, C., SASAKI, T., RULAND, J., PENNINGER, J. M., SIDEROVSKI, D. P. & MAK, T. W. 1998. Negative Regulation of PKB/Akt-Dependent Cell Survival by the Tumor Suppressor PTEN. *Cell*, 95, 29-39.
- STEINIGER, B. & BARTH, P. 2000. Microanatomy and function of the spleen. *Adv Anat Embryol Cell Biol*, 151, lii-ix, 1-101.
- STEVEN, A. C., BISHOP, M. E., ROOP, D. R. & STEINERT, P. M. 1990. Biosynthetic pathways of filaggrin and loricrin—two major proteins expressed by terminally differentiated epidermal keratinocytes. *Journal of Structural Biology*, 104, 150-162.
- STILES, B. L., KURALWALLA-MARTINEZ, C., GUO, W., GREGORIAN, C., WANG, Y., TIAN, J., MAGNUSON, M. A. & WU, H. 2006. Selective deletion of Pten in pancreatic beta cells leads to increased islet mass and resistance to STZ-induced diabetes. *Mol Cell Biol*, 26, 2772-81.
- STRICKLAND, J. E., GREENHALGH, D. A., KOCEVA-CHYLA, A., HENNINGS, H., RESTREPO, C., BALASCHAK, M. & YUSPA, S. H. 1988. Development of murine epidermal cell lines which contain an activated rasHa oncogene and form papillomas in skin grafts on athymic nude mouse hosts. *Cancer Res*, 48, 165-9.
- SUBAUSTE, M. C., NALBANT, P., ADAMSON, E. D. & HAHN, K. M. 2005. Vinculin controls PTEN protein level by maintaining the interaction of the adherens junction protein beta-catenin with the scaffolding protein MAGI-2. *J Biol Chem*, 280, 5676-81.
- SUNDBERG, J. P. 2004. Chapter 12 - Skin and Adnexa of the Laboratory Mouse. In: BULLOCK, P. H. J. H. G. (ed.) *The Laboratory Mouse*. London: Academic Press.
- SUZUKI, A., ITAMI, S., OHISHI, M., HAMADA, K., INOUE, T., KOMAZAWA, N., SENOO, H., SASAKI, T., TAKEDA, J., MANABE, M., MAK, T. W. & NAKANO, T. 2003. Keratinocyte-specific Pten Deficiency Results in Epidermal Hyperplasia, Accelerated Hair Follicle Morphogenesis and Tumor Formation. *Cancer Research*, 63, 674-681.
- TOPLEY, G. I., OKUYAMA, R., GONZALES, J. G., CONTI, C. & DOTTO, G. P. 1999. p21(WAF1/Cip1) functions as a suppressor of malignant skin tumor formation and a determinant of keratinocyte stem-cell potential. *Proceedings of the National Academy of Sciences of the United States of America*, 96, 9089-9094.
- VASUDEVAN, K. M., BURIKHANOV, R., GOSWAMI, A. & RANGNEKAR, V. M. 2007. Suppression of PTEN expression is essential for antiapoptosis and cellular transformation by oncogenic Ras. *Cancer Res*, 67, 10343-50.
- VIVANCO, I. & SAWYERS, C. L. 2002. The phosphatidylinositol 3-Kinase AKT pathway in human cancer. *Nat Rev Cancer*, 2, 489-501.
- WANG, S., GAO, J., LEI, Q., ROZENGURT, N., PRITCHARD, C., JIAO, J., THOMAS, G. V., LI, G., ROY-BURMAN, P., NELSON, P. S., LIU, X. & WU, H. 2003. Prostate-specific deletion of the murine Pten tumor suppressor gene leads to metastatic prostate cancer. *Cancer Cell*, 4, 209-21.
- WANG, X. J., GREENHALGH, D. A., DONEHOWER, L. A. & ROOP, D. R. 2000. Cooperation between Ha-ras and fos or transforming growth factor α overcomes a paradoxical tumor-inhibitory effect of p53 loss in transgenic mouse epidermis. *Molecular Carcinogenesis*, 29, 67-75.
- WICKMAN, G. R., SAMUEL, M. S., LOCHHEAD, P. A. & OLSON, M. F. 2010. The Rho-Regulated ROCK Kinases in Cancer. In: GOLEN, K. V. (ed.) *The Rho GTPases in Cancer*. Springer Science.
- WILKINSON, S., PATERSON, H. F. & MARSHALL, C. J. 2005. Cdc42-MRCK and Rho-ROCK signalling cooperate in myosin phosphorylation and cell invasion. *Nat Cell Biol*, 7, 255-261.
- WU, H., GOEL, V. & HALUSKA, F. G. 2003. PTEN signaling pathways in melanoma. *Oncogene*, 22, 3113-3122.
- YAMADA, K. M. & ARAKI, M. 2001. Tumor suppressor PTEN: modulator of cell signaling, growth, migration and apoptosis. *Journal of Cell Science*, 114, 2375-2382.
- YAMASHIRO, S., TOTSUKAWA, G., YAMAKITA, Y., SASAKI, Y., MADAULE, P., ISHIZAKI, T., NARUMIYA, S. & MATSUMURA, F. 2003. Citron kinase, a Rho-dependent kinase, induces di-phosphorylation of regulatory light chain of myosin II. *Mol Biol Cell*, 14, 1745-56.
- YANG, S. & KIM, H. M. 2012. The RhoA-ROCK-PTEN pathway as a molecular switch for anchorage dependent cell behavior. *Biomaterials*, 33, 2902-15.
- YAO, D., ALEXANDER, C. L., QUINN, J. A., CHAN, W.-C., WU, H. & GREENHALGH, D. A. 2008. Fos cooperation with PTEN loss elicits keratoacanthoma not carcinoma, owing to p53/p21WAF-induced differentiation triggered by GSK3 β inactivation and reduced AKT activity. *Journal of Cell Science*, 121, 1758-1769.
- YAO, D., ALEXANDER, C. L., QUINN, J. A., PORTER, M. J., WU, H. & GREENHALGH, D. A. 2006. PTEN Loss Promotes ras^{Ha}-Mediated Papillomatogenesis via Dual Up-Regulation of AKT

- Activity and Cell Cycle Deregulation but Malignant Conversion Proceeds via PTEN-Associated Pathways *Cancer Research*, 66, 1302-1312.
- YASWEN, P. & CAMPISI, J. 2007. Oncogene-Induced Senescence Pathways Weave an Intricate Tapestry. *Cell*, 128, 233-234.
- YOSHIOKA, K., NAKAMORI, S. & ITOH, K. 1999. Overexpression of Small GTP-binding Protein RhoA Promotes Invasion of Tumor Cells. *Cancer Research*, 59, 2004-2010.
- YUSPA, S. H. 1994. The Pathogenesis of Squamous Cell Cancer: Lessons Learned from Studies of Skin Carcinogenesis—Thirty-third G. H. A. Clowes Memorial Award Lecture. *Cancer Research*, 54, 1178-1189.
- YUSPA, S. H. 1998. The pathogenesis of squamous cell cancer: lessons learned from studies of skin carcinogenesis. *Journal of Dermatological Science*, 17, 1-7.
- YUSPA, S. H., BEN, T., HENNINGS, H. & LICHTI, U. 1982. Divergent responses in epidermal basal cells exposed to the tumor promoter 12-O-tetradecanoylphorbol-13-acetate. *Cancer Res*, 42, 2344-9.
- YUSPA, S. H., HAWLEY-NELSON, P., STANLEY, J. R. & HENNINGS, H. 1980. Epidermal cell culture. *Transplant Proc*, 12, 114-22.
- YUSPA, S. H., KILKENNY, A., CHENG, C., ROOP, D. R., HENNINGS, H., KRUSZEWSKI, F., LEE, E., STRICKLAND, J. & GREENHALGH, D. A. 1991. Alterations in epidermal biochemistry as a consequence of stage-specific genetic changes in skin carcinogenesis. *Environmental Health Perspectives*, 93, 3-10.
- YUSPA, S. H., KILKENNY, A. E., STEINERT, P. M. & ROOP, D. R. 1989. Expression of murine epidermal differentiation markers is tightly regulated by restricted extracellular calcium concentrations in vitro. *J Cell Biol*, 109, 1207-17.
- YUSPA, S. H. & POIRIER, M. C. 1988. Chemical carcinogenesis: from animal models to molecular models in one decade. *Adv. Cancer Res.*, 50, 25-70.
- ZHANG, Z., REN, J. H., LI, Z. Y., NONG, L. & WU, G. 2012. Fasudil inhibits lung carcinoma-conditioned endothelial cell viability and migration. *Oncol Rep*, 27, 1561-6.
- ZOHN, I. M., CAMPBELL, S. L., KHOSRAVU-FAR, R., ROSSMAN, K. L. & DER, C. J. 1998. Rho family proteins and Ras transformation: the RHOad less traveled gets congested. *Oncogene*, 17, 1415-1438.